Case reports in
cancer genetics
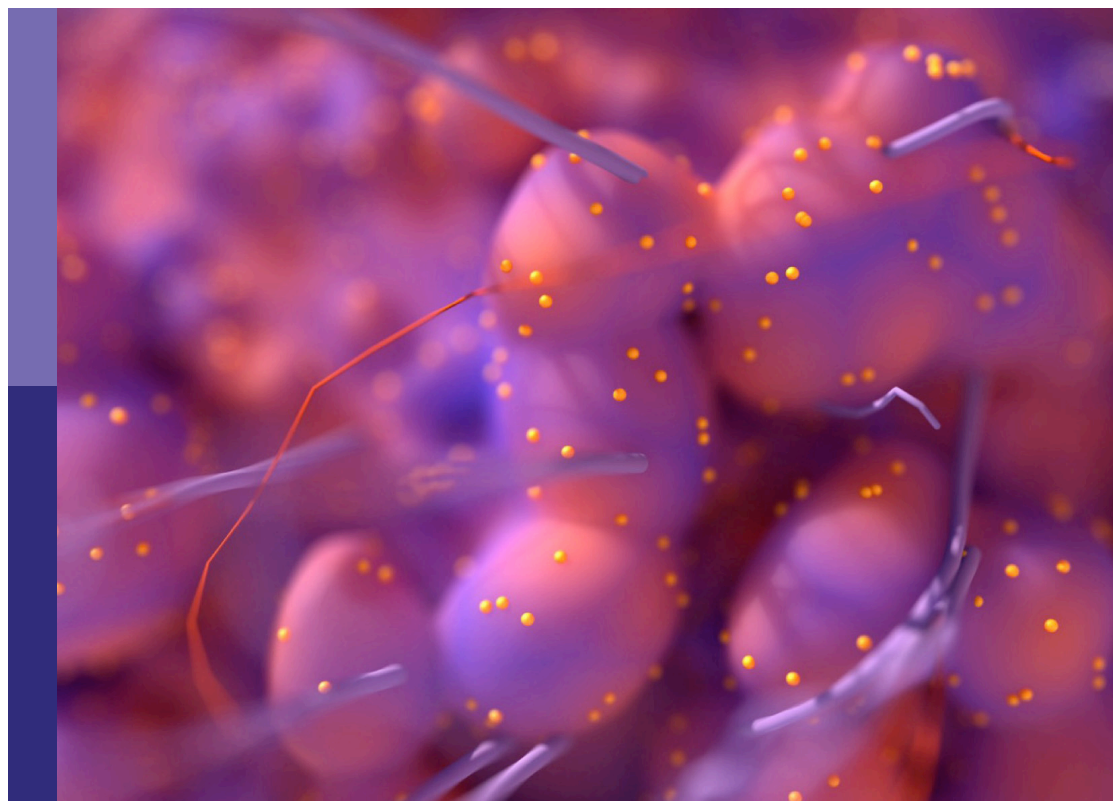# 2022

Edited by
Haidong Gao, Athina Markou and Emilio Cordova

About Frontiers

Frontiers is more than just an open access publisher of scholarly articles: it is a pioneering approach to the world of academia, radically improving the way scholarly research is managed. The grand vision of Frontiers is a world where all people have an equal opportunity to seek, share and generate knowledge. Frontiers provides immediate and permanent online open access to all its publications, but this alone is not enough to realize our grand goals.

Frontiers journal series

The Frontiers journal series is a multi-tier and interdisciplinary set of open-access, online journals, promising a paradigm shift from the current review, selection and dissemination processes in academic publishing. All Frontiers journals are driven by researchers for researchers; therefore, they constitute a service to the scholarly community. At the same time, the *Frontiers journal series* operates on a revolutionary invention, the tiered publishing system, initially addressing specific communities of scholars, and gradually climbing up to broader public understanding, thus serving the interests of the lay society, too.

Dedication to quality

Each Frontiers article is a landmark of the highest quality, thanks to genuinely collaborative interactions between authors and review editors, who include some of the world's best academicians. Research must be certified by peers before entering a stream of knowledge that may eventually reach the public - and shape society; therefore, Frontiers only applies the most rigorous and unbiased reviews. Frontiers revolutionizes research publishing by freely delivering the most outstanding research, evaluated with no bias from both the academic and social point of view. By applying the most advanced information technologies, Frontiers is catapulting scholarly publishing into a new generation.

What are Frontiers Research Topics?

Frontiers Research Topics are very popular trademarks of the *Frontiers journals series*: they are collections of at least ten articles, all centered on a particular subject. With their unique mix of varied contributions from Original Research to Review Articles, Frontiers Research Topics unify the most influential researchers, the latest key findings and historical advances in a hot research area.

Find out more on how to host your own Frontiers Research Topic or contribute to one as an author by contacting the Frontiers editorial office: frontiersin.org/about/contact

Case reports in cancer genetics : 2022

Topic editors

Haidong Gao — Shandong University, China

Athina Markou — National and Kapodistrian University of Athens, Greece

Emilio Cordova — National Institute of Genomic Medicine (INMEGEN), Mexico

Citation

Gao, H., Markou, A., Cordova, E., eds. (2023). *Case reports in cancer genetics : 2022*. Lausanne: Frontiers Media SA. doi: 10.3389/978-2-8325-3064-1

Table of
contents

A Novel Intergenic Gene Between *SLC8A1* and *PKDCC-ALK* Fusion Responds to *ALK* TKI WX-0593 in Lung Adenocarcinoma: A Case Report

Jia Du[1†], Baoming Wang[2†], Mengxia Li[1], Chunyang Wang[2], Tonghui Ma[2] and Jinlu Shan[1]*

[1] Cancer Center, Daping Hospital, Army Medical University, Chongqing, China, [2] Department of Translational Medicine, Genetron Health (Beijing), Co. Ltd., Beijing, China

Background: Expanding the druggable novel anaplastic lymphoma kinase (*ALK*) fusions list is crucial to the precise treatment of patients with cancer with positive *ALK* fusions. The *intergenic-ALK* fusions accounted for a substantial proportion of *ALK* fusions. However, they were typically considered of limited clinical significance due to the obscure functional partners. In this case report, a patient carrying *intergenic-ALK* fusion presents an excellent outcome after taking the new second-generation tyrosine kinase inhibitor (TKI) candidate, WX-0593.

Case Presentation: A 47-year-old Chinese female patient diagnosed with IVB lung adenocarcinoma was admitted to the hospital with large dimension lesions in the left lobe of the lung. After 1 week of first line chemotherapy, no response was found. A novel *ALK* rearrangement generated by a fusion of the intergenic region between *SLC8A1* and *PKDCC* to the intron 19 of *ALK* was presented after next-generation sequencing and was further confirmed by Sanger's sequencing. High expression of *ALK* was revealed by immunohistochemistry. The patient was directed to engage in phase III clinical trial (NCT04632758) and received an orally active second-generation *ALK* inhibitor WX-0593. Over the course of 17 months, the partial response was obtained without significant side effects.

Conclusion: In summary, a patient with non–small cell lung cancer harboring a novel *intergenic-ALK* fusion, whose intergenic breakpoint was located between *SLC8A1* and *PKDCC*, benefited from a potent *ALK* TKI candidate WX-0593. This finding extended the scope of targetable *ALK* fusions. More importantly, it highlighted the advantages of next-generation sequencing in identifying rare but functional *ALK* fusions, which eventually benefit patients.

Keywords: fusion, *intergenic-ALK*, inhibitor, WX-0593, *SLC8A1*, *PKDCC*

INTRODUCTION

Anaplastic lymphoma kinase (*ALK*) gene fusions drive genetic alterations and critical molecular targets in around 3%~5% of non–small cell lung cancer (NSCLC) (1). For the treatment of patients with *ALK* rearrangement-positive NSCLC, the first-generation *ALK* tyrosine kinase inhibitor (TKI) crizotinib (2), second-generation [ceritinib (3), alectinib (4), and brigatinib (5)], and third-generation [lorlatinib (6)] *ALK* TKIs have been approved as an effective treatment. Because of their rarity, newly confirmed *ALK* fusions, in addition to the conventional *EML4-ALK* fusion, represent significant difficulties in targeted *ALK* TKI therapy in the clinic. Clinical outcomes vary according to fusion partners and specific TKIs (7). Therefore, an accurate diagnosis of functional *ALK* fusions is crucial for successful NSCLC treatment. In contrast to the typical form of *ALK* fusions, the rare *intergenic-ALK* fusions, whose breakpoint localized in the intergenic regions, are theoretically to be unfunctional due to the missing chimeric full coding transcripts. Here, for the first time, we reported a novel *intergenic-ALK* fusion, whose intergenic region was between *SLC8A1* and *PKDCC* and fused with the exon 20 of ALK in a patient with NSCLC. The patient achieved a long-term therapeutic benefit after receiving the potent second-generation candidate *ALK* TKI WX-0593 treatment.

CASE PRESENTATION

This case report was approved by the Ethics Committee of Daping Hospital [2022(03)]. A 47-year-old Chinese female patient was admitted to the hospital with paroxysmal abdominal pain in June 2020. Computed tomography (CT) scans revealed a space-occupying lesion in the left lung lobe, as well as multiple masses in the liver and skeleton. IVB lung adenocarcinoma (cT2N1M1c) was diagnosed on the basis of the pathological results from tissue biopsy and CT. Lung tumor biopsies were submitted to Genetron Health Inc. (Beijing, China) for Next Generation Sequencing (NGS) with an 825 cancer-related gene DNA panel (Onco Panscan™) for comprehensive molecular profiling. During the DNA-NGS analysis, the patient received 1 week of chemotherapy with pemetrexed disodium (0.8 g) and nedaplatin (100 mg) and did not show any response (**Figure 1**).

The DNA sequencing identified a novel *ALK* fusion with a mutation frequency of 5.3% (**Figure 2A**). Integrative Genomics Viewer revealed a novel *intergenic-ALK* rearrangement generated by a fusion of the intergenic region between *SLC8A1* and *PKDCC* to the intron 19 of *ALK*, and Sanger's sequencing result supported the accuracy of DNA-NGS detection. Furthermore, the gene fusion was confirmed by fluorescence *in situ* hybridization (FISH) with *ALK* break-apart probe (Healthcare, NMPA: 20183400004) (**Figure 2B**). A high level of *ALK* protein expression was further validated with immunohistochemistry (Ventana ALK (D5F3®) XP®, #3633, Cell Signaling Technology) (**Figure 2C**).

The patient was referred to enroll in phase III clinical trial (NCT04632758) and was randomly administered an orally active second-generation *ALK* inhibitor WX-0593. An initial dose of 60 mg was administered for 1 week, followed by a maintenance dose of 180 mg. According to the Response Evaluation Criteria for

FIGURE 1 | The treatment scheme and representative CT scan images during treatment. ADC, adenocarcinoma; SD, stable disease; PR, partial response.

FIGURE 2 | Identification of a novel intergenic ALK fusion. **(A)** Sequence analysis of the *intergenic-ALK* fusion. Upper panel showed reads of fusion on Integrative Genomic Viewer. Lower panel showed a schematic presentation of breakpoints and the Sanger's sequencing result. **(B)** FISH analysis showed fused yellow signals (negative signal), single green signals (positive signal), and single red signals (positive signal) in the patient's specimen. **(C)** Immunohistochemical staining with anti-ALK antibody (D5F3) revealed a high level of ALK protein.

Solid Tumors 1.1 guidelines, the CT scan indicated a partial response (PR) lasting longer than 22 months, with no noticeable side effects (**Figure 1**).

DISCUSSION

With the development of NGS technology, more than 90 *ALK* fusion partners have been discovered to date (8). It is generally believed that the functional protein of the partner gene at the N-terminus of *ALK* could result in continuous *ALK* gene activation driven by the promoter of the partner gene. Theoretically, the rare type of *intergenic-ALK* fusion, whose partner lacked a promoter, will fail to respond to TKIs. Sporadic cases showed that some *intergenic-ALK* fusions were sensitive to the *ALK* TKIs (8). However, it has not been fully identified due to a lack of knowledge concerning the precise mechanism (9). Therefore, it is vital to expand the list of targetable intergenic fusions.

To date, three generations of *ALK* TKIs, including but not limited to crizotinib, alectinib, and lorlatinib, have been developed. These inhibitors present an exceptional capacity to lengthen the lives of patients with *ALK* fusions. Despite the excellent results of these TKIs, newly developed local *ALK* TKIs

were required to reduce the financial burden on the patients and national health insurance. *In vitro* and *in vivo* preclinical models revealed that WX-0593, a potent orally active second-generation *ALK* and ROS1 inhibitor, showed robust antitumor activity. Furthermore, it presented the noticeable safety and efficacy in patients with *ALK*-positive and *ROS1*-positive NSCLC in phase I clinical trial (NCT03389815) (10).

In this study, the patient with novel *intergenic-ALK* (chr2_42048364; A20) fusion showed an excellent prognosis outcome after being treated with WX-0593. The soft tissue masses in the lung and liver diminished dramatically, which had obtained a PR after 17 months of therapy. The patient continues to receive WX-0593 medication while preparing this manuscript. Positive therapeutic outcomes in our investigation demonstrated that *intergenic-ALK* fusion could be considered as a potential oncogenic mutation by stimulating the overexpression of *ALK* proteins. We infer that the intergenic region at the 5' end functions as a strong promoter in this unique fusion variant. Nonetheless, the oncogenic and molecular processes of this fusion will need to be further investigated.

Despite the great novelty of our results, several limitations still need to be discussed. RNA-based NGS is preferred to DNA-based NGS for fusion detection based on the NCCN Guidelines

Version 1.2022 for NSCLC. However, because of the limited number of retained specimens, the RNA-NGS was not performed. It could not be precisely annotated whether the newly discovered fusion forms differed at the DNA and RNA levels. To confirm the biological function of the *intergenic-ALK* fusion in cancer, additional research is required.

CONCLUSION

In summary, an *ALK*-TKI candidate, WX-0593, was effectively treated a patient with NSCLC with novel *intergenic-ALK* fusion. This case broadened the breadth of *ALK* fusions that can be targeted and highlighted the utility of NGS in mining rare but functional *ALK* fusions, which eventually bring benefits to the patients.

DATA AVAILABILITY STATEMENT

The original contributions presented in the study are included in the article/supplementary materials. Further inquiries can be directed to the corresponding author.

ETHICS STATEMENT

This case report was approved by the Ethics Committee of Daping Hospital [2022(03)]. The patients/participants provided their written informed consent to participate in this study. Written informed consent was obtained from the individual(s) for the publication of any potentially identifiable images or data included in this article.

AUTHOR CONTRIBUTIONS

JD and BW contributed to the experiment performing and manuscript writing. CW and TM participated to the data analysis. ML provided the clinical samples and relevant information. JS designed and optimized the experiment. All authors contributed to the article and approved the submitted version.

REFERENCES

1. Du X, Shao Y, Qin HF, Tai YH, Gao HJ. ALK-Rearrangement in Non-Small-Cell Lung Cancer (NSCLC). *Thorac Cancer* (2018) 9:423–30.
2. Shaw AT, Kim D-W, Nakagawa K, Seto T, Crinó L, Ahn M-J, et al. Crizotinib Versus Chemotherapy in Advanced ALK-Positive Lung Cancer. *N Engl J Med* (2013) 368:2385–94.
3. Shaw AT, Kim D-W, Mehra R, Tan DS, Felip E, Chow LQ, et al. Ceritinib in ALK-Rearranged Non–Small-Cell Lung Cancer. *N Engl J Med* (2014) 370:1189–97.
4. Peters S, Camidge DR, Shaw AT., Gadgeel S, Ahn JS, Kim D-W, et al. Alectinib Versus Crizotinib in Untreated ALK-Positive Non–Small-Cell Lung Cancer. *N Engl J Med* (2017) 377:829–38.
5. Camidge DR, Kim HR, Ahn M-J, Yang JC-H, Han J-Y, Lee J-S, et al. Brigatinib Versus Crizotinib in ALK-Positive non–Small-Cell Lung Cancer. *N Engl J Med* (2018) 379:2027–39.
6. Solomon BJ, Besse B, Bauer TM, Felip E, Soo RA, Camidge DR, et al. Lorlatinib in Patients With ALK-Positive Non-Small-Cell Lung Cancer: Results From a Global Phase 2 Study. *Lancet Oncol* (2018) 19:1654–67.
7. Childress MA, Himmelberg SM, Chen H, Deng W, Davies MA, Lovly C. M.. ALK Fusion Partners Impact Response to ALK Inhibition: Differential Effects on Sensitivity, Cellular Phenotypes, and Biochemical Properties. *Mol Cancer Res MCR* (2018) 16:1724–36. doi: 10.1158/1541-7786.Mcr-18-0171
8. Ou S-HI, Zhu VW, Nagasaka M. Catalog of 5'fusion Partners in ALK-Positive NSCLC Circa 2020. *JTO Clin Res Rep* (2020) 1:100015.
9. Li W, Liu Y, Li W, Chen L, Ying J. Intergenic Breakpoints Identified by DNA Sequencing Confound Targetable Kinase Fusion Detection in NSCLC. *J Thorac Oncol Off Publ Int Assoc Study Lung Cancer* (2020) 15:1223–31. doi: 10.1016/j.jtho.2020.02.023
10. Shi Y-K, Fang J, Zhang S, Liu Y, Wang L, Si M, et al. Safety and Efficacy of WX-0593 in ALK-Positive or ROS1-Positive Non-Small Cell Lung Cancer. *Ann Oncol* (2019) 30:v607–8.

Case Report: Malignant Brain Tumors in Siblings With *MSH6* Mutations

Di Wu[1†], Qingshan Chen[2†] and Jian Chen[1,3*]

[1] Institute of Functional Nano and Soft Materials (FUNSOM) and Collaborative Innovation Center of Suzhou Nano Science and Technology, Soochow University, Suzhou, China, [2] Department of Neurosurgery, The Second People's Hospital of Liaocheng of Shandong Province, Liaocheng, China, [3] Chinese Institute for Brain Research, Beijing, Research Unit of Medical Neurobiology, Chinese Academy of Medical Sciences, Beijing, China

Background: Familial brain tumor incidences are low. Identifying the genetic alterations of familial brain tumors can help better understand the pathogenesis and make therapy regimens for these tumors.

Case Presentation: An elder female and a younger male were diagnosed with brain tumors at the age of 10 and 5, respectively. Whole-genome sequencing analysis of the two patients' blood, primary brain tumor tissues, and their parents' blood samples was performed, which revealed that the two tumor samples harbored extremely high somatic mutation loads. Additionally, we observed pigmentation on the male patient's skin.

Conclusion: Germline, biallelic mutation of *MSH6*—a gene related to DNA mismatch repair whose defect will result in constitutional mismatch repair deficiency (CMMRD)—is causal for the brain tumors of these two siblings.

Keywords: brain tumor, genome sequencing, *MSH6*, DNA Mismatch Repair, CMMRD, case report

INTRODUCTION

Brain tumors are the most common and lethal type of solid tumors in children (1). They range from the least common, non-invasive, surgically curable pilocytic astrocytoma to the common, highly malignant glioblastoma (GBM) and medulloblastoma (MB) (2–5). Both of GBM and MB are classified as grade IV in malignancy by the World Health Organization (WHO) (6). Familial brain tumor incidences, on the other hand, are relatively low. Gorlin syndrome patients caused by inherited *PTCH1* mutations can develop MB and Li-Fraumeni syndrome patients resulted from germline *TP53* inactivation are associated with malignant gliomas (7, 8). Constitutional mismatch repair deficiency (CMMRD) syndrome, which was called Turcot syndrome for many years, is also associated with an increased risk of brain cancer (9).

CMMRD syndrome is a distinct childhood cancer predisposition syndrome characterized by diverse malignancies in hematological organs, the brain, the large intestine and other organs (10). Patients mostly fail in reaching their adulthood (11). The most prevalent are brain tumors and the

age at diagnosis has been estimated to be 10.3 years old (12). The majority of the brain tumors are malignant gliomas, but MB and other central nervous system tumors have also been reported (10, 13). GBM is the most lethal tumor in CMMRD patients (14). The disease is caused by biallelic germline mutations that occur in one of the four mismatch repair (MMR) genes (*MLH1*, *MSH2*, *MSH6*, *PMS2*) (15). The protein products of these MMR genes are highly conserved from bacteria to humans, which are responsible for the correction of mismatches, insertions and deletions during DNA replication and recombination (16). Humans have two types of MMR enzymes: MutS (hMSH2, hMSH3 and hMSH6) and MutL (hMLH1, hMLH3, PMS1 and PMS2) (17). MutS enzymes first recognize mismatched nucleotides in DNA and then work in combination with MutL enzymes to activate other proteins to remove the mismatched DNA strand and synthesize a new DNA strand (18, 19). In MutS, hMSH6 and hMSH2 function as a heterodimer to recognize single base mismatches as well as 1-2 base insertions and deletions, while the complex of hMSH3 and hMSH2 recognizes larger insertion or deletion loops up to 13 nucleotides (16, 20). Patients with *MSH6* nullizygous mutations commonly develop brain tumors before the age of 10 (9).

The diagnosis of CMMRD syndrome is difficult due to many reasons. Firstly, CMMRD syndrome is caused by biallelic germline mutations of MMR genes but their parents with only one allelic mutation show a low risk of cancer predisposition (21). Secondly, CMMRD syndrome lacks unique clinical features and clear diagnostic criteria. Its clinical presentation varies and the phenotypes also overlap with other tumor syndromes such as Li-Fraumeni syndrome (22).

In this case report, an elder sister and a younger brother were diagnosed with GBM and MB, respectively. Further genomic sequencing confirmed that both patients harbored biallelic *MSH6* mutations, thus confirming the diagnosis of CMRRD syndrome.

CASE PRESENTATION

The two patients were siblings, and their parents were nonconsanguineous, healthy, and had no family history of genetic or infectious diseases. The elder female and the younger male were diagnosed with brain tumors at the age of 10 and 5 years old, respectively. The male patient repeatedly vomited without any obvious causes five days before being admitted to the hospital and became slightly worse mentally and ate less after the illness. The female patient had similar symptoms with paroxysmal headaches. Computed tomography (CT) showed that the female had a tumor in the right frontal lobe and the male had a tumor in the cerebellar region (**Figures 1A, B**), and subsequent histopathology confirmed the diagnoses of GBM and MB, respectively (**Figures 1C**). Then both of them underwent surgery for total tumor resection. One month later, Intensity-modulated radiation therapy (IMRT) was followed in the female, where a DT dose of 50 Gy in 2 Gy daily fractions in GTV and 45 Gy in 1.8 Gy daily fractions in PTV were delivered with

instruction from the radiation oncologist. The frequency of administration is 5 times weekly. For the male, the radiotherapy was administered in the dose of 36 Gy in 1.8 Gy daily fractions. The siblings tolerated radiation therapy very well and the follow-up brain MRI revealed no brain tumor. However, one and a half years later, tumor recurrence was suspected in the female through MRI and she received the second radiotherapy (dose of DT: 39.6 Gy in 1.8 Gy daily fractions) combined with temozolomide (TMZ) chemotherapy (100 mg daily for 5 days). For the male, a neoplasm lesion was detected in the spinal canal after 6 months. The second surgery was performed and followed by radiotherapy one month later (dose of DT: 42 Gy in 2.1 Gy daily fractions). The siblings have already resumed normal schooling and daily activities. The timeline from the episode of care in the two cases have been illustrated in **Supplementary Figure 1**.

We performed whole-genome sequencing of the patients' tumor tissue and blood samples, as well as their parents' blood samples, to obtain an overview of the somatic mutation landscape. The tumors were sequenced at 50X and the blood samples were sequenced at 30X (**Figure 2A**). Both tumor cases harbored millions of somatic mutations, many hundreds of folds higher than the average somatic mutation numbers in either GBM or MB (23, 24) (**Figure 2D**). In both tumors, the predominant mutations were single base mutations (**Figure 2C**) and about half of the mutations in exons were non-synonymous mutations (**Figure 2B**). We also observed some well-known somatic mutations such as mutations in *NF1*, *RB1*, *CDKN2A*, *TP53* and *PTEN* in the GBM case and mutations in *TP53*, *NF1*, *SF3B1* and *PTCH* in the MB case (**Figure 2E**).

Somatic mutations can occur in all cells of the body throughout the whole lifetime. They may arise due to mistakes in DNA replication, modification or repair processes. The development of cancer is often accompanied by somatic mutations (25). Based on this, the concept of Mutational Signatures has been proposed, which represents the unique set of characteristics of mutational profiles on the genome (25). Single base substitution (SBS) signatures have been identified by frequencies of 96 different contexts, considering the mutated base and the bases immediately 5' and 3' (26, 27). Based on the assessment of 1,865 whole genomes and 19,184 exomes, 60 SBS signatures have been defined (available at the Cosmic website) (26). We compared the mutational signatures of the two cases with the known mutational signatures and the result indicated strong signals of the SBS44 and SBS14 signatures for both cases; note that both of these signatures are associated with DNA mismatch repair (**Figures 3A–C**).

Our sequencing results showed that the parents had a heterozygous defect and the two patients had homozygous defects in *MSH6*. The mother carried an *MSH6 c.2731C>T* nonsense mutation and the father carried a single nucleotide deletion that resulted in a frameshift of the protein (**Figure 4A**). We performed immunohistochemical (IHC) staining to verify the loss of MSH6 protein in both tumor cases (**Figure 4B**). *MSH6* nullizygous usually causes CMMRD syndrome, which is typically accompanied by a visible symptom called café-au-lait macules
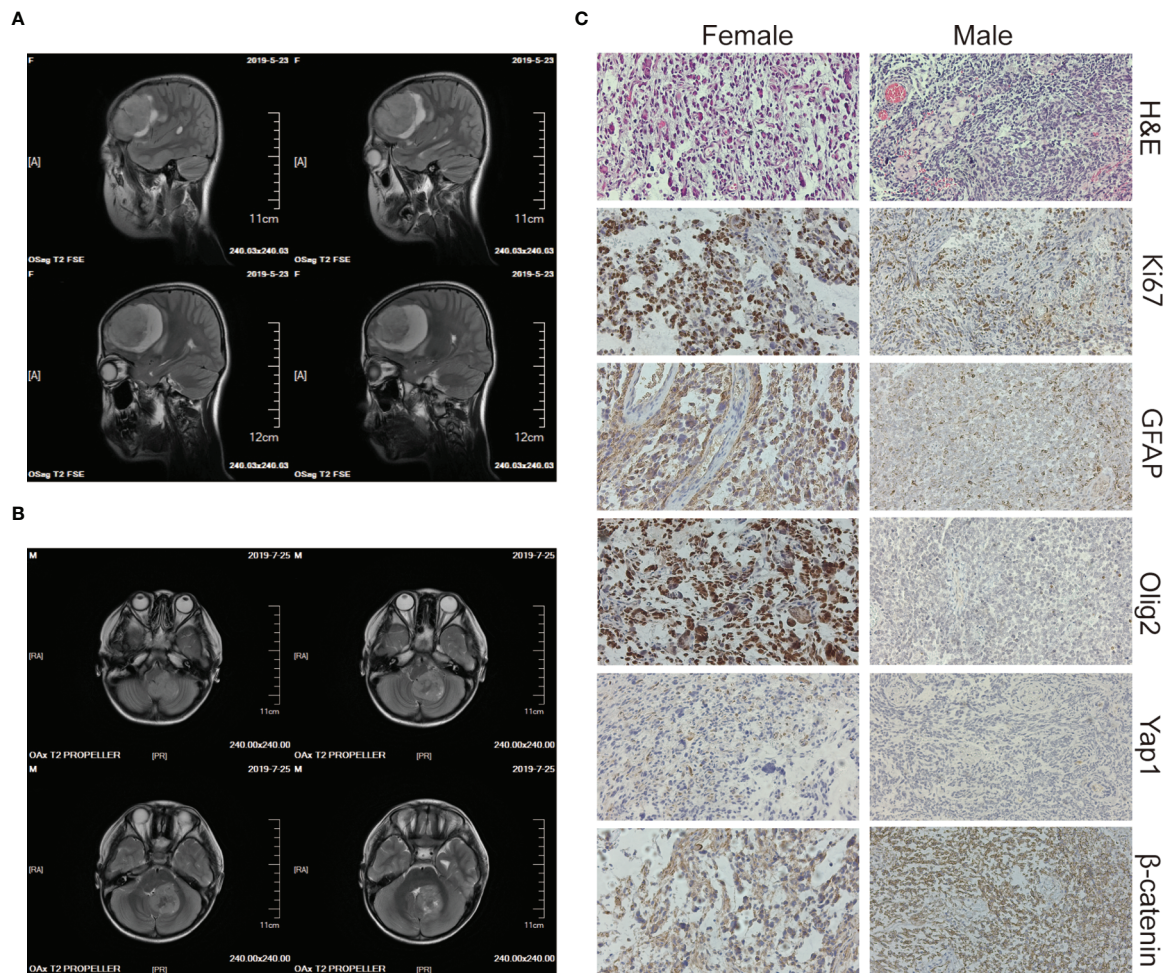
FIGURE 1 | Imaging and histology of the brain tumors. **(A, B)** CT scan images of the brain tumor tissue of the female (upper panels) and the male (lower panels). **(C)** H&E, Ki67, GFAP, Olig2, Yap1, and β-catenin staining of the female's (left panels) and the male's (right panels) brain tumor tissue. The magnification is 20×.

(CALM) (22). We detected multiple flat patches of skin that were darker than the surrounding area in the male (**Figure 4C**).

CONCLUSION AND DISCUSSION

CMMRD syndrome is a rare childhood cancer susceptibility syndrome. The lack of awareness and broad cancer spectrum of malignancies contributes to diagnosis difficulty. Most CMMRD patients have multiple CALM reminiscent of neurofibromatosis type 1 (NF1) (10, 28). It has been demonstrated that *NF1* is a frequent somatic mutation target of MMR deficiency. Parents of CMMRD patients commonly have no symptoms of NF1, while the offspring may present NF1-associated signs when they inherit both of the mutant MMR alleles from their parents (28). In the two cases, for clinicians, CMMRD syndrome was not taken into consideration, and the two patients were diagnosed as common brain tumors in the beginning because of scarce knowledge of this syndrome and little attention to the

diffuse and irregular hyperpigmented macules and the absence of a family history of neoplasms. The diagnosis was confirmed only when germline biallelic inactivation of *MSH6* and a huge somatic mutation load in the tumor were discovered by high throughput sequencing. Of note, microsatellite instability (MSI) is a recognized biomarker for MMR deficiency, which is also can be an auxiliary index for diagnoses (29). In addition, immunohistochemistry to detect the expression of MMR proteins could be an inexpensive alternative method to help CMMRD diagnosis.

The parents of the two cases had no history of colorectal cancers but they did carry a heterozygous mutation of *MSH6*. Compared with *MSH2* and *MLH1*, the clinical severity of heterozygous *MSH6* and *PMS2* mutations is lower, and the diagnosis of CMMRD syndrome often lacks a family history of cancer (21). It is significant for clinicians to be aware of CMMRD syndrome and assess cancer risk in these patients and their relatives. Early cancer surveillance and timely interventions may benefit their future lifetime. There have been clinical diagnostic
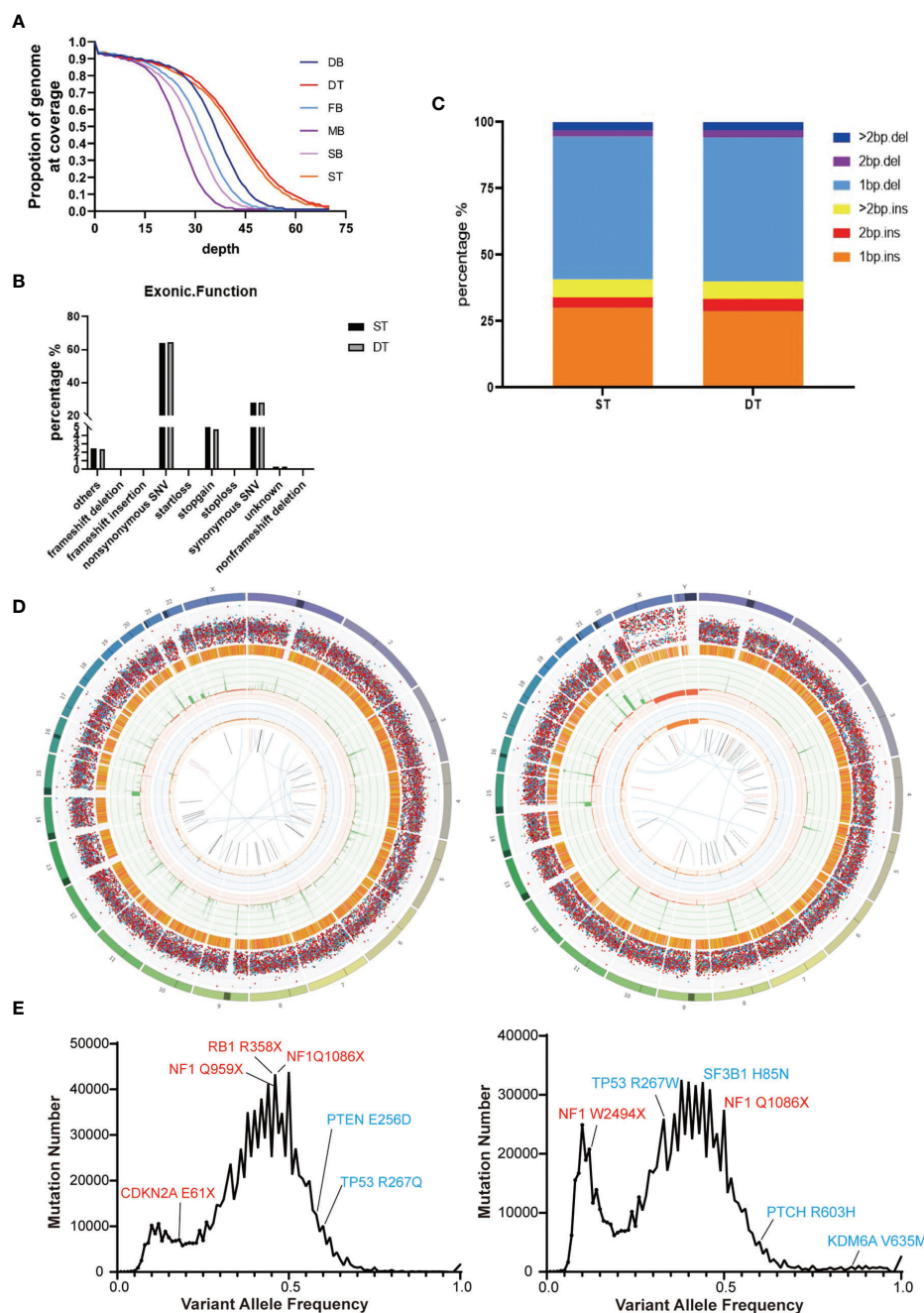
FIGURE 2 | Summary of the whole-genome sequencing results of the two brain tumor cases. **(A)** Sequencing depth and coverage of the tumor and blood samples. D refers to the female patient (daughter); S refers to the male patient (son); F refers to the patients' father; M refers to the patients' mother. B refers to blood samples. T refers to tumor tissue. **(B)** The proportion of different somatic mutation types in exons. **(C)** The distribution of somatic Indel length. **(D)** Circos plots of the female's (left) and the male's (right) brain tumor tissue illustrated distributions of all exonic mutations across the chromosomes. The outer first circle showed the chromosomes and the darker shaded areas represented large gaps. The second circle showed the somatic variants and each dot represented a single somatic variant. The third circle showed all observed tumor purity adjusted copy number changes, including both focal and chromosomal somatic events. The fourth circle represented the observed minor allele copy numbers across the chromosome. The innermost circle displayed the observed structural variants within the chromosomes. **(E)** Mutation number vs. Variant allele frequency (VAF) plot of the female's (left) and the male's (right) brain tumor tissue. Potential driver mutations are labeled (Red: Truncation mutation; Blue: Non-synonymous mutation).
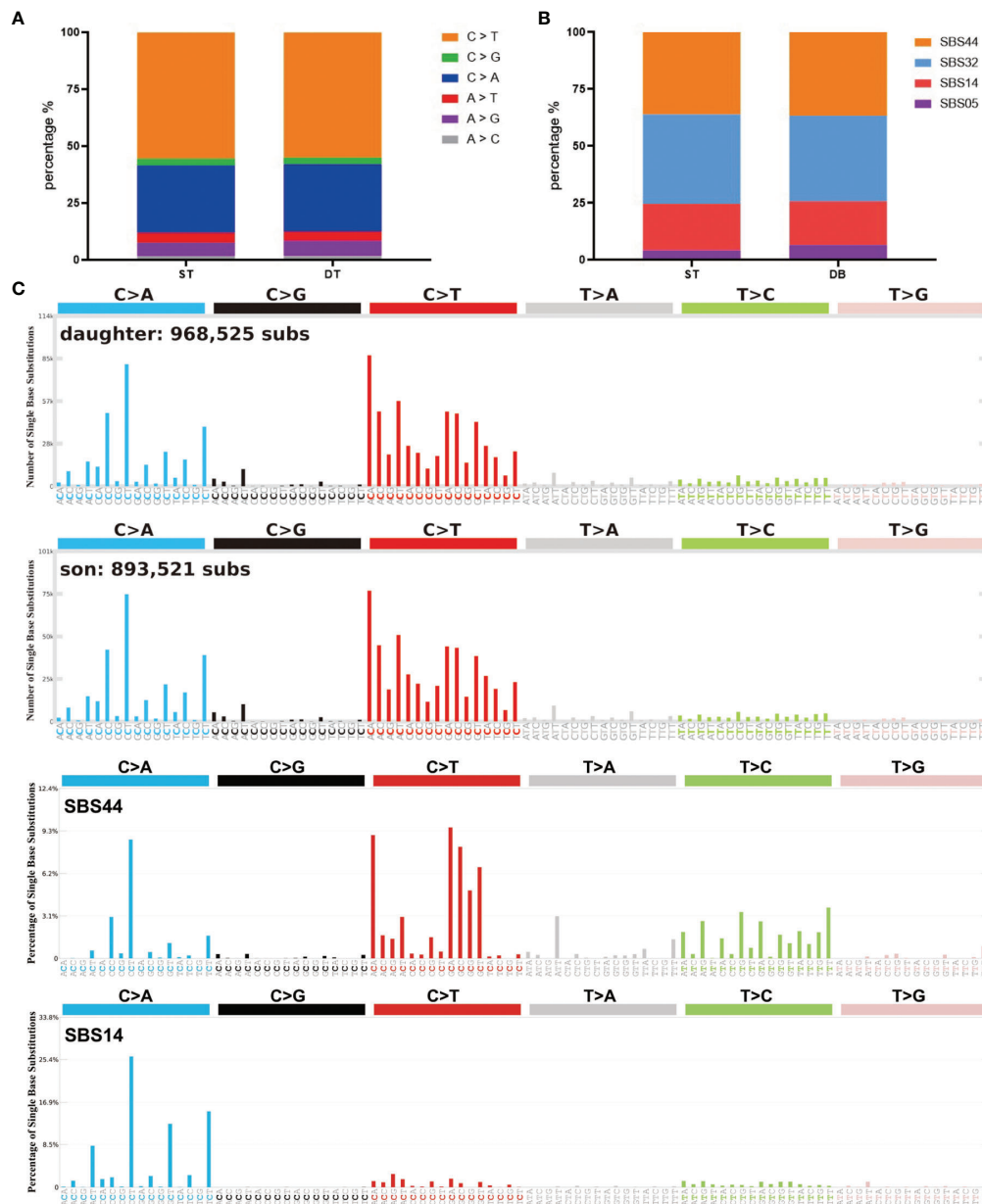
FIGURE 3 | Summary of SBS signatures of the two brain tumor cases. **(A)** The distribution of different single base substitution types. **(B, C)** SBS signatures of the two brain tumor cases and two comparable mutational signatures: SBS44 and SBS14.

criteria and guidelines for surveillance proposed by the European Consortium "Care for CMMR-D" (C4CMMR-D) (10, 14). Commencing MRI scanning at 2 years old and scanning once every 6–12 months is suggested, but whether it will help improve survival has not been validated (14).

In the two cases, radiotherapy received an effective therapeutic outcome, but the information available for optimal treatment is still an urgent requirement. Radiotherapy and adjuvant TMZ chemotherapy are the commonly used treatment for brain tumors (30). However, for CMMRD patients with brain tumors, chemotherapy is typically not a

feasible choice because commonly used chemotherapeutic alkylating agents can only initiate efficient tumor damage with a functional MMR system (31). According to the statistics collected by the European C4CMMRD Consortium, five out of six patients showed poor response to chemotherapy (14). The therapeutic efficiency of TMZ has also been reported to be limited in two patients with *MSH6*-mutated recurrent GBM, and its use should be avoided due to its known ability to accumulate somatic mutations and promote neoplastic progression (32, 33). In the previous case reports regarding children with brain tumors carrying biallelic *MSH6* mutations,
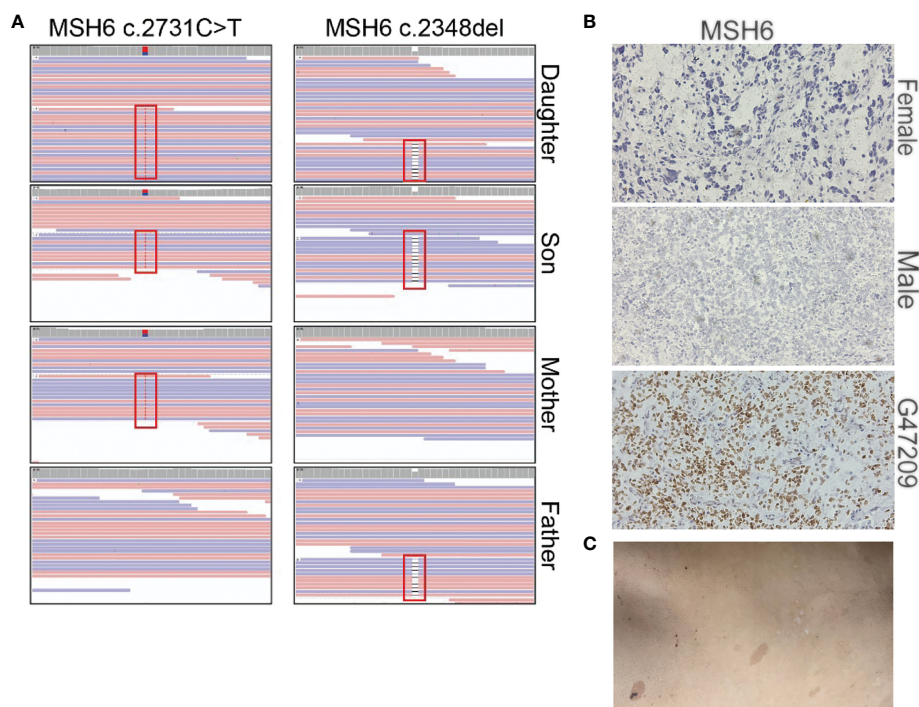
FIGURE 4 | Summary of the *MSH6* mutation in the two brain tumor cases. **(A)** Mutation positions of *MSH6* in the two brain tumor cases and their parents. **(B)** MSH6 staining in the two brain tumor cases and the positive control from a glioma case (G47209) expressing MSH6. The magnification is 20×. **(C)** Hyperpigmented skin lesions in the male case.

the survival was mostly 12-36 months after surgery and subsequent chemoradiotherapy, and many demonstrated resistance to TMZ (11, 32–40). Effective chemotherapeutic drugs for CMMRD syndrome are still lacking, but early detection of tumors may allow for the most effective chemotherapeutic approach (33).

In summary, accurate diagnoses, long-time surveillance and effective therapies for CMMRD patients are still difficulties to be overcome. Several case reports have elaborated immune checkpoint inhibitor (ICPI) can improve the survival of CMMRD patients with malignant gliomas (41–44). One of them reported that a 5-year-old female GBM patient with biallelic *MSH6* mutations was treated with nivolumab and showed a durable response to ICPI treatment and regression of the tumor. For the siblings in this report, ICPI may be taken into consideration if the tumor reoccurs.

METHODS

Whole-Genome Sequencing (WGS)

Genomic DNA was extracted from the tumor and blood samples using a genomic DNA extraction kit (Tiangen Biotech, DP304). The library was constructed and sequenced using Illumina NovaSeq 6000 platform with 150 bp pair-end reads (GeneWiz Inc.).

Bioinformatic Analysis

The raw 150 bp pair-end reads were trimmed using fastp (45) and aligned to hg38 human genome using Sentieon's bwa mem algorithm (Sentieon Inc, San Jose, CA). The germline variations were called following Sentieon's DNAseq pipeline (https://support.sentieon.com/manual/DNAseq_usage/dnaseq/) and the somatic variations were called using TNseq pipeline (https://support.sentieon.com/manual/TNseq_usage/tnseq/). The germline and somatic variations were annotated by Annovar (46). The genomic alignment result was visualized by Integrative Genomics viewer (IGV) (47). MutSignatures (48) was used to analyze and visualize mutation signatures. Circos map was produced using Circos (49).

DATA AVAILABILITY STATEMENT

The datasets presented in this study can be found online at: https://ngdc.cncb.ac.cn/gsa-human/. The accession number is HRA002310.

ETHICS STATEMENT

Patient information was de-identified. The studies involving human participants were reviewed and approved by the

institutional review board of The Second People's Hospital of Liaocheng of Shandong Province. Written informed consent to participate in this study was provided by the participants' legal guardian.

AUTHOR CONTRIBUTIONS

JC conceived and designed the experiments. DW performed the experiments and analyzed the data. QSC collected the clinical samples and analyzed clinical data. DW and JC wrote the paper. All authors read and approved the final manuscript.

SUPPLEMENTARY MATERIAL

The Supplementary Material for this article can be found online at: https://www.frontiersin.org/articles/10.3389/fonc.2022.920305/full#supplementary-material

REFERENCES

1. Smith MA, Reaman GH. Remaining Challenges in Childhood Cancer and Newer Targeted Therapeutics. *Pediatr Clin North Am* (2015) 62(1):301–12. doi: 10.1016/j.pcl.2014.09.018

2. Aldape K, Brindle KM, Chesler L, Chopra R, Gajjar A, Gilbert MR, et al. Challenges to Curing Primary Brain Tumours. *Nat Rev Clin Oncol* (2019) 16(8):509–20. doi: 10.1038/s41571-019-0177-5

3. Nabors LB, Portnow J, Ahluwalia M, Baehring J, Brem H, Brem S, et al. Central Nervous System Cancers, Version 3.2020, NCCN Clinical Practice Guidelines in Oncology. *J Natl Compr Canc Netw* (2020) 18(11):1537–70. doi: 10.6004/jnccn.2020.0052

4. Northcott PA, Robinson GW, Kratz CP, Mabbott DJ, Pomeroy SL, Clifford SC, et al. Medulloblastoma. *Nat Rev Dis Primers* (2019) 5(1):11. doi: 10.1038/s41572-019-0063-6

5. Smoll NR, Drummond KJ. The Incidence of Medulloblastomas and Primitive Neurectodermal Tumours in Adults and Children. *J Clin Neurosci* (2012) 19(11):1541–4. doi: 10.1016/j.jocn.2012.04.009

6. Louis DN, Perry A, Reifenberger G, von Deimling A, Figarella-Branger D, Cavenee WK, et al. The 2016 World Health Organization Classification of Tumors of the Central Nervous System: A Summary. *Acta Neuropathol* (2016) 131(6):803–20. doi: 10.1007/s00401-016-1545-1

7. Fang Z, Su Y, Sun H, Ge M, Qi Z, Hao C, et al. Case Report : Li-Fraumeni Syndrome With Central Nervous System Tumors in Two Siblings. *BMC Pediatr* (2021) 21(1):588. doi: 10.1186/s12887-021-03070-8

8. Sereflican B, Tuman B, Sereflican M, Halicioglu S, Ozyalvacli G, Bayrak S. Gorlin-Goltz Syndrome. *Turk Pediatri Ars* (2017) 52(3):173–7. doi: 10.5152/TurkPediatriArs.2017.2992

9. Abedalthagafi M. Constitutional Mismatch Repair-Deficiency: Current Problems and Emerging Therapeutic Strategies. *Oncotarget* (2018) 9(83):35458–69. doi: 10.18632/oncotarget.26249

10. Wimmer K, Kratz CP, Vasen HF, Caron O, Colas C, Entz-Werle N, et al. Diagnostic Criteria for Constitutional Mismatch Repair Deficiency Syndrome: Suggestions of the European Consortium 'Care for CMMRD' (C4CMMRD). *J Med Genet* (2014) 51(6):355–65. doi: 10.1136/jmedgenet-2014-102284

11. Ilencikova D, Sejnova D, Jindrova J, Babal P. High-Grade Brain Tumors in Siblings With Biallelic *MSH6* Mutations. *Pediatr Blood Cancer* (2011) 57(6):1067–70. doi: 10.1002/pbc.23217

12. Lavoine N, Colas C, Muleris M, Bodo S, Duval A, Entz-Werle N, et al. Constitutional Mismatch Repair Deficiency Syndrome: Clinical Description in a French Cohort. *J Med Genet* (2015) 52(11):770–8. doi: 10.1136/jmedgenet-2015-103299

13. Bakry D, Aronson M, Durno C, Rimawi H, Farah R, Alharbi QK, et al. Genetic and Clinical Determinants of Constitutional Mismatch Repair Deficiency Syndrome: Report From the Constitutional Mismatch Repair Deficiency Consortium. *Eur J Cancer* (2014) 50(5):987–96. doi: 10.1016/j.ejca.2013.12.005

14. Vasen HF, Ghorbanoghli Z, Bourdeaut F, Cabaret O, Caron O, Duval A, et al. Guidelines for Surveillance of Individuals With Constitutional Mismatch Repair-Deficiency Proposed by the European Consortium "Care for CMMR-D" (C4CMMR-D). *J Med Genet* (2014) 51(5):283–93. doi: 10.1136/jmedgenet-2013-102238

15. Wimmer K, Etzler J. Constitutional Mismatch Repair-Deficiency Syndrome: Have We So Far Seen Only the Tip of an Iceberg? *Hum Genet* (2008) 124(2):105–22. doi: 10.1007/s00439-008-0542-4

16. Muro Y, Sugiura K, Mimori T, Akiyama M. DNA Mismatch Repair Enzymes: Genetic Defects and Autoimmunity. *Clin Chim Acta* (2015) 442:102–9. doi: 10.1016/j.cca.2015.01.014

17. Liu D, Keijzers G, Rasmussen LJ. DNA Mismatch Repair and its Many Roles in Eukaryotic Cells. *Mutat Res Rev Mutat Res* (2017) 773:174–87. doi: 10.1016/j.mrrev.2017.07.001

18. Li GM. Mechanisms and Functions of DNA Mismatch Repair. *Cell Res* (2008) 18(1):85–98. doi: 10.1038/cr.2007.115

19. Baretti M, Le DT. DNA Mismatch Repair in Cancer. *Pharmacol Ther* (2018) 189:45–62. doi: 10.1016/j.pharmthera.2018.04.004

20. Eso Y, Shimizu T, Takeda H, Takai A, Marusawa H. Microsatellite Instability and Immune Checkpoint Inhibitors: Toward Precision Medicine Against Gastrointestinal and Hepatobiliary Cancers. *J Gastroenterol* (2020) 55(1):15–26. doi: 10.1007/s00535-019-01620-7

21. Tabori U, Hansford JR, Achatz MI, Kratz CP, Plon SE, Frebourg T, et al. Clinical Management and Tumor Surveillance Recommendations of Inherited Mismatch Repair Deficiency in Childhood. *Clin Cancer Res* (2017) 23(11):e32–e7. doi: 10.1158/1078-0432.CCR-17-0574

22. Aronson M, Colas C, Shuen A, Hampel H, Foulkes WD, Baris Feldman H, et al. Diagnostic Criteria for Constitutional Mismatch Repair Deficiency (CMMRD): Recommendations From the International Consensus Working Group. *J Med Genet* (2022) 59(4):318–27. doi: 10.1136/jmedgenet-2020-107627

23. Stratton MR, Campbell PJ, Futreal PA. The Cancer Genome. *Nature* (2009) 458(7239):719–24. doi: 10.1038/nature07943

24. Alexandrov LB, Nik-Zainal S, Wedge DC, Aparicio SA, Behjati S, Biankin AV, et al. Signatures of Mutational Processes in Human Cancer. *Nature* (2013) 500(7463):415–21. doi: 10.1038/nature12477

25. Alexandrov LB, Stratton MR. Mutational Signatures: The Patterns of Somatic Mutations Hidden in Cancer Genomes. *Curr Opin Genet Dev* (2014) 24:52–60. doi: 10.1016/j.gde.2013.11.014

26. Alexandrov LB, Kim J, Haradhvala NJ, Huang MN, Tian Ng AW, Wu Y, et al. The Repertoire of Mutational Signatures in Human Cancer. *Nature* (2020) 578(7793):94–101. doi: 10.1038/s41586-020-1943-3

27. Alexandrov LB, Nik-Zainal S, Wedge DC, Campbell PJ, Stratton MR. Deciphering Signatures of Mutational Processes Operative in Human Cancer. *Cell Rep* (2013) 3(1):246–59. doi: 10.1016/j.celrep.2012.12.008

28. Wimmer K, Rosenbaum T, Messiaen L. Connections Between Constitutional Mismatch Repair Deficiency Syndrome and Neurofibromatosis Type 1. *Clin Genet* (2017) 91(4):507–19. doi: 10.1111/cge.12904

29. Carrato C, Sanz C, Munoz-Marmol AM, Blanco I, Pineda M, Del Valle J, et al. The Challenge of Diagnosing Constitutional Mismatch Repair Deficiency Syndrome in Brain Malignancies From Young Individuals. *Int J Mol Sci* (2021) 22(9):4629. doi: 10.3390/ijms22094629

30. Zhang J, Stevens MF, Bradshaw TD. Temozolomide: Mechanisms of Action, Repair and Resistance. *Curr Mol Pharmacol* (2012) 5(1):102–14. doi: 10.2174/1874467211205010102

31. Fink D, Aebi S, Howell SB. The Role of DNA Mismatch Repair in Drug Resistance. *Clin Cancer Res* (1998) 4:1–6. PMID: 9516945.

32. Hunter C, Smith R, Cahill DP, Stephens P, Stevens C, Teague J, et al. A Hypermutation Phenotype and Somatic MSH6 Mutations in Recurrent Human Malignant Gliomas After Alkylator Chemotherapy. *Cancer Res* (2006) 66(8):3987–91. doi: 10.1158/0008-5472.CAN-06-0127

33. Scott RH, Mansour S, Pritchard-Jones K, Kumar D, MacSweeney F, Rahman N. Medulloblastoma, Acute Myelocytic Leukemia and Colonic Carcinomas in a Child With Biallelic MSH6 Mutations. *Nat Clin Pract Oncol* (2007) 4 (2):130–4. doi: 10.1038/ncponc0719

34. Ostergaard JR, Sunde L, Okkels H. Neurofibromatosis Von Recklinghausen Type I Phenotype and Early Onset of Cancers in Siblings Compound Heterozygous for Mutations in MSH6. *Am J Med Genet A* (2005) 139A (2):96–105. doi: 10.1002/ajmg.a.30998

35. Etzler J, Peyrl A, Zatkova A, Schildhaus HU, Ficek A, Merkelbach-Bruse S, et al. RNA-Based Mutation Analysis Identifies an Unusual MSH6 Splicing Defect and Circumvents PMS2 Pseudogene Interference. *Hum Mutat* (2008) 29(2):299–305. doi: 10.1002/humu.20657

36. Auclair J, Leroux D, Desseigne F, Lasset C, Saurin JC, Joly MO, et al. Novel Biallelic Mutations in MSH6 and PMS2 Genes: Gene Conversion as a Likely Cause of PMS2 Gene Inactivation. *Hum Mutat* (2007) 28(11):1084–90. doi: 10.1002/humu.20569

37. Hegde MR, Chong B, Blazo ME, Chin LH, Ward PA, Chintagumpala MM, et al. A Homozygous Mutation in MSH6 Causes Turcot Syndrome. *Clin Cancer Res* (2005) 11(13):4689–93. doi: 10.1158/1078-0432.CCR-04-2025

38. Menko FH, Kaspers GL, Meijer GA, Claes K, van Hagen JM, Gille JJ. A Homozygous MSH6 Mutation in a Child With Cafe-Au-Lait Spots, Oligodendroglioma and Rectal Cancer. *Fam Cancer* (2004) 3(2):123–7. doi: 10.1023/B:FAME.0000039893.19289.18

39. Yip S, Miao J, Cahill DP, Iafrate AJ, Aldape K, Nutt CL, et al. MSH6 Mutations Arise in Glioblastomas During Temozolomide Therapy and Mediate Temozolomide Resistance. *Clin Cancer Res* (2009) 15(14):4622–9. doi: 10.1158/1078-0432.CCR-08-3012

40. Poley JW, Wagner A, Hoogmans MM, Menko FH, Tops C, Kros JM, et al. Biallelic Germline Mutations of Mismatch-Repair Genes: A Possible Cause for Multiple Pediatric Malignancies. *Cancer* (2007) 109(11):2349–56. doi: 10.1002/cncr.22697

41. Bouffet E, Larouche V, Campbell BB, Merico D, de Borja R, Aronson M, et al. Immune Checkpoint Inhibition for Hypermutant Glioblastoma Multiforme Resulting From Germline Biallelic Mismatch Repair Deficiency. *J Clin Oncol* (2016) 34(19):2206–11. doi: 10.1200/JCO.2016.66.6552

42. Mishra AK, Achari RB, Zameer L, Achari G, Gehani A, Roy P, et al. Germline Biallelic Mismatch Repair Deficiency in Childhood Glioblastoma and Implications for Clinical Management. *Neurol India* (2022) 70(2):772–4. doi: 10.4103/0028-3886.344608

43. Rittberg R, Harlos C, Rothenmund H, Das A, Tabori U, Sinha N, et al. Immune Checkpoint Inhibition as Primary Adjuvant Therapy for an IDH1-Mutant Anaplastic Astrocytoma in a Patient With CMMRD: A Case Report-Usage of Immune Checkpoint Inhibition in CMMRD. *Curr Oncol* (2021) 28 (1):757–66. doi: 10.3390/curroncol28010074

44. AlHarbi M, Ali Mobark N, AlMubarak L, Aljelaify R, AlSaeed M, Almutairi A, et al. Durable Response to Nivolumab in a Pediatric Patient With Refractory Glioblastoma and Constitutional Biallelic Mismatch Repair Deficiency. *Oncologist* (2018) 23(12):1401–6. doi: 10.1634/theoncologist.2018-0163

45. Chen S, Zhou Y, Chen Y, Gu J. Fastp: An Ultra-Fast All-in-One FASTQ Preprocessor. *Bioinformatics* (2018) 34(17):i884–i90. doi: 10.1093/bioinformatics/bty560

46. Wang K, Li M, Hakonarson H. ANNOVAR: Functional Annotation of Genetic Variants From High-Throughput Sequencing Data. *Nucleic Acids Res* (2010) 38(16):e164. doi: 10.1093/nar/gkq603

47. Robinson JT, Thorvaldsdottir H, Winckler W, Guttman M, Lander ES, Getz G, et al. Integrative Genomics Viewer. *Nat Biotechnol* (2011) 29(1):24–6. doi: 10.1038/nbt.1754

48. Fantini D, Vidimar V, Yu Y, Condello S, Meeks JJ. MutSignatures: An R Package for Extraction and Analysis of Cancer Mutational Signatures. *Sci Rep* (2020) 10(1):18217. doi: 10.1038/s41598-020-75062-0

49. Krzywinski M, Schein J, Birol I, Connors J, Gascoyne R, Horsman D, et al. Circos: An Information Aesthetic for Comparative Genomics. *Genome Res* (2009) 19(9):1639–45. doi: 10.1101/gr.092759.109

Case Report: A rare case of familial lung cancer requiring pneumonectomy in three male siblings

Andrey Kaprin[1,2], Oleg Pikin[1], Andrey Ryabov[1],
Oleg Aleksandrov[1]*, Evgeniy Toneev[3], Ludmila Lubchenko[1]
and Ekaterina Zelenova[2]

[1]P.Herzen Moscow Oncology Research Institute (MORI), Moscow, Russia, [2]Peoples' Friendship
University of Russia, Moscow, Russia, [3]Ulyanovsk Oncology Center, Ulyanovsk, Russia

Lung cancer is a disease with a unique genetic pattern and is occasionally related to hereditary syndromes such as Lynch, Louis−Bar, and Li−Fraumeni. In some patients, germinal mutations may be discovered in combination with somatic alterations. For instance, Li−Fraumeni syndrome often reveals a mixture of *TP53* and *EGFR* mutations. The development of new target therapies necessitates an extensive search for new pathogenic mutations. In this article, we present a rare case report of lung cancer, requiring a pneumonectomy, in three sibling brothers.

KEYWORDS

lung cancer, familial cancer, genome sequencing, pneumonectomy, immunotherapy

Introduction

Lung cancer is a major socioeconomic threat to modern society and is recognized to play a significant role in morbidity and mortality, even in the most developed countries (1). One of the best-known risk factors is smoking, along with pollution.

In recent years, DNA profiling of malignant diseases has become increasingly popular and widely used in clinical practice. Investigation of pathological mutations may provide an accurate treatment plan, including target therapy, thus having been a cornerstone in modern oncology. Key mutations for lung cancer are *EGFR*, *BRAF*, and *KRAS* and alterations in *PDL-1*, *ALK*, and *ROS1* expression. The current clinical guidelines covering the appropriate administration of immunotherapy and tyrosine kinase inhibitors were devised with consideration of target gene mutations (2).

Germinal mutations are not as common in lung cancer as they are in other tumors, but they are more regularly accompanied with family history. It may be a part of the Lynch, Louis−Bar, or Li−Fraumeni syndromes (3). Given the connection with the latter,

germinal mutations in *p53* and *EGFR* are commonly diagnosed (4, 5). To elaborate an explicit and personalized management plan, it is imperative to consider all available options on an extended tumor board with the participation of a geneticist.

Case history

Three male patients, sibling brothers, were independently diagnosed with lung cancer in the left lung. Patient A (56 years old, the oldest one), patient B (63 years old), and patient C (58 years old) were assessed in 2008, 2016, and 2018, respectively. Each of them was referred to the Regional Cancer Centre in Ulyanovsk for further diagnosis and management.

Presentation

All patients were admitted with productive cough, associated with occasional bloody expectoration in patients A and B. They had neither significant comorbidities nor environmental or occupational hazards.

Objective findings

CT scan showed a peripheral 7-cm lesion of the left lower lobe in patient A, a perihilar lesion of the left upper lobe and a tumor with N1 lymph node involvement in patient B, and a centrally located lesion with hypermetabolism of para-aortic lymph nodes with an SUVmax of 7.34 in patient C (Figure 1). In all three cases, a preoperative endoscopic biopsy was performed, which revealed squamous cell carcinoma in patient A and lung adenocarcinoma in patients B and C.

Diagnosis and management

All patients successfully underwent left-sided pneumonectomy. To downstage the tumor in patient A and because of mediastinal lymph node involvement in patient C, neoadjuvant chemotherapy consisting of etoposide + cisplatin for four cycles was performed.

Postoperative histology showed pT4N0M0, G2, stage IIIa, in patient A; pT2bN1M0, stage IIb, in patient B; and pT2aN2M0, stage IIIa, in patient C. Patients B and C received adjuvant chemotherapy.

After the blood relationship between the patients was revealed, they were referred to a geneticist. Somatic mutations in *EGFR*, *BRAF*, *KRAS*, and *PIK3CA* genes were ordered first and showed no evidence of presence in any of them. Because of serious concerns about familial history, we evaluated the *CHEK2* gene, responsible for the development of different types of cancer, but no mutation was identified. After that, an analysis of microsatellite instability (MSI) was performed, provided by TrueMark MSI Assay (Applied Biosystems, USA) (Tables 1, 2).

Furthermore, in patient A, a complex molecular genetic testing was completed with the usage of a broad genetic panel: *APC*, *ATM*, *AXIN2*, *BARD1*, *BLM*, *BMPR1A*, *BRCA1*, *BRCA2*, *BRIP1*, *CDH1*, *CDKN2A*, *CHEK2*, *DICER1*, *EPCAM*, *GALNT12*, *GREM1*, *MEN1*, *MLH1*, *MLH3*, *MSH2*, *MSH3*, *MSH6*, *MUTYH*, *NBN*, *NF1*, *NTHL1*, *PALB2*, *PMS2*, *POLD1*, *POLE*, *PTCH1*, *PTCH2*, *PTEN*, *RAD51C*, *RAD51D*, *RET*, *SMAD4*, *STK11*, *SUFU*, *TP53*, *TSC1*, *TSC2*, *VHL*, and *WT1*. For the naming of
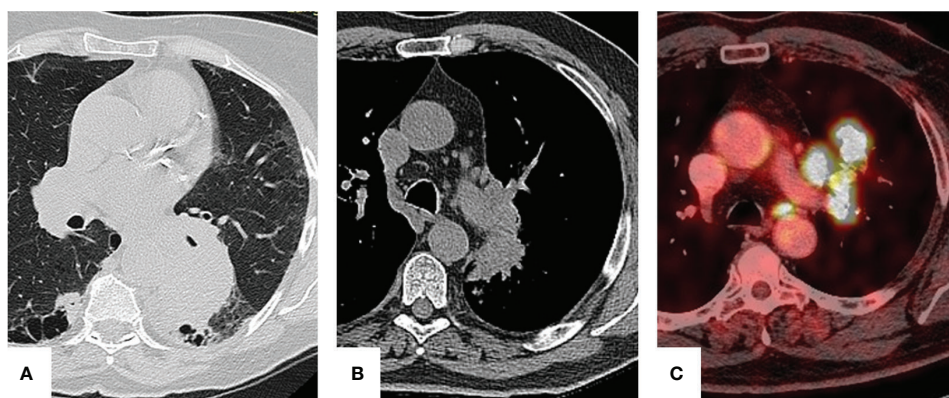
FIGURE 1
Preoperative imaging. Patient **A**: a 7-cm lesion is seen in the left lower lobe. Patient **B**: perihilar lesion with infiltration of bronchopulmonary lymph nodes. Patient **C**: para-aortic lymph node hypermetabolism.

TABLE 1   Results of activation mutations and MSI status.

Patient	EGFR	BRAF	KRAS	PIK3CA	CHEK2	MSI
A	–	–	–	–	Wt	–
B	Wt	Wt	Wt	Wt	Wt	MSI-high
C	Wt	Wt	Wt	Wt	Wt	MSI-high

the revealed variations, we utilized the nomenclature from http://varnomen.hgvs.org/.

Data processing was carried out with an automated algorithm, comprised of translation alignment of Genome Reference Consortium Human Build 38 (GRCh38), post-processing of alignment, and detection of variants and quality filter, along with the annotation of revealed variants of all known transcripts for each gene from RefSeq based on the usage of the pathogenic potential of substitution prediction (SIFT, PolyPhen2-HDIV, PolyPhen2-HVAR, MutationTaster, MetaSVM) and evolutionary conservative position calculations by PhyloP and PhastCons.

For an appraisal of population prevalence, we adopted samples from the Genome Aggregation Database (gnomAD), Exome Aggregation Consortium (ExAC), 1000 Genomes, and NHLBI Exome Sequencing Project (ESP6500). The classification of nucleotide sequence was accomplished according to a technical standard of next-generation sequencing (NGS), American College of Medical Genetics and Genomics (ACMG) (Table 3).

After amplification and extensive sequencing of lymphocyte's DNA, we revealed the germinal missense mutation NM_000264.5(PTCH1):c.3941C>T (p.Pro1314Leu, rs1400282737, COSM9550521) in a heterozygous state.

The mutation NM_000264.5(PTCH1):c.3941C>T in the gene *PTCH1* is registered in ClinVar and COSMIC databases as a pathologically relevant variant (score 1.00), associated with a high risk of different malignant tumors (Figure 2).

Discussion

According to GLOBOCAN (2021), lung cancer includes 11.6% of all malignant tumors worldwide and is associated with a large amount of 1-year lethality. Despite significant advances in treatment, it is still a remarkably fatal disease with an average rate of 48.4% of those who die within a year since diagnosis (1).

Genetics, environment, and length of affection may influence the possibility and timing of familial lung cancer cases. A meta-analysis, conducted by The International Lung Cancer Consortium (ILCCO) in 2021, revealed a 1.5-fold increased rate of lung cancer in relatives in the first degree (6). The same findings were shown by Cannon-Albright LA (2019) and Loiola de Alencar (2020), which even stated a two-fold increased rate (7, 8). Ang et al. (2020) appraised high-risk factors of lung cancer, such as Asian race compared to non-Asians, age below 50, smoking, and individuals whose two or more relatives are affected (7). This evidence entails a comprehensive study of

TABLE 2   MSI status associated with functional alteration of the mismatch repair system in patients B and C.

Locus	Chromosome	Instability
NR27	4q12	Stable
NR21	2q11.1	Unstable for C
NR24	14q11.2	Stable
BAT25	1p12	Stable
BAT26	7q34	Unstable for B and C
CAT25	11q24.2	Stable
BAT40	11q22.2	Unstable for B and C
NR22	1q42.3	Unstable for B and C
ABI-19	1q21.3	Stable
ABI-20B	17p12	Stable
ABI-17	17p13.2	Stable
ABI-16	2p21	Unstable for B and C
ABI-20A	12q24.13	Stable
TH01	11p15.5 (HID)	Match
PentaD	21q22.3 (HID)	Match

TABLE 3 Properties of the study.

Total sequences	818,529
Sequence length	2 × 150
Overall nucleotides	116,694,169
Mean coverage	251.8
Revealed variants	467
Variants after pathogenic criteria filtering	1

genetic factors to determine the optimal pathways for diagnosis, management, and subsequent follow-up.

At the present time, over 754 genes are correlated with lung cancer (8). To establish target genes, DNA diagnostics with polymerase chain reaction are widely implicated. More recently, modern approaches such as NGS have been introduced. The technology is used to determine the order of nucleotides in entire genomes or targeted regions of DNA.

The common pathway for DNA analysis in lung cancer is straightforward. In the case of adenocarcinoma (even in dimorphic combination with squamous cell carcinoma), a molecular genetic assay of *EGFR* mutations (18–21 exons), *BRAF*, *V600E*, *ALK*, and *ROS1* is recommended. For negative or unknown results, further investigation must be proceeded with *PDL-1* testing (2).

For a correct perception of the results and to deliberate the familial prepossession, a discussion with a geneticist is advocated. If a connection with one of the genetic syndromes is suspected, a comprehensive DNA testing must be performed.

The *PTCH1* gene encodes the patched homolog 1 protein. PTCH1, a 12-pass transmembrane protein, encompasses two large extracellular loops and two large intracellular loops. The PTCH1 protein is one of the membranous receptors involved in Hedgehog signaling (9). Hedgehog signaling is important for embryonic development and tumorigenesis.

PTCH1 is altered in 2.76% of non-small cell lung carcinoma patients with *PTCH1* mutation present in 2.56% of all non-small cell lung carcinoma patients (10). The available data on lung cancer features associated with *PTCH1* mutation are limited, and no previous study has focused on the long-term survival of these patients. However, it was found that patients with breast cancer and *PTCH1* mutation had more metastasis in the lungs and worse recurrence-free survival (11). The features of lung cancer associated with *PTCH1* mutation remain to be investigated. In view of the poor prognosis in patient A, a regular follow-up should be provided for life.

It is believed that one of the most important universal causes of cancer development is genomic instability. DNA mismatch repair deficiency leads to microsatellite instability and occurs in 15% of colorectal cancers, leading to the ineffectiveness of standard 5-fluorouracil-based chemotherapy (12).
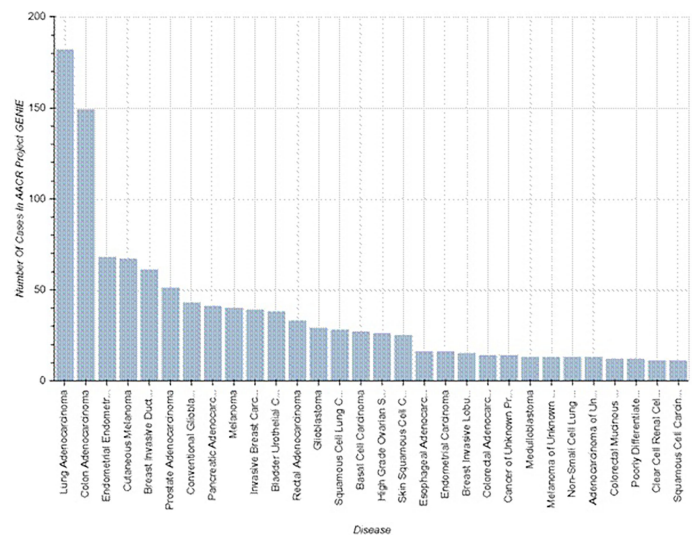
FIGURE 2
Known cases of malignancy associated with *PTCH1* mutations (https://www.mycancergenome.org/content/alteration/ptch1-mutation/).

The MSI-H rate in lung adenocarcinoma has been shown to be rare (0.8%) (13). Patients B and C had MSI-high status; therefore, nivolumab or pembrolizumab can be administered in case of progression.

Overall follow-up comprised 11 years for patient A, 5 years for patient B, and 2 years for patient C with no evidence of recurrence. In case of tumor progression, the thorough genetic testing performed in this study may facilitate the selection of an appropriate treatment option.

Conclusion

This rare observation of familial NSCLC indicates the necessity of a scrupulous analysis of genealogy and elaborate genetic testing. Genetic counseling is mandatory in patients with a familial history of malignancy and the usage of broad panels is advised.

Data availability statement

The original contributions presented in the study are included in the article/supplementary material. Further inquiries can be directed to the corresponding author.

Ethics statement

The studies involving human participants were reviewed and approved by the Hertsen Moscow Oncology Research Institute Ethics Committee (#039-B, 23.06.2022). The patients/participants provided their written informed consent to participate in this study. Written informed consent was obtained from the individual(s) for the publication of any potentially identifiable images or data included in this article.

Author contributions

Conflict of interest

The authors declare that the research was conducted in the absence of any commercial or financial relationships that could be construed as a potential conflict of interest.

Publisher's note

References

1. Sung H, Ferlay J, Siegel RL, Laversanne M, Soerjomataram I, Jemal A, et al. Global cancer statistics 2020: GLOBOCAN estimates of incidence and mortality worldwide for 36 cancers in 185 countries. *CA Cancer J Clin* (2021) 71:209–49. doi: 10.3322/caac.21660

2. Ettinger DS, Wood DE, Aisner DL, Akerley W, Bauman JR, Bharat A, et al. Non-small cell lung cancer, version 3.2022, NCCN clinical practice guidelines in oncology. *J Natl Compr Canc Netw* (2022) 20(5):497–530. doi: 10.6004/jnccn.2022.0025

3. Benusiglio PR, Fallet V, Sanchis-Borja M, Coulet F, Cadranel J. Lung cancer is also a hereditary disease. *Eur Respir Rev* (2021) 30(162):210045. doi: 10.1183/16000617.0045-2021

4. Barbosa MVR, Cordeiro de Lima VC, Formiga MN, Andrade de Paula CA, Torrezan GT, Carraro DM, et al. High prevalence of EGFR mutations in lung adenocarcinomas from Brazilian patients harboring the TP53 p.R337H variant. *Clin Lung Cancer* (2020) 21:e37–44. doi: 10.1016/j.cllc.2019.11.012

5. Mezquita L, Jové M, Nadal E, Kfoury M, Morán T, Ricordel C, et al. High prevalence of somatic oncogenic driver alterations in patients with NSCLC and Li-fraumeni syndrome. *J Thorac Oncol* (2020) 15:1232–9. doi: 10.1016/j.jtho.2020.03.005

6. Cotu ML, Liu M, Bonassi S, Neri M, Schwartz AG, Christiani DC, et al. Increased the risk of lung cancer in individuals with a family history of the disease: a pooled analysis from the international lung cancer consortium. *Eur J Cancer* (2012) 48:1957–68. doi: 10.1016/j.ejca.2012.01.038

7. Ang L, Chan C, Yau WP, Seow WJ. Association between family history of lung cancer and lung cancer risk: a systematic review and meta-analysis. *Lung Cancer* (2020) 148:129–37. doi: 10.1016/j.lungcan.2020.08.012

8. Wang CY, Chang YC, Kuo YL, Lee KT, Chen PS, Cheung CHA, et al. Common 5p15.33 and 6p21.33 variants influence lung cancer risk. *Nat Genet* (2008) 40(12):1407–9. doi: 10.1038/ng.273

9. Harvey MC, Fleet A, Okolowsky N, Hamel PA. Distinct effects of the mesenchymal dysplasia gene variant of murine patched-1 protein on canonical and non-canonical hedgehog signaling pathways. *J Biol Chem* (2014) 289 (15):10939–49. doi: 10.1074/jbc.M113.514844

10. The AACR Project GENIE Consortium. AACR project GENIE: powering precision medicine through an international consortium. *Cancer Discov* (2017) 7 (8):818–31. doi: 10.1158/2159-8290.CD-17-0151

11. Wang CY, Chang YC, Kuo YL, Lee KT, Chen PS, Cheung CHA, et al. Mutation of the PTCH1 gene predicts recurrence of breast cancer. *Sci Rep* (2019) 9:16359. doi: 10.1038/s41598-019-52617-4

12. Devaud N, Gallinger S. Chemotherapy of MMR-deficient colorectal cancer. *Fam Cancer* (2013) 12(2):301–6. doi: 10.1007/s10689-013-9633-z

13. Warth A, Körner S, Penzel R, Muley T, Dienemann H, Schirmacher P, et al. Microsatellite instability in pulmonary adenocarcinomas: a comprehensive study of 480 cases. *Virchows Arch* (2016) 468(3):313–9. doi: 10.1007/s00428-015-1892-7

Case report: Identification of a novel heterozygous germline *ERCC2* mutation in a patient with dermatofibrosarcoma protuberans

Qing Zhang[1]*, Yongzhi Ju[2,3,4], Xia You[2,3,4], Tingting Sun[2,3,4] and Yi Ding[5]

[1]Department of Orthopaedic Oncology, Beijing Ji Shui Tan Hospital, Peking University, Beijing, China, [2]The Medical Department, Jiangsu Simcere Diagnostics Co., Ltd, Nanjing, China, [3]The Medical Department, Nanjing Simcere Medical Laboratory Science Co.,Ltd, Nanjing, China, [4]The State Key Lab of Translational Medicine and Innovative Drug Development, Jiangsu Simcere Diagnostics Co., Ltd, Nanjing, China, [5]Department of Pathology, Beijing Ji Shui Tan Hospital, Peking University, Beijing, China

Dermatofibrosarcoma protuberans (DFSP) is a kind of soft tissue sarcoma, mostly occurs in the trunk, followed by proximal extremities and head and neck. Surgical resection is the most important treatment for DFSP, but the local recurrence rate of DFSP is high. Except reported specific chromosomal tran7slocations occurred in DFSP, the association between DNA repair gene mutations and DFSP still unknown. In this report we found a 19-year-old boy with DFSP carries a novel heterozygous germline *ERCC2* mutation, which belongs to the nucleotide excision repair (NER) pathway and genetic defects in *ERCC2* may contribute to the cancer susceptibility xeroderma pigmentosum (XP), Cocaine syndrome (CS), and trichothiodystrophy (TTD). Different mutations of the *ERCC2* gene can lead to diverse diseases, but there are no targeted therapies. In summary, our results enlarged the mutation spectrum of the DFSP patients. It also provides new insights into genetic counseling and targeted therapeutic strategies for patients with DFSP.

Introduction

There are more than 50 subtypes of soft tissue sarcomas, 30% of which are associated with specific genetic alterations, including translocations (1). Several studies have reported associations between cancer risk and DNA repair gene polymorphisms in the nucleotide excision repair (NER) pathway. NER involves more than 20 proteins, including xeroderma pigmentosum (XP) factors (group A to F) and cockayne syndrome (CS) factors (A and B), whose inactivation can cause xeroderma pigmentosum (XP) or Cockayne syndrome (CS) (2).

ERCC2 gene is a member of the nucleotide excision repair system (NER). *ERCC2* gene encodes xeroderma pigmentosum group D (XPD) protein, one of the subunits of the TFIIH complex, which plays an important role in nucleotide excision repair function and basic transcription (3). *ERCC2* gene mutations can lead to XP, CS, and trichothiodystrophy (TTD). XP is a hereditary disease, harbored heterozygous mutations in R638W and R616P of *ERCC2* which decreased helicase activity (3). Patients with XP are extremely sensitive to sunlight and have an increased risk of skin cancer (4, 5). More epidemiological studies have reported that *ERCC2* SNPs can increase the risk of skin cancer, lung cancer, breast cancer, ovarian cancer, and bladder cancer (6–8). *ERCC2* somatic mutation has a high incidence in bladder cancer, accounting for about 10%, and is related to chemotherapy response (9). Meanwhile, more studies have reported the importance of DNA damage repair gene mutation in predicting tumorigenesis and tumor treatment response.

Dermatofibrosarcoma protuberans is (DFSP) a rare cutaneous soft tissue sarcoma, accounting for approximately 1.8% of all soft tissue sarcomas and 0.1% of all tumors (10, 11). DFSP progress slowly, mostly showing skin-colored plaque. It expands slowly for months or years, and finally becomes a nodule, which is easy to be ignored in the early stage (12). The most common form of DFSP is adhesion to the dermis, but it can move freely to the deeper cortex, may also adhere to bone or fascia, and the tumor may fester or have pain (13, 14). Although about 85-90% of DFSPs are low-grade lesions, about 10-15% of DFSPs contain high-grade differentiated fibrosarcomatous, which is more likely to recurrence and metastasis (15, 16). Surgical resection is the most important treatment for DFSP, but the local recurrence rate of DFSP is high, and it less metastasizes to the distal end.

In this case, we found a heterozygous germline mutation *ERCC2* c.105+1 G > C may be related to the occurrence of DFSP.

Case presentation

A 19-year-old boy had pain in his right toe during exercise in 2020. No bone destruction was found, and the pain was gradually relieved. The tubercle in the right toe proximal dorsal was found in June 2021 but without any treatments. In December 2021, due to the influence of enlarged nodules on wearing shoes, he went to the local hospital and underwent unplanned resection of the inner mass of the right back. The pathological examination was DFSP (Figure 1). The tumor is about 2×1cm, it was tough, tender, movable, had a clear boundary, and did not adhere to the deep tissue. PET/CT was performed in January 2022, and no distal organ or lymphatic metastasis was found (Figure 2). However, the patient's local subcutaneous soft tissue thickening and small nodules have increased metabolic activity, which may be considered a possible postoperative residual or recurrence. At the same time, next gene sequencing (NGS) was performed on tissue and blood samples.

The 551-gene NGS panel revealed a novel heterozygous germline *ERCC2* c.105+1 G > C mutation. This variation has never been reported in any database or any publications, such as the Exome Aggregation Consortium and 1000 Genomes Project. The variant is predicted to be pathogenic by MutationTaster and dbscSNV, which are used for functional prediction of splice variants. The splice-site variant in *ERCC2* (c.105+1 G > C) destroys a canonical splice donor site in intron 2, which may leading to an abnormal splicing of mRNA and affect its function (Figure 3). Loss-of-function variants in *ERCC2* are known to be pathogenic (3, 17–19). The ClinVar database records that the downstream *ERCC2*:c.594+2_594+5del is pathogenic/likely pathogenic. Based on the above analysis, we classified the variant as (likely) pathogenic according to the criteria of the American College of Medical Genetics and Genomics (ACMG).

In April 2022, sanger sequencing of blood samples from the patient's parents was carried out for family verification. The father's diagnosis of polyliposarcoma also harbored this mutation, while variations were not detected in the unaffected mother (Figure 4).

Discussion

Soft tissue sarcomas represent a heterogeneous group of rare tumors, 30% of which are associated with simple genetic alterations, including specific translocations. Studies have demonstrated that DNA repair plays a vital role in genomic maintenance to prevent carcinogenesis. *ERCC2* encodes the XPD protein, which is part of the TFIIH complex, has ATP-dependent DNA helicase activity, and belongs to the RAD3/XPD subfamily of helicases. *ERCC2* plays an important role in gene transcription and gene transcription-coupled nucleotide excision repair (20). Genetic defects in *ERCC2* may contribute to the cancer susceptibility XP, CS, and TTD.

XP patients are particularly sensitive to light, the risk of cutaneous tumors in sun-exposed areas of the body is 1000 fold that of normal individuals. The deficient NER system of XP patients cannot repair the UV damage, resulting in specific
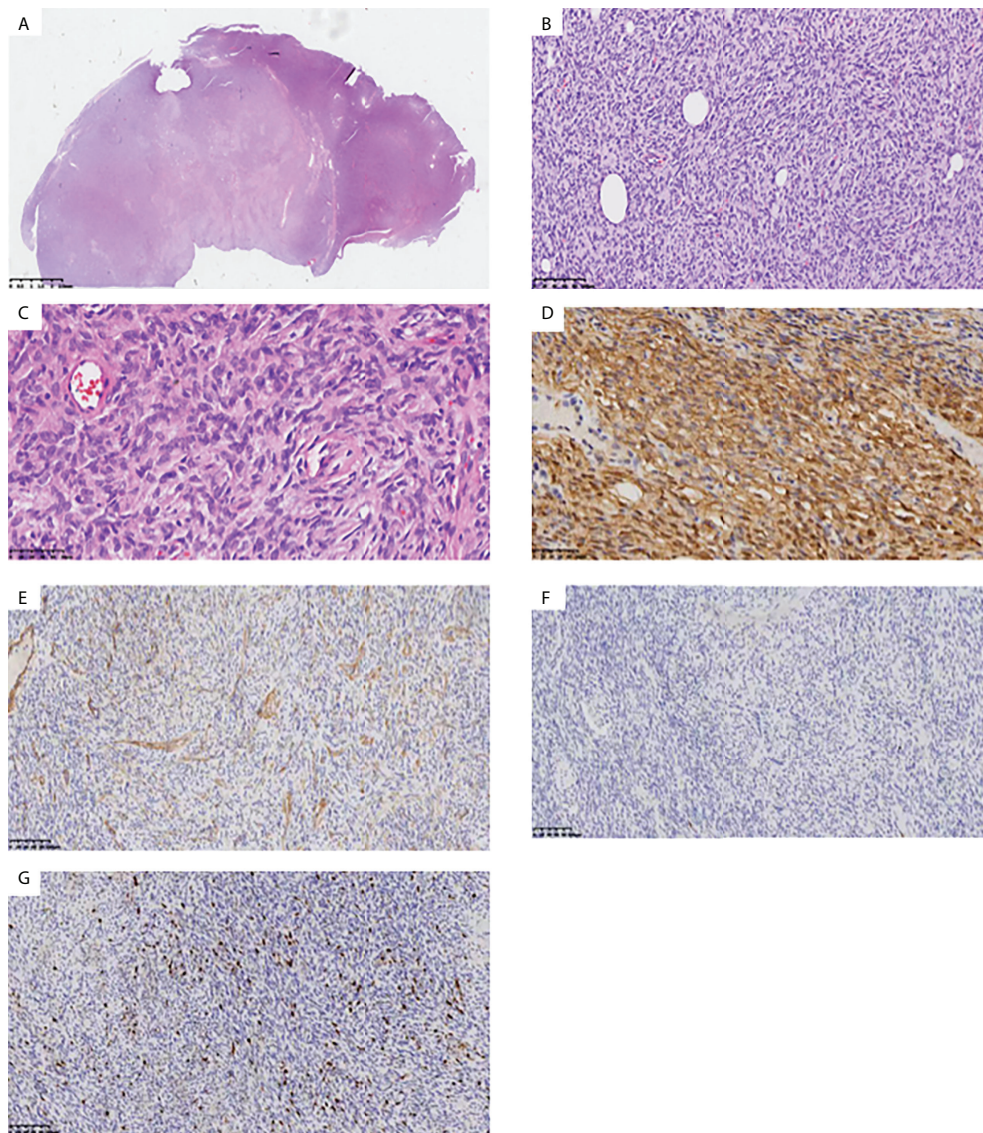
FIGURE 1

Histopathologic stains from the inner mass of the right back. HE staining results suggested spindle cell tumor. Low-power **(A)**, medium-power **(B)**, and high-power **(C)** view demonstrating a partially encapsulated nodular mass without dermal connection. Immunohistochemistry results suggested dermatofibrosarcoma protuberans: CD34 (+) **(D)**, SMA (-) **(E)**, S100 (-) **(F)**, Ki67+ 5-10% **(G)**.

mutations accumulation in key regulatory genes in the skin, eye, ocular, and oral cells (21). Different mutations of the *ERCC2* gene can lead to diverse diseases, but there are no targeted therapies. With the increasing number of defects in genes regulating double-strand break (DSB) repair/homologous recombination (HR), such as *BRCA1/2* and mismatch repair (MMR) genes, other NER genes related to cancer pathogenesis, diagnosis, and treatment are also receiving increasing attention (22). There are *in vitro* experiments and case reports showing that the combination of different drugs with platinum-based chemotherapy (such as carboplatin and gemcitabine, irofulven,

and cisplatin) can significantly improve the efficacy of patients with *ERCC2* mutations (22, 23). More studies are now exploring the association of platinum-based chemotherapy sensitivity with *ERCC2* mutations, which may be a potential therapeutic target.

In our case, the splice-site variant in *ERCC2* c.105+1 G > C identified in a young DFSP patient as well as his father who was diagnosis of polyliposarcoma. This variant was absent from all public DNA sequence databases. Previously reported mutations in the human *ERCC2* are mainly single residue changes and sometimes at adjacent which could case strikingly different genetic disorders, meanwhile, proved mutations in G47R
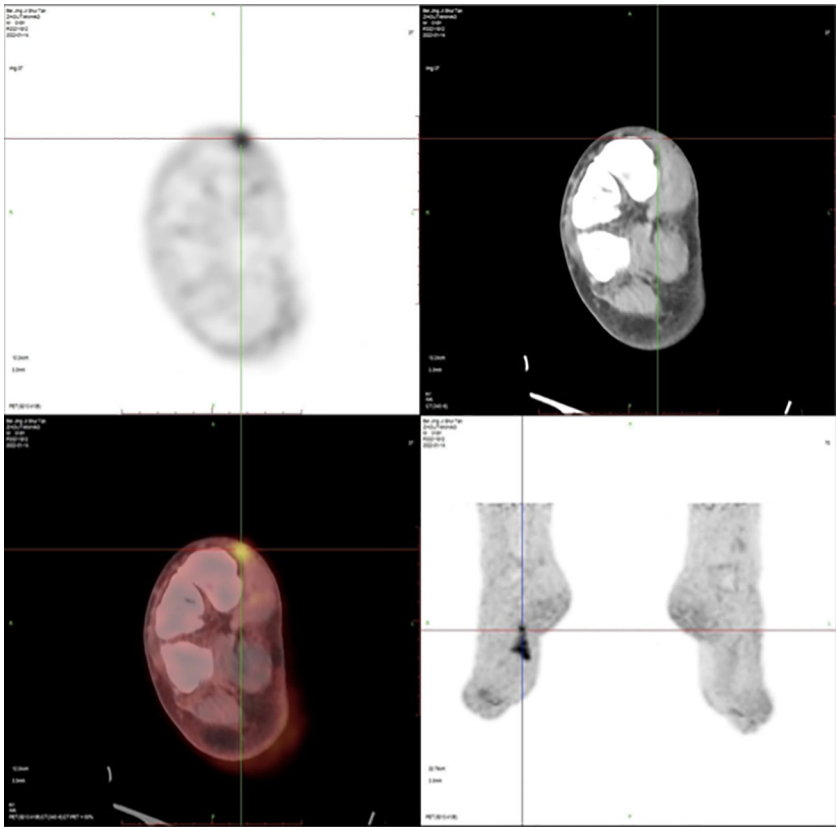
FIGURE 2
Positron emission tomography/computed tomography (PET/CT) imaging after unplanned resection of DFSP showed an increased radioactive uptake (SUVmax = 5.2) of soft tissue density as well as small nodules in the local subcutaneous soft tissue and have increased metabolic activity.
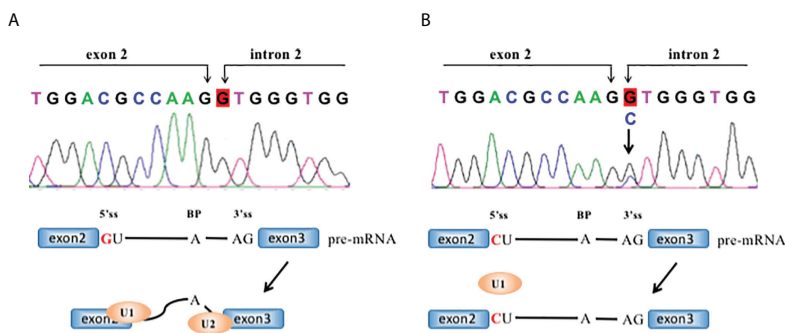
FIGURE 3
The *ERCC2* intron2 c.105+1 G>C mutation and its effect in RNA splicing. RNA splicing of wild-type **(A, B)** mutant *ERCC2*. Each intron has guanine and uracil (GU) at the 5′-end and adenine and guanine (AG) at the 3′-end. 5′ss: 5′ splice site; 3′ ss: 3′ splice site; BP, branch site.

(located in HD1 helicase motifI), T76A, D234N, G602D, and R683W showed greatly reduced helicase activity (24). Therefore, we can only study the significance of the mutation by itself. In principle, the RNA splicing process is tightly regulated, and may be dependent in part on whether the donor or acceptor site is affected. Aberrant RNA splicing is closely related to tumor development, growth, and progression to therapy-resistant tumors (25, 26). For example, a heterozygous splice-site
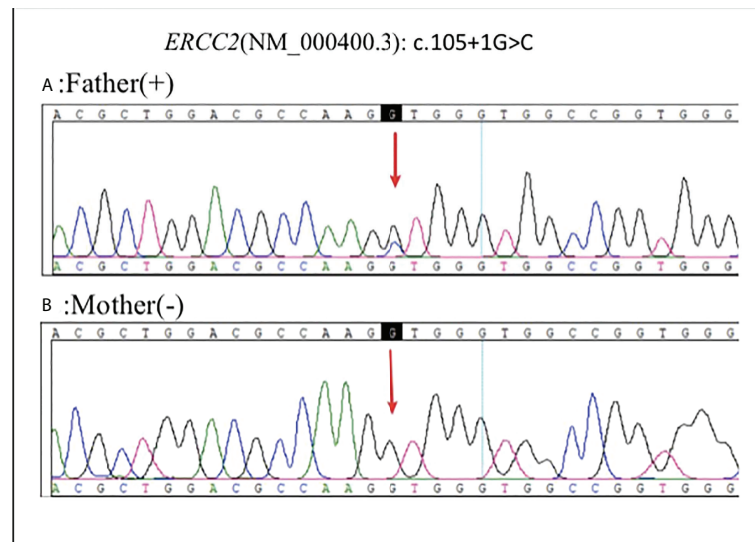
mutation (c.619+1 G > C) at the 5' end of intron 6 in *WDR77* is present in familial papillary thyroid cancers (27). The mutation caused exon 6 skipping, consequently leading to a frameshift and creating a premature stop codon for the new reading frame. It resulted in a shorter transcript and was only observed at very low levels, suggesting that the mutation triggers the nonsense-mediated messenger RNA (mRNA) decay (NMD) process. Splice-site mutation of *FLCN* in the 5' end of intron 9 (c.1062+1 G > A) causing partial retention of intron, which was associated with Birt-Hogg-Dubé syndrome (28). A family with hereditary multiple osteochondroma (HMO) from Guangxi Province, China, harbored the pathogenic heterozygous c.1056+1 G > A mutation of *EXT1* (29). These studies suggest that guanine (G) mutation at the exon-intron junction was a very important event. In our case, the heterozygous c.105+1 G > C mutation destroys a canonical splice donor site in intron 2, which are most likely to cause changes in its function.

In summary, we identified a novel germline *ERCC2* mutation in a patient with DFSP. Our results enlarged the mutation spectrum of the DFSP patients. It also provides new insights into genetic counseling and targeted therapeutic strategies for patients with DFSP.

Data availability statement

The original contributions presented in the study are included in the article/supplementary material. Further inquiries can be directed to the corresponding author.

Ethics statement

Written informed consent was obtained from the individual(s) for the publication of any potentially identifiable images or data included in this article.

Author contributions

YJ and XY prepared the manuscript and the literature search. TS reviewed and edited the manuscript. QZ treated and observed the patient. YD performed the histopathological and immunohistochemical examinations. All authors contributed to the article and approved the submitted version.

Conflict of interest

Authors YJ, XY, and TS were employed by Jiangsu Simcere Diagnostics Co., Ltd and Nanjing Simcere Medical Laboratory Science Co., Ltd.

The remaining authors declare that the research was conducted in the absence of any commercial or financial relationships that could be construed as a potential conflict of interest.

Publisher's note

All claims expressed in this article are solely those of the authors and do not necessarily represent those of their affiliated organizations, or those of the publisher, the editors and the reviewers. Any product that may be evaluated in this article, or claim that may be made by its manufacturer, is not guaranteed or endorsed by the publisher.

References

1. Sbaraglia M, Bellan E. Dei tos a P.The 2020 WHO classification of soft tissue tumours: news and perspectives. *Pathologica* (2021) 113(2):70–84. doi: 10.32074/1591-951X-213

2. Le Morvan V, Longy M, Bonaïti-Pellié C, Bui B, Houédé N, Coindre JM, et al. Genetic polymorphisms of the XPG and XPD nucleotide excision repair genes in sarcoma patients. *Int J Cancer* (2006) 119(7):1732–5. doi: 10.1002/ijc.22009

3. Taylor EM, Broughton BC, Botta E, Stefanini M, Sarasin A, Jaspers NG, et al. Xeroderma pigmentosum and trichothiodystrophy are associated with different mutations in the XPD (*ERCC2*) repair/transcription gene. *Proc Natl Acad Sci U S A* (1997) 94(16):8658–63. doi: 10.1073/pnas.94.16.8658

4. Marteijn JA, Lans H, Vermeulen W, Hoeijmakers JHJ. Understanding nucleotide excision repair and its roles in cancer and ageing. *Nat Rev Mol Cell Biol* (2014) 15(7):465–81. doi: 10.1038/nrm3822

5. Lehmann J, Schubert S, Emmert S. Xeroderma pigmentosum: diagnostic procedures, interdisciplinary patient care, and novel therapeutic approaches. *J Dtsch Dermatol Ges* (2014) 12(10):867–72. doi: 10.1111/ddg.12419

6. Benhamou S, Sarasin A. *ERCC2*/XPD gene polymorphisms and cancer risk. *Mutagenesis* (2002) 17(6):463–9. doi: 10.1093/mutage/17.6.463

7. Stern MC, Lin J, Figueroa JD, Kelsey KT, Kiltie AE, Yuan JM, et al. Polymorphisms in DNA repair genes, smoking, and bladder cancer risk: findings from the international consortium of bladder cancer. *Cancer Res* (2009) 69(17):6857–64. doi: 10.1158/0008-5472.CAN-09-1091

8. Simone M, Daunia V, Donato N. DNA Repair gene polymorphisms and risk of cutaneous melanoma: A systematic review and meta-analysis. *Carcinogenesis* (2009) 30(10):1735–43. doi: 10.1093/carcin/bgp207

9. Van Allen EM, Mouw KW, Kim P, Iyer G, Wagle N, Al-Ahmadie H, et al. Somatic *ERCC2* mutations correlate with cisplatin sensitivity in muscle-invasive urothelial carcinoma. *Cancer Discovery* (2014) 4(10):1140–53. doi: 10.1158/2159-8290.CD-14-0623

10. Chang CK, Jacobs IA, Salti GI. Outcomes of surgery for dermatofibrosarcoma protuberans. *Eur J Surg Oncol* (2004) 30(3):341–5. doi: 10.1016/j.ejso.2003.12.005

11. Bowne WB, Antonescu CR, Leung DH, Katz SC, Hawkins WG, Woodruff JM, et al. Dermatofibrosarcoma protuberans: A clinicopathologic analysis of patients treated and followed at a single institution. *Cancer* (2000) 88(12):2711–20. doi: 10.1002/1097-0142(20000615)88:12<2711::aid-cncr9>3.0.co;2-m

12. Bogucki B, Neuhaus I, Hurst EA. Dermatofibrosarcoma protuberans: a review of the literature. *Dermatol Surg* (2012) 38(4):537–51. doi: 10.1111/j.1524-4725.2011.02292.x

13. Gloster JrHM. Dermatofibrosarcoma protuberans. *J Am Acad Dermatol* (1996) 35(3 Pt 1):355–74. doi: 10.1016/s0190-9622(96)90597-6

14. Taylor HB, Helwig EB. Dermatofibrosarcoma protuberans. a study of 115 cases. *Cancer* (1962) 15:717–25. doi: 10.1002/1097-0142(196207/08)15:4<717::aid-cncr2820150405>3.0.co;2-2

15. Abbott JJ, Oliveira AM, Nascimento AG. The prognostic significance of fibrosarcomatous transformation in dermatofibrosarcoma protuberans. *Am J Surg Pathol* (2006) 30(4):436–43. doi: 10.1097/00000478-200604000-00002

16. Mentzel T, Beham A, Katenkamp D, Dei Tos AP, Fletcher CD. Fibrosarcomatous ("high-grade") dermatofibrosarcoma protuberans: clinicopathologic and immunohistochemical study of a series of 41 cases with emphasis on prognostic significance. *Am J Surg Pathol* (1998) 22(5):576–87. doi: 10.1097/00000478-199805000-00009

17. Bergmann E, Egly JM. Trichothiodystrophy, a transcription syndrome. *Trends Genet* (2001) 17(5):279–86. doi: 10.1016/s0168-9525(01)02280-6

18. Botta E, Nardo T, Orioli D, Guglielmino R, Ricotti R, Bondanza S, et al. Genotype–phenotype relationships in trichothiodystrophy patients with novel splicing mutations in the XPD gene. *Hum Mutat* (2009) 30(3):438–45. doi: 10.1002/humu.20912

19. Ueda T, Compe E, Catez P, Kraemer KH, Egly JM. Both XPD alleles contribute to the phenotype of compound heterozygote xeroderma pigmentosum patients. *J Exp Med* (2009) 206(13):3031–46. doi: 10.1084/jem.20091892

20. Schaeffer L, Moncollin V, Roy R, Staub A, Mezzina M, Sarasin A, et al. The *ERCC2*/DNA repair protein is associated with the class II BTF2/TFIIH transcription factor. *EMBO J* (1994) 13(10):2388–92. doi: 10.1002/j.1460-2075.1994.tb06522.x

21. Lehmann AR, McGibbon D, Stefanini M. Xeroderma pigmentosum. *Orphanet J Rare Dis* (2011) 6:70. doi: 10.1186/1750-1172-6-70

22. Topka S, Steinsnyder Z, Ravichandran V, Tkachuk K, Kemel Y, Bandlamudi C, et al. Targeting germline- and tumor-associated nucleotide excision repair defects in cancer. *Clin Cancer Res* (2021) 27(7):1997–2010. doi: 10.1158/1078-0432.CCR-20-3322

23. Hirotsu Y, Yokoyama H, Amemiya K, Hagimoto T, Hosaka K, Oyama T, et al. Genomic profiling identified *ERCC2* E606Q mutation in helicase domain respond to platinum-based neoadjuvant therapy in urothelial bladder cancer. *Front Oncol* (2020) 10:1643. doi: 10.3389/fonc.2020.01643

24. Fan L, Fuss JO, Cheng QJ, Arvai AS, Hammel M, Roberts VA, et al. XPD helicase structures and activities: Insights into the cancer and aging phenotypes from XPD mutations. *Cell* (2008) 133:789–800. doi: 10.1016/j.cell.2008.04.030

25. Wang E, Aifantis I. RNA Splicing and cancer. *Trends Cancer* (2020) 6:631–44. doi: 10.1016/j.trecan.2020.04.011

26. Dong X, Chen R. Understanding aberrant RNA splicing to facilitate cancer diagnosis and therapy. *Oncogene* (2020) 39:2231–42. doi: 10.1038/s41388-019-1138-2

27. Zhao Y, Yu T, Sun J, Wang F, Cheng C, He S, et al. Germ-line mutations in WDR77 predispose to familial papillary thyroid cancer. *Proc Natl Acad Sci USA* (2021) 118(31):e2026327118. doi: 10.1073/pnas.2026327118

28. Furuya M, Kobayashi H, Baba M, Ito T, Tanaka R, Nakatani Y. Splice-site mutation causing partial retention of intron in the FLCN gene in birt-Hogg-Dubé syndrome: A case report. *BMC Med Genomics* (2018) 11(1):42. doi: 10.1186/s12920-018-0359-5

29. Yuan G, Su Q, Liao W, Hou W, Huang L, Wang P, et al. Mutational analysis of *EXT1* in a Chinese family affected by hereditary multiple osteochondroma. *BioMed Res Int* (2021) 2021:8888948. doi: 10.1155/2021/8888948

Check for updates

Congenital midline spinal hamartoma in an infant with DICER1 syndrome: A case report

Rawan Hammad[1,2]*, Winnie Lo[3], Haiying Chen[3],
Manohar Shroff[4], David Malkin[1],
Anita Villani[1] and Avram Denburg[1]

[1]Division of Pediatric Hematology and Oncology, The Hospital for Sick Children, Toronto, ON,
Canada, [2]Division of Hematology, Faculty of Medicine, King Abdulaziz University, Jeddah, Saudi
Arabia, [3]Department of Pediatric Laboratory Medicine, The Hospital for Sick Children, Toronto, ON,
Canada, [4]Department of Diagnostic Imaging, The Hospital for Sick Children, Toronto, ON, Canada

Congenital spinal hamartomas are rare benign tumors. They are mostly seen in infants and are typically asymptomatic at presentation. Spinal hamartomas have not been associated with any known cancer predisposition syndrome. DICER1 syndrome is a well-characterized cancer predisposition syndrome caused by a germline mutation in the *DICER1* gene, which shows variable expressivity. To our knowledge, spinal hamartoma has never been described in individuals with DICER1 syndrome. Here, we describe a rare association of congenital spinal hamartoma and DICER1 syndrome in a 5-week-old infant, with molecular findings suggestive of the implication of *DICER1* in the pathogenesis of this tumor.

KEYWORDS

congenital midline spinal hamartoma, DICER1, infant, case report, cancer predisposition

Introduction

Congenital midline spinal hamartomas are a rare but increasingly well-described clinical entity. They are benign tumors, characterized by a well-differentiated and mature overgrowth of local ectodermal and mesodermal elements, present in a disorganized manner (1). Spinal hamartomas typically present in infants and have been associated with skin dimples, cutaneous angiomata, subcutaneous masses or intact overlying skin. At presentation, most patients with spinal hamartomas are neurologically intact with no significant signs of spinal cord compression (2). Hamartomas have been described in patients with spinal dysraphism (3) and in most cases are not associated with any other congenital malformations or cancer predisposition syndromes.

DICER1 syndrome (OMIM #601200) is a rare tumor predisposition syndrome, with tendency to develop a wide range of benign and malignant tumors beginning in childhood and continuing into adulthood. DICER1 syndrome is caused by a germline pathogenic variant in the tumor suppressor gene, *DICER1* (4). Typical DICER1-associated tumors include pleuropulmonary blastoma, cystic

nephroma, nasal chondromesenchymal hamartoma (NCMH), thyroid nodules, and ovarian Sertoli-Leydig cell tumor (5). Central nervous system (CNS) manifestations of DICER1 syndrome include pituitary blastoma, pineoblastoma, ciliary body medulloepithelioma, Embryonal tumor with multilayered rosettes (ETMR)-like infantile cerebellar tumor and primary DICER1 CNS-sarcoma (6). To our knowledge, spinal hamartomas have never been described in patients with DICER1 syndrome.

Herein, we present the case of a 5-week-old infant with an extremely atypical presentation of congenital midline spinal hamartoma of the cervical spine, who was found to harbor a pathogenic germline *DICER1* variant and a second somatic hit in the spinal hamartoma.

Case presentation

A 5-week-old full-term female infant presented with progressive bilateral upper limb weakness and diminished spontaneous movements beginning at the age of 1 week. Her perinatal history was unremarkable, with no history of traumatic delivery and a normal physical exam at birth. At presentation, there was bilateral upper limb flaccid hypotonia on the right more than the left, absent grasp reflex in both hands, absent bilateral upper limb deep tendon reflexes and loss of upper limb sensation bilaterally. Magnetic resonance imaging (MRI) of the brain and spine revealed a cervical spine extramedullary lesion extending from C2-C6 with extension through several neuronal foramina on the right (Figure 1) and severe compression of the spinal cord.

Based on her age and radiographic features, neuroblastoma with cord compression was suspected. Staging Computed tomography (CT) of the neck, chest abdomen and pelvis were unremarkable. Her urine catecholamines (HVA and VMA) were both within normal limits on two occasions. She received a single cycle of carboplatin and etoposide as well as dexamethasone on an emergent basis. The patient continued to demonstrate symptomatic cord compression, so a decision was made to undergo surgical resection of the lesion to protect her cord from ongoing damage and obtain a histologic diagnosis.
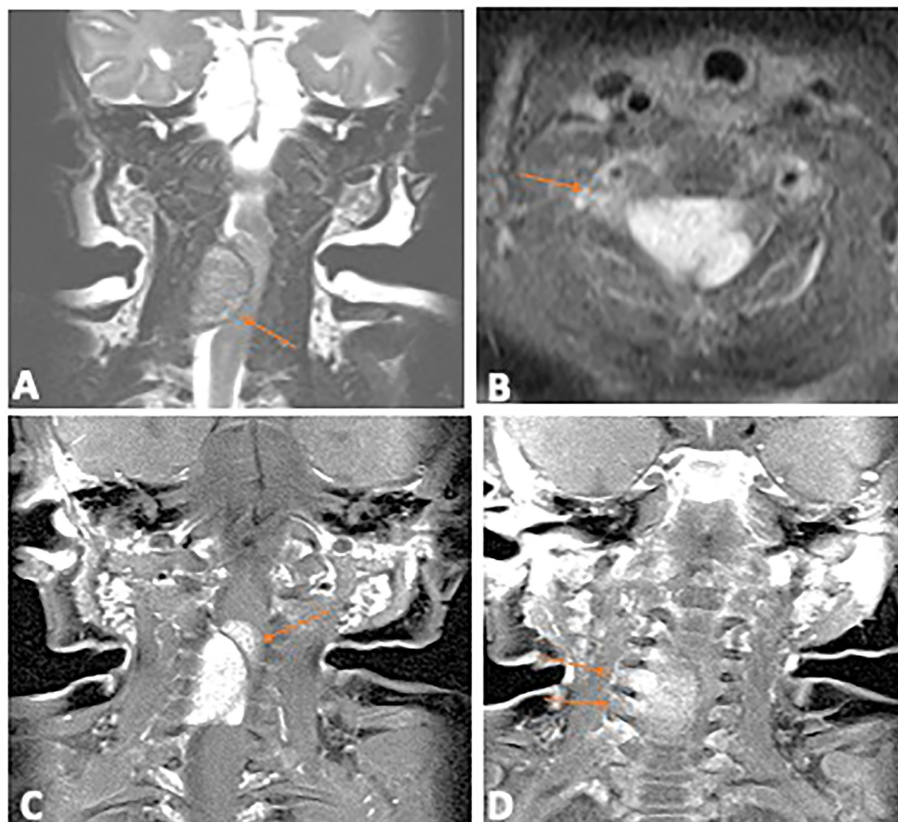
FIGURE 1
Diagnostic Magnetic Resonance Imaging of the primary spinal hamartoma. **(A)** Coronal T2 image of the cervical spine shows an intraspinal extramedullary mass (arrow) which is iso to hypointense, compressing the cord. **(B)** Contrast enhanced axial T1 image with fat saturation showing the enhancing intraspinal mass (arrow); **(C)** Coronal contrast enhanced T1 image with fat saturation showing the lobulated intraspinal component (arrow) which infiltrated into the cord. **(D)** Coronal contrast enhanced T1 image, arrows show extension through multiple neural foramina on the right.

Intra-operatively, a well circumscribed cartilaginous tumor was identified on the right side of the dura. A gross total resection of the extradural component was achieved and a small intradural residual tumor was left as it was adherent to the nerve root. Pathologic examination revealed a benign lesion with similar features in the intraspinal, extradural and intradural components. The lesion showed anastomosing islands of hyaline cartilage with loose fibrous stroma (including nerve-like tissue) in between (Figures 2A, B). Immunohistochemistry (IHC) stains of the nerve-like tissue were positive for neurofilament and S100, consistent with nerve differentiation (Figures 2C, D). IHC stains for glial fibrillary acidic protein (GFAP), pan-cytokeratin and desmin were negative. Overall, the features favor a diagnosis of spinal hamartoma.

Postoperatively, the patient developed respiratory failure secondary to accessory muscle weakness requiring ventilation and eventually a tracheostomy. Post-operative MRI showed two areas of extradural enhancement in the right aspect of the spinal canal suggestive of residual tumor.

Her family history revealed non-consanguineous parents of European descent. The mother had developed thyroid nodules at age 16 years and an ovarian Sertoli-Leydig cell tumor which was diagnosed and resected at age 30 years, following the diagnosis of our patient's spinal hamartoma. There was no other family history of cancers or cancer predisposition in the family.

The evolution of this family's cancer history prompted further evaluation. A salivary sample was obtained from the mother for germline *DICER1* sequencing using an external *DICER1* DNA sequencing panel (Prevention Genetics, Marshfield, WI). Results revealed a heterozygous pathogenic variant in the *DICER1* gene designated c.3118_3119insCA (p.IIe1040Thrfs*27), which is predicted to result in a frameshift and premature translational stop site, expected to result in an absent or disrupted protein product. This variant was reported as pathogenic given its predicted functional consequence and has not been previously reported in the literature nor in population controls (gnomAD). There was no tumor specimen available from the mother for sequencing.

Following the mother's confirmed germline *DICER1* finding, the patient was enrolled in our institutional precision oncology program KiCS (SickKids Cancer Sequencing) Program, through which germline and tumor samples were sequenced using a clinically validated DNA cancer sequencing panel (supplementary material). The same heterozygous germline frameshift variant in the *DICER1* gene was detected in the patient who at that point was 3 years of age.

Sequence analysis of the patient's tumor revealed a second missense variant in the *DICER1* gene, namely, c.5113G>A (p.Glu1705Lys). This is a somatic hot spot variant and is frequently identified somatically in DICER1 associated tumors such as Sertoli–Leydig cell tumor and pleuropulmonary blastoma (7, 8). Somatic hot spot missense variants in *DICER1*
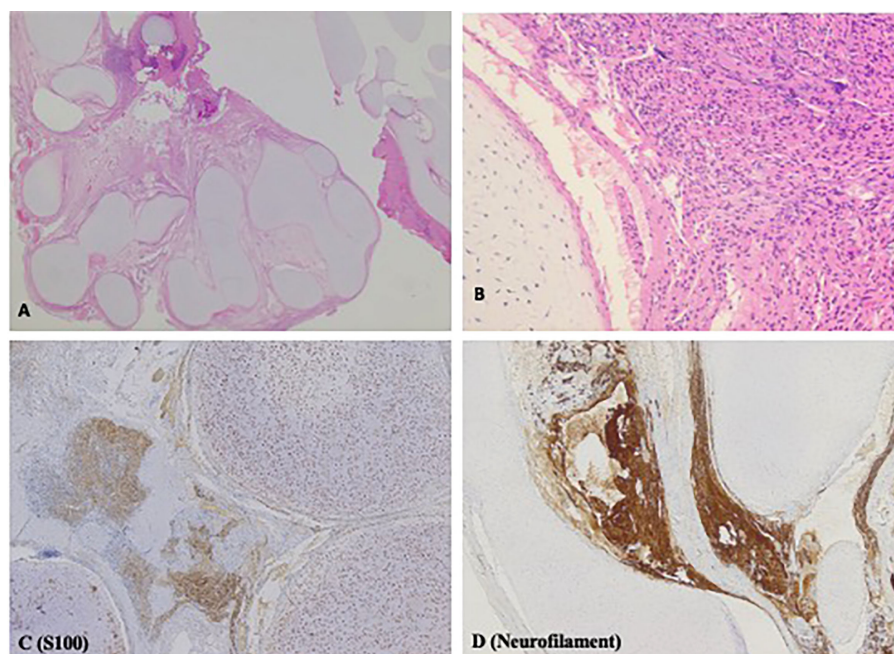
FIGURE 2
H&E and Immunohistochemistry (IHC) stains displaying histopathologic features of spinal hamartoma. **(A)** H&E stain; original magnification x12.5. Irregular lobules of hyaline cartilage, with loose fibrous stroma in between. Irregular nerve-like tissue is found in the loose fibrous stroma **(B)** H&E stain; original magnification x200. High power view of the cartilage and nerve-like tissue. **(C)** IHC stain for S100; original magnification x 50. Both the cartilage and the nerve-like tissue are positive for S100. **(D)** IHC stain for neurofilament; original magnification x50. The nerve-like tissue is positive for neurofilament.

are clustered in the RNase IIIb domain and functional studies have shown that they lead to defective cleavage of 5p-derived miRNAs from the pre-miRNA loop sequence and results in the retention of the pre-miRNA loop sequence in *DICER1* mutant cancers (8). This was detected at a variant allele frequency (VAF) of 41.56%. No other gene variants were detected in the tumor. The tumor mutational burden was 0.33 mutations/Mb and copy number analysis showed a stable genome.

At her last follow up, at the age of four years, the patient remained tracheostomy-dependent but had shown marked interval improvement in her limb function. Serial surveillance MRIs of the spine showed stable residual with no signs of recurrence. Ongoing Surveillance with 6 monthly abdominal/ pelvic ultrasound and chest X-ray and annual ophthalmologic assessment has not revealed any other DICER1-associated manifestations to date (9) (Figure 3).

Discussion

In this report, we describe the first case of congenital midline spinal hamartoma in an infant with a germline *DICER1* pathogenic variant, an association not previously reported in the literature. The presence of a second somatic hotspot missense *DICER1* variant provides evidence that this tumor is a DICER-1 syndrome related manifestation in this patient.

DICER1 syndrome was first described by Priest et al. when several family members of children with pleuropulmonary blastema (PPB) were noted to develop other neoplasms (10). *DICER1* germline pathogenic variants were subsequently identified as an inciting genetic event in the development of this syndrome when families with PPB underwent germline DNA sequencing (11). Since the *DICER1* gene discovery, the list of associated benign and malignant neoplasms continues to expand (9). NCMH was the first and remains the most commonly reported type of hamartoma linked to *DICER1* syndrome (5). In 2014, Stewart et al. established the association in a case series in which 6/8 evaluable patients with PPB and NCMH were found to harbor a germline *DICER1* mutation; two of these were found to have an acquired somatic *DICER1* mutation (12). Further studies supported the association, and NCMH is now a well-established *DICER1*-associated tumor (5, 13, 14). Recently, Apellaniz-Ruiz described two patients with DICER1 syndrome and mesenchymal hamartoma of the liver (MHL). These authors hypothesized the direct implication of the *DICER1* gene in the
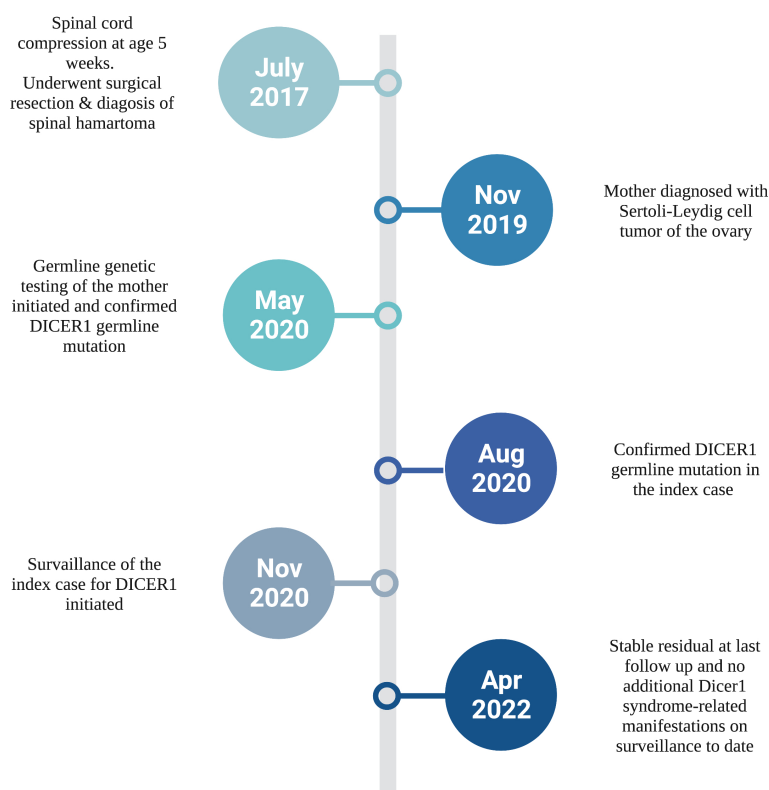
FIGURE 3
Diagnostic timeline of our infant with congenital spinal hamartoma and DICER1 Syndrome. Created with BioRender.com.

pathogenesis of MHL, through dysregulation of miRNA expression, suggesting that MHL is a DICER1 phenotype (15). This variety of tumors supports the variable expressivity observed in DICER1 syndrome and indicates the possibility of further expansion of DICER1 associated neoplasms.

Our patient developed a congenital spinal hamartoma, which is an extremely rare benign, but locally aggressive, tumor of infancy and childhood. Intracranial hamartomas are commonly associated with neurofibromatosis type 1, consisting of neural-crest derived neurons, glial cells and Schwann cells (16). Congenital midline spinal hamartomas differ histopathologically as they are composed of mature native tissue which is present in a disordered manner (1). It was first reported as a distinct entity by Tibbs et al. in 1976, where the clinicopathologic characteristics of five infants with spinal hamartoma was described. The initial description noted the histologic distinctive features from teratomas, namely the presence of mesodermal elements, the well differentiated tissue and lack of malignant transformation in the former (17). The definition of spinal hamartomas was later refined to the presence of disorganized mature local tissue (1, 18). Since its early description, only a few case series and case reports have been reported in the literature, with the majority describing it as an asymptomatic, benign lesion lacking the potential for malignant transformation (2, 3, 19, 20). The pathogenesis of these hamartomas is unknown and has not been molecularly characterized.

DICER1 is a tumor suppressor gene which encodes an RNase III-family endonuclease responsible for cleavage of precursor microRNA into active miRNA (21). Tumorigenesis in DICER1 syndrome is typically caused by a loss of function germline variant and a second somatic missense variant in one of the "hotspot" codons within the RNase IIIb domain (4). Functional studies of these somatic DICER1 RNase IIIb domain missense variants have shown that they lead to defective cleavage of 5p-derived miRNAs from the pre-miRNA loop sequence resulting in the retention of pre-miRNA loop sequence in DICER1 mutant cancers (8). This is consistent with the two-hit hypothesis implicated in the development of cancers in most patients with DICER1 syndrome (9). Our patient's DICER1 germline pathogenic variant was a c.3118_3119insCA frameshift. The second hit identified in our patient's tumor was a missense mutation in the DICER1 gene (c.5113G>A (p.Glu1705Lys)). This variant is one of the hot spot mutations in DICER1 and is frequently identified somatically in Sertoli–Leydig cell tumors, pleuropulmonary blastomas and other cancer types. It is often found with a loss of function germline DICER1 variant in patients with DICER1 tumor predisposition syndrome (7).

It is interesting to note that our patient's spinal hamartoma is quite atypical in many ways. First, the hamartoma developed in the cervical spine, contrary to the thoracic and lumbosacral predominance that is generally described in the literature (1). Additionally, spinal hamartomas are usually asymptomatic, whereas our patient presented with significant symptomatic spinal cord compression, which has only been reported once previously (20). It is not clear if the pathogenesis and clinical behavior of this hamartoma is influenced by the DICER1 drivers, differentiating its natural history from sporadic forms of spinal hamartoma.

In summary, DICER1-associated hamartoma has been described in the nasal cavity, liver and now spine. As described in this report, congenital spinal hamartoma is a newly associated, albeit rare manifestation of the DICER1 syndrome phenotype.

Data availability statement

The original contributions presented in the study are included in the article/Supplementary Material. Further inquiries can be directed to the corresponding author/s.

Ethics statement

Ethical review and approval was not required for the study on human participants in accordance with the local legislation and institutional requirements. Written informed consent to participate in this study was provided by the participants' legal guardian/next of kin. Written informed consent was obtained from the individual (s), and minor(s)' legal guardian/next of kin, for the publication of any potentially identifiable images or data included in this article.

Author contributions

RH, data acquisition and original draft preparation. WL, carried out molecular genetic studies and annotation. HC, pathologist provided histology images. MS, radiologist provided MRI images. DM, AV, and AD, conceptualization, writing- review and editing. All authors contributed to the article and approved the submitted version.

Conflict of interest

The authors declare that the research was conducted in the absence of any commercial or financial relationships that could be construed as a potential conflict of interest.

Publisher's note

All claims expressed in this article are solely those of the authors and do not necessarily represent those of their affiliated organizations, or those of the publisher, the editors and the reviewers. Any product that may be evaluated in this article, or claim that may be made by its manufacturer, is not guaranteed or endorsed by the publisher.

Supplementary material

The Supplementary Material for this article can be found online at: https://www.frontiersin.org/articles/10.3389/fonc.2022.963768/full#supplementary-material

References

1. Castillo M, Smith MM, Armao D. Midline spinal cord hamartomas: MR imaging features of two patients. *AJNR Am J Neuroradiol* (1999) 20(6):1169–71.

2. Morris GF, Murphy K, Rorke LB, James HE. Spinal hamartomas: a distinct clinical entity. *J Neurosurg* (1998) 88(6):954–7. doi: 10.3171/jns.1998.88.6.0954

3. Malelak EB, Lauren C, Argie D, Nugraheni T. Congenital midline spinal hamartoma in a 5-Month-Old infant. *World Neurosurg* (2021) 145:142–7. doi: 10.1016/j.wneu.2020.09.065

4. Brenneman M, Field A, Yang J, Williams G, Doros L, Rossi C, et al. Temporal order of RNase IIIb and loss-of-function mutations during development determines phenotype in pleuropulmonary blastoma / DICER1 syndrome: a unique variant of the two-hit tumor suppression model. *F1000Res* (2015) 4:214. doi: 10.12688/f1000research.6746.1

5. Stewart DR, Best AF, Williams GM, Harney LA, Carr AG, Harris AK, et al. Neoplasm risk among individuals with a pathogenic germline variant in DICER1. *J Clin Oncol* (2019) 37(8):668–76. doi: 10.1200/JCO.2018.78.4678

6. de Kock L, Priest JR, Foulkes WD, Alexandrescu S. An update on the central nervous system manifestations of DICER1 syndrome. *Acta Neuropathol* (2020) 139 (4):689–701. doi: 10.1007/s00401-019-01997-y

7. Conlon N, Schultheis AM, Piscuoglio S, Silva A, Guerra E, Tornos C, et al. A survey of DICER1 hotspot mutations in ovarian and testicular sex cord-stromal tumors. *Mod Pathol* (2015) 28(12):1603–12. doi: 10.1038/modpathol.2015.115

8. Pugh TJ, Yu W, Yang J, Field AL, Ambrogio L, Carter SL, et al. Exome sequencing of pleuropulmonary blastoma reveals frequent biallelic loss of TP53 and two hits in DICER1 resulting in retention of 5p-derived miRNA hairpin loop sequences. *Oncogene* (2014) 33(45):5295–302. doi: 10.1038/onc.2014.150

9. Schultz KAP, Williams GM, Kamihara J, Stewart DR, Harris AK, Bauer AJ, et al. DICER1 and associated conditions: Identification of At-risk individuals and recommended surveillance strategies. *Clin Cancer Res* (2018) 24(10):2251–61. doi: 10.1158/1078-0432.CCR-17-3089

10. Priest JR, Watterson J, Strong L, Huff V, Woods WG, Byrd RL, et al. Pleuropulmonary blastoma: a marker for familial disease. *J Pediatr* (1996) 128 (2):220–4. doi: 10.1016/S0022-3476(96)70393-1

11. Hill DA, Ivanovich J, Priest JR, Gurnett CA, Dehner LP, Desruisseau D, et al. DICER1 mutations in familial pleuropulmonary blastoma. *Science* (2009) 325 (5943):965. doi: 10.1126/science.1174334

12. Stewart DR, Messinger Y, Williams GM, Yang J, Field A, Schultz KA, et al. Nasal chondromesenchymal hamartomas arise secondary to germline and somatic mutations of DICER1 in the pleuropulmonary blastoma tumor predisposition disorder. *Hum Genet* (2014) 133(11):1443–50. doi: 10.1007/s00439-014-1474-9

13. Mason KA, Navaratnam A, Theodorakopoulou E, Chokkalingam PG. Nasal chondromesenchymal hamartoma (NCMH): a systematic review of the literature with a new case report. *J Otolaryngol Head Neck Surg* (2015) 44:28. doi: 10.1186/s40463-015-0077-3

14. Vasta LM, Nichols A, Harney LA, Best AF, Carr AG, Harris AK, et al. Nasal chondromesenchymal hamartomas in a cohort with pathogenic germline variation in DICER1. *Rhinol Online* (2020) 3:15–24. doi: 10.4193/RHINOL/20.007

15. Apellaniz-Ruiz M, Segni M, Kettwig M, Gluer S, Pelletier D, Nguyen VH, et al. Mesenchymal hamartoma of the liver and DICER1 syndrome. *N Engl J Med* (2019) 380(19):1834–42. doi: 10.1056/NEJMoa1812169

16. Katz BH, Quencer RM. Hamartomatous spinal cord lesion in neurofibromatosis. *AJNR Am J Neuroradiol* (1989) 10(5 Suppl):S101.

17. Tibbs PA, James HE, Rorke LB, Schut L, Bruce DA. Midline hamartomas masquerading as meningomyeloceles or teratomas in the newborn infant. *J Pediatr* (1976) 89(6):928–33. doi: 10.1016/S0022-3476(76)80598-7

18. Takeyama J, Hayashi T, Saito M, Shimanuki Y, Watanabe M, Sasano H, et al. Spinal hamartoma associated with spinal dysraphism. *Childs Nerv Syst* (2006) 22(9):1098–102. doi: 10.1007/s00381-005-0016-0

19. Bining HJ, Saigal G, Goswami RS, Gill D, McNeely PD. Spinal hamartoma in a neonate: Unusual presentation and MR imaging findings. *AJNR Am J Neuroradiol* (2006) 27(4):810–2.

20. Samak EM, Abdel Latif AM, Ghany WA, Hewedi IH, Amer A, Moharram H, et al. Spinal intramedullary hamartoma with acute presentation in a 13-month old infant: case report. *J Neurosurg Pediatr* (2016) 18(2):177–82. doi: 10.3171/2016.2.PEDS15561

21. Denli AM, Tops BB, Plasterk RH, Ketting RF, Hannon GJ. Processing of primary microRNAs by the microprocessor complex. *Nature* (2004) 432 (7014):231–5. doi: 10.1038/nature03049

Check for updates

Case report: Unique FLT4 variants associated with differential response to anlotinib in angiosarcoma

Yuanyuan Gu[1†], Jing Meng[2†], Yongzhi Ju[3], Xia You[3], Tingting Sun[3], Jun Lu[4] and Yin Guan[1*]

[1]Department of Medical Oncology, Beijing Chao-Yang Hospital, Capital Medical University, Beijing, China, [2]Department of Medical Oncology, The Chinese People's Liberation Army (PLA) General Hospital, Beijing, China, [3]The Medical Department, Jiangsu Simcere Diagnostics Co., Ltd., Nanjing, China, [4]Department of Pathology, Beijing Chao-Yang Hospital, Capital Medical University, Beijing, China

Angiosarcoma (AS) is a rare, clinically aggressive tumor with limited treatment options and a poor prognosis. Mutations involving the angiogenesis-related genesTP53, PTPRB, PLCG1, KDR as well as FLT4 amplification have been observed in AS. There is a potential therapeutic value of inhibition of the VEGF pathway against angiosarcoma. Our case first described a patient with two sites of cutaneous angiosarcomas (cASs) that responded differently to anlotinib. And genetic analysis revealed that those two sites had different FLT4 variants, suggesting that FLT4 amplification could be the cause of anlotinib non-response.

KEYWORDS

cutaneous angiosarcomas, vascular endothelial growth factor receptor (VEGFR), FLT4, anlotinib, soft tissue sarcomas

Introduction

Angiosarcomas (ASs) are rare, aggressive tumors of vascular or lymphatic endothelial cell origin that account for about 2%–3% of all adult soft tissue sarcomas. They can arise from anywhere on the body, with cutaneous angiosarcomas (about 60% of all cases) involving the head and neck, particularly the scalp, followed by the breast, extremity, trunk, liver, and other sites (1, 2). ASs can be divided into primary cutaneous (in the absence of lymphoedema or radiation), parenchymal tissue/visceral (which includes primary breast lesions), deep soft tissue, and lymphoedema-associated and post-radiation angiosarcomas, according to lesion location and underlying risk factors (1, 3). The prognosis of ASs is poor, with approximately 16%–44% of advanced or metastatic patients presenting at the time of diagnosis (2, 4). ASs have a 5-year survival rate of 30%–

40% with overall survival ranging from 6 to 16 months depending on tumor stage, surgical resection, and distant metastases (5, 6).

When compared to Western countries, approximately 50%–60% of cutaneous angiosarcomas (cASs) originate in the head and neck, with Asians involving up to 90% of the scalp and face (7). cASs are more common in elderly men between the ages of 60 and 70 who have distinct clinical causative factors, such as chronically sun-damaged skin or chronic lymphedema/irradiated skin (8). Patients with angiosarcoma of the head and neck have a higher tumor mutation burden and a dominant UV damage mutational signature (9, 10).

Surgical resection with wide excisional margins is the main therapy for R0 resection cASs, but due to insufficient surgical excision and the infiltrative growth pattern, local recurrences or metastases are common, particularly in head and neck locations, with 5-year overall survival of 10%–15% (11, 12). Several studies revealed that age, tumor size, tumor location, resection with positive margins, and advanced stage are the poor prognosis factors for cASs (13–15).

Amplifications of *MYC*, *KLT4*, *FLT4*, and recurrent mutations in *TP53*, *PLCG1* (R707), and *PTPRB*, as well as genetic alterations in the mitogen-activated protein kinase (MAPK) pathway, have been reported in ASs (9, 16–19). Many antiangiogenic targeted agents, including vascular endothelial growth factor/receptor inhibitors, such as

bevacizumab (20), or multi-kinase inhibitors, pazopanib (21, 22), and sunitinib, have demonstrated clinical efficacy in ASs, including cASs, when used alone or in combination with standard therapies. Clinical success with angiogenesis targeting agents, on the other hand, has so far been lacking.

Case description

In December 2018, a 73-year-old male patient discovered on his own a swelling in the left parotid area, initially the size of peanut rice, with local pressure pain but no fever, facial palsy, or taste disturbance. One month later, the swelling had grown to the size of a small date and was diagnosed as a "parotid cyst" at an outside hospital and underwent "left parotid abscess excision." In March 2019, the patient visited our hospital for a reexamination. The CT scan revealed an irregular mass in the posterior and inferior portion of the left parotid gland, measuring 3.7 × 3.4 cm. This mass had uneven density, mild to moderate enhancement, uneven edges, a poor boundary with the parotid gland, and local skin thickening. Pathological findings postoperatively showed that vascular endothelial derived cells were responsible for the infection, and the immunohistochemical staining showed that CD31 was diffusely positive and the Ki-67 proliferation index was 50%–60%, whereas CD34 was negative (Figures 1A–C), with
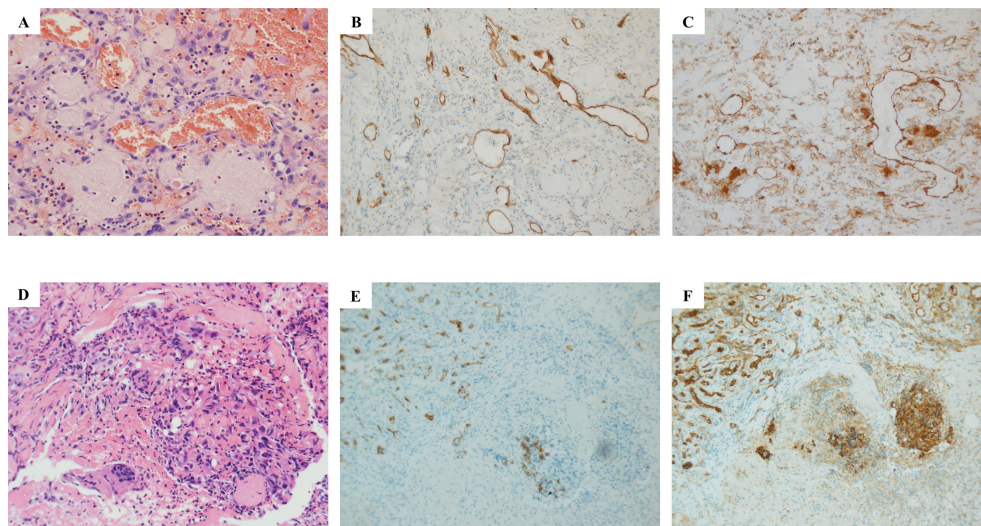
FIGURE 1
Histopathological examination results of parotid gland and scalp metastasis. Hematoxylin−eosin (HE) staining showed that salivary gland tissue was found in the sample tissue of the left parotid gland mass, and fibrous tissue hyperplasia was observed in some areas (A−C) Atypical cells were seen near the granulation tissue, which was indicated by immunophenotype as endovascular cells, and infiltration of lymphocytes and plasma cells was also observed, accompanied by bleeding (A). Immunohistochemical results showed CD34 negative (B) and CD31 positive (C). As for the HE result of scalp metastasis (D, E), squamous mucosa, epithelial erosion, a small amount of increased cytoplasmic ratio, irregular karyotype, and trace lesion tissue (D) were shown. Immunohistochemical results showed CD34 negative (E) and CD31 positive (F).

lymphoid and plasma cell infiltration and bleeding. The presence of two lymph nodes surrounding the tissue led to a preliminary diagnosis of poorly differentiated AS.

However, a relapse of the local bump behind the left ear 2 months after the operation. Meanwhile, a lesion appeared on the scalp. The scalp was broken locally, the wound was poorly healed, and the surrounding tissues were eroded. A local biopsy revealed CD31, ERG, and Ki-67 were positive, P53 was partially positive, while CK, CD34, CD117, CEA, and P40 were negative, indicating that this was a metastasis (Figures 1D–F). Given the size of the lesion, the patient's old age, and physical condition, surgery and chemotherapy were risky treatments, and the patient made an informed decision to decline them. So anlotinib, a multi-targeted tyrosine kinase inhibitor approved as second-line treatment for advanced soft-tissue sarcoma, was recommended after complete informed consent in July 2019. During the treatment, the tumor behind the left ear was quickly relieved until it disappeared (Figures 2A–E), but anlotinib was not effective for scalp metastasis, and the lesions continued to deteriorate until they were uncontrollable (Figures 2F–O). This patient died in May 2020 without a relapse behind the left ear.

There was a significant difference in the response to anlotinib between recurrent parotid lesions and scalp metastases. We sequenced the scalp metastatic and the surgically resected primary tissues by Next Generation Sequencing (NGS). The sequencing results showed that the primary lesions only had the *FLT4* p.G1276E mutation. However, in addition to the *FLT4* p.G1276E mutation, scalp metastasis also exhibited *FLT4* amplification and mutations of *FLT1/ARID1A/CHEK2/IRS1* (Table 1).

Identification of genomic alterations to confirm predictive biomarkers for anti-angiogenesis therapy is always on the way. The predictive value of the *FLT4* F131S mutation to regorafenib was not ruled out because of its extracellular location and complicated genomic profiles (23). Although a 6-month clinical stable response to pazopanib caught our attention in *VEGFR*-2 or 3 amplified angiosarcoma (24), we should not ignore the potential responsive mechanism of the *VEGFR3* R1070L mutation in the tyrosine kinase domain. In our description, the unique and pure *FLT4* G1276E mutation may be a reasonable explanation for this rapid and durable response to anlotinib. The amplification of *FLT4* by metastatic lesions may be the reason for the

FIGURE 2
Different responses of retro auricular and scalp angiosarcoma metastases to anlotinib treatment. Changes in retro auricular recurrence and overhead metastases during anlotinib treatment on 13 July, 22 July, 25 July, 28 July, and 1 August 2019, respectively. Among them, the retro auricular tumor was relieved quickly after anlotinib treatment, and the bump was gradually reduced to disappear, achieving recovery **(A−E)**. However, the scalp metastasis of the same period was not effective, and the lesion gradually deteriorated until it was uncontrollable **(F−O)**. Continuous deterioration of the scalp metastatic during anlotinib maintenance on 4 August **(K)**, 12 August **(L)**, 8 October **(M)**, 19 November **(N)**, and 10 December 2019 **(O)**.

TABLE 1   DNA-NGS detection results of the patient.

Genes	Primary tumor	Scalp metastasis
FLT4	p.Gly1276Glu (25.58%)	p.Gly1276Glu (68.23%)
FLT4		Amplification (CN: 4.9)
FLT1		p.Gly181Glu (4.86%)
ARID1A		p.Gln425* (3.25%)
CHEK2		p.Arg3Trp (3.72%)
IRS1		p.Thr1103Ala (2.91%)
TMB	0.8 Muts/Mb	4.0 Muts/Mb
MSI	MSS	MSS

muts/Mb, mutations per megabase; NGS, next-generation sequencing; TMB, tumor mutational burden; MSI, microsatellite Instability; CN, Copy number.

unresponsiveness after constructional analysis of other gene alterations. Further study is ongoing and warranted.

Conclusion

AS is a rare, highly heterogeneous sarcoma with a variety of clinical characteristics. The prognosis of ASs is poor, with a 5-year survival rate of only 30%–40% from primary diagnosis, but once metastasized, the average survival period is less than 1 year. Based on the stage and the location, radical surgery remains the curative treatment for Ass, and adjuvant radiochemotherapy is mainly used to treat locally advanced or progressive patients (6). Targeted agents, including mono-target antibodies, bevacizumab, or multi-target small molecules in tyrosine kinases, pazopanib, and regorafenib, have shown significant clinical efficacy (25). There are some immunotherapy drugs, and combination strategies are being investigated in various subtypes of soft tissue sarcomas, including ASs (26). Due to the complex correlation between drug efficiency and pathological subtype heterogeneity as well as genetic characteristics, treatment options for ASs remain limited (27).

Anlotinib is a new oral molecular multi-target tyrosine kinase inhibitor (TKI) that targets vascular endothelial growth factor receptor (VEGFR) 1, VEGFR3, VEGFR2/KDR, platelet-derived growth factor receptor a (PDGFR-a), c-Kit, and fibroblast growth factor receptor (FGFR) 1–3 and inhibits tumor angiogenesis and tumor cell proliferation. It has been approved as a third-line treatment for patients with advanced non-small-cell lung cancer (NSCLC) (28). Based on a preclinical study, anlotinib showed high selectivity for VEGF family members, especially VEGFR2 and VEGFR3, with IC50 values of 0.2 and 0.7 nmol/L, showing high selectivity and inhibitory potency to sunitinib (29). A phase 2 clinical trial involving 166 patients to evaluate anlotinib in recurrent metastatic soft tissue sarcomas found that the overall 12-week PFS and ORR rates were 68% and 13%, respectively, with easily controllable adverse events (30). More trials are being conducted to investigate the efficacy of anlotinib monotherapy, anlotinib plus immunotherapy, and anlotinib plus chemotherapy in advanced sarcomas, particularly soft tissue sarcomas (31). So far, there have been few reports on the efficacy of anlotinib treatment in ASs, with only a few case reports referring to various lesions in head and neck AS (32) and cardiac AS (33) or combined immunotherapy in metastatic primary splenic AS (34). In the case we present, the patient experienced local recurrence in the ear as well as scalp metastases following surgery. Anlotinib was an option chosen when the patient declined chemotherapy and surgery. However, the two lesions respond differently to treatment, with the lesion behind the ear disappearing quickly and the lesion on the scalp worsening. FLT4 p.G1276E mutation rate doubled, and newly added FLT4 amplification as well as point mutation of FLT1/ARID1A/CHEK2/IRS1, according to genetic alterations from primary and metastatic tissues.

The FLT4 gene encodes VEGFR3 and is involved in lymphatic differentiation. It has been reported that inappropriate genetic abnormalities of VEGFR signaling are critical in the genesis of angiosarcomas (35, 36). FLT4 gene amplification, along with MYC, is present in approximately 25% of secondary angiosarcomas (17). A case report described a 6-month clinically stable response to pazopanib in an angiosarcoma patient with VEGFR-2, VEGFR-3 amplification, and a novel VEGFR3 R1070L mutation (24). Arnaud-Coffin et al. (37) also reported a partial response to pazopanib in an FLT4 amplified angiosarcoma patient, but with a worse PFS of 3.1 months. FLT4 amplification was also reported to be a poor prognostic factor for ASs (38). Several basket trials with FLT4 gene amplification subgroups are also being conducted (NCT02693535, NCT02029001, NCT03297606). The FLT1 gene encodes VEGFR1 and is a member of the VEGFR family. The point mutation c.542G>A was found in FLT1's Ig-like domain 2, which is a high-affinity ligand-binding region (29). Some studies have found that soluble FLT1 expression is associated with poor clinical outcomes and may be a biomarker of intrinsic resistance to anti-angiogenic therapies that selectively inhibit the VEGFR-2 signaling pathway (39). However, no studies have been conducted to investigate the impact of FLT1 extracellular domain mutations on the efficacy of kinase inhibitor therapy.

ARID1A encodes BAF250A, which is a member of the SWI/SNF chromatin-remodeling complex. *ARID1A* is a tumor suppressor, and most mutations seen in cancers are frameshift or nonsense mutations that result in inactivation and reduced expression of *ARID1A* (40). The overall mutation rate of *ARID1A* in cancers is about 6%, with clear-cell ovarian cancer (45%) and endometrial cancer (37%) being the most common (41, 42). There is a lot of evidence that *ARID1A* loss-of-function mutations can activate the PI3K/Akt/mTORpathway (43, 44) and increase the sensitivity of ARID1A-deficient cells to treatment with the PI3K/AKT inhibitor in gastric cancer cells (45) or cholangiocarcinoma (46). Checkpoint kinase 2 (CHEK2) is a cancer susceptibility gene that codes for the serine/threonine CHK2 kinase involved in DNA damage response (DDR). A higher frequency of germline mutations is significantly associated with breast and ovarian cancers (47). Insulin receptor substrate-1 (IRS1) is a mediator of oncogenic IGF signaling and is overexpressed in a variety of malignant tumor types, where it also mediates EGFR or mTOR inhibitor resistance (48–50). Although these mutations are linked to sarcoma development to some extent, there have been no reports of these mutations being linked to sarcoma-targeted therapy resistance.

In our case, *FLT4* p.G1276E is a novel mutation localized in the carboxyterminal domain of *VEGFR3* that may be the primary reason for the response to anlotinib in the recurrence site, but the *FLT4* amplification in the metastatic site may be a worse prognosis factor and showed no response to anlotinib. Our findings may broaden the spectrum of the *FLT4* gene mutations while also providing guidance for clinical anlotinib treatment of local recurrence and metastatic ASs.

Data availability statement

The original contributions presented in the study are included in the article/supplementary material. Further inquiries can be directed to the corresponding author.

Ethics statement

Written informed consent was obtained from the individual(s) for the publication of any potentially identifiable images or data included in this article.

Author contributions

YiG treated and observed the patient. YuG, JM, and YiG collected the clinical information, diagnostic information, therapeutic information, and images of the patients. JL performed the histopathological and immunohistochemical examinations. YiG, YuG, JM, and JL prepared the manuscript and the literature search. YJ, XY, and TS performed data analysis and interpretation. YiG and JM reviewed and edited the manuscript. All authors contributed to the article and approved the submitted version.

Conflict of interest

Publisher's note

References

1. Young RJ, Brown NJ, Reed MW, Hughes D, Woll PJ. Angiosarcoma. *Lancet Oncol* (2010) 11(10):983–91. doi: 10.1016/S1470-2045(10)70023-1

2. Singla S, Papavasiliou P, Powers B, Gaughan J, von Mehren M, Watson JC, et al. Challenges in the treatment of angiosarcoma: a single institution experience. *Am J Surg* (2014) 208(2):254–9. doi: 10.1016/j.amjsurg.2014.01.007

3. Gaballah AH, Jensen CT, Palmquist S, Pickhardt PJ, Duran A, Broering G, et al. Angiosarcoma: Clinical and imaging features from head to toe. *Br J Radiol* (2017) 90(1075):20170039. doi: 10.1259/bjr.20170039

4. Buehler D, Rice SR, Moody JS, Rush P, Hafez GR, Attia S, et al. Angiosarcoma outcomes and prognostic factors: a 25-year single institution experience. *Am J Clin Oncol* (2014) 37(5):473–9. doi: 10.1097/COC.0b013e31827e4e7b

5. Cao J, Wang J, He C, Fang M. Angiosarcoma: a review of diagnosis and current treatment. *Am J Cancer Res* (2019) 9(11):2303–13.

6. Boichard A, Wagner MJ, Kurzrock R. Angiosarcoma heterogeneity and potential therapeutic vulnerability to immune checkpoint blockade: insights from genomic sequencing. *Genome Med* (2020) 12(1):61. doi: 10.1186/s13073-020-00753-2

7. Farid M, Ong WS, Lee MJ, Jeevan R, Ho ZC, Sairi AN, et al. Cutaneous versus non-cutaneous angiosarcoma: clinicopathologic features and treatment outcomes in 60 patients at a single Asian cancer centre. *Oncology* (2013) 85(3):182–90. doi: 10.1159/000354215

8. Ronchi A, Cozzolino I, Zito Marino F, De Chiara A, Argenziano G, Moscarella E, et al. Primary and secondary cutaneous angiosarcoma: Distinctive clinical, pathological and molecular features. *Ann Diagn Pathol* (2020) 48:151597. doi: 10.1016/j.anndiagpath.2020.151597

9. Painter CA, Jain E, Tomson BN, Dunphy M, Stoddard RE, Thomas BS, et al. The angiosarcoma project: enabling genomic and clinical discoveries in a rare

cancer through patient-partnered research. *Nat Med* (2020) 26(2):181–7. doi: 10.1038/s41591-019-0749-z

10. Chan JY, Lim JQ, Yeong J, Ravi V, Guan P, Boot A, et al. Multiomic analysis and immunoprofiling reveal distinct subtypes of human angiosarcoma. *J Clin Invest* (2020) 130(11):5833–46. doi: 10.1172/JCI139080

11. Holden CA, Spittle MF, Jones EW. Angiosarcoma of the face and scalp, prognosis and treatment. *Cancer* (1987) 59(5):1046–57. doi: 10.1002/1097-0142 (19870301)59:5<1046::aid-cncr2820590533>3.0.co;2-6

12. Lee BL, Chen CF, Chen PC, Lee HC, Liao WC, Perng CK, et al. Investigation of prognostic features in primary cutaneous and soft tissue angiosarcoma after surgical resection: A retrospective study. *Ann Plast Surg* (2017) 78(3 Suppl 2):S41–6. doi: 10.1097/SAP.0000000000001004

13. Perez MC, Padhya TA, Messina JL, Jackson RS, Gonzalez RJ, Bui MM, et al. Cutaneous angiosarcoma: a single-institution experience. *Ann Surg Oncol* (2013) 20(11):3391–7. doi: 10.1245/s10434-013-3083-6

14. Dettenborn T, Wermker K, Schulze HJ, Klein M, Schwipper V, Hallermann C. Prognostic features in angiosarcoma of the head and neck: a retrospective monocenter study. *J Craniomaxillofac Surg* (2014) 42(8):1623–8. doi: 10.1016/j.jcms.2014.05.002

15. Goerdt LV, Schneider SW, Booken N. Cutaneous angiosarcomas: Molecular pathogenesis guides novel therapeutic approaches. *J Dtsch Dermatol Ges* (2022) 20 (4):429–43. doi: 10.1111/ddg.14694

16. Manner J, Radlwimmer B, Hohenberger P, Mössinger K, Küffer S, Sauer C, et al. MYC high level gene amplification is a distinctive feature of angiosarcomas after irradiation or chronic lymphedema. *Am J Pathol* (2010) 176(1):34–9. doi: 10.2353/ajpath.2010.090637

17. Cornejo KM, Deng A, Wu H, Cosar EF, Khan A, St Cyr M, et al. The utility of MYC and FLT4 in the diagnosis and treatment of postradiation atypical vascular lesion and angiosarcoma of the breast. *Hum Pathol* (2015) 46(6):868–75. doi: 10.1016/j.humpath.2015.02.014

18. Behjati S, Tarpey PS, Sheldon H, Martincorena I, Van Loo P, Gundem G, et al. Recurrent PTPRB and PLCG1 mutations in angiosarcoma. *Nat Genet* (2014) 46(4):376–9. doi: 10.1038/ng.2921

19. Murali R, Chandramohan R, Möller I, Scholz SL, Berger M, Huberman K, et al. Targeted massively parallel sequencing of angiosarcomas reveals frequent activation of the mitogen activated protein kinase pathway. *Oncotarget* (2015) 6 (34):36041–52. doi: 10.18632/oncotarget.5936

20. Agulnik M, Yarber JL, Okuno SH, von Mehren M, Jovanovic BD, Brockstein BE, et al. An open-label, multicenter, phase II study of bevacizumab for the treatment of angiosarcoma and epithelioid hemangioendotheliomas. *Ann Oncol* (2013) 24(1):257–63. doi: 10.1093/annonc/mds237

21. Ogata D, Yanagisawa H, Suzuki K, Oashi K, Yamazaki N, Tsuchida T. Pazopanib treatment slows progression and stabilizes disease in patients with taxane-resistant cutaneous angiosarcoma. *Med Oncol* (2016) 33(10):116. doi: 10.1007/s12032-016-0831-z

22. Fujiwara S, Nakano E, Nakamura K, Washio K, Ogura K, Nishigori C. Pazopanib as a potential chemotherapy for cutaneous angiosarcoma: A case series of 10 patients from a single institution. *J Dermatol* (2020) 47(7):e273–4. doi: 10.1111/1346-8138.15381

23. Korphaisarn K, Loree JM, Nguyen V, Coulson R, Holla V, Litzenburger BC, et al. Genomic analysis of exceptional responder to regorafenib in treatment-refractory metastatic rectal cancer: a case report and review of the literature. *Oncotarget* (2017) 8(34):57882–8. doi: 10.18632/oncotarget.18357

24. Ravi V, Sanford EM, Wang WL, Ross JS, Ramesh N, Futreal A, et al. Antitumor response of VEGFR2- and VEGFR3-amplified angiosarcoma to pazopanib. *J Natl Compr Canc Netw* (2016) 14(5):499–502. doi: 10.6004/jnccn.2016.0058

25. Florou V, Wilky BA. Current management of angiosarcoma: Recent advances and lessons from the past. *Curr Treat Options Oncol* (2021) 22(7):61. doi: 10.1007/s11864-021-00858-9

26. Tang F, Tie Y, Wei YQ, Tu CQ, Wei XW. Targeted and immuno-based therapies in sarcoma: mechanisms and advances in clinical trials. *Biochim Biophys Acta Rev Cancer* (2021) 1876(2):188606. doi: 10.1016/j.bbcan.2021.188606

27. Weidema ME, Versleijen-Jonkers YMH, Flucke UE, Desar IME, van der Graaf WTA. Targeting angiosarcomas of the soft tissues: A challenging effort in a heterogeneous and rare disease. *Crit Rev Oncol Hematol* (2019) 138:120–31. doi: 10.1016/j.critrevonc.2019.04.010

28. Han B, Li K, Wang Q, Zhang L, Shi J, Wang Z, et al. Effect of anlotinib as a third-line or further treatment on overall survival of patients with advanced non-small cell lung cancer: The ALTER 0303 phase 3 randomized clinical trial. *JAMA Oncol* (2018) 4(11):1569–75. doi: 10.1001/jamaoncol.2018.3039

29. Tanaka K, Yamaguchi S, Sawano A, Shibuya M. Characterization of the extracellular domain in vascular endothelial growth factor receptor-1 (Flt-1

tyrosine kinase). *Jpn J Cancer Res* (1997) 88(9):867–76. doi: 10.1111/j.1349-7006.1997.tb00463.x

30. Chi Y, Fang Z, Hong X, Yao Y, Sun P, Wang G, et al. Safety and efficacy of anlotinib, a multikinase angiogenesis inhibitor, in patients with refractory metastatic soft-tissue sarcoma. *Clin Cancer Res* (2018) 24(21):5233–8. doi: 10.1158/1078-0432.CCR-17-3766

31. Li S. Anlotinib: A novel targeted drug for bone and soft tissue sarcoma. *Front Oncol* (2021) 11:664853. doi: 10.3389/fonc.2021.664853

32. Ren B, Wang W, Tan J, Yuan B, Chen G, Mo X, et al. Efficacy of anlotinib for the treatment of angiosarcoma of the face and neck: A case report. *Front Oncol* (2021) 11:596732. doi: 10.3389/fonc.2021.596732

33. Fang X, Zheng S. Primary cardiac angiosarcoma: a case report. *J Int Med Res* (2021) 49(8):3000605211033261. doi: 10.1177/03000605211033261

34. Xu W, Wang K, Gu W, Nie X, Zhang H, Tang C, et al. Case report: Complete remission with anti-PD-1 and anti-VEGF combined therapy of a patient with metastatic primary splenic angiosarcoma. *Front Oncol* (2022) 12:809068. doi: 10.3389/fonc.2022.809068

35. Antonescu CR, Yoshida A, Guo T, Chang NE, Zhang L, Agaram NP, et al. KDR activating mutations in human angiosarcomas are sensitive to specific kinase inhibitors. *Cancer Res* (2009) 69(18):7175–9. doi: 10.1158/0008-5472.CAN-09-2068

36. Itakura E, Yamamoto H, Oda Y, Tsuneyoshi M. Detection and characterization of vascular endothelial growth factors and their receptors in a series of angiosarcomas. *J Surg Oncol* (2008) 97(1):74–81. doi: 10.1002/jso.20766

37. Arnaud-Coffin P, Brahmi M, Vanacker H, Eberst L, Tredan O, Attignon V, et al. Therapeutic relevance of molecular screening program in patients with metastatic sarcoma: Analysis from the ProfiLER 01 trial. *Transl Oncol* (2020) 13 (12):100870. doi: 10.1016/j.tranon.2020.100870

38. Huang SC, Zhang L, Sung YS, Chen CL, Kao YC, Agaram NP, et al. Recurrent CIC gene abnormalities in angiosarcomas: A molecular study of 120 cases with concurrent investigation of PLCG1, KDR, MYC, and FLT4 gene alterations. *Am J Surg Pathol* (2016) 40(5):645–55. doi: 10.1097/PAS.0000000000000582

39. Meyerhardt JA, Ancukiewicz M, Abrams TA, Schrag D, Enzinger PC, Chan JA, et al. Phase I study of cetuximab, irinotecan, and vandetanib (ZD6474) as therapy for patients with previously treated metastatic colorectal cancer. *PloS One* (2012) 7(6):e38231. doi: 10.1371/journal.pone.0038231

40. Huang J, Zhao YL, Li Y, Fletcher JA, Xiao S. Genomic and functional evidence for an ARID1A tumor suppressor role. *Genes Chromosomes Cancer* (2007) 46(8):745–50. doi: 10.1002/gcc.20459

41. Jiang T, Chen X, Su C, Ren S, Zhou C. Pan-cancer analysis of ARID1A alterations as biomarkers for immunotherapy outcomes. *J Cancer* (2020) 11 (4):776–80. doi: 10.7150/jca.41296

42. Mullen J, Kato S, Sicklick JK, Kurzrock R. Targeting ARID1A mutations in cancer. *Cancer Treat Rev* (2021) 100:102287. doi: 10.1016/j.ctrv.2021.102287

43. Hideshima T, Nakamura N, Chauhan D, Anderson KC. Biologic sequelae of interleukin-6 induced PI3-K/Akt signaling in multiple myeloma. *Oncogene* (2001) 20(42):5991–6000. doi: 10.1038/sj.onc.1204833

44. Yang Y, Wang X, Yang J, Duan J, Wu Z, Yang F, et al. Loss of ARID1A promotes proliferation, migration and invasion *via* the akt signaling pathway in NPC. *Cancer Manag Res* (2019) 11:4931–46. doi: 10.2147/CMAR.S207329

45. Lee D, Yu EJ, Ham IH, Hur H, Kim YS. AKT inhibition is an effective treatment strategy in ARID1A-deficient gastric cancer cells. *Onco Targets Ther* (2017) 10:4153–9. doi: 10.2147/OTT.S139664

46. Tessiri S, Techasen A, Kongpetch S, Namjan A, Loilome W, Chan-On W, et al. Therapeutic targeting of ARID1A and PI3K/AKT pathway alterations in cholangiocarcinoma. *PeerJ* (2022) 10:e12750. doi: 10.7717/peerj.12750

47. Weitzel JN, Neuhausen SL, Adamson A, Tao S, Ricker C, Maoz A, et al. Pathogenic and likely pathogenic variants in PALB2, CHEK2, and other known breast cancer susceptibility genes among 1054 BRCA-negative hispanics with breast cancer. *Cancer* (2019) 125(16):2829–36. doi: 10.1002/cncr.32083

48. Sun Y, Zhou J, Shi L, Li J, Chen J. MicroRNA–466 inhibits cell proliferation and invasion in osteosarcoma by directly targeting insulin receptor substrate 1. *Mol Med Rep* (2019) 19(4):3345–52. doi: 10.3892/mmr.2019.9956

49. Reuveni H, Flashner-Abramson E, Steiner L, Makedonski K, Song R, Shir A, et al. Therapeutic destruction of insulin receptor substrates for cancer treatment. *Cancer Res* (2013) 73(14):4383–94. doi: 10.1158/0008-5472.CAN-12-3385

50. Xie C, Wan X, Quan H, Zheng M, Fu L, Li Y, et al. Preclinical characterization of anlotinib, a highly potent and selective vascular endothelial growth factor receptor-2 inhibitor. *Cancer Sci* (2018) 109(4):1207–19. doi: 10.1111/cas.13536

Check for updates

Case Report: A novel *LHFPL3::NTRK2* fusion in dysembryoplastic neuroepithelial tumor

Yanming Chen[1†], Qing Zhu[1†], Ye Wang[2], Xiaoxiao Dai[3], Ping Chen[4], Ailin Chen[1], Sujuan Zhou[4,5], Chungang Dai[1], Shengbin Zhao[4], Sheng Xiao[6] and Qing Lan[1*]

[1]Department of Neurosurgery, The Second Affiliated Hospital of Soochow University, Suzhou, China, [2]Heath Management Center, The Second Affiliated Hospital of Soochow University, Suzhou, China, [3]Department of Pathology, The Second Affiliated Hospital of Soochow University, Suzhou, China, [4]Molecular Genetics Laboratory, Suzhou Sano Precision Medicine Ltd., Suzhou, China, [5]Pathology and Pathophysiology, Soochow University Medical College, Suzhou, China, [6]Department of Pathology, Brigham and Women's Hospital, Boston, BS, United States

Neurotrophic tyrosine receptor kinase (*NTRK*) rearrangements are oncogenic drivers of various types of adult and pediatric tumors, including gliomas. However, *NTRK* rearrangements are extremely rare in glioneuronal tumors. Here, we report a novel *NTRK2* rearrangement in a 24-year-old female with dysembryoplastic neuroepithelial tumor (DNT), a circumscribed WHO grade I benign tumor associated with epilepsy. By utilizing targeted RNA next-generation sequencing (NGS), fluorescence *in situ* hybridization (FISH), reverse transcriptase PCR (RT-PCR), and Sanger sequencing, we verified an in-frame fusion between *NTRK2* and the lipoma *HMGIC* fusion partner-like 3 (*LHFPL3*). This oncogenic gene rearrangement involves 5' *LHFPL3* and 3' *NTRK2*, retaining the entire tyrosine kinase domain of *NTRK2* genes. Moreover, the targeted DNA NGS analysis revealed an *IDH1* (p.R132H) mutation, a surprising finding in this type of tumor. The pathogenic mechanism of the *LHFPL3::NTRK2* in this case likely involves aberrant dimerization and constitutive activation of RTK signaling pathways.

KEYWORDS

dysembryoplastic neuroepithelial tumors, NTRK2, LHFPL3, next-generation sequencing, IDH1

Introduction

The neurotrophic tyrosine receptor kinase (*NTRK*) family includes *NTRK1*, *NTRK2*, and *NTRK3* which encode neurotrophin receptors TrkA, TrkB, and TrkC, respectively. Fusions involving the *NTRK* family are one of the most common mechanisms of oncogenic Trk activation (1) and occur sporadically in low-grade gliomas and

glioblastoma (2). A variety of N-terminal gene fusion partners are described (3), which replace the ligand-binding site of the Trk, resulting in ligand-independent dimerization and phosphorylation of the Trk (4).

We describe here a novel *NTRK2::LHFPL3* fusion in a Dysembryoplastic neuroepithelial tumor (DNT), a low-grade glioneuronal tumor. While the signaling pathways of TrkB are well-studied, not much is known about the *LHFPL3*. Lipoma *HMGIC* fusion partner-like 3 (*LHFPL3*) is a member of the superfamily of tetra-span transmembrane proteins. RNA-Seq expression data from GTEx showed a dominant *LHFPL3* expression in the brain, including amygdala, anterior cingulate cortex, caudate, front cortex, hippocampus, hypothalamus, nucleus accumbens, putamen, and substantia nigra, while its expression is minimal in other non-brain tissues. Two human diseases have been linked to this group of genes. One *LHFP*-like gene is fused to the high mobility group AT-Hook 2 (*HMGA2*) in lipomas (5). Mutations in an *LHFP*-like gene result in deafness (6).

DNTs represent a type of glioneuronal and neuronal tumor (WHO, grade I) in the central nervous system (CNS) (7) and is the second most prevalent CNS neoplasm associated with epilepsy onset (8). DNT was first described by Daumas-Duport in 1988 (9), characterized by a multinodular growth of specific glioneuronal elements, with the columnar architecture of oligodendrocyte-like cells oriented perpendicular to the cortical surface and floating neurons in an abundant mucinous matrix (10, 11). DNT has shown genetic diversity and lacks molecular characteristics (12). Although studies have indicated *FGFR1* mutations are more common in DNTs (10), other genetic alterations were also reported (13). While certain pediatric gliomas have been shown to harbor *NTRK* fusions with frequencies of 5–25% (14), only one case of mixed neuronal-glial tumors (MNGT) with *SPECC1L::NTRK2* fusion was reported (12). Due to the exceeding rare *NTRK* rearrangement in this group of glioneuronal and neuronal tumors, we conducted a comprehensive integrating analysis of imaging, conventional histopathology, and molecular profiling.

Materials and methods

Immunohistochemistry

The tumor tissue was fixed by formalin and embedded in paraffin. The embedded tumor tissue was cut into 5μm thick slices. For immunohistochemistry, the primary antibodies were utilized according to the manufacturer's protocol. The immunohistochemical staining of pan-TRK (ab181560, Abcam, UK), Synaptophysin (36406, CST, USA), CD34 (Kit-0004, MXB, China), NSE (MAB-0791, MXB, China), Olig2 (ab109186, Abcam,

UK), ATRX (sc-55584, Santa Cruz, USA), P53 (2527, CST, USA), IDH1 (R132H) (H09, Dianova, Germany), and Ki67 (9449, CST, USA) followed the protocol as the previous report (15).

Targeted RNA next-generation sequencing

Total RNA from fresh tumor tissue was extracted with TRIzol™ LS Reagent following the manufacturer's instructions (10296010, ThermoFisher, Invitrogen, USA). 100ng total RNA was utilized for reverse transcription. End repairing and adaptor ligation were performed according to standard NGS protocols (E7771 and E6111, NEB, USA). PCR enrichment was performed using 390 gene-specific primers specific to a group of 63 genes commonly involved in solid tumors, and the enriched PCR products were sequenced in an Illumina NovaSeq 6000 platform (San Diego, USA). Sequencing results were analyzed with SeqNext software (JSI, Germany).

Fluorescence *in situ* hybridization

FISH was performed on 5μm paraffin slides of tumor tissue with dual-color break-apart probes for *NTRK2* (Betrue, China). A total of 50 interphases were studied. FISH was applied as previously described (16).

Reverse transcriptase PCR and Sanger sequencing

Total RNA was extracted with TRIzol™ LS Reagent according to the manufacturer's instructions (10296010, ThermoFisher, Invitrogen, USA). The RNA integrity was evaluated in agarose gel electrophoresis. cDNA was synthesized with random priming and SuperScript™ IV reverse transcriptase (18090050, ThermoFisher, USA). The first PCR was performed as the previous report (17). The primers were specific for *LHFPL3* and *NTRK2* (*LHFPL3*-F: 5'-CTTCAAAGCCGCCTCCTTCTT, *NTRK2*-R: 5'-TCCTGCTCAGGACAGAGGTTA). The first PCR condition was 95℃ 3 min for 1 cycle followed by 35 cycles of 95℃ 30s, 58℃ 60 sec, and 72℃ 60 sec, extend 72℃ 5 min. 1μL of the first PCR product was utilized for nested PCR with the nested primers (*LHFPL3*-F: 5'-TCCGCTGCCTGCCTTGTGCTT, *NTRK2*-R: 5'-GCTGAACAAATGTGTCTGGC). Nested PCR condition was 95℃ 3 min for 1 cycle followed by 40 cycles of 95℃ 30s, 58℃ 60 sec, and 72℃ 60 sec, extend 72℃ 5 min. Eventually, Sanger sequencing was performed to confirm the breakpoint on both *LHFPL3* exon2 and *NTRK2* exon16.

Case presentation

A 24-year-old female presented with a history of more than a decade of recurrent and unprovoked seizures. T2 weighted magnetic resonance imaging (MRI) of the brain showed an inhomogeneous hyperintense lesion located in the left frontal lobe (Figure 1A), measuring 2.0 × 1.5 × 1.7 cm in dimension, while T1 weighted MR image revealed hypo-intensity without peri-tumoral edema (Figure 1B). Contrast-enhanced MRI exhibited no significant enhancement (Figures 1C, D).

The patient received extensive tumor resection after careful preoperative planning. The tumor was soft and confined in the lobe

(Figure 1E). A postoperative MRI confirmed complete resection of the tumor. The fresh tumor tissues were sent for histology and molecular profiling analysis. H&E staining revealed a multinodular glial element, and a honeycomb appearance of oligodendrocyte-like cells was observed, with neurons floating in the matrix (Figure 1F). Immunohistochemistry analysis showed positive ATRX nuclear stain and negative P53 expression (Figures 1G, I), consistent with the genomic analysis showed wild-type *ATRX* and *TP53*. Scattered CD34 expression was seen in tumor cells in addition to vascular endothelial cells (Figure 1H), which was consistent with a previous report showing frequent CD34 expression in mixed or diffuse DNT (18). Tumor cells also expressed synaptophysin (Syn) (Figure 1K),
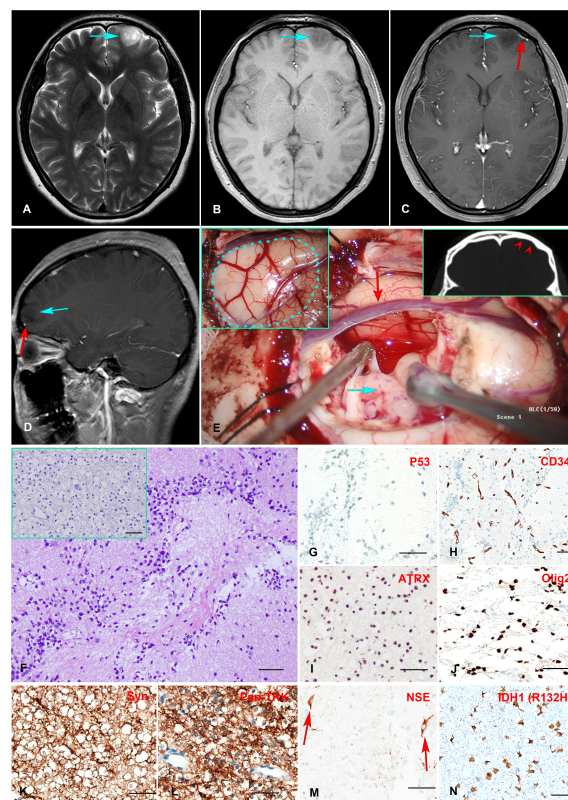
FIGURE 1

(A–E) Preoperative MR imaging and intraoperative stills. T2-weighted MRI revealed an inhomogeneous hyperintense lesion in the left frontal lobe **(A)**. T1-weighted MRI showed a hypointensity of the lesion **(B)**. Enhanced T1-weighted MR images indicated no enhancement of the mass, with a vessel (red arrow) underneath the tumor **(C, D)**. The intraoperative stills revealed the tumor was regionally confined in a lobe. The dotted blue line in the panel delineated the region of the tumor. The red arrowheads indicate left frontal bone deformation and thinning caused by long-term tumor compression**(E)**. **(F–N)** Histopathology and immunohistochemistry staining of the Formalin-fixed paraffin-embedded (FFPE) tissue tumor tissue sections. H&E staining revealed numerous round monotonous oligodendrocyte-like cells, with neurons floating in the matrix. The multinodular glial architecture was also observed (inserted) **(F)**. Immunohistochemical staining indicates negative P53-negative expression **(G)**, scattered positive CD34 expression in tumor cells in addition to vascular endothelial cells **(H)**, positive ATRX expression **(I)**, positive Olig2 expression **(J)**, positive Syn and Pan-TRK expression **(K, L)**, positive NSE expression in neurons **(M)**, and positive mutant IDH1 (R132H) expression **(N)**. Scale bar = 50μm.

oligodendrocyte transcription factor 2 (Olig2) (Figure 1J), and Ki-67 positivity less than 5%. Neuron-specific enolase (NSE) expression was observed in the neurons as expected (Figure 1M). Taken together, the histopathological and molecular pathological profiles were consistent with a complex subtype DNT. Moreover, Anti-Pan TRK antibody staining revealed a strong signal in tumor cells, consistent with the TrkB rearrangement (Figure 1L).

An RNA NGS assay with 390 'bait' probes targeting 63 genes commonly rearranged in solid tumors revealed an *LHFPL3::NTRK2* transcript (Figure 2A). The *LHFPL3::NTRK2* fusion gene contained the first two exons of *LHFPL3* and the last 6 exons of *NTRK2*, starting at exon 16 (Figure 2B). FISH analysis with a break-apart *NTRK2* probe confirmed the *NTRK2* rearrangement in tumor cell touch preparation (Figures 2C, D).

RT-PCR analysis of tumor RNA with primers specific for *LHFPL3* and *NTRK2* showed 3 bands. The dominant band (Figure 2E) was Sanger sequenced and was identical to the transcript obtained from the RNA NGS. The other 2 minor bands were not sequenced, likely from differential splicing. A targeted DNA NGS (Figure 2F) analysis revealed an isocitrate dehydrogenase 1 (*IDH1*) mutation (p.R132H) (Figure 3A) and

copy number gains of the chromosomes 7p, 9q, and X (Figure 3B). Immunohistochemistry analysis also confirmed the expression of mutant *IDH1* (R132H) (Figure 1N). *IDH1* mutations are often seen in diffuse gliomas including astrocytoma or oligodendroglioma but are rarely reported in DNTs (19). Other mutations, including *ATRX* and *TP53* mutations in astrocytoma and chromosome 1p/19q co-deletion in oligodendroglioma, were not observed in this tumor.

Discussion

A variety of genomic alterations have been reported in DNTs, although diagnostically specific changes are not established. Nevertheless, fibroblast growth factor 1 receptor (*FGFR1*) has been frequently activated in DNTs (10, 20). Among *FGFR1* alterations, internal tandem duplication (ITD) of the tyrosine kinase domain (TKD) is the most common mutation, which was reported in 40~60% of DNTs. In addition, hotspot missense mutations of *FGFR1* were also reported. Other genomic alterations include *BRAF* p.V600E and copy number chromosome gains (21).
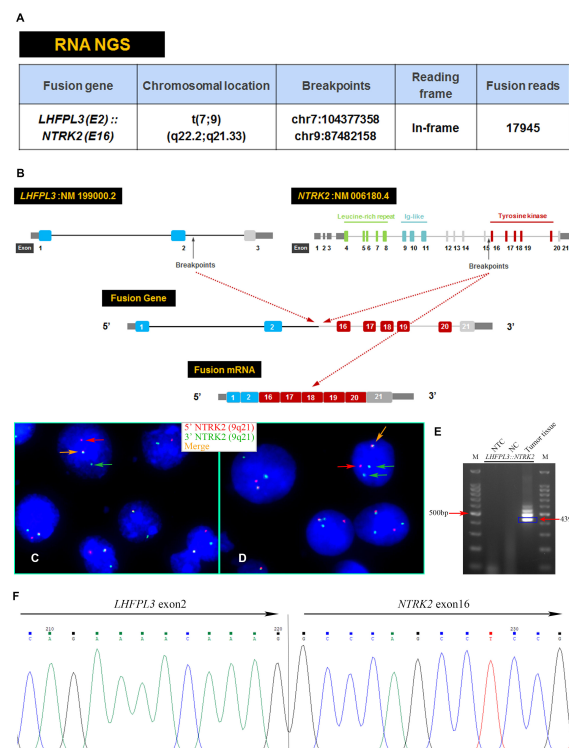
FIGURE 2
Characterization of the *LHFPL3::NTRK2* fusion. **(A)** Targeted RNA NGS revealed an *LHFPL3::NTRK2* fusion transcript with an intact reading frame. **(B)** A schematic diagram showed the breakpoints of *LHFPL3* and *NTRK2*, with the fused gene retaining the tyrosine kinase domain of the *NTRK2*. **(C, D)** FISH with an *NTRK2* split-apart probe showed the separation of the 5' *NTRK2* (Red) from the 3' *NTRK2* (Green), consistent with the *NTRK2* gene rearrangement. **(E)** RT-PCR confirmed the expression of *LHFPL3::NTRK2* fusion transcript. **(F)** Sanger sequencing of the PCR product confirmed the breakpoints of *LHFPL3* and *NTRK2* genes. NTC, No Template Control; NC, Negative Control.
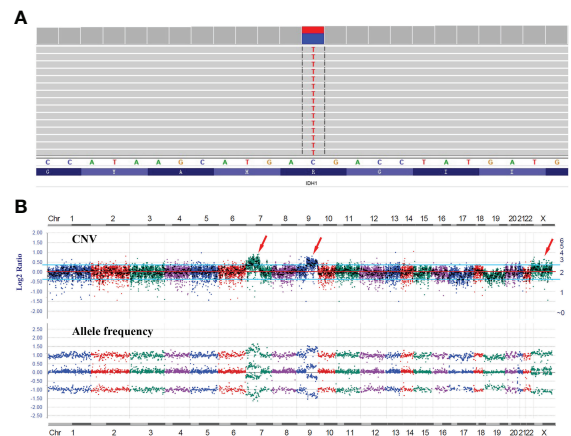
FIGURE 3
DNA NGS results of the tumor. **(A)** IGV image of the *IDH1* mutation (p.R132H). **(B)** Copy number variation (CNV) analysis showed gains of the chromosomes 7p, 9q, and X with no evidence of 1p/19q co-deletion.

Thefrequency of *BRAF* alterations in DNTs remains inconclusive among different studies (22, 23), with several studies failing to identify *BRAF* alterations in their DNTs cohorts (20, 24).

NTRK rearrangements in glioneuronal tumors were extremely rare. *STRN1::NTRK2* and *ARHGEF2::NTRK1* were reported in a single case of malignant glioneuronal tumor, respectively (25, 26). Alvarez-Breckenridge (27) described a case of low-grade glioneuronal tumor with *BCAN::NTRK1* fusion. Surrey (12) reported a case of mixed neuronal-glial tumors (MNGT) with *SPECC1L::NTRK2* fusion. Torre et al. reported a cohort of gliomas harboring *NTRK* fusions, most infantile or adult cases were histologically high-grade (89.7%, 26/29), while pediatric cases demonstrated high-grade histology (15.4%, 2/13) were rare. The median follow-up period after diagnosis was 23 months. During the follow-up period, 57.0% of the cases suffered tumor recurrence or progression (28).

IDH1/2 mutations are rare in DNTs, different from low-grade diffuse gliomas. In a cohort of 100 DNTs, 3 *IDH1* mutations were observed (19). Jayapalan (29) reported a rosette-forming glioneuronal tumor with *IDH1* mutation, which recurred *in situ* and progressed to glioblastoma 6 years after partial resection. Authors speculated that *IDH1* mutation may lead to the malignant transformation of this type of benign glioneuronal tumor. Nevertheless, the biological and prognostic implications of *IDH1/2* mutations in DNTs remain to be clarified.

In conclusion, we report a rare DNT with a novel *LHFPL3::NTRK2* fusion and an *IDH1* mutation. These findings provide additional evidence for a heterogeneous genomic profile of DNTs. Further functional evaluation of the *LHFPL3::NTRK2* fusion oncoprotein will not only detail the oncogenic signaling mechanism but also shed light on the cellular function of *LHFPL3*, a CNS-specifically expressed gene with no studies.

Data availability statement

The original contributions presented in the study are included in the article/Supplementary Material. Further inquiries can be directed to the corresponding author.

Ethics statement

This study was reviewed and approved by the Ethics Committee of the Second Affiliated Hospital of Soochow University. Written informed consent to participate in this study was provided by the participant herself.

Author contributions

YC designed this study. XD, PC, SuZ, and ShZ performed histopathological and molecular pathological examinations. XD and SX were responsible for the pathological diagnosis. QZ, YW, AC, and CD supported clinical data. QL and SX guided this work. All authors contributed to the article and approved the submitted version.

Funding

Conflict of interest

Authors PC, SuZ, and ShZ were employed by Suzhou Sano Precision Medicine Ltd.

The remaining authors declare that the research was conducted in the absence of any commercial or financial relationships that could be construed as a potential conflict of interest.

Publisher's note

All claims expressed in this article are solely those of the authors and do not necessarily represent those of their affiliated organizations, or those of the publisher, the editors and the reviewers. Any product that may be evaluated in this article, or claim that may be made by its manufacturer, is not guaranteed or endorsed by the publisher.

References

1. Vaishnavi A, Le AT, Doebele RC. TRKing down an old oncogene in a new era of targeted therapy. *Cancer Discov* (2015) 5:25–34. doi: 10.1158/2159-8290.CD-14-0765

2. Gambella A, Senetta R, Collemi G, Vallero SG, Monticelli M, Cofano F, et al. NTRK fusions in central nervous system tumors: A rare, but worthy target. *Int J Mol Sci* (2020) 21(3):1–24. doi: 10.3390/ijms21030753

3. Solomon JP, Benayed R, Hechtman JF, Ladanyi M. Identifying patients with NTRK fusion cancer. *Ann Oncol* (2019) 30:viii16–22. doi: 10.1093/annonc/mdz384

4. Cocco E, Scaltriti M, Drilon A. NTRK fusion-positive cancers and TRK inhibitor therapy. *Nat Rev Clin Oncol* (2018) 15(12):731–47. doi: 10.1038/s41571-018-0113-0

5. Petit MMR, Schoenmakers EFPM, Huysmans C, Geurts JMW, Mandahl N, Van De Ven WJM. LHFP, a novel translocation partner gene of HMGIC in a lipoma, is a member of a new family of LHFP-like genes. *Genomics* (1999) 57:438–41. doi: 10.1006/geno.1999.5778

6. Lerat J, Bonnet C, Cartault F, Loundon N, Jacquemont ML, Darcel F, et al. High prevalence of congenital deafness on reunion island is due to a founder variant of LHFPL5. *Clin Genet* (2019) 95:177–81. doi: 10.1111/cge.13460

7. Louis DN, Perry A, Wesseling P, Brat DJ, Cree IA, Figarella-Branger D, et al. The 2021 WHO classification of tumors of the central nervous system: a summary. *Neuro Oncol* (2021) 23(8):1231–51. doi: 10.1093/neuonc/noab106

8. Blumcke I, Aronica E, Urbach H, Alexopoulos A, Gonzalez-Martinez JA. A neuropathology-based approach to epilepsy surgery in brain tumors and proposal for a new terminology use for long-term epilepsy-associated brain tumors. *Acta Neuropathologica* (2014) 128:39–54. doi: 10.1007/s00401-014-1288-9

9. Daumas-Duport C, Scheithauer BW, Chodkiewicz J-P, Laws ER, Vedrenne C. Dysembryoplastic neuroepithelial tumor: A surgically curable tumor of young patients with intractable partial seizures. *Neurosurgery* (1988) 23:545–56. doi: 10.1227/00006123-198811000-00002

10. Sontowska I, Matyja E, Malejczyk J, Grajkowska W. Dysembryoplastic neuroepithelial tumour: insight into the pathology and pathogenesis. *Folia Neuropathol* (2017) 55(1):1–13. doi: 10.5114/fn.2017.66708

11. Caporalini C, Scagnet M, Moscardi S, Di Stefano G, Baroni G, Giordano F, et al. Dysembryoplastic neuroepithelial tumors: A single-institutional series with special reference to glutamine synthetase expression. *Ann Diagn Pathol* (2021) 54:151774. doi: 10.1016/j.anndiagpath.2021.151774

12. Surrey LF, Jain P, Zhang B, Straka J, Zhao X, Harding BN, et al. Genomic analysis of dysembryoplastic neuroepithelial tumor spectrum reveals a diversity of molecular alterations dysregulating the MAPK and PI3K/mTOR pathways. *J Neuropathol Exp Neurol* (2019) 78(12):1100–11. doi: 10.1093/jnen/nlz101

13. Lee D, Cho YH, Kang SY, Yoon N, Sung CO, Suh Y-L. BRAF V600E mutations are frequent in dysembryoplastic neuroepithelial tumors and subependymal giant cell astrocytomas. *J Surg Oncol* (2015) 111:359–64. doi: 10.1002/jso.23822

14. Amatu A, Sartore-Bianchi A, Siena S. NTRK gene fusions as novel targets of cancer therapy across multiple tumour types. *ESMO Open* (2016) 1:e000023. doi: 10.1136/esmoopen-2015-000023

15. Lan Q, Chen Y, Dai C, Li S, Fei X, Dong J, et al. Novel enhanced GFP-positive congenic inbred strain establishment and application of tumor-bearing nude mouse model. *Cancer Sci* (2020) 111(10):3626–38. doi: 10.1111/cas.14545

16. Panagopoulos I, Gorunova L, Andersen HK, Pedersen TD, Lomo J, Lund-Iversen M, et al. Genetic characterization of myoid hamartoma of the breast. *Cancer Genomics Proteomics* (2019) 16(6):563–8. doi: 10.21873/cgp.20158

17. Chen Y, Wang Y, He Q, Wang W, Zhang T, Wang Z, et al. Integrative analysis of TP73 profile prognostic significance in WHO grade II/III glioma. *Cancer Med* (2021) 10(13):4644–57. doi: 10.1002/cam4.4016

18. Blümcke I, Wiestler OD. Gangliogliomas: An intriguing tumor entity associated with focal epilepsies. *J Neuropathol Exp Neurol* (2002) 61:575–84. doi: 10.1093/jnen/61.7.575

19. Thom M, Toma A, An S, Martinian L, Hadjivassiliou G, Ratilal B, et al. One hundred and one dysembryoplastic neuroepithelial tumors: An adult epilepsy series with immunohistochemical, molecular genetic, and clinical correlations and a review of the literature. *J Neuropathol Exp Neurol* (2011) 70:859–78. doi: 10.1097/NEN.0b013e3182302475

20. Rivera B, Gayden T, Carrot-Zhang J, Nadaf J, Boshari T, Faury D, et al. Germline and somatic FGFR1 abnormalities in dysembryoplastic neuroepithelial tumors. *Acta Neuropathol* (2016) 131(6):847–63. doi: 10.1007/s00401-016-1549-x

21. Kakkar A, Majumdar A, Kumar A, Tripathi M, Pathak P, Sharma MC, et al. Alterations in BRAF gene, and enhanced mTOR and MAPK signaling in dysembryoplastic neuroepithelial tumors (DNTs). *Epilepsy Res* (2016) 127:141–51. doi: 10.1016/j.eplepsyres.2016.08.028

22. Blumcke I, Coras R, Wefers AK, Capper D, Aronica E, Becker A, et al. Review: Challenges in the histopathological classification of ganglioglioma and DNT: microscopic agreement studies and a preliminary genotype-phenotype analysis. *Neuropathol Appl Neurobiol* (2019) 45(2):95–107. doi: 10.1111/nan.12522

23. Blumcke I, Aronica E, Becker A, Capper D, Coras R, Honavar M, et al. Low-grade epilepsy-associated neuroepithelial tumours - the 2016 WHO classification. *Nat Rev Neurol* (2016) 12(12):732–40. doi: 10.1038/nrneurol.2016.173

24. Matsumura N, Nobusawa S, Ito J, Kakita A, Suzuki H, Fujii Y, et al. Multiplex ligation-dependent probe amplification analysis is useful for detecting a copy number gain of the FGFR1 tyrosine kinase domain in dysembryoplastic neuroepithelial tumors. *J Neurooncol* (2019) 143(1):27–33. doi: 10.1007/s11060-019-03138-7

25. Boyer J, Birzu C, Bielle F, Goulas C, Savatovsky J, Karachi C, et al. Dramatic response of STRN-NTRK -fused malignant glioneuronal tumor to larotrectinib in adult. *Neuro-Oncology* (2021) 23:1200–2. doi: 10.1093/neuonc/noab080

26. Kurozumi K, Nakano Y, Ishida J, Tanaka T, Doi M, Hirato J, et al. High-grade glioneuronal tumor with an ARHGEF2-NTRK1 fusion gene. *Brain Tumor Pathol* (2019) 36(3):121–8. doi: 10.1007/s10014-019-00345-y

27. Alvarez-Breckenridge C, Miller JJ, Nayyar N, Gill CM, Kaneb A, D'Andrea M, et al. Clinical and radiographic response following targeting of BCAN-NTRK1 fusion in glioneuronal tumor. *NPJ Precis Oncol* (2017) 1(1):5. doi: 10.1038/s41698-017-0009-y

28. Torre M, Vasudevaraja V, Serrano J, DeLorenzo M, Malinowski S, Blandin AF, et al. Molecular and clinicopathologic features of gliomas harboring NTRK fusions. *Acta Neuropathol Commun* (2020) 8(1):107. doi: 10.1186/s40478-020-00980-z

29. Jayapalan RR, Mun KS, Wong KT, Sia SF. Malignant transformation of a rosette-forming glioneuronal tumor with IDH1 mutation: A case report and literature review. *World Neurosurg X* (2019) 2:100006. doi: 10.1016/j.wnsx.2018.100006

A case report of *CIC–DUX4* fusion-positive sarcoma in the pelvic cavity with targeted next-generation sequencing results

Qian Wu[1,2,3] and Ying He[1,2,3]*

[1]Department of Pathology, West China Second Hospital of Sichuan University, Chengdu, Sichuan, China, [2]Key Laboratory of Birth Defects and Related Diseases of Women and Children (Sichuan University), Ministry of Education, Chengdu, Sichuan, China, [3]NHC Key Laboratory of Chronobiology (Sichuan University), Chengdu, Sichuan, China

CIC–DUX4 fusion-positive sarcoma is a subtype of undifferentiated small round cell sarcoma that is rarely reported. As far as we know, less than 200 cases have been reported worldwide to date. The clinicopathologic characteristics of this kind of tumor are non-specific, which makes it difficult to be diagnosed. Therefore, more cases are required to enrich the diagnosis and treatment experience. Here, we present a 17-year-old Asian girl diagnosed with *CIC–DUX4* fusion-positive sarcoma after targeted next-generation sequencing. Her clinical manifestation was abdominal pain. Furthermore, a mass in the pelvic cavity and massive ascites were found after an imaging examination. After resection, the mass was sent to the pathology department for a definite diagnosis, and the micromorphology showed an undifferentiated sarcoma with massive necrosis. The tumor cells were round to spindle with clear to eosinophilic cytoplasm and vesicular nuclei. Rhabdoid cells and myxoid mesenchyme were focally shown. Immunohistochemical staining showed diffusely positive for vimentin, cyclin D1, Fli-1, and WT-1 and very focally positive for CD99. Moreover, the targeted next-generation sequencing also revealed other genetic changes in this tumor including LongInDel of *POLE*, copy number variation of *CD79*, low tumor mutational burden, and microsatellite stability. With a follow-up time of 6 months, the patient survived the disease and received chemotherapy routinely. This report presented a rare primary site CIC–DUX4 fusion-positive sarcoma (CDS) and revealed novel genetic changes that enrich the manifestation, histology, and cytogenetic scales of this rare sarcoma. In addition, we have summarized the clinicopathologic characteristics of this tumor by reviewing the literature to have a better understanding of *CIC–DUX4* fusion-positive sarcomas, which may be helpful for diagnosis and treatment.

KEYWORDS

CIC–DUX4, undifferentiated small round cell sarcoma, target next generation sequencing, low tumor mutational burden, *POLE*

Introduction

Undifferentiated small round cell sarcomas (USRCSs) are a group of tumors with similar morphology, which makes it difficult to identify and diagnose. However, with the rapidly developing molecular pathology, it is possible to clarify them by genetic changes. *CIC*-rearranged sarcoma is one of the new tumor types of the USRCS, which used to be considered Ewing-like sarcoma.

Somers et al. (1) presented a case of an unusual and more aggressive cutaneous and subcutaneous primitive neuroectodermal tumor/Ewing sarcoma (PNET/ES), which showed a complex karyotype with t(4;19)(q33~q35;q13.1). Two years later, Kawamura-Saito et al. (2) found a recurrent chromosomal translocation t(4;19)(q35;q13) in two cases and recognized the fusion of *CIC–DUX4*. Afterward, Italiano et al. implicated that *CIC* was fused to copies of *DUX4* gene not only on 4q35 but also on 10q26.3 (3). Moreover, more fusion partners of *CIC* were found, such as *FOXO4* (4, 5) and *NUTM1* (6, 7). More cases were included to summarize the characteristics of this kind of tumor and showed a distinct immunoprofile, karyotype, and worse outcome as compared to ES (8, 9), suggesting that it was a new pathologic entity.

To date, more than 200 cases of *CIC*-rearranged sarcoma have been reported, among which the *CIC–DUX4* was the most common fusion (1–3, 7–32). Here, we report a case of *CIC–DUX4* fusion-positive sarcoma (CDS) arising in the pelvic cavity of a 17-year-old girl with targeted next-generation sequencing results, which enriches the manifestation, histology, and cytogenetic scales of this rare sarcoma.

Case report

A 17-year-old Asian girl came to the hospital with complaints of abdominal pain. A computed tomography (CT) scan showed a cystic and solid mass measured 12.1 cm × 8.2 cm × 13.6 cm in the pelvic cavity with heterogeneous enhancement in an enhanced scan (Figure 1). Ultrasound detected fluid dark areas in multiple abdominal spaces. The serum level of carbohydrate antigen 125 was 447.6 U/ml. After adequate evaluation and preparation, the patient received surgery. During the surgery, ascites with a volume of 3,000 ml were drained from the abdominal cavity. Both the mass and ascites were sent for pathologic examination.

Grossly, the tumor showed a fused-nodular mass with an appearance of color and a touch of tenderness when being cut. The histological examination demonstrated the tumor consisted of round to spindle malignant cells with clear to eosinophilic cytoplasm and vesicular nuclei. Rhabdoid cells and myxoid mesenchyme were focally shown. Moreover, necrosis and pathologic mitoses were apparent (Figures 2A–F). Tumor cells were also detected in the peritoneal lavage. Immunohistochemical (IHC) staining showed diffusely positive for vimentin, Fli-1, cyclin D1, and WT-1 and very focally positive for CD99 (Figures 2G–I). Pan-CK, ER, PR, CD117, DOG-1, NSE, Syn, CD34, S100, desmin, caldesmon, CD10, and Sall-4 were all negative. The index of Ki-67 was >90%.

For diagnosis and further treatment strategy, the paraffin section of the tumor was sent for targeted next-generation sequencing (NGS) on the Illumina platform. The exons of 672 and 633 genes were detected by DNA sequencing and RNA sequencing, respectively. The results were as follows: 1) fusion between *CIC* exon 20 and *DUX4* exon 1 (Figure 3A), 2) LongInDel of *POLE* (exon22_exon31del) (Figure 3B), 3) copy number variation (CNV) of *CD79A* (5.8 copies), 4) low tumor mutational burden (TMB) at 0.5 Muts/Mb, and 5) microsatellite stability (MSS). Finally, this tumor was diagnosed as CDS.

After the surgery, the patient went to another medical institution for further treatment. At a follow-up of 6 months, the patient was still alive.

Discussion

In the latest (2020) World Health Organization (WHO) classification of tumors of soft tissue and bone, *CIC*-rearranged sarcomas were categorized as a new entity of USRCS (33). So far,
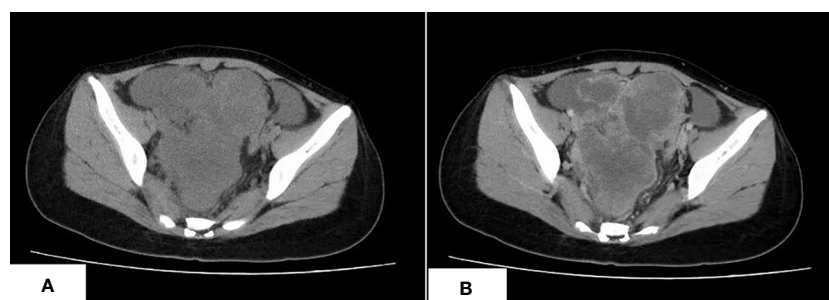
FIGURE 1
The CT scan of CDS. **(A)** An irregular lobulated mass in pelvic cavity, which has unclear margin with peripheral structure, is shown. **(B)** The tumor shows heterogeneous enhancement in the contrast-enhanced CT scan.
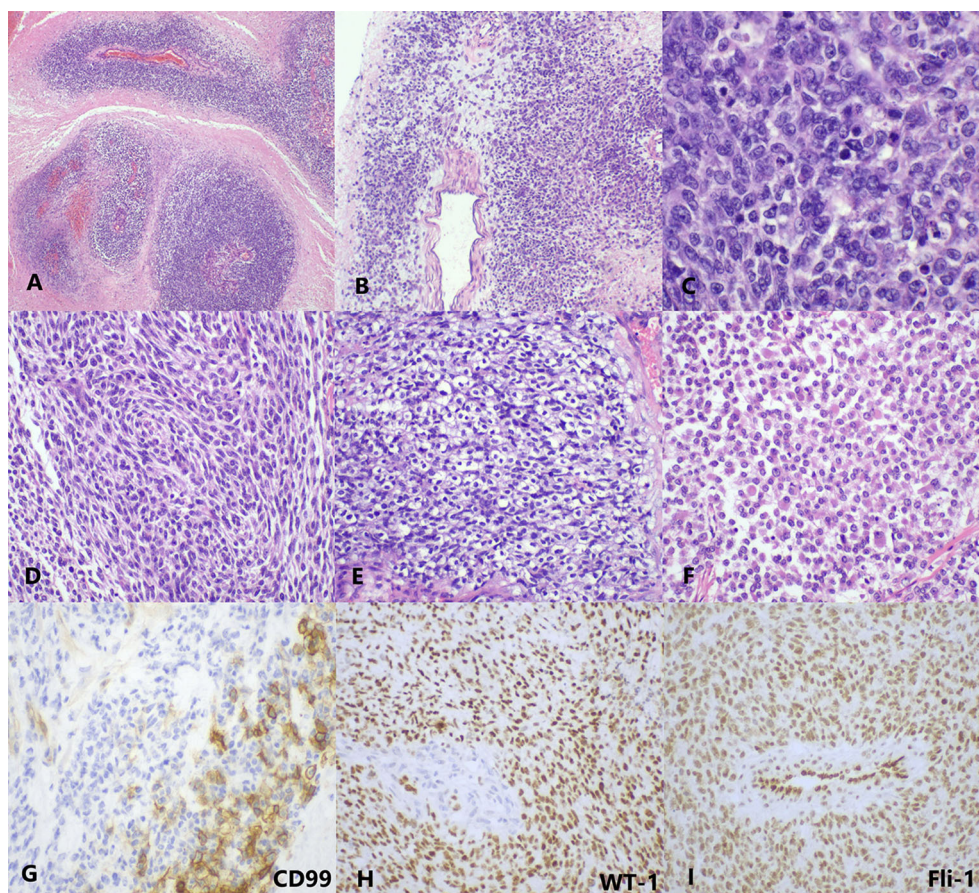
FIGURE 2

The histopathology and immunohistology of CDS. **(A)** At low magnification, the tumor cells are separated by massive necrosis, arranged in nest-like and perivascular (H&E, ×40). **(B)** Focal myxoid stroma (H&E, ×40). **(C)** At high magnification, the tumor cells show round-to-oval shape with lightly eosinophilic cytoplasm and vesicular nuclei; several mitotic figures are visible (H&E, ×400). Moreover, **(D)** spindle cell-like (H&E, ×200), **(E)** clear cell-like (H&E, ×200), and **(F)** rhabdoid plasmacytoid tumor cells (H&E, ×200) are also exhibited in some areas. **(G)** CD99 is focally membranous positive (IHC, ×400). **(H)** WT-1 (IHC, ×200) and **(I)** Fli-1 (IHC, ×200) are diffusely nuclear positive. IHC, immunohistochemistry.

less than 200 cases have been reported, including 157 cases of CDS, among which 88 cases are available for clinicopathologic information. The age ranged from 8 to 69 years (average at 30.7 and median at 29.5). Gender, 41 male (46.6%) and 47 female (53.4%), did not yield much difference. The most common primary sites are the soft tissue of the limbs (43/88, 48.9%), followed by the soft tissue of the trunk (35/88, 39.8%) and parenchymal organs (7/88, 7.9%). Only three cases originated from bones (3/88, 3.4%) (18, 26), which was distinguished from ES. Only two cases arose from the pelvic cavity: one is a 45-year-old man, and the other is the current case report. The maximum diameter of tumors was mentioned in 35 cases, which ranged from 1.5 to 20 cm (mean at 8.2 cm and median at 8 cm). The manifestations are usually not special, mostly occasionally discovery of mass. However, some unique manifestations are also reported, such as mimicking a phlegmon (27), cardiac tamponade (31), vaginal bleeding (28), and massive ascites in this report, which are caused by the tumor

invasion of particular organs. The most common metastasis organ of CDS is the lung, followed by the brain and liver.

For morphology, the typical CDS usually consists of undifferentiated small round-to-oval tumor cells with clear to eosinophilic cytoplasm and vesicular nucleus, arranged in sheets and nests. Pathologic mitoses and geographic necrosis are easy to see. Focal myxoid matrix (1, 3, 7–9, 11, 13, 14, 18, 25, 26, 30) and spindle tumor cells (3, 8–11, 14, 18, 19, 21, 27) are also reported in some studies. Other less common morphologies include rhabdoid appearance or plasmacytoid appearance (3, 9, 12, 18, 19, 25, 32), epithelioid (18, 32), formation of microcystic spaces or pseudoacinar arrangements (8, 9, 15, 21, 23, 32), or single cell cords (13). There is one case in that focal hyaline cartilage formations appeared after chemotherapy (19).

During immunohistochemistry, almost all CDS showed vimentin positivity, and most showed weak and focal membranous CD99 positivity. Specht et al. (8) found that WT-1
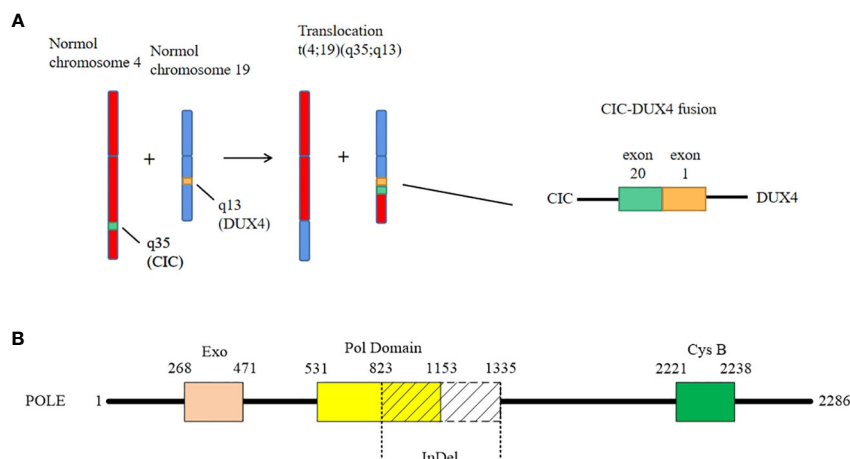
FIGURE 3

The genetic changes of the case. **(A)** The case shows a classical fusion of *CIC–DUX4*, which is generated by translocation of chromosome t (4;19)(q35;q13). The breakpoints are located in exon 20 of *CIC* and exon 1 of *DUX4*, respectively. **(B)** The LongInDel of *POLE* (exon22_exon31del) causes deletion of amino acid residues 823–1,335 of POLE protein, which may lead to frameshift and loss of polymerase domain 25 and CysB motif (amino acid residues 2,221–2,238).

was strongly positive in all CDS cases but negative in all ES cases. Therefore, they proposed that consistent WT-1 expression might provide a useful clue in the diagnosis of CDS. However, it may be a pitfall in diagnosis when CDS is primarily in the kidney. There is a report that a renal CDS was originally diagnosed as a stromal Wilms tumor (WT) because of the expression of WT-1 and rare recognition of CDS (21). In addition, CDS also frequently expresses Fli-1 and ERG, the ETS transcription factor family members (14). Cytokeratin is usually very focal positive. Bcl-2 positivity (3, 20, 21), ETV4 positivity (24), and C-MYC protein expression (15) were also reported. Moreover, Yoshimoto and his colleagues found that cyclin D2 and MUC5AC were novel biomarkers and were useful for distinguishing CDS from ES (34).

For diagnosis, although clinical, histological, and immunochemical characteristics of CDS are well recognized, none of them are entirely sensitive or specific. Therefore, a molecular testing result of *CIC–DUX4* fusion is necessary to reach the final diagnosis. Fluorescence *in situ* hybridization (FISH) and targeted RNA sequencing are the most popular methods to detect *CIC* rearrangement. However, Yoshida et al. described four cases that showed negative results by CIC break-apart FISH assays but identified *CIC–DUX4* and its fusion breakpoint through high-throughput RNA sequencing (24), suggesting there may be a false-negative rate for FISH to detect CDS. Moreover, ETV transcriptional upregulation (22), DNA methylation profiling, and next-generation sequencing (29) were suggested to be more sensitive than FISH and RNA sequencing. Therefore, when histology and immunoprofiles highly indicate the diagnosis of CDS but the result of FISH or RNA sequencing is negative, conclusions must not be drawn yet; it is necessary to consider another detection technique.

For pathogenesis, Kawamura-Saito and his colleagues found that *CIC–DUX4* protein transforms NIH 3T3 cells and is a strong transcriptional activator that upregulates *PEA3* family genes (2). Other researchers revealed that *CIC–DUX4* sarcomas demonstrate frequent *MYC* amplification and ETS-family transcription factor expression (14). These studies uncovered the downstream targets of *CIC–DUX4* protein. Subsequently, the upstream factors were found by Lin et al. (35), who suggested that negative *MAPK-ERK* regulation sustained *CIC–DUX4* oncoprotein expression. Moreover, targeted NGS was also performed to characterize potential somatic driver alterations of CDS. Vega et al. analyzed 11 CDS cases by targeted NGS. Although no recurrent somatic mutations were identified, they detected low mutational burden and recurrent chromosome 1p loss (36). Other researchers also found a low mutational burden by targeted NGS, as well as stable microsatellite status (28), which is consistent with this report. However, we found mutations of *POLE* and *CD79A*, which have not been reported before. Moreover, Ricker and her colleagues noticed the overexpression of the translation factor *eEF1A1* when whole-genome sequencing and RNA sequencing were performed in a case of CDS (30) (Table 1). Furthermore, cell lines were established for drug sensitivity tests, and bortezomib, crizotinib (37), and inhibition of the CCNE–CDK2 complex (38) seemed to be able to suppressed the growth of CDS cells. However, more studies are needed to better understand this rare sarcoma.

What is worthy to be mentioned is that we found a novel mutation of *POLE*. It is well known that exonuclease domain mutations of *POLE* were mostly reported in some epithelial tumors such as colorectal cancer and endometrial carcinoma, which lead to a deficiency of proofreading activity and usually

TABLE 1 The summary of studies about next-generation sequencing (NGS) of *CIC−DUX4* sarcomas.

Authors	Case(s)	Methods	Discoveries
Vega et al.	11	Targeted NGS (409 genes)	1) Low mutational burden 2) Recurrent chromosome 1p loss 3) *ARID1A* R963X non-sense mutation in a recurrence sample
Sedighim et al.	1	Targeted NGS	1) Low mutational burden 2) Stable microsatellite status
Ricker et al.	1	Whole-genome sequencing and RNA sequencing	Overexpression of the translation factor *eEF1A1*
This report	1	Targeted NGS (672 genes) and RNA sequencing (633 genes)	1) *POLE* exon 22–exon 31 LongIndel 2) *CD79A* copy number variation (CNV) 3) Low mutational burden 4) Stable microsatellite status

NGS, next-generation sequencing.

high TMB ([39]). However, in this case, the mutation of *POLE* is LongInDel from exon 22 to exon 31 (823–1,335 amino acid residues), which causes the loss of part of the polymerase domain and CysB motif (2,221–2,238 amino acid residues) ([Figure 3B]). The site of mutation is beyond the exonuclease domain, which means it is a non-proofreading mutation. A study suggested that tumors with *POLE* proofreading mutation showed a significantly higher TMB than tumors with non-proofreading mutations ([40]), which may explain why this sarcoma has a *POLE* mutation but low TMB. Moreover, we revealed the CNV of *CD79A*, which may lead to the increase of its mRNA and protein expression levels and influence the B lymphocyte antigen. However, the significance of these mutations needs more exploration in the future.

Conclusions

We report a case of CDS arising from the pelvic cavity, which is a rare primary site for the tumor. Moreover, the results of the targeted NGS, which is LongInDel of *POLE* and CNV of *CD79A*, were the first to be reported. Therefore, our case enriches the clinical and genetic scales of CDS.

Data availability statement

The original contributions presented in the study are included in the article/supplementary materials. Further inquiries can be directed to the corresponding author.

Ethics statement

Ethical review and approval were not required for the study on human participants in accordance with the local legislation and institutional requirements. Written informed consent was obtained from the minor(s)' legal guardian/next of kin for the publication of any potentially identifiable images or data included in this article.

Author contributions

QW wrote the manuscript. YH diagnosed the case and revised the manuscript. Both authors contributed to the article and approved the submitted version.

Funding

Conflict of interest

The authors declare that the research was conducted in the absence of any commercial or financial relationships that could be construed as a potential conflict of interest.

Publisher's note

All claims expressed in this article are solely those of the authors and do not necessarily represent those of their affiliated organizations, or those of the publisher, the editors and the reviewers. Any product that may be evaluated in this article, or claim that may be made by its manufacturer, is not guaranteed or endorsed by the publisher.

References

1. Somers GR, Shago M, Zielenska M, Chan H, Bo YN. Primary subcutaneous primitive neuroectodermal tumor with aggressive behavior and an unusual karyotype: Case report. *Pediatr Dev Pathol* (2004) 7:538–45. doi: 10.1007/s10024-004-2024-6

2. Kawamura-Saito M, Yamazaki Y, Kaneko K, Kawaguchi N, Kanda H, Mukai H, et al. Fusion between CIC and DUX4 up-regulates PEA3 family genes in Ewing-like sarcomas with t (4,19)(q35;q13) translocation. *Hum Mol Genet* (2006) 15:2125–37. doi: 10.1093/hmg/ddl136

3. Italiano A, Yun SS, Lei Z, Singer S, Maki RG, Coindre JI, et al. High prevalence of CIC fusion with double-homeobox (DUX4) transcription factors in EWSR1-negative undifferentiated small blue round cell sarcomas. *Genes Chromosomes Cancer* (2012) 51:207–18. doi: 10.1002/gcc.20945

4. Sugita S, Arai Y, Tonooka A, Hama N, Totoki Y, Fujii T, et al. A novel CIC-FOXO4 gene fusion in undifferentiated small round cell sarcoma: a genetically distinct variant of Ewing-like sarcoma. *Am J Surg Pathol* (2014) 38:1571–6. doi: 10.1097/PAS.0000000000000286

5. Solomon DA, Brohl AS, Khan J, Miettinen M. Clinicopathologic features of a second patient with Ewing-like sarcoma harboring CIC-FOXO4 gene fusion. *Am J Surg Pathol* (2014) 38:1724–5. doi: 10.1097/PAS.0000000000000335

6. Le Loarer F, Pissaloux D, Watson S, Godfraind C, Galmiche-Rolland L, Silva K, et al. Clinicopathologic features of CIC-NUTM1 sarcomas, a new molecular variant of the family of CIC-fused sarcomas. *Am J Surg Pathol* (2019) 43:268–76. doi: 10.1097/PAS.0000000000001187

7. Yan Y, Liu L, Kong F, Yan T, Shen D. Clinicopathological and molecular genetic features of 72 cases of small round cell sarcoma of bone and soft tissue. *CH J Pathol* (2021) 50:919–23. doi: 10.3760/cma.j.cn112151-20201108-00833

8. Specht K, Sung YS, Zhang L, Richter G, Fletcher CD, Antonescu CR. Distinct transcriptional signature and immunoprofile of CIC-DUX4 fusion–positive round cell tumors compared to EWSR1-rearranged ewing sarcomas: Further evidence toward distinct pathologic entities. *Genes Chromosomes Cancer* (2014) 53:622–33. doi: 10.1002/gcc.22172

9. Antonescu CR, Owosho AA, Zhang L, Chen S, Deniz K, Huryn JM, et al. Sarcomas with CIC-rearrangements are a distinct pathologic entity with aggressive outcome: A clinicopathologic and molecular study of 115 cases. *Am J Surg Pathol* (2017) 41:941–9. doi: 10.1097/PAS.0000000000000846

10. Rakheja D, Goldman S, Wilson KS, Lenarsky C, Schultz RA. Translocation (4;19)(q35;q13.1)–associated primitive round cell sarcoma: Report of a case and review of the literature. *Pediatr Dev Pathol* (2008) 11:239–44. doi: 10.2350/07-06-0296.1

11. Graham C, Chilton-Macneill S, Zielenska M, Somers GR. The CIC-DUX4 fusion transcript is present in a subgroup of pediatric primitive round cell sarcomas. *Hum Pathol* (2012) 43:180–9. doi: 10.1016/j.humpath.2011.04.023

12. Machado I, Cruz J, Lavernia J, Rubio L, Campos J, Barrios M, et al. Superficial EWSR1-negative undifferentiated small round cell sarcoma with CIC/DUX4 gene fusion: a new variant of Ewing-like tumors with locoregional lymph node metastasis. *Virchows Archiv* (2013), 463; 837–42. doi: 10.1007/s00428-013-1499-9

13. Choi E, Thomas DG, Mchugh JB, Patel RM, Lucas DR. Undifferentiated small round cell sarcoma with t(4;19)(q35;q13.1) CIC-DUX4 fusion: a novel highly aggressive soft tissue tumor with distinctive histopathology. *Am J Surg Pathol* (2013) 37:1379–86. doi: 10.1097/PAS.0b013e318297a57d

14. Smith SC, Buehler D, Choi E-YK, McHugh JB, Rubin BP, Billings SD, et al. CIC-DUX sarcomas demonstrate frequent MYC amplification and ETS-family transcription factor expression. *Modern Pathol* (2015), 28; 57–68. doi: 10.1038/modpathol.2014.83

15. Tardío JC, Machado I, Navarro L, Idrovo F, Sanz-Ortega J, Pellín A, et al. Ewing-Like sarcoma with CIC-DUX4 gene fusion in a patient with neurofibromatosis type 1. a hitherto unreported association. *Pathol - Res Pract* (2015) 211:1–6. doi: 10.1016/j.prp.2015.08.003

16. Haidar A, Arekapudi S, DeMattia F, Abu-Isa E, Kraut M. High-grade undifferentiated small round cell sarcoma with t(4;19)(q35;q13.1) CIC-DUX4 fusion: Emerging entities of soft tissue tumors with unique histopathologic features – a case report and literature review. *Am J Case Rep* (2015) 16:87–94. doi: 10.12659/AJCR.892551

17. Chebib I, Vickie Y. Round cell sarcoma with CIC-DUX4 gene fusion: Discussion of the distinctive cytomorphologic, immunohistochemical, and molecular features in the differential diagnosis of round cell tumors. *Cancer Cytopathol* (2016) 124:350–61. doi: 10.1002/cncy.21685

18. Gambarotti M, Benini S, Gamberi G, Cocchi S, Palmerini E, Sbaraglia M, et al. CIC-DUX4 fusion-positive round-cell sarcomas of soft tissue and bone: a single-institution morphological and molecular analysis of seven cases. *Histopathol* (2016) 69:624–34. doi: 10.1111/his.12985

19. Yoshida A, Goto K, Kodaira M, Kobayashi E, Kawai A. CIC-rearranged sarcomas: A study of 20 cases and comparisons with Ewing sarcomas. *Am J Surg Pathol* (2015) 40:313–23. doi: 10.1097/PAS.0000000000000570

20. Bergerat S, Barthelemy P, Mouracade P, Lang H, Saussine C, Lindner V, et al. Primary CIC-DUX4 round cell sarcoma of the kidney: A treatment-refractory tumor with poor outcome. *Pathol Res Pract* (2017) 213:154–60. doi: 10.1016/j.prp.2016.11.015

21. Mangray S, Somers GR, He J, Zhong S, Shago M, Treaba DO, et al. Primary undifferentiated sarcoma of the kidney harboring a novel variant of CIC-DUX4 gene fusion. *Am J Surg Pathol* (2016) 40:1298. doi: 10.1097/PAS.0000000000000688

22. Kao Y-C, Sung Y-S, Chen C-L, Zhang L, Dickson BC, Swanson D, et al. ETV transcriptional upregulation is more reliable than RNA sequencing algorithms and FISH in diagnosing round cell sarcomas with CIC gene rearrangements. *Gene Chromo Canc* (2017) 56:501–10. doi: 10.1002/gcc.22454

23. Owosho AA, Estilo CL, Huryn JM, Zhang L, Fletcher CDM, Antonescu CR. Head and neck round cell sarcomas: A comparative clinicopathologic analysis of 2 molecular subsets: Ewing and CIC-rearranged sarcomas. *Head Neck Pathol* (2017) 11:450–9. doi: 10.1007/s12105-017-0808-z

24. Yoshida A, Arai Y, Kobayashi E, Yonemori K, Ogura K, Hama N, et al. CIC break-apart fluorescence in-situ hybridization misses a subset of CIC-DUX4 sarcomas: a clinicopathological and molecular study. *Histopathol Off J Br Division Int Acad Pathol* (2017) 71: 461–469. doi: 10.1111/his.13252

25. Donahue JE, Yakirevich E, Zhong S, Treaba DO, Lakis NS, Ali SM, et al. Primary spinal epidural CIC-DUX4 undifferentiated sarcoma in a child. *Pediatr Devel Pathol* (2018) 4:411–7. doi: 10.1177/1093526617707856

26. Brcic I, Brodowicz T, Cerroni L, Kashofer K, Serbanescu GL, Kasseroler MT, et al. Undifferentiated round cell sarcomas with CIC-DUX4 gene fusion: expanding the clinical spectrum. *Pathol* (2020) 52:236–42. doi: 10.1016/j.pathol.2019.09.015

27. Donthi D, Malik P, Prenshaw KL, Hong H. A rare case of round cell sarcoma with CIC-DUX4 mutation mimicking a phlegmon: Review of literature. *Am J Case Rep* (2020) 21:1–4. doi: 10.12659/AJCR.925683

28. Sedighim S, Burke J, Schneider D, Kamdjou T, Diaz-Perez JA, Trent J, et al. CIC-rearranged round cell (Ewing-like) sarcoma of the uterus: Review of the literature. *Gyneco Oncol Rep* (2020) 33:100592. doi: 10.1016/j.gore.2020.100592

29. Miele E, Vito RD, Ciolfi A, Pedace L, Russo I, Pasquale MDD, et al. DNA Methylation profiling for diagnosing undifferentiated sarcoma with capicua transcriptional receptor (CIC) alterations. *Int J Mol Sci* (2020) 21:1818. doi: 10.3390/ijms21051818

30. Ricker CA, Berlow NE, Crawford KA, Georgopapadakos T, Huelskamp AN, Woods AD, et al. Undifferentiated small round cell sarcoma in a young male: a case report. *Mol Case Stud* (2020) 6:1–22. doi: 10.1101/mcs.a004812

31. Maekawa A, Matsunobu T, Nabeshima A, Fukushima S, Makihara K, Hisaoka M, et al. Cardiac tamponade as an unusual initial clinical manifestation of CIC-DUX4 sarcoma. *Am J Case Rep* (2021) 22:e929349. doi: 10.12659/AJCR.929349

32. Vieira AC, Xavier CB, Vieira TD, Carvalho FM, Scaranti M, Munhoz RR, et al. CIC-DUX4 rearranged uterine cervix round-cell sarcoma exhibiting near-complete pathologic response following radiation and neoadjuvant chemotherapy: A case report. *Gyneco Oncol Rep* (2021) 36:100745–5. doi: 10.1016/j.gore.2021.100745

33. Antonescu CR, Yoshida A. Undifferentiated small round cell sarcomas of bone and soft tissue/CIC-rearranged sarcoma. In: *WHO classification of tumours of soft tissue and bone 5th edition*, Lyon(France): International Agency for Research on Cancer 2020. vol. 3. (2020). p. 330.

34. Yoshimoto T, Tanaka M, Homme M, Yamazaki Y, Takazawa Y, Antonescu CR, et al. CIC-DUX4 induces small round cell sarcomas distinct from Ewing sarcoma. *Cancer Res* (2017) 77:2927–37. doi: 10.1158/0008-5472.CAN-16-3351

35. Kawe Lin Y, Wu W, Ponce RK, Kim JW, Okimoto RA. Negative MAPK-ERK regulation sustains CIC-DUX4 oncoprotein expression in undifferentiated sarcoma. *P Natl A Sci India B* (2020) 117:20776–84. doi: 10.1073/pnas.2009137117

36. Lazo de la Vega L, Hovelson DH, Cani AK, Liu C-J, McHugh JB, Lucas DR, et al. Targeted next-generation sequencing of CIC-DUX4 soft tissue sarcomas demonstrates low mutational burden and recurrent chromosome 1p loss. *Hum Pathol* (2016) 58:161–70. doi: 10.1016/j.humpath.2016.09.004

37. Oyama R, Takahashi M, Yoshida A, Sakumoto M, Takai Y, Kito F, et al. Generation of novel patient-derived CIC- DUX4 sarcoma xenografts and cell lines. *Sci Rep* (2017) 7:4712–2. doi: 10.1038/s41598-017-04967-0

38. Okimoto RA, Wu W, Nanjo S, Olivas V, Lin YK, Ponce RK, et al. CIC-DUX4 oncoprotein drives sarcoma metastasis and tumorigenesis *via* distinct regulatory programs. *J Clin Invest* (2019) 129:3401–6. doi: 10.1172/JCI126366

39. Kane DP, Shcherbakova PV. A common cancer-associated DNA polymerase ϵ mutation causes an exceptionally strong mutator phenotype, indicating fidelity defects distinct from loss of proofreading. *Cancer Res* (2014) 74:1895–901. doi: 10.1158/0008-5472.Can-13-2892

40. He J, Ouyang W, Zhao W, Shao L, Li B, Liu B, et al. Distinctive genomic characteristics in POLE/POLD1-mutant cancers can potentially predict beneficial clinical outcomes in patients who receive immune checkpoint inhibitor. *Ann Transl Med* (2021) 9:129. doi: 10.21037/atm-20-7553

Check for updates

Case report: Neurofibromatosis type 1 gastrointestinal stromal tumor and small bowel adenocarcinoma with a novel germline *NF1* frameshift mutation

Wuming Zhang[1,2,3], Xianqin Hu[1,2,3], Zhikang Chen[1,2,3] and Chen Lai[1,2,3]*

[1]Department of General Surgery, Xiangya Hospital of Central South University, Changsha, Hunan, China, [2]Hunan Key Laboratory of Precise Diagnosis and Treatment of Gastrointestinal Tumor, Xiangya Hospital of Central South University, Changsha, Hunan, China, [3]International Joint Research Center of Minimally Invasive Endoscopic Technology Equipment & Standardization, Xiangya Hospital of Central South University, Changsha, Hunan, China

A synchronous case of small bowel adenocarcinoma(SAB) is reported, accompanied with gastrointestinal stromal tumor(GIST),and gangliocytomain in an elderly woman with neurofibromatosis type 1 (NF-1). A 67-year-old female was hospitalized with the chief complaint of abdominal pain, the computed tomography scan indicated a large bowel mass. Multiple tumors were found in the small intestine, through which two larger tumors (7 cm and 1.5 cm) were resected. A novel germline *NF1* mutation and a *PMS2* mutation were identified after genetic testing, followed by the exploration of possible relationship between them in promoting tumorigenesis. Our results suggest multiple gastrointestinal tumors emerging in NF1 patients, and genetic testing can better guide postoperative treatment in a more efficient way.

KEYWORDS

NF1 mutation, NF-1 = neurofibromatosis type 1, small bowel adenocarcinoma, GIST - gastrointestinal stromal tumor, PMS2 gene

Introduction

Neurofibromatosis type 1(NF-1) occurs as an autosomal dominant genetic disease induced by a mutation in the *NF1* gene on chromosome 17 with an incidence of 1 in 3000 (1). The *NF1* gene spans approximately 280kb of genomic DNA, which is composed of 57 constitutive exons and 4 alternate splicing exons (9a, 10a2, 23a, and 48a), serving as a

cancer suppressor gene. *NF1* gene known to encode neurofibrin, accompanied with a functional domain, RAS-GAP. This domain plays a role in accelerating the conversion of active RAS-GTP to inactive RAS-GDP, acting as a negative regulator of RAS signaling pathway, which is involved in cell growth and differentiation (2). Neurofibromatosis type 1 is manifested by multiple flat, light-brown patches of skin pigment, skin fold freckling, visible neurofibromas under the skin and Lisch nodules (3).Severe complications, including learning disabilities, scoliosis, osteoporosis and malignancy may present, which can affect all parts of the body, followed by serious impacts on the physical and mental health of patients (4). Only neurofibromas with symptoms requires treatment. Large skin neurofibromas can be removed by surgery. While small and medium-sized neurofibromatosis can be treated with Carbon dioxide laser under anesthesia. The most recent treatments, such as Cabozantinib, is remaining in the experimental stage II (5).

Gastrointestinal stromal tumor (GIST) is a mesenchymal tumor developed from pacemaker cells in the gastrointestinal tract, called Cajal cells, which play an essential role in gastrointestinal peristalsis. Abdominal pain, gastrointestinal obstruction and upper gastrointestinal tract bleeding are presented as the primary manifestations of GIST (6).

Small bowel adenocarcinoma (SBA) occupies 40% of small bowel cancers with a low incidence rate of 7.3 per million people, mainly occurring in the duodenum, jejunum and ileum (7). SBA generally accompanied by local tumor complications. A duodenal SBA is often associated with gastric outlet obstruction, and a jejunal or ileal SBA with abdominal cramps, of which approximately 1/4-1/3 report gastrointestinal bleeding (8). Despite the occupation of 75% of the length and 90% of the mucosal surface of the gastrointestinal tract (9), the incidence of small bowel adenocarcinoma is much decreased compared to colorectal cancer, so most treatments are proposed based on the treatment model of colorectal cancer. This discrepancy may result from a lower incidence of *APC* mutations, where the lower bacterial load, faster food flow and more intestinal juice dilute cause less exposure of harmful material and small intestine has abundant lymph nodes, the higher the IgA levels are correlated with the better immune response (10).

Here, we report a case of multiple primary malignant tumors (NF-1, GIST, SBA and Gangliocytomain), and investigate the possible relationship between them.

Case presentation

Clinical evaluation

On June 30 2022, a 67-year-old woman was admitted to hospital with the chief complaint of abdominal pain over 2 months. The patient has undergone colonoscopy at another hospital, which revealed multiple circular lumps in the terminal

ileum and small polyps in the rectum and colon. On admission, a physical examination was performed, with neurofibroma, café au lait macules, skin fold freckling detected all over the patient's body (Figure 1), which were diagnosed as gastrointestinal neoplasms and neurofibromatosis type 1 (11). A detailed family history survey revealed that the patient's sons and granddaughter also had neurofibromatosis (Figure 2). Improvement of relevant tests: blood routine, urine, feces, coagulation function, tumor markers were normal, fecal latent blood test was positive. Computed tomography for thoracic, abdominal and pelvic examination revealed a terminal ileal tumor with secondary intussusception, diffuse osteoporosis (secondary right second costal old fracture with callus formation), lumps behind the bilateral sacral bone, sacral bone resorption. Multiple subcutaneous nodules were observed on the chest, neck, abdomen and back. (Supplementary Figure 1) MRI of head showed no abnormality.

Surgical findings

On July 04 2022, the exploratory laparotomy was performed under general anesthetic. During the operation, a mass with the size of about 5 cm × 7 cm was found within 10 cm of the ileocecal area, with significant enlargement and edema of the proximal small bowel. A mass approximately 1.5 cm in diameter can be seen on the lateral wall of the small intestine, approximately 120 cm from the Treitz ligament (Supplementary Figure 2). The ileocecal tumor was resected, accompanied with its corresponding mesentery, and the mass on the lateral wall of the small intestine.

Postoperative pathology

Postoperative pathology (Supplementary Figure 1) confirmed the mass on the ileocecal area of the small intestine as moderate-differentiated adenocarcinoma, invading the subserosal connective tissues, without metastasis to the mesenteric lymph nodes (0/15). The mass on the lateral wall of small intestine was identified as gastrointestinal stromal tumor, with the maximum diameter of the tumor was 1.5 cm, the tumor envelope was intact, the mitosis count was ≤5/5 mm2, indicating a rather low risk of invasion.

Postoperative therapy

The proband's postoperative course went well and the patient was discharged from the hospital one week later. In this case, the metastasis of small bowel adenocarcinoma was not found, also without high-risk features, such as positive resection margins, <8 lymph nodes, tumor perforation, perineural or
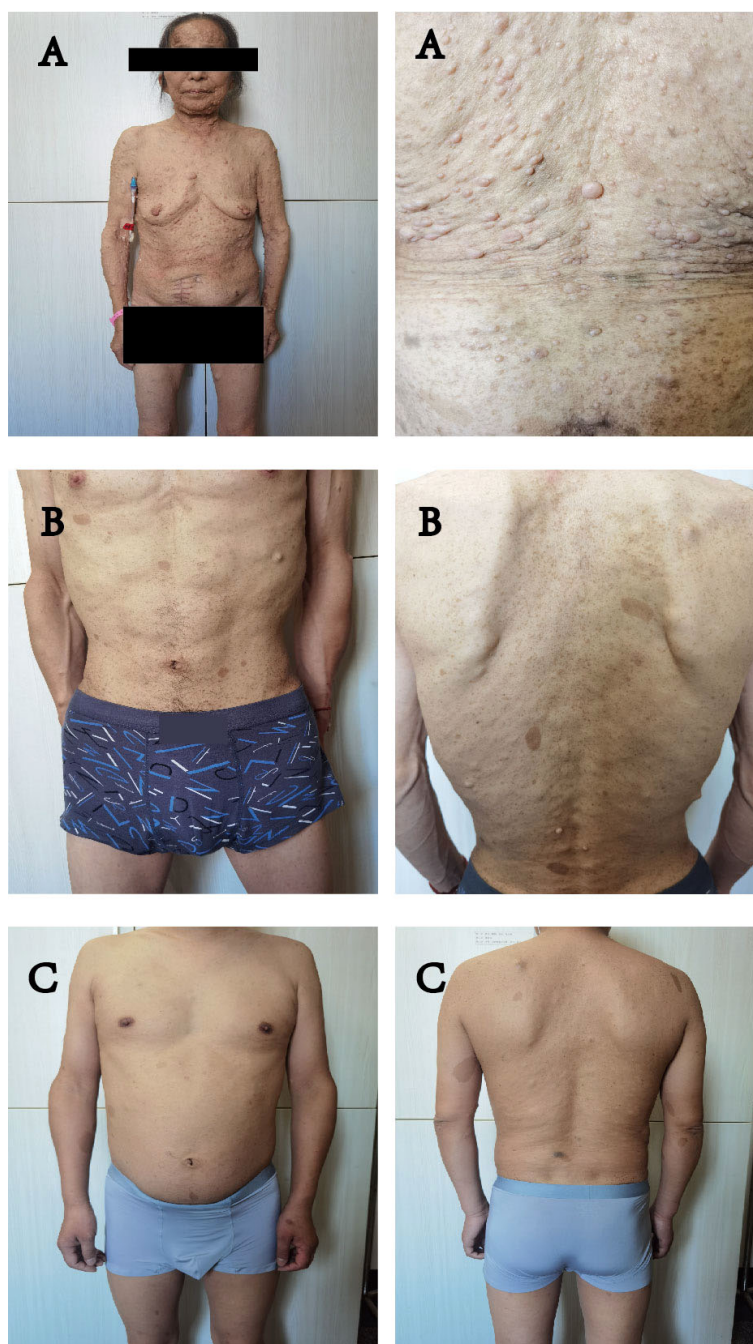
FIGURE 1
(A–C) all showed symptoms of NF1: multiple flat, light-brown patches of skin pigment, skin fold wrecking, visible neurofibromas under the skin. **(A)** is the mother of **(B, C)**.

lymphovascular invasion and poor-differentiated histology. Moreover, the Immunohistochemistry results suggested defective mismatch repair (dMMR). According to NCCN guidelines (8), this case dose not require chemotherapy. In the first three years, it is suggested be observed every three months.

Gene analysis

The resected SBA tumor tissues fixed by formalin and embedded with paraffin were subjected to next-generation sequencing (NGS) accompanied with peripheral blood from
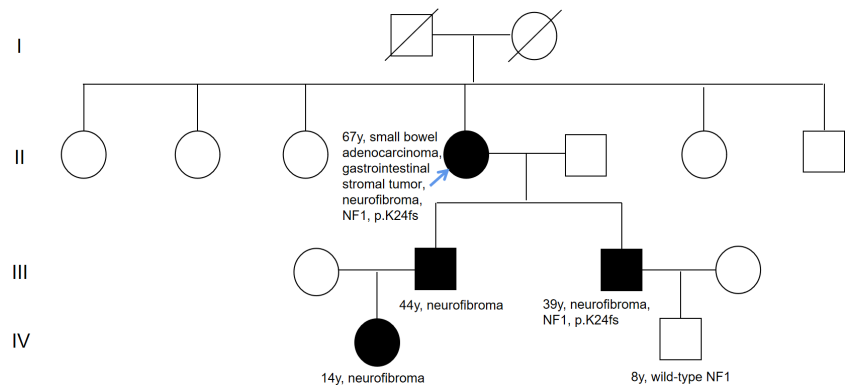
FIGURE 2
Pedigree of family. The black symbols indicate neurofibromatosis type 1. Numbers on right-top gives the current age. The blue arrow means the proband.

the proband, with a 1123-gene panel utilized (ChosenMed Technology [Beijing] Co. Ltd, Beijing, China). First, genomic DNA was extracted from the FFPE sections of tumor tissues using AllPrep FFPE DNA/RNA Kit (Qiagen). Pure DNA was eluted in elution buffer. Afterwards, DNA sample library were prepared according to the protocols, which was eventually sequenced with Illumina NextSeq 550Dx (12–14). The next-generation sequencing outcomes revealed a somatic *PIK3CA* mutation (NM_006218: exon10: c.1633G>A: p.E545K), with an allele frequency of 1.43%, followed by, a novel *NF1* germline frameshift mutation (NM_000267: exon2: c.71_75del: p.K24fs), with the variant allele frequency of 45.51%. This *NF1* variation has never been reported in any population database or publications, including the Exome Aggregation Consortium

and 1000 Genomes Project. The Integrative Genome Viewer snapshot of *NF1* is depicted in Figure 3. In addition, *PMS2* and *PTEN* missense mutations were also detected (Table 1). The resected GIST tumor tissues fixed with formalin and embedded with paraffin from the proband were also subjected to next-generation sequencing by the same gene panel. The results revealed no other mutations detected (such as *KIT*, *PDGFRA*) except the same *NF1* frameshift mutation (NM_000267: exon2: c.71_75del: p. K24fs).

Considering the impacts of neurofibroma on several family member, gene sequencing was conducted among this family using a hereditary-cancer-gene panel. The results indicted the same *NF1* mutation in the peripheral blood of proband's younger son, who is 39 years old and diagnosed with
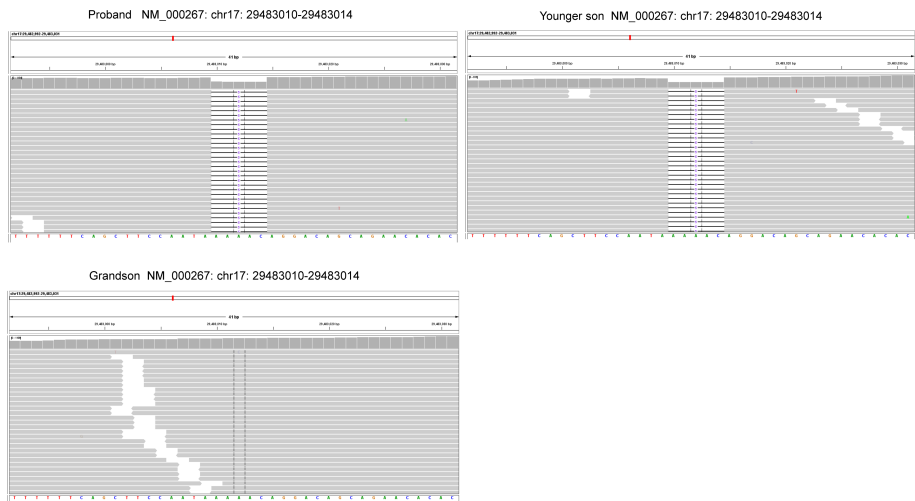
FIGURE 3
The Integrative Genome Viewer (IGV) snapshot of NF1.

TABLE 1 Genetic test results using the resected formalin fixed and paraffin embedded small bowel adenocarcinoma tumor tissues.

Germline mutations							
Gene	Chromosome	Exon	Nucleotide	Amino acid	ClinVar annotation	MutationTaster prediction	SIFT prediction
NF1	17	2	c.71_75del	p. K24fs		Disease causing	Disease causing
PMS2	7	5	c.379G>A	p. A127T	Conflicting interpretations of pathogenicity		
PTEN	10	8	c.949G>A	p. V317I	Uncertain significance		
Somatic mutations							
Gene	Chromosome	Exon	Nucleotide	Amino acid	OncoKB annotation		
PIK3CA	3	10	c.1633G>A	p. E545K	Oncogenic		

neurofibroma. The proband's grandson detected with wild-type *NF1* (Figure 3).

Of note, a germline *NF1* mutation (NM_000267: exon2: c.71_75del: p.K24fs) was detected in the peripheral blood of the proband through next-generation sequencing, which was also detected in one family member affected with NF-1. As the silico analysis with the MutationTaster and SIFT software predicted (15), the *NF1* mutation is disease-causing as the c.71_75del introduced a premature stop codon early in the translation, which resulted in a truncated proteins (Table 1). These results indicated that the novel *NF1* mutation might be responsible for the occurrence of NF1 in this family.

Discussion

Neurofibromatosis usually emerges as a relatively common autosomal dominant disease. Cases of *NF1* combined with stromal tumor have also been occasionally reported, but not cases of NF-1, GIST and SBA.

Neurofibromatosis can be considered a tumor susceptibility syndrome as it brings the increased risk of multiple tumors (16). A study in Finland reported that the cumulative cancer risk of 38% on *NF1* carriers at age 50, and the lifetime cancer risk of 59.6%, which were 3.9% and 30.8% in the general population, respectively. *NF1*-related tumors included malignant peripheral nerve sheath tumor, gastrointestinal adenocarcinoma, GIST, breast cancer, and pheochromocytoma (4).

At present, GISTs are mainly induced by *KIT* gene or *PDGFRA* gene mutations, which are observed in approximately 83% of GIST cases (17). These patients, except for the *PDGFRA-D842V* mutation, exhibit a satisfactory response to imatinib (18). However, *NF1*-related GIST is significantly distinguished from sporadic GIST. First, sporadic GIST is mainly distributed in the stomach (50%-70%), while *NF1*-related GIST is mostly found in the small bowel (68%); Most *NF1*-related GIST is spindle cell type

(75%), while the prognosis is better than sporadic GIST (19). Secondly, *KIT* and *PDGFRA* mutations are rarely reported in *NF1*-associated GIST. *NF1*-related GIST is a tumor with low malignancy and risk, with resistance to imatinib, which generally do not require treatment (20). There may exist a common pathway between *NF1*-related GIST and sporadic GIST, that is, *NF1* gene mutation destroys the normal function of neurofibromin and activates structural RAS, which increases downstream signaling *via* the mitogen-activated protein kinase (MAPK) pathway (21). The constitutive activation of the RAS-MAPK cascade could also result from mutations of *KIT* (22). Therefore, the activation of the MAPK cascade can be concluded that the activation of this common pathway leads to the development of GIST (23).

Due to a germline mutation in the *PMS2* gene, Lynch syndrome was diagnosed despite no family history of the tumor. GLTen Kate demonstrated the lifetime risk of SBA in Lynch syndrome to be 4.2% (24). Neurofibromatosis, Lynch syndrome and SBA seem to be correlated to each other. In early embryonic development, the *NF1* gene is a mutational target of MMR deficiency, that its inactivation is a critical step in the malignant progression of MMR-deficient ells (25). Homozygous MMR gene mutations (*MLH1, MSH2, PMS2, MSH6* biallelic mutations) are associated with neonatal neurofibromatosis and are more prone to early severe malignancies, including hematological malignancies, lymphomas and gastrointestinal malignancies (26–28).

Small bowel adenocarcinoma is generally characterized by dMMR associated with Lynch syndrome. The largest retrospective study on SBA identified dMMR protein in 26% (26/100) of tumors, which identified 10% (10/100) of Lynch syndrome in SBA, and 38.5% (10/26) of Lynch syndrome in dMMR tumors (29). In the study of Schrock et al., SBA is associated with a higher mutation rate of NF1 compared to gastric cancer (P=0.049) and colorectal cancer (P<0.01) (30). As a tumor suppressor gene, NF1 mutation may be more likely to lead to the occurrence of SBA under some mechanism. In this

case, genetic analysis may contribute to further revealing an association between SBA and NF-1.

Conclusion

We revealed a novel *NF1* germline frameshift mutation, which exerts a certain contribution to analyzing the relationship between NF-1, GIST, and SBA. If there occur gastrointestinal symptoms in the patients with *NF1* mutation, the possibility of a gastrointestinal tumor should be suspected. Genetic testing is also recommended in these patients for formulating effective treatments.

Data availability statement

The original contributions presented in the study are included in the article/Supplementary Material. Further inquiries can be directed to the corresponding author.

Ethics statement

Written informed consent was obtained from the individual(s) for the publication of any potentially identifiable images or data included in this article.

Author contributions

XH and ZC contributed to data acquisition and analysis. WZ and CL contributed to study design, data acquisition, analysis and the writing of the manuscript. All authors contributed to the article and approved the submitted version.

Conflict of interest

The authors declare that the research was conducted in the absence of any commercial or financial relationships that could be construed as a potential conflict of interest.

Publisher's note

All claims expressed in this article are solely those of the authors and do not necessarily represent those of their affiliated organizations, or those of the publisher, the editors and the reviewers. Any product that may be evaluated in this article, or claim that may be made by its manufacturer, is not guaranteed or endorsed by the publisher.

Supplementary material

The Supplementary Material for this article can be found online at: https://www.frontiersin.org/articles/10.3389/fonc.2022.1052799/full#supplementary-material

References

1. Tamura R. Current understanding of neurofibromatosis type 1, 2, and schwannomatosis. *Int J Mol Sci* (2021) 22(11):5850. doi: 10.3390/ijms22115850

2. DeClue JE, Cohen BD, Lowy DR. Identification and characterization of the neurofibromatosis type 1 protein product. *Proc Natl Acad Sci U S A.* (1991) 88 (22):9914–8. doi: 10.1073/pnas.88.22.9914

3. Gutmann DH, Ferner RE, Listernick RH, Korf BR, Wolters PL, Johnson KJ. Neurofibromatosis type 1. *Nat Rev Dis Primers* (2017) 3:17004. doi: 10.1038/nrdp.2017.4

4. Uusitalo E, Rantanen M, Kallionpaa RA, Poyhonen M, Leppavirta J, Yla-Outinen H, et al. Distinctive cancer associations in patients with neurofibromatosis type 1. *J Clin Oncol* (2016) 34(17):1978–86. doi: 10.1200/JCO.2015.65.3576

5. Wilson BN, John AM, Handler MZ, Schwartz RA. Neurofibromatosis type 1: New developments in genetics and treatment. *J Am Acad Dermatol* (2021) 84 (6):1667–76. doi: 10.1016/j.jaad.2020.07.105

6. Joensuu H. Gastrointestinal stromal tumor (GIST). *Ann Oncol* (2006) 17 Suppl 10:x280–6. doi: 10.1093/annonc/mdl274

7. Raghav K, Overman MJ. Small bowel adenocarcinomas–existing evidence and evolving paradigms. *Nat Rev Clin Oncol* (2013) 10(9):534–44. doi: 10.1038/nrclinonc.2013.132

8. Benson AB, Venook AP, Al-Hawary MM, Arain MA, Chen YJ, Ciombor KK, et al. Small bowel adenocarcinoma, version 1.2020, NCCN clinical practice guidelines in oncology. *J Natl Compr Canc Netw* (2019) 17(9):1109–33. doi: 10.6004/jnccn.2019.0043

9. DeSesso JM, Jacobson CF. Anatomical and physiological parameters affecting gastrointestinal absorption in humans and rats. *Food Chem toxicol: an Int J published Br Ind Biol Res Assoc* (2001) 39(3):209–28. doi: 10.1016/S0278-6915 (00)00136-8

10. Lowenfels AB. Why are small-bowel tumours so rare? *Lancet* (1973) 1 (7793):24–6. doi: 10.1016/S0140-6736(73)91228-2

11. Torpy JM, Burke AE, Glass RM. JAMA patient page. neurofibromatosis. *JAMA* (2009) 302(19):2170. doi: 10.1001/jama.302.19.2170

12. Han P, Wei G, Cai K, Xiang X, Deng WP, Li YB, et al. Identification and functional characterization of mutations in LPL gene causing severe

hypertriglyceridaemia and acute pancreatitis. *J Cell Mol Med* (2020) 24(2):1286–99. doi: 10.1111/jcmm.14768

13. Dai Y, Liang S, Dong X, Zhao Y, Ren H, Guan Y, et al. Whole exome sequencing identified a novel DAG1 mutation in a patient with rare, mild and late age of onset muscular dystrophy-dystroglycanopathy. *J Cell Mol Med* (2019) 23 (2):811–8. doi: 10.1111/jcmm.13979

14. Zheng Y, Xu J, Liang S, Lin D, Banerjee S. Whole exome sequencing identified a novel heterozygous mutation in HMBS gene in a Chinese patient with acute intermittent porphyria with rare type of mild anemia. *Front Genet* (2018) 9:129. doi: 10.3389/fgene.2018.00129

15. Zhang R, Chen S, Han P, Chen F, Kuang S, Meng Z, et al. Whole exome sequencing identified a homozygous novel variant in CEP290 gene causes meckel syndrome. *J Cell Mol Med* (2020) 24(2):1906–16. doi: 10.1111/jcmm.14887

16. Philpott C, Tovell H, Frayling IM, Cooper DN, Upadhyaya M. The NF1 somatic mutational landscape in sporadic human cancers. *Hum Genomics* (2017) 11(1):13. doi: 10.1186/s40246-017-0109-3

17. Blay JY, Kang YK, Nishida T, von Mehren M. Gastrointestinal stromal tumours. *Nat Rev Dis Primers.* (2021) 7(1):22. doi: 10.1038/s41572-021-00254-5

18. Cassier PA, Fumagalli E, Rutkowski P, Schoffski P, Van Glabbeke M, Debiec-Rychter M, et al. Outcome of patients with platelet-derived growth factor receptor alpha-mutated gastrointestinal stromal tumors in the tyrosine kinase inhibitor era. *Clin Cancer research: an Off J Am Assoc Cancer Res* (2012) 18 (16):4458–64. doi: 10.1158/1078-0432.CCR-11-3025

19. Mussi C, Schildhaus HU, Gronchi A, Wardelmann E, Hohenberger P. Therapeutic consequences from molecular biology for gastrointestinal stromal tumor patients affected by neurofibromatosis type 1. *Clin Cancer Res* (2008) 14 (14):4550–5. doi: 10.1158/1078-0432.CCR-08-0086

20. Miettinen M, Fetsch JF, Sobin LH, Lasota J. Gastrointestinal stromal tumors in patients with neurofibromatosis 1: a clinicopathologic and molecular genetic study of 45 cases. *Am J Surg Pathol* (2006) 30(1):90–6. doi: 10.1097/01.pas.0000176433.81079.bd

21. Maruta H, Burgess AW. Regulation of the ras signalling network. *Bioessays* (1994) 16(7):489–96. doi: 10.1002/bies.950160708

22. Duensing A, Medeiros F, McConarty B, Joseph NE, Panigrahy D, Singer S, et al. Mechanisms of oncogenic KIT signal transduction in primary gastrointestinal stromal tumors (GISTs). *Oncogene* (2004) 23(22):3999–4006. doi: 10.1038/sj.onc.1207525

23. Maertens O, Prenen H, Debiec-Rychter M, Wozniak A, Sciot R, Pauwels P, et al. Molecular pathogenesis of multiple gastrointestinal stromal tumors in NF1 patients. *Hum Mol Genet* (2006) 15(6):1015–23. doi: 10.1093/hmg/ddl016

24. Ten Kate GL, Kleibeuker JH, Nagengast FM, Craanen M, Cats A, Menko FH, et al. Is surveillance of the small bowel indicated for lynch syndrome families? *Gut* (2007) 56(9):1198–201. doi: 10.1136/gut.2006.118299

25. Wang Q, Montmain G, Ruano E, Upadhyaya M, Dudley S, Liskay RM, et al. Neurofibromatosis type 1 gene as a mutational target in mismatch repair-deficient cell type. *Hum Genet* (2003) 112(2):117–23. doi: 10.1007/s00439-002-0858-4

26. Gallinger S, Aronson M, Shayan K, Ratcliffe EM, Gerstle JT, Parkin PC, et al. Gastrointestinal cancers and neurofibromatosis type 1 features in children with a germline homozygous MLH1 mutation. *Gastroenterology* (2004) 126(2):576–85. doi: 10.1053/j.gastro.2003.11.008

27. Kruger S, Kinzel M, Walldorf C, Gottschling S, Bier A, Tinschert S, et al. Homozygous PMS2 germline mutations in two families with early-onset haematological malignancy, brain tumours, HNPCC-associated tumours, and signs of neurofibromatosis type 1. *Eur J Hum Genet* (2008) 16(1):62–72. doi: 10.1038/sj.ejhg.5201923

28. Raevaara TE, Gerdes AM, Lonnqvist KE, Tybjaerg-Hansen A, Abdel-Rahman WM, Kariola R, et al. HNPCC mutation MLH1 P648S makes the functional protein unstable, and homozygosity predisposes to mild neurofibromatosis type 1. *Genes Chromosomes Cancer.* (2004) 40(3):261–5. doi: 10.1002/gcc.20040

29. Latham A, Shia J, Patel Z, Reidy-Lagunes DL, Segal NH, Yaeger R, et al. Characterization and clinical outcomes of DNA mismatch repair-deficient small bowel adenocarcinoma. *Clin Cancer Res* (2021) 27(5):1429–37. doi: 10.1158/1078-0432.CCR-20-2892

30. Schrock AB, Devoe CE, McWilliams R, Sun J, Aparicio T, Stephens PJ, et al. Genomic profiling of small-bowel adenocarcinoma. *JAMA Oncol* (2017) 3 (11):1546–53. doi: 10.1001/jamaoncol.2017.1051

Check for updates

Identification of KIT and BRAF mutations in thyroid tissue using next-generation sequencing in an Ecuadorian patient: A case report

Santiago Cadena-Ullauri[1†], Elius Paz-Cruz[1†],
Rafael Tamayo-Trujillo[1†], Patricia Guevara-Ramírez[1],
Viviana Ruiz-Pozo[1], Paola Solis-Pazmino[2,3], Cristhian Garcia[3],
Richard Godoy[3], Eddy Lincango-Naranjo[3,4,5]
and Ana Karina Zambrano[1*]

[1]Centro de Investigación Genética y Genómica, Facultad de Ciencias de la Salud Eugenio Espejo,
Universidad UTE, Quito, Ecuador, [2]Surgery Group of Los Angeles, Department of Colorectal Surgery,
Los Angeles, CA, United States, [3]Instituto de la Tiroides y Enfermedades de Cabeza y Cuello (ITECC),
Department of Head and Neck Surgery, Quito, Ecuador, [4]Department of Teaching and Research,
Hospital Vozandes, Quito, Ecuador, [5]CaTaLiNA Research Initiative (Cáncer de tiroides en Latinoamérica),
Quito, Ecuador

Background: The incidence of thyroid cancer has increased worldwide. Ecuador presents the highest incidence among Latin American countries and the second around the world. Genetic alteration is the driving force for thyroid tumorigenesis and progression. The change from valine (V) to glutamic acid (E) at codon 600 of the BRAF gene (BRAF^{Val600Glu}) is the most commonly reported mutation in thyroid cancer. Moreover, the BRAF mutation is not the only mutation that has been correlated with TC. For instance, mutations and overexpression of the KIT gene has been associated with different types of cancer, including lung and colon cancer, and neuroblastoma.

Case presentation: A woman in her early fifties, self-identified as mestizo, from Otavalo, Imbabura-Ecuador had no systemic diseases and denied allergies, but she had a family history of a benign thyroid nodule. Physical examination revealed a thyroid gland enlargement. The fine-needle aspiration biopsy indicated papillary thyroid cancer. The patient underwent a successful total thyroidectomy with an excellent recovery and no additional treatments after surgery. Using Next-Generation sequencing a heterozygous mutation in the BRAF gene, causing an amino acid change Val600Glu was identified. Similarly, in the KIT gene, a heterozygous mutation resulting in an amino acid change Leu678Phe was detected. Moreover, an ancestry analysis was performed, and the results showed 3.1% African, 20.9% European, and 76% Native American ancestry.

Conclusions: This report represents the genetic characteristics of papillary thyroid cancer in an Ecuadorian woman with a mainly Native American ethnic component. Further studies of pathological variants are needed to determine if the combined demographic and molecular profiles are useful to develop targeted treatments focused on the Ecuadorian population.

Background

The incidence of thyroid cancer (TC) has increased worldwide (1). In the United States, thyroid cancer incidence has tripled over the last three decades from 5.5 to 14.0 per 100,000 people in 2019. TC ranks as the fifth most common cancer in Ecuadorian women (2, 3).

TC is classified into differentiated TC (DTC), poorly differentiated TC (PDTC), and anaplastic TC (ATC) (4). The most common type is differentiated TC (DTC) including papillary thyroid cancer (PTC), and particularly thyroid cancers of 1 cm or less in size, called papillary thyroid microcarcinoma (5). DTC, including PTC, is relatively indolent and highly curable; however, a significant recurrence rate, about 20% at 10 years and 30% at 30 years after initial treatment, is seen.

Genetic alteration is the driving force for thyroid tumorigenesis and progression. The main metabolic pathways associated with TC oncogenesis are the mitogen-activating protein kinase (MAPK) signaling pathway and the Phosphatidylinositol-3-kinase (PI3K)-AKT pathway (4). Mutations in protein components of these metabolic pathways lead to the translocation of transcription factors upregulating gene transcription and promoting oncogenesis 4). The change from valine (V) to glutamic acid (E) at codon 600 of the BRAF gene (BRAF^{Val600Glu}) is the most commonly reported mutation in PTC (4, 6). The BRAF mutation leads to the activation of the BRAF kinase in the MAPK pathway; this is considered the initial event in the oncogenesis and progression of PTC (4). An association between the BRAF^{Val600Glu} variant presence and worse prognosis, extrathyroidal extension, and lymph node metastasis has also been established (6, 7). Moreover, the BRAF mutation is not the only mutation that has been correlated with TC. For instance, mutations and overexpression of the KIT gene has been associated with different types of cancer, including lung cancer, neuroblastoma, and colon (8–10). Hence, it is important to identify mutations that along with the BRAF^{Val600Glu} mutation are driving the tumorigenesis.

The present case report describes a woman in her early fifties who underwent total thyroidectomy with malignant histopathologic features and the presence of a BRAF^{Val600Glu} and a KIT^{Leu678Phe} variants.

Case presentation

The present case report describes a woman in her early fifties, self-identified as mestizo, from Otavalo, Imbabura-Ecuador. In her familial history, the mother and father did not report any type of cancer, and only one of her brothers, among six, presented thyroid nodules; however, they were categorized as benign. The patient attended to the physician due to a lump in the neck that had been gradually enlarging for about 2 years. She had no symptoms of dysphagia and denied odynophagia or shortness of breath. The patient had no systemic diseases and denied allergies.

Physical examination revealed a thyroid gland enlargement. The ultrasound confirmed the thyroid growth (29 x 17 x 22 mm) and showed a solid nodule located in the left lobule with irregular borders, microcalcifications, highly vascularized. The fine-needle aspiration biopsy

Abbreviations: TC, Thyroid cancer; DTC, Differentiated thyroid cancer; PTC, Papillary thyroid cancer; FTC, Follicular thyroid cancer; MAPK, Mitogen-activated protein kinase; (PI3K)-AKT, Phosphatidylinositol 3-kinase.

indicated a Bethesda VI consistent with papillary thyroid cancer. Based on the results, a total thyroidectomy was chosen as the best option (11). The subject's blood tests were normal; therefore, the patient could undergo surgery. The procedure was successful with an excellent recovery. Posterior medical checkups did not show any complication.

Moreover, an ancestral composition analysis was performed, and the results showed 3.1% African, 20.9% European, and 76% Native American. A timeline of the relevant episodes of care is depicted in Figure 1.

Genomic analyses

Next-generation sequencing was performed using the TruSight Tumor 15 kit from Illumina ®; this panel includes 15 genes commonly mutated in solid tumors. Among the mutated genes, two had an in silico pathogenic status: BRAF and KIT, as described in the Table 1. The BRAF gene suffered a heterozygous mutation, a change from adenine to thymine at position 1799; this caused an amino acid change from Valine to Glutamic acid at position 600 (Figure 2), confirmed with Sanger Sequencing. Similarly, in the KIT gene, a heterozygous mutation led to a thymine change to cytosine at position 2032, which resulted in an amino acid change from Leucine to Phenylalanine at position 678 (Figure 3).

Methods

Sample collection and DNA extraction

After the total thyroidectomy procedure, a tissue sample (21.3 mg) was sent to the Centro de Investigación Genética y Genómica for the genomic analyses. The patient's informed consent was signed before the surgery. The DNA extraction was performed using the PureLink Genomic DNA Mini Kit, according to the manufacturer's instructions (Invitrogen, USA), and was quantified using spectrophotometry.

PCR amplification and genotyping for ancestral composition analysis

A multiplex reaction was performed for the amplification of 46 ancestry-informative markers (AIMs)-InDels. The amplification procedure was based on the protocol by Pereira et al. with a 10ul final reaction volume, using a Qiagen Multiplex PCR Master Mix (Qiagen), 46 (AIMs)-InDels primers and genomic DNA (13). Positive DNA control 2800M was included in the reaction along with the patient sample. The PCR amplification program was 95°C for 15 min; 30 cycles at 94°C for 30 sec, 60°C for 90 sec, and 72°C for 45 sec; and a final extension at 72°C for 60 min (13). A 3500 Genetic Analyzer (Applied Biosystems) was used for fragment separation and detection. The results were collected in Data Collection v4.0 and Gene Mapper v5 (Applied Biosystems)

Statistical analyses

The statistical analyses were performed according to Zambrano, et al. (14) using the software STRUCTURE v2.3.4. The ancestry
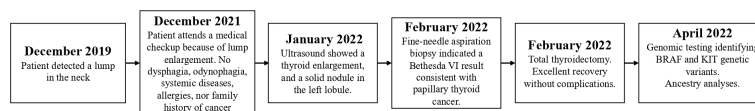
FIGURE 1

Subject's relevant episodes of care. The disease-associated episodes of care are presented in the figure.

TABLE 1 Genetic variants identified using next generation sequencing.

Gene	Chromosome	HGVS DNA Reference	HGVS Protein Reference	Predicted Effect	dbSNP/dbVar ID	Genotype
BRAF	7	NM_004333.4:c.1799T>A	NM_004333.4:p.(Val600Glu)	Missense variant	rs113488022	Heterozygous
KIT	4	NM_000222.2:c.2032C>T	NM_000222.2:p.(Leu678Phe)	Missense variant	N/A	Heterozygous
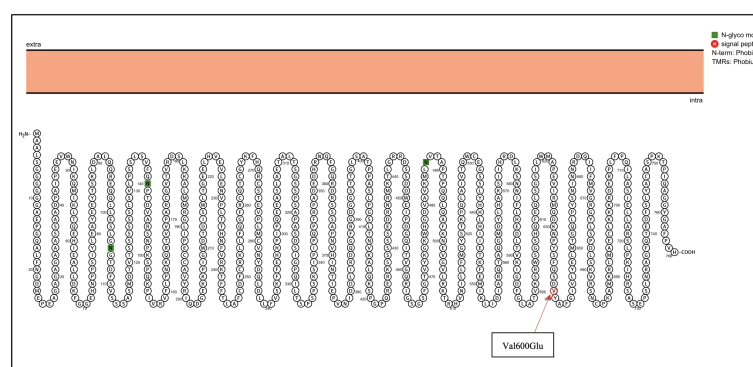
FIGURE 2

BRAF genetic mutation identified in the patient by NGS. Proteins were visualized with Protter (12). The red circle highlights the identified Val600Glu mutation in the BRAF gene.

inferences compared the subject and each reference population from HGDP-CEPH (Africans, Europeans, and Native Americans) subset H952. The run consisted of a burn-in length of 10 000, and 10 000 Markov Chain Monte Carlo (MCMC) interactions.

Next-generation sequencing

The TruSight Tumor 15 kit from Illumina® was used for sequencing on a MiSeq platform, according to the manufacturer's instructions (Illumina, USA). Data analyses, including variant calling, were performed on the TruSight Tumor 15 v2.0.1 for mapping, Pisces 5.1.7.52 for variant caller, Sift and PolyPhen for *in silico* prediction and COSMIC and ClinVar for clinical association.

Discussion and conclusions

Thyroid cancer (TC) is a malignant tumor with the most rapid increase in the incidence rate in the last three decades (2, 15–20). The incidental finding is a worldwide phenomenon. However, few studies have reported that the prevalence of large and aggressive tumors is also increasing (21–23), suggesting that factors other than

overdiagnosis might be affecting the increase of PTC incidence (24–28). Another factor that may be associated with a higher incidence of PTC is the use of radioactive drugs in hyperthyroid patients (29).

Several pieces of research suggest that thyroid cancer incidence is different among populations. In the USA, non-Hispanic Caucasians are less affected than the Hispanic and African-American populations (20, 30). Population-specific factors, such as American Indian ancestry, which influences other cancer patterns, may increase the risk of PTC in the Ecuadorian population (31–33). Moreover, Salazar-Vega et al. (2019) found that the mestizo population had a higher incidence of thyroid cancer in Ecuador (17). In the same study, they found that most of the thyroid cancer patients came from the highlands (2358masl), in comparison of those from the coast (93masl) and Amazon (731masl) regions (17); this is similar to what was found by Zeng, R. et al. (34) where high altitude was correlated with a higher thyroid cancer incidence (34). The subject comes from Otavalo a region located at 2532masl; hence the high altitude could be a risk factor for the presence of her thyroid cancer.

Furthermore, diet has been associated with an increased thyroid cancer predisposition (35). In Ecuador, grains are the most consumed food, especially in the highlands, and starch has been associated with an increased thyroid cancer predisposition (35); therefore, the Ecuadorian diet could also have a role in the increased thyroid cancer incidence.
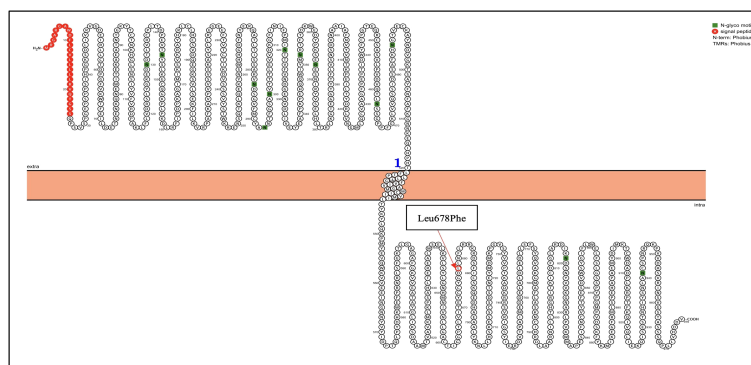
FIGURE 3
KIT genetic mutation identified in the patient by NGS. Proteins were visualized with Protter (12). The red circle highlights the identified Leu678Phe mutation in the KIT gene.

In Ecuador, genetic studies are scarce. Solis et al. (21). found a BRAF$^{\text{Val600Glu}}$ mutation in 130 of 169 (76,9%) PTC patients from the northern Ecuadorian Andes treated at the Hospital Eugenio Espejo in Quito, Ecuador (21), similar to other populations around the world (22, 23, 32, 36–38). The BRAF$^{\text{Val600Glu}}$ mutation constitutively activates the MAPK pathway, promoting cell survival, proliferation, and growth, thus tumorigenesis (39, 40). The Supplementary Figure 1 represents the difference between the wild-type and mutant residues. There is a significant difference in size, hydrophobicity, and charge. Studies *in vitro* have identified a 500-fold greater activity of BRAF$^{\text{Val600Glu}}$ in comparison with the wild type (40). The BRAF$^{\text{Val600Glu}}$ mutation has been widely described, and nowadays, specific treatments have been designed for this mutation. For example, the FDA has approved a combination of dabrafenib and trametinib for the treatment of anaplastic thyroid cancer patients, carrying the BRAF$^{\text{Val600Glu}}$ mutation (41).

In silico modeling of the BRAF proteins was performed using the Swissmodel and Hope tools. It was observed that the overall structure of the protein (Supplementary Figure 1) was not altered (QMEAN score 0.57 ± 0.05 for both models); however, the mutation causes a change in residue Val600Glu. The mutated residue is located in a domain that is crucial for the activity of the protein, thus the mutation affects its function and interaction with other proteins.

A small number of studies have researched the role of KIT in PTC. Sanlorenzo et al. (42) mentioned that the proto-oncogene KIT encodes for the tyrosine kinase receptor and is involved in cell signal transduction with different downstream pathways: MAPK, phosphatidylinositol 3-kinases (PI3K), Janus kinase (JAK)/signal transducers and activators of transcription (STAT), SRC family kinases (SFK) and phospholipase Cγ (42). On the other hand, the mitogen-activated protein kinase (MAPK) pathway has been extensively researched, and the role of point mutations in the BRAF and RAS genes and RET/PTC rearrangements in PTC molecular pathogenesis has been described (43, 44).

In silico modeling of the KIT proteins was analyzed using the Swiss-Model and Hope tools. It was observed that the overall structure of the protein (Supplementary Figure 2) was not altered (QMEAN score 0.71 ± 0.05 for both models), but the mutation causes a change in residue Leu678Phe. The mutated residue is located in a domain that is important for binding of other molecules and also is in contact with residues in a domain that is important for the activity of the protein. Therefore, the mutation might disturb the interaction between protein domains and as such affect the function of the protein.

The 3D molecular structure obtained using the HOPE tool shows that the mutant residue is bigger than the wild-type residue (Supplementary Figures 1, 2). The wild-type residue was buried in the core of the protein, and the fact that it is bigger, probably causes that it does not fit.

The precise role of KIT in cancer is still unknown, and numerous investigations present discrepancies depending on the type of tumor. Studies show that it is highly expressed or mutated in small cell lung cancer, leukemia cells, colon cancer, and neuroblastoma. Other studies demonstrate that the KIT expression is lost in breast cancer and melanoma (8). Similarly, a low expression of the KIT gene has been reported during the transformation of normal thyroid epithelium to papillary carcinoma, suggesting a possible role of the gene in the differentiation of thyroid tissue (8, 45, 46).

The strength of the used approach relies on the high analytical sensitivity of NGS. NGS can efficiently detect variants even in tissue samples; moreover, it allows to analyze several genes at once, compared to Sanger (∼1000 bp at once) (47). On the other hand, NGS limitations include higher costs and the need of specialized bioinformatic tools (48).

To conclude, we believe that this report represents the genetic characteristics of PTC in an Ecuadorian woman with a mainly Native American ethnic component. Further studies of pathological variants are needed to determine if the combined demographic and molecular profiles are useful to develop targeted treatments focused on the Ecuadorian population.

Data availability statement

The original contributions presented in the study are included in the article/Supplementary Material. Further inquiries can be directed to the corresponding author.

Ethics statement

The studies involving human participants were reviewed and approved by CEISH- UTE (CEISH-2021-014). The patients/participants provided their written informed consent to participate in this study. Written informed consent was obtained from the patient for publication of this case report.

Author contributions

Conceptualization, SC-U, EP-C, RT-T and AZ. Resources, PS-P, CG, RG, EL-N, AZ. Methodology, AZ, SC-U, EP-C, RT-T, PG-R and VR-P. Formal Analysis, SC-U, EP-C, RT-T and AZ. Writing – Review and Editing, SC-U, EP-C, RT-T and AZ, PS-P. Supervision, AZ. Project Administration, AZ. Funding Acquisition, AZ. All authors contributed to the article and approved the submitted version.

Funding

Acknowledgments

The authors are grateful to the patients for participating in the study, and to the Instituto de la Tiroides y Enfermedades de Cabeza y Cuello (ITECC) for their collaboration.

Conflict of interest

The authors declare that the research was conducted in the absence of any commercial or financial relationships that could be construed as a potential conflict of interest.

Publisher's note

All claims expressed in this article are solely those of the authors and do not necessarily represent those of their affiliated organizations, or those of the publisher, the editors and the reviewers. Any product that may be evaluated in this article, or claim that may be made by its manufacturer, is not guaranteed or endorsed by the publisher.

Supplementary material

The Supplementary Material for this article can be found online at: https://www.frontiersin.org/articles/10.3389/fonc.2022.1101530/full#supplementary-material

SUPPLEMENTARY FIGURE 1
Three-dimensional structures of wild and mutant proteins, obtained with the Swissmodel tool. **(A)** Wild Type BRAF Protein (P15056, extracted from UniProt). **(B)** Mutant protein (p.Val600Glu). **(C)** Close-up of the BRAF genetic mutation identified in the patient by NGS. The wild-type residue is in red, whereas the mutant residue is in green.

SUPPLEMENTARY FIGURE 2
Three-dimensional structures of wild and mutant proteins, obtained with the Swissmodel tool. **(A)** Wild Type KIT Protein (P10721-1, extracted from UniProt). **(B)** Mutant protein (p.Leu678Phe). **(C)** Close-up of the mutation. The KIT protein is colored grey, the side chains of both, the wild-type and the KIT[Leu678Phe] variant residue are shown and colored green and red respectively.

References

1. Khatami F, Mohammad Tavangar S, Tavangar SM. A review of driver genetic alterations in thyroid cancers. *Iran J Pathol* (2018) 13(2):125–35. doi: 10.30699/ijp.13.2.125

2. López Gavilanez E, Bautista Litardo N, Navarro Chávez M, Hernández Bonilla M, Segale Bajaña A. Thyroid cancer in Ecuador. *BMC Cancer* (2020) 20(1):1–3. doi: 10.1186/s12885-020-07137-0

3. Pacheco-Ojeda L, Martínez-Jaramillo A, Romo-Castillo H, Mario Montalvo-Burbano M. Differentiated thyroid cancer clinical trends in Quito, Ecuador. *Int J Med Surg Sci* (2021) 8(2):1–10. doi: 10.32457/ijmss.v8i2.1347

4. Nylén C, Mechera R, Maréchal-Ross I, Tsang V, Chou A, Gill AJ, et al. Molecular markers guiding thyroid cancer management. *Cancers (Basel)* (2020) 12(8):1–26. doi: 10.3390/cancers12082164

5. Brito JP, Hay ID. Management of papillary thyroid microcarcinoma. *Endocrinol Metab Clin North Am* (2019) 48(1):199–213. doi: 10.1016/j.ecl.2018.10.006

6. Silver JA, Bogatchenko M, Pusztaszeri M, Forest VI, Hier MP, Yang JW, et al. BRAF V600E mutation is associated with aggressive features in papillary thyroid carcinomas ≤ 1.5 cm. *J Otolaryngol - Head Neck Surg* (2021) 50(1):1–8. doi: 10.1186/s40463-021-00543-9

7. Al-Masri M, Al-Shobaki T, Al-Najjar H, Iskanderian R, Younis E, Abdallah N, et al. BRAF V600E mutation in papillary thyroid carcinoma: its relation to clinical features and oncologic outcomes in a single cancer centre experience. *Endocr Connect* (2021) 10(12):1531–7. doi: 10.1530/EC-21-0410

8. Franceschi S, Lessi F, Panebianco F, Tantillo E, La Ferla M, Menicagli M, et al. Loss of c-KIT expression in thyroid cancer cells. *PLoS One* (2017) 12(3):1–15. doi: 10.1371/journal.pone.0173913

9. Chen EC, Karl TA, Kalisky T, Gupta SK, O'Brien CA, Longacre TA, et al. KIT signaling promotes growth of colon xenograft tumors in mice and is upregulated in a subset of human colon cancers. *Gastroenterology* (2015) 149(3):705–17. doi: 10.1053/j.gastro.2015.05.042

10. Yu G, Yin C, Jiang L, Zheng Z, Wang Z, Wang C, et al. Amyloid precursor protein cooperates with c-KIT mutation/overexpression to regulate cell apoptosis in AML1-ETO-positive leukemia *via* the PI3K/AKT signaling pathway. *Oncol Rep* (2016) 36(3):1626–32. doi: 10.3892/or.2016.4963

11. American Cancer Society. *Treatment of thyroid cancer by type and stage*. American Cancer Society (2021) Atlanta, Georgia. USA. p. 1–4. Available at: http://www.cancer.org/cancer/thyroidcancer/detailedguide/thyroid-cancer-treating-by-stage.

12. Omasits U, Ahrens CH, Müller S, Wollscheid B. Protter: Interactive protein feature visualization and integration with experimental proteomic data. *Bioinformatics* (2014) 30(6):884–6. doi: 10.1093/bioinformatics/btt607

13. Pereira R, Phillips C, Pinto N, Santos C, dos Santos SEB, Amorim A, et al. Straightforward inference of ancestry and admixture proportions through ancestry-informative insertion deletion multiplexing. *PLoS One* (2012) 7(1). doi: 10.1371/journal.pone.0029684

14. Zambrano AK, Gaviria A, Cobos-Navarrete S, Gruezo C, Rodríguez-Pollit C, Armendáriz-Castillo I, et al. The three-hybrid genetic composition of an Ecuadorian population using AIMs-InDels compared with autosomes, mitochondrial DNA and y chromosome. *Sci Rep* (2019) 9(1):1–8. doi: 10.1038/s41598-019-45723-w

15. GLOBOCAN. *Age-standardized rate (Ecuador) per 100 000, incidence, males and females thyroid* (2022). Available at: https://gco.iarc.fr/overtime/en/dataviz/trends?populations=82610&sexes=1_2&types=0&multiple_populations=1&cancers=2.

16. Cordero FC, Ayala PC, Maldonado JY, Montenegro WT. Trends in cancer incidence and mortality over three decades in Quito-Ecuador. *Colomb Med* (2018) 49(1):35–41. doi: 10.25100/cm.v49i1.3785

17. Salazar-Vega J, Ortiz-Prado E, Solis-Pazmino P, Gómez-Barreno L, Simbaña-Rivera K, Henriquez-Trujillo AR, et al. Thyroid cancer in Ecuador, a 16 years population-based analysis (2001-2016). *BMC Cancer* (2019) 19(1):1–8. doi: 10.1186/s12885-019-5485-8

18. Xing MM, Alzahrani AS, Carson KA, Viola D, Elisei R, Bendlova B, et al. Association between BRAF V600E mutation and mortality in patients with papillary thyroid cancer. *JAMA - J Am Med Assoc* (2013) 309(14):1493–501. doi: 10.1001/jama.2013.3190

19. Solis-Pazmino P, Salazar-Vega J, Lincango-Naranjo E, Garcia C, Koupermann GJ, Ortiz-Prado E, et al. Thyroid cancer overdiagnosis and overtreatment: a cross- sectional study at a thyroid cancer referral center in Ecuador. *BMC Cancer* (2021) 21(1):1–10. doi: 10.1186/s12885-020-07735-y

20. Johnston LE, Tran Cao HS, Chang DC, Bouvet M. Sociodemographic predictors of survival in differentiated thyroid cancer: Results from the SEER database. *ISRN Endocrinol* (2012) 2012:1–8. doi: 10.5402/2012/384707

21. Solis-Pazmino P, Cucalon J, Jaramillo Koupermann G, Galvez G, Salazar-Vega J, Ortiz-Prado E, et al. High prevalence of BRAFV600E mutation in patients with papillary thyroid cancer from Northern Ecuadorian andes. *Am Thyroid Assoc* (2018) 28. doi: 10.1089/thy.2018.29065.abstracts

22. Pessôa-Pereira D, Medeiros MF da S, Lima VMS, da Silva JC, Cerqueira TL de O, da Silva IC, et al. Association between BRAF (V600E) mutation and clinicopathological features of papillary thyroid carcinoma: A brazilian single-centre case series. *Arch Endocrinol Metab* (2019) 63(2):97–106. doi: 10.20945/2359-3997000000120

23. Rashid FA, Munkhdelger J, Fukuoka J, Bychkov A. Prevalence of BRAFV600E mutation in Asian series of papillary thyroid carcinoma–a contemporary systematic review. *Gland Surg* (2020) 9(5):1878–900. doi: 10.21037/gs-20-430

24. Wang F, Zhao S, Shen X, Zhu G, Liu R, Viola D, et al. BRAF V600E confers male sex disease-specific mortality risk in patients with papillary thyroid cancer. *J Clin Oncol* (2018) 36(27):2787–95. doi: 10.1200/JCO.2018.78.5097

25. Pellegriti G, Frasca F, Regalbuto C, Squatrito S, Vigneri R. Worldwide increasing incidence of thyroid cancer: Update on epidemiology and risk factors. *J Cancer Epidemiol* (2013) 2013. doi: 10.1155/2013/965212

26. Liu R, Bishop J, Zhu G, Zhang T, Ladenson PW, Xing M. Mortality risk stratification by combining BRAF V600E and TERT promoter mutations in papillary thyroid cancer genetic duet of BRAF and TERT promoter mutations in thyroid cancer mortality. *JAMA Oncol* (2017) 3(2):202–8. doi: 10.1001/jamaoncol.2016.3288

27. Chakraborty A, Narkar A, Mukhopadhyaya R, Kane S, D'Cruz A, Rajan MGR. BRAFV600E mutation in papillary thyroid carcinoma: Significant association with node metastases and extra thyroidal invasion. *Endocr Pathol* (2012) 23(2):83–93. doi: 10.1007/s12022-011-9184-5

28. Vigneri R, Malandrino P, Vigneri P. The changing epidemiology of thyroid cancer: Why is incidence increasing? *Curr Opin Oncol* (2015) 27(1):1–7. doi: 10.1097/CCO.0000000000000148

29. Metso S, Auvinen A, Huhtala H, Salmi J, Oksala H, Jaatinen P. Increased cancer incidence after radioiodine treatment for hyperthyroidism. *Cancer* (2007) 109(10):1972–9. doi: 10.1002/cncr.22635

30. Aschebrook-Kilfoy B, Kaplan EL, Chiu BCH, Angelos P, Grogan RH. The acceleration in papillary thyroid cancer incidence rates is similar among racial and ethnic groups in the united states. *Ann Surg Oncol* (2013) 20(8):2746–53. doi: 10.1245/s10434-013-2892-y

31. Hoffman J, Fejerman L, Hu D, Huntsman S, Li M, John EM, et al. Identification of novel common breast cancer risk variants at the 6q25 locus among latinas 06 biological sciences. *Breast Cancer Res* (2019) 21(1):1–12. doi: 10.1186/s13058-018-1085-9

32. Estrada-Flórez AP, Bohórquez ME, Vélez A, Duque CS, Donado JH, Mateus G, et al. BRAF and TERT mutations in papillary thyroid cancer patients of Latino ancestry. *Endocr Connect* (2019) 8(9):1310–7. doi: 10.1530/EC-19-0376

33. Fejerman L, Ahmadiyeh N, Hu D, Huntsman S, Beckman KB, Caswell JL, et al. Genome-wide association study of breast cancer in latinas identifies novel protective variants on 6q25. *Nat Commun* (2014) 5(May). doi: 10.1038/ncomms6260

34. Zeng R, Shou T, Yang KX, Shen T, Zhang JP, Zuo RX, et al. Papillary thyroid carcinoma risk factors in the yunnan plateau of southwestern China. *Ther Clin Risk Manage* (2016) 12:1065–74. doi: 10.2147/TCRM.S105023

35. Fiore M, Cristaldi A, Okatyeva V, Lo Bianco S, Oliveri Conti G, Zuccarello P, et al. Dietary habits and thyroid cancer risk: A hospital-based case–control study in Sicily (South Italy). *Food Chem Toxicol* (2020) 146:111778. doi: 10.1016/j.fct.2020.111778

36. Cho U, Oh WJ, Bae JS, Lee S, Lee YS, Park GS, et al. Clinicopathological features of rare BRAF mutations in korean thyroid cancer patients. *J Korean Med Sci* (2014) 29 (8):1054–60. doi: 10.3346/jkms.2014.29.8.1054

37. Ye Z, Xia X, Xu P, Liu W, Wang S, Fan Y, et al. The prognostic implication of the BRAF V600E mutation in papillary thyroid cancer in a Chinese population. *Int J Endocrinol* (2022) 2022:1–7. doi: 10.1155/2022/6562149

38. Frasca F, Nucera C, Pellegriti G, Gangemi P, Attard M, Stella M, et al. BRAF (V600E) mutation and the biology of papillary thyroid cancer. *Endocr Relat Cancer* (2008) 15(1):191–205. doi: 10.1677/ERC-07-0212

39. McCain J. The MAPK (ERK) pathway: Investigational combinations for the treatment of BRAF- mutated metastatic melanoma. *P T* (2013) 38(2):96-108.

40. Li C, Lee KC, Schneider EB, Zeiger MA. BRAF V600E mutation and its association with clinicopathological features of papillary thyroid cancer: A meta-analysis. *J Clin Endocrinol Metab* (2012) 97(12):4559–70. doi: 10.1210/jc.2012-2104

41. National Cancer Institute. *Dabrafenib – trametinib braf combination approved for solid tumors with BRAF mutations*. Cancer Currents Blog (2022) Bethesda, Maryland. USA. p. 1–6. Available at: https://www.cancer.gov/news-events/cancer-currents-blog/2022/fda-dabrafenib-trametinib-braf-solid-tumors#:~:text=FDA. cited 2022 Sep 28previously approved the dabrafenib,melanoma%2C and anaplastic thyroid cancer.

42. Sanlorenzo M, Vujic I, Posch C, Ma J, Lin K, Lai K, et al. Oncogenic KIT mutations in different exons lead to specific changes in melanocyte phospho-proteome. *J Proteomics* (2016) 144:140–7. doi: 10.1016/j.jprot.2016.05.019

43. Zou M, Baitei EY, Alzahrani AS, Binhumaid FS, Alkhafaji D, Al-Rijjal RA, et al. RET/PTC, or BRAF mutations in advanced stage of papillary thyroid carcinoma. *Thyroid* (2014) 24(8):1256–66. doi: 10.1089/thy.2013.0610

44. Guerra PTCA, Zeppa P, Bifulco M, Vitale M. Concomitant BRAF(V600E) mutation and RET/PTC rearrangement is a frequent occurrence in papillary thyroid carcinoma. *Thyroid* (2014) 24,2:1–20. doi: 10.1089/thy.2013.0235

45. Tanaka T, Umeki K, Yamamoto I, Kotani T, Sakamoto F, Tanaka T, et al. C-kit proto-oncogene is more likely to lose expression in differentiated thyroid carcinoma than three thyroid-specific genes: Thyroid peroxidase, thyroglobulin, and thyroid stimulating hormone receptor. *Endocr J* (1995) 42(5):723–8. doi: 10.1507/endocrj.42.723

46. Tomei S, Mazzanti C, Marchetti I, Rossi L, Zavaglia K, Lessi F, et al. C-KIT receptor expression is strictly associated with the biological behaviour of thyroid nodules. *J Transl Med* (2012) 10(1):1–9. doi: 10.1186/1479-5876-10-7

47. Chin ELH, da Silva C, Hegde M. Assessment of clinical analytical sensitivity and specificity of next-generation sequencing for detection of simple and complex mutations. *BMC Genet* (2013) 14(1):1. doi: 10.1186/1471-2156-14-6

48. Alkan C, Sajjadian S, Eichler EE. Limitations of next generation genome sequence assembly. *Nat Methods* (2011) 8(1):1–7. doi: 10.1038/nmeth.1527

Frontiers | Frontiers in Oncology

Check for updates

Case report: Application of morphology in the diagnosis of siderosis in a patient with tuberculosis infection

Yuli Zhou[1], Ying Wang[2†], Wenbing Liu[3†], Haibin Wang[4], Daqiang He[1], Juan Jin[5], Qiaoyun Li[6], Junying Li[7], Qiong Chen[1], Senlin Ruan[1], Shenghai Wu[1*†] and Jiyu Tang[8*]

[1]Department of Laboratory, Hangzhou First People's Hospital, Zhejiang University School of Medicine, Hangzhou, China, [2]Department of Laboratory, Shenzhen Second People's Hospital, Shenzhen, China, [3]Department of Cardiopulmonary Medicine, Zhejiang Rehabilitation Medical Center, Hangzhou, China, [4]Department of Radiology, Hangzhou First People's Hospital, Zhejiang University School of Medicine, Hangzhou, China, [5]Hangzhou Medical College, Lin'an people's Hospital, Hangzhou, China, [6]Department of Pathology, Hangzhou First People's Hospital, Zhejiang University School of Medicine, Hangzhou, China, [7]Agricultural and Biological Ring Testing Center, Zhejiang University, Hangzhou, China, [8]Department of Nephrology, Zhejiang Provincial People's Hospital, Hangzhou Medical College, Zhejiang Chinese Medical University, Hangzhou, China

A 49-year-old male who had been working in welding for more than 30 years was admitted to the hospital for a medical checkup that revealed a lung shadow without specific symptoms such as coughing and sputum. Imaging studies showed diffuse ground-glass changes in both lungs, wall cavities with wall nodules, multiple peripheral nodules, and some nodules with calcification. The patient has been engaged in welding work for more than 30 years and exposed to iron dust. Lung tissue biopsy, routine morphological and pathological fluid basis examination of alveolar lavage fluid, can be considered as pulmonary iron particles, which can be regarded as iron dust lung. Acid-fast bacilli were detected in both fibrobronchoscopic brush extract and alveolar lavage fluid acid-fast staining. As the pathological examination revealed granulomatous inflammation showed caseation necrosis, the patient was judged to have concomitant pulmonary TB. After the diagnosis was made, the patient was no longer exposed to dust and was treated with appropriate anti- tuberculosis (TB) therapy. Lung lesions caused by welding have been reported, but the simultaneous finding of siderosis with pulmonary TB is specific to the case presented here. By describing the imaging features, combining different staining methods of alveolar lavage fluid and pathological examination of lung tissue, we showed various morphological manifestations of this case, aiming at improving the morphological diagnosis level of laboratory physicians and enabling patients to be diagnosed and treated early.

KEYWORDS

welder, siderosis, tuberculosis, morphology, case report

Introduction

At first described by Zenker in 1866 (1), iron dust lung is a rare occupational disease characterized by the accumulation of iron particles within the alveolar macrophages as a result of iron oxide in welding fumes, especially in welders, generally without associated symptoms or dysfunction. When the lungs are examined at autopsy, large deposits of iron oxide are observed yet there is no fibrosis. This condition is called siderosis and is typically classed as benign pneumoconiosis, but patients can develop chronic bronchitis and interstitial fibrosis due to persistent exposure. The literature has reported honeycomb-like interstitial pneumonia and varying degrees of fibrosis in welder autopsy materials (2–4). Both silicosis and TB result in impaired pulmonary function, and both have an appreciable mortality, even when occurring as single disease entities. TB represents a major health hazard to silicotics living in high TB prevalence areas, because of their increased susceptibility to disease. Based on the relationship between silicosis increasing the prevalence of TB among workers, we naturally speculate that the deposition of iron particles in the lungs causes lung function damage and changes in immune response, and iron pneumoconiosis patients are also greatly susceptible to TB. As a result, people engaged in welding and other occupations for a long time need to be well protected to prevent occupational disease and TB, early detection is important for reversible siderosis recovery. As such, differential diagnosis might be difficult. Here, we present a case of iron dust lung in a patient who has no symptoms but has nodular lesions visible on Computed Tomography(CT). The alveolar lavage fluid was examined by various staining methods and pathological examination of lung tissue, to show the different morphological manifestations of the case. All above can improve the morphological identification ability of inspectors and make a quick diagnosis, so as to provide laboratory basis for the prevention and treatment of iron pneumoconiosis.

Case description

A 49-year-old male patient who came to our hospital for three weeks of lung shadow found on physical examination had no cough and sputum, no dyspnea, no appetite or weight loss, no fever, chest pain or hemoptysis, no previous diabetes, no history of trauma or radiation exposure. He had surgery for a fracture of the left clavicle five years ago, the pre-operative chest X-ray have not showed any siderosis changes, and postoperative recovery is satisfactory. When he came to our hospital for examination, the patient performed well in all aspects of his body, body temperature: 36.6°C, pulse: 69 times/min, breathing: 20 times/min, blood pressure: 122/82 mmHg. The patient was mind and spirit, with clear breath sounds in both lungs and no obvious rales of dry and wet, and the remaining physical examination revealed no obvious anomalies. There were no significant abnormalities in common laboratory tests. No significant abnormalities were seen in the routine Electrocardiogram (ECG). Examination of epigastric ultrasonography did not suggest abnormalities associated with this disorder. Pulmonary ventilation function measurement: mild obstructive pulmonary ventilation dysfunction, normal lung diffusion function, negative drug relaxation test. The patient has been working as an "electric welder" for more than thirty years and had a history of smoking for well over twenty years, ten cigarettes per day. He quit smoking after lung shadow was revealed in physical examination. Chest CT done three weeks ago suggested diffuse lesions and localized emphysema, thick-walled cavities and multiple nodules seen in both pulmonary and mediastinal windows (Figures 1A, B). The diffuse ground-glass changes in two lungs were considered as diffuse alveolar exudation, at the same time under the two pulmonary interstitial changes, combined with occupational history, considering pneumoconiosis may. Although welding-associated pulmonary fibrosis was the most likely diagnosis for this patient, for further differential diagnosis, we communicate with the patient and his family and inform them of the necessity and risks, and after having their consent, we perform a fiberoptic bronchoscopy. We performed fiber bronchoscopy for differential diagnosis and obtained bronchoalveolar lavage fluid from the posterior segment of the right upper lobe and lingual segment of the left upper lobe. Thecell counts and leukocyte classification results: the posterior upper lobe lavage fluid of the right lung had a bloody turbid appearance, a nucleated cell count of 510/μl and neutrophils accounted for 60%, and the appearance of the lingual segment of the left upper lobe is colorless and micro-muted,
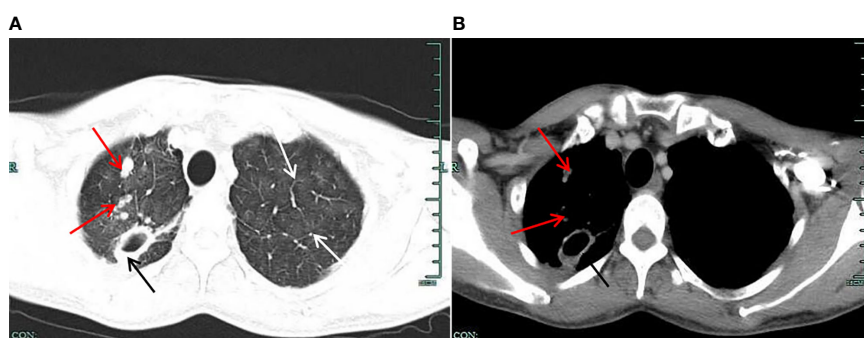
FIGURE 1
(A) Lung window on chest CT. The figure shows the multiple "ground glass" blurred shadows on both lungs (shown by the white arrow); the upper lobe of the right lung shows multiple nodular foci, one of which is larger (shown by the black arrow), showing a thick-walled cavity, and the edge of the lesion has multiple small nodule foci (shown by the red arrow). **(B)** Mediastinal window on chest CT. The figure shows a thick-walled cavity shadow (shown by a black arrow) in a larger nodular foci of the upper lobe of the right lung. The inner wall of the cavity is still smooth, the adjacent pleural traction is changed, the marginal small nodule foci are slightly displayed (shown by the red arrow), and the deposition of granular materials is visible.

with a nucleated cell count of 63/µl, neutrophils 6%. The St. Regis staining of Bronohoalveolarlavage (BAL) fluid showed macrophages engulfing a large number of brown-black particles of varying sizes (Figure 2A). Positive Prussian blue staining (Figure 2B), alveolar lavage fluid pathological fluid base, and lung biopsy (Figures 2C–E), is composed of substantial iron particles. Under the electron microscope visible macrophage cytoplasm containing large size, structure, irregular iron particles (Figure 2F), which are brown-yellow or brown-black with different sizes, metallic luster, and strong refraction. The patient's macrophage iron particles differ significantly from those in cases of pulmonary hemorrhage, in which the hemosiderin-containing particles are bluish-black, uneven in size, metallic, and non-refractive. According to pneumoconiosis diagnostic criteria (5), the patient was diagnosed with pneumoconiosis; also chest CT showed wall cavities with mural nodules, multiple nodules around them, and some nodules with calcification, considering the possibility of old TB. Further acid-fast staining of bronchoscopic brush smears and alveolar lavage fluid showed that acid-fast bacilli were positive (6 in 300 fields) (Figure 2G). Acid-fast bacilli were also detected by electron microscopy (Figure 2H), biopsy of the posterior right upper lobe of the lung is granulomatous inflammation with necrosis, and the patient was diagnosed with siderosis and TB.

The diagnosis of TB in this patient was clear. No obvious abnormalities in Cryptococcus antigen detection, Mycobacterium TB identification, and for rifampicin resistance testing. Mycobacterium tuberculosis and RIF resistance gene testing is detected by the export kit, as long as the sample is added to the kit, and after a period of time, the instrument can display the results. We contacted the patient, learned that he had no family history of TB, and recommended that he go to the local TB hospital for regular chest CT check-ups. The patient also followed our advice to change jobs to avoid further lung damage.

Literature review and discussions

Pneumoconiosis is a class of diseases caused by the build-up of inhaled dust, which may cause a reaction to the tissues of the lungs. Such diseases exist in two different clinical pathologic forms, one is fibrotic (e.g., silicosis, coal workers' pneumoconiosis (CWP), asbestosis, beryllium poisoning, and talc), which can be focal nodular or diffuse fibrosis; the other form is nonfibrotic (e.g., siderosis, stannosis, and baritosis), consisting of granules-laden macrophages with very low or no fibrosis (6, 7). The most common type of pneumoconiosis is the fibrotic form of pneumoconiosis, including silicosis, CWP, and asbestosis. Here we discuss the rare siderosis due to welding.
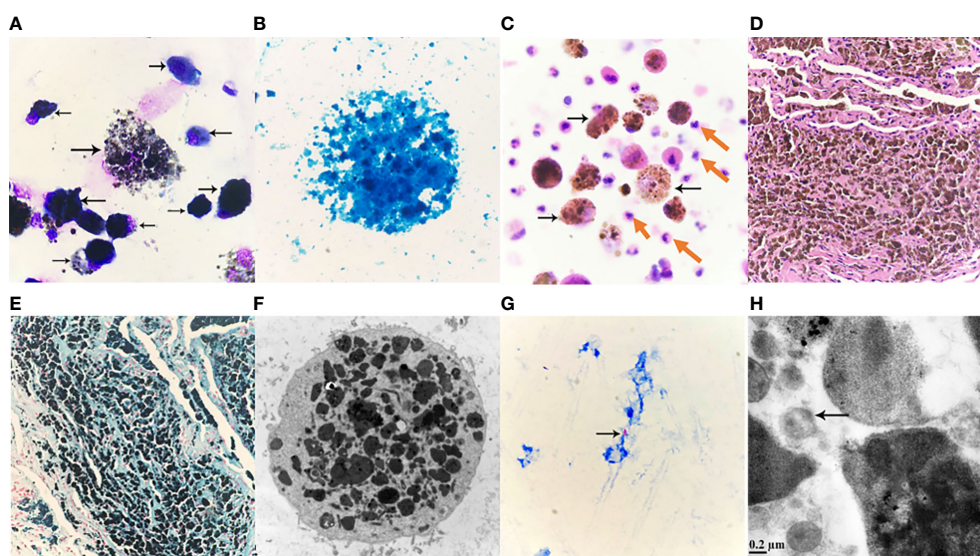
FIGURE 2

(A) Alveolar lavage fluid Wright-Giemsa Stained ×1000. Nucleated cells are significantly increased, easy to see piles, or scattered macrophages, macrophages can be seen round, or circular; soma medium in size, or enlarged; Swallow a large number of black gray, or brown-black particles, different sizes, different shades of coloring, cytoplasmic internal cause is full of a large number of particles, so that the soma swells, cytoplasm is aggregated or scattered black masses, the nucleus is squeezed by particles, distributed at the edge of the cell, or because of particle covering, the structure of the nucleus cannot be seen clearly, macrophage soma that swallows a large number of particles is easy to apoptosis, rupture, nucleus chromatin is loose, granules are scattered due to cell rupture. (B) Alveolar lavage solution, Prussian blue staining ×1000. Cytoplasmic macrophages filled with iron granules stained blue. Prussian blue staining positive reaction, a large number of granules covered leading to unclear cell structure. (C) Pathological fluid-based Hematoxylin-eosin staining (HE staining) of the posterior right upper lobe of the lung ×400. Significantly increased nucleated cells, scattered cells, evenly distributed, mainly neutrophils (pointed by red arrows), easy to see macrophages (pointed by black arrows), macrophage soma enlarged, round, or circular, it can be seen that macrophages engulf a large number of different sizes, lumpy, or fine, brownish-yellow, brownish-black particles; Macrophages and neutrophils are at different levels of visual field. (D) Pathological HE staining of lung tissue slices ×100. Visible lung tissue filled with brownish-yellow or brownish-black particles of varying sizes. (E) Lung tissue section, Prussian blue staining ×100. Visible lung tissue cloth granular, lumpy full blue, or blue-black particles, Prussian blue staining positive reaction. (F) Alveolar lavage fluid, transmission electron microscopy ×8000. The enlarged macrophage cytoplasm is filled with gray-black iron particles of different sizes and irregular shapes, and the nucleus cannot be seen due to the facet; Marked reduction in organelles may be associated with impaired macrophage immune function. (G) Fibrotic brush sample smear, acid-fast stained. Acid-fast bacilli (pointed by the arrow) can be seen: 6 Bars can be seen in 300 fields (×1000). (H) Alveolar lavage fluid, transmission electron microscopy ×50,000. M. tuberculosis (indicated by arrow).

Chronic effects of welding on the lungs include asthma, pneumosiderosis, and relatively rare lung cancer. Iron dust lung, a rare but most common welding-related occupational disease that causes the accumulation of iron particles in alveolar macrophages (8), was originally used by Zenker in 1866 to describe lung pathology caused by long-term sustained inhalation of iron or iron oxide dust (1). It was also described in 1936 by Doig and McLaughlin in a prospective study that examined the clinical and chest X-ray results of 16 welders. In chest X-rays, small circular shadows could be detected, while lung function was not impaired. As in this case, many patients are asymptomatic, and it takes years for them to develop symptoms. The most common complaints are shortness of breath, cough, and sputum production. Doig and McLaughlin followed up 15 of them for nine years, who remained healthy without any respiratory symptoms or dysfunction (4).

Unfortunately, iron has also been proved to cause fibrosis in some cases, especially when mixed with large amounts of sílica. Iron deposition can also lead to changes in symptoms and function of lung. In 1988, Funahashi (9) et al. surveyed 10 symptomatic welders, and histological examination revealed some degree of interstitial pulmonary fibrosis in all cases. Interstitial pulmonary fibrosis is a rare clinical disorder commonly associated with long-term and heavy exposure to welding fumes in poorly ventilated workplaces, which can appear with emphysema, especially in smokers. It is assumed to be a response to iron-containing particles, many of which were found within the fibrotic alveolar septum. The elemental content of these lung tissues was also analyzed by energy-dispersive X-rays, suggesting that the welder's iron dust lung may be associated with interstitial fibrosis (2, 3, 8).

Epidemiological studies and case reports have confirmed that inhalation of silica dust increases the prevalence of TB among workers, but the magnitude of the impact remains uncertain. Recent findings suggest that patients without silicone lung may be susceptible to TB when exposed to silica, and even if exposure is stopped, the risk appears to be lifelong (6). The mechanism of this relationship is unclear. Is reported in the literature a few possible reasons, such as inhalation of silica altering the immune response of the lungs, impairing the function of macrophages, and causing their apoptosis; an excess of surfactant protein A in BAL fluid appears to be associated with an increased risk of TB; and finally, *M. tuberculosis* can remain dormant within silicone nodules, direct damage of macrophages and the low permeability of drugs in these nodules may lead to subsequent treatment failure and high recurrence rates in these patients (10). It remains unclear whether coal miners with pneumoconiosis are also at risk of TB. A study with 53753 coal miners reported that miners were at three times higher risk of TB than the general population in the same area (11). Since both iron and silicone are pneumoconioses, we reasonably suspect that iron dust lung and TB also have the aforementioned concern.

In ordinary cases, the diagnosis of mycobacterial infection is based on the presence of typical clinical features of TB, such as persistent cough, hemoptysis, weight loss, fever, or changes in imaging findings. Meanwhile, sputum smears and cultures are needed to confirm the disease. However, in patients with pneumoconiosis, due to the deformation of bronchial stenosis and even occlusion caused by the contraction of scars in the lungs, TB bacteria are often not detected in sputum, and even if checked repeatedly, most patients still have negative results. At the same time, in patients with a high staging of pneumoconiosis, imaging often shows complex and variable, the

nodules are fused into clumps, showing irregular clumps, or patchy, fibrous cord-like shadows, blurred edges, and have lost the characteristic changes of TB. At this time pneumoconiosis complicated by TB is difficult to distinguish (7, 12).

In this case, a welder with more than 30 years of experience, iron-containing particles were most likely to be inhaled and deposited in the lungs. Similar to previous reports, the patient's main finding on chest CT was diffuse ground glass-like changes in both lungs, which has been described as the most common finding among welders. These ambiguous micro nodes do not reflect pathologically reactive fibrosis but do correlate with iron-bearing macrophages located in the alveolar space as indicated by Prussian blue staining. In the morphological analysis of alveolar lavage fluid, when macrophages engulf a large number of iron particles, different staining methods and electron microscopy show different morphological characteristics.

In discussing this case, we should also distinguish between siderosis, desquamative interstitial pneumonia, and idiopathic pulmonary hemosiderosis. In most cases, desquamative interstitial pneumonia is associated with smoking, and its histological manifestations include involvement of parenchymal lobes and significant accumulation of alveolar macrophages, but macrophage Prussian blue stain is negative. While hemoptysis, iron deficiency anemia and a triple sign of lung parenchymal infiltration on chest x-ray are three of the hallmarks of idiopathic pulmonary hemosiderosis, which often occurs in children. Our diagnosis can exclude desquamative interstitial pneumonia and idiopathic pulmonary hemosiderosis because macrophage iron stain is positive and there is no iron deficiency anemia (2). In addition, morphologically, we also need to identify between iron-containing granule cells, dust cells, hemosiderin cells, and melanocytes (Table 1). Iron particles in iron-containing granule cells have a brownish-yellow metallic luster, strong refractive index, and vary in size (13, 14); hemosiderin cells and dust cells belong to macrophages, but the contents of the phagocytosis are different. Hemosiderin-containing cells are the macrophage that engulfs erythrocytes. Hemoglobin broken down to form hemosiderin granules suggestsold bleeding, more common in bloody specimens. Hemosiderin that truly comes from alveolar hemorrhage is usually blue-black and lumpy, with a single block reaching a diameter of 7 to 8 μm (15) (Figure 3A), fresh red blood cells or old red blood cells can be seen in the background, and phagocytes or red blood cell debris in the macrophage cytoplasm can also be seen. Dust cells are formed by engulfing non-decomposable substances such as dust (Figure 3B), the particles are mostly dark black in size and more common seen in patients who smoke, and also in patients with occupational pneumoconiosis. Besides black particles, blue lipid droplets formed by tar can also be seen in the dust cells of patients who smoke. Under electron microscopy, the particles of both types of cells are black (Figure 3C) and need to be identified by other methods. Melanoma cells (Figure 3D) have moderate to rich cytoplasm and eccentric nuclei, cell morphology is characteristic of malignant tumor cells, chromatin is loose, and cells have fine and uniform granules. Melanin particles can be found in the cytoplasm of tumor cells or melanoma macrophages and may be indistinguishable from hemosiderin. The latter is usually coarser and more refractive than melanin particles, and histochemical staining (Fontana-Masson for the diagnosis of melanoma and Perls for hemosiderin) may be helpful. The immunochemistry of melanoma cell markers also contributes to the diagnosis of melanoma (16).

TABLE 1 Cytological characteristics of iron-containing granules, dust cells, hemosideranocytes, and melanocytes, differences in particles in cells, and suggestive diseases.

Cells	Cytologic features	Characteristics of particles in cells	Diseases
Iron-containing granule cells	The main component are macrophages that digest iron fragments (macrophages engulf foreign iron particles that cannot be digested and absorbed)	Blue-black and black iron particles of different sizes, with metallic luster and a high index of refraction, there are many large pieces of iron in the macrophages	Siderosis
Dust cells	Macrophages that mainly engulf substances that cannot be broken down, such as dust	Black particles and droplets of blue lipids formed by tar	Pneumoconiosis/smoking
Dust cells	Macrophages that mainly engulf substances that cannot be broken down, such as dust	Black particles and droplets of blue lipids formed by tar	Pneumoconiosis/smoking
Hemosiderin cells	Metabolites after macrophages engulf red blood cells or red blood cell fragments are hemosiderosin granules	Blue-black and uniform in size without metallic luster and refraction	Pulmonary hemorrhage
Melanoma cells	Mesothelial-like cells with moderate to abundant cytoplasm and eccentric nuclei with characteristics of tumor cells	Black, finer and more uniform than iron particles, less refractive	Melanoma
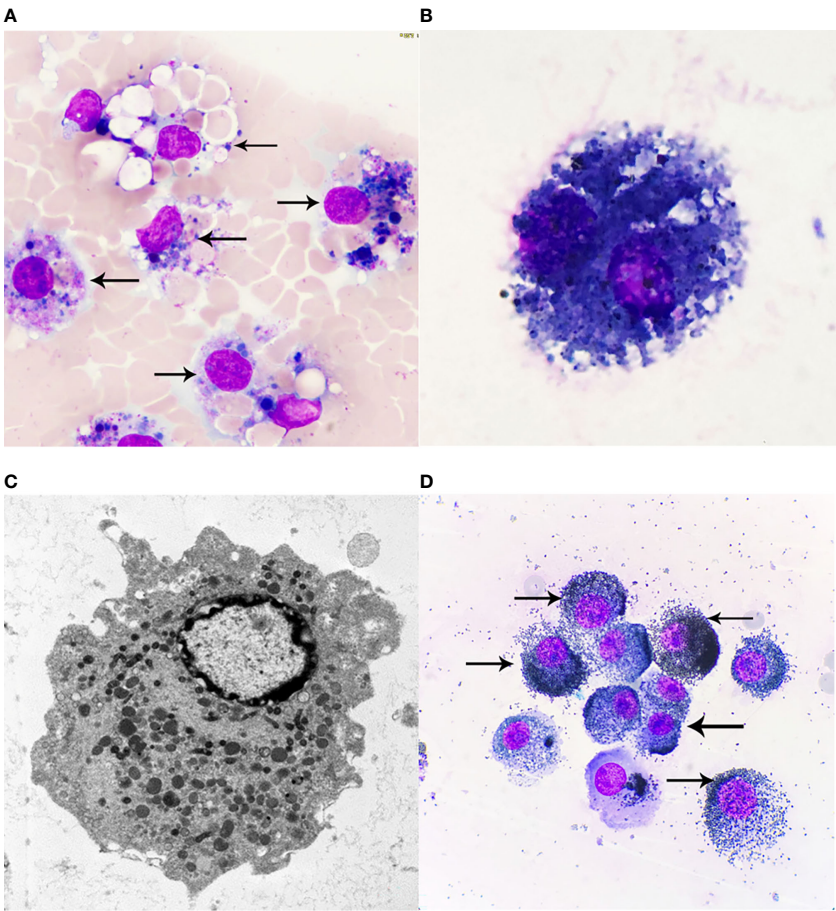
FIGURE 3

(A) Hemosiderin cells, Wright-Giemsa Stained ×1000. Macrophages engulf fresh red blood cells or red blood cell fragments, and after Wright-Giemsa Staining, intracytoplasmic digestion can be seen to form vacuole areas, and blue or blue-black hemosiderin granules of different sizes can also be seen, that is, hemosiderin cells. (B) Dust cells, Wright-Giemsa Stained ×1000. Macrophages that mainly engulf substances that cannot be broken down, such as dust. Black particles and droplets of blue lipids formed by tar can be seen. (C) Electron microscopy of macrophages ×10000. Macrophages are diverse in morphology and vary due to their different functional states, generally round or oval in shape, with short protrusions, and those with active functions often extend longer pseudopodia and are irregular. The nucleus is small, round or oval in shape, and darkly colored. Under transmission electron microscopy, the cytoplasm contains a large number of primary lysosomes, secondary lysosomes, phagocytosic vesicles and phagosomes, in addition to the more developed Golgi complex, a small number of mitochondria and a rough endoplasmic reticulum. (D) Melanoma cells, Wright-Giemsa Stained ×1000. Melanoma cells have moderate to rich cytoplasm and eccentric nuclei, and cell morphology is characteristic of malignant tumor cells, chromatin is loose, and melanoma cells have fine, uniform granules; melanin particles can be found in the cytoplasm of tumor cells or melanoma macrophages. The arrows of (A) refer to more typical Hemosiderin cells, the arrows of (D) refer to more typical Melanoma cells.

Conclusions

In summary, this report describes a case of iron dust lung with concomitant TB. To avoid further lung injury, such patients should be discontinued from occupational exposure. Regular and long-term monitoring is required for patients with a history of exposure to welding fumes, as the risk of TB in this group is significantly elevated, and this risk may be long-standing even if exposure is stopped. As with our patient, any typical but non-specific features of TB in patients with siderosis should be thoroughly examined, such as persistent cough, weight loss, and fever, to rule out TB. In addition, any radiological findings, such as asymmetrical nodules, rapid progression, or cavities, should be of concern. TB treatment in these patients may be prolonged because sputum specimens may remain smear-positive for a longer period. Finally, patients with siderosis should receive close and regular follow-up for early detection of any new TB cases or recurrences. When clinicians encounter such rare cases, while referring to the patient's symptoms and imaging performance, a detailed understanding of the work history, combined with a variety of morphological results, such as conventional morphological examination of alveolar lavage fluid, alveolar lavage fluid pathological fluid-based examination, lung tissue biopsy and Prussian blue staining, etc., will be very helpful for diagnosis and differential diagnosis.

Data availability statement

The datasets presented in this study can be found in online repositories. The names of the repository/repositories and accession number(s) can be found in the article/supplementary material.

Ethics statement

The studies involving human participants were reviewed and approved by the Ethics Committee of Hangzhou First People's Hospital, Zhejiang University School of Medicine. The patients/participants provided their written informed consent to participate in this study. Written informed consent was obtained from the individual(s) for the publication of any potentially identifiable images or data included in this article.

Author contributions

Acknowledgments

Conflict of interest

The authors declare that the research was conducted in the absence of any commercial or financial relationships that could be construed as a potential conflict of interest.

Publisher's note

All claims expressed in this article are solely those of the authors and do not necessarily represent those of their affiliated organizations, or those of the publisher, the editors and the reviewers. Any product that may be evaluated in this article, or claim that may be made by its manufacturer, is not guaranteed or endorsed by the publisher.

References

1. Spalgais S, Kumar R, Mrgipuri P. Symptomatic pulmonary siderosis in Scissors/Knife sharpening worker: A case report. *Indian J Occup Environ Med* (2020) 24(1):42–4. doi: 10.4103/ijoem.IJOEM_77_19

2. Ji C, Chen G, Cai HR, Meng FQ, Chen YB, Guo LC, et al. An unusual case of welder's siderosis with local massive fibrosis: a case report. *Chin Med J (Engl)* (2012) 125 (3):552–4. doi: 10.3760/cma.j.issn.0366-6999.2012.03.030

3. Fidan F, Esme H, Unlu M, Acar M, Albayrak R, Dilek FH. Welder's lung associated with pneumothorax. *J Thorac Imaging* (2005) 20(2):120–2. doi: 10.1097/01.rti.0000155039.51662.fc

4. Yamamoto Y, Tsujino K, Urasaki K, Matsuki T, Fukushima K, Kida. Arc-welders' pneumoconiosis with atypical radiological H. And bronchoalveolar lavage fluid findings: A case report. *Respir Med Case Rep* (2020) 29:101023. doi: 10.1016/j.rmcr.2020.101023

5. Qi XM, Luo Y, Song MY, Liu Y, Shu T, Liu Y, et al. Pneumoconiosis: current status and future prospects *Chin Med J (Engl)* (2021) 134(8):898–907. doi: 10.1097/CM9.0000000000001461

6. Ehrlich R, Akugizibwe P, Siegfried N, Rees. The association between silica exposure D. Silicosis and tuberculosis: a systematic review and meta-analysis. *BMC Public Health* (2021) 21(1):953. doi: 10.1186/s12889-021-10711-1

7. Jun JS, Jung JI, Kim HR, Ahn MI, Han DH, Ko JM, et al. Complications of pneumoconiosis: radiologic overview. *Eur J Radiol* (2013) 82(10):1819–30. doi: 10.1016/j.ejrad.2013.05.026

8. Koksal D, Karcioglu O, Babaoglu E, Sarinc Ulasli S, Onder S. The contribution of bronchoalveolar lavage in the diagnosis of welder's lung in a patient with pulmonary fibrosis. *Arch Environ Occup Health* (2020) 75(1):56–9. doi: 10.1080/19338244.2018.1544113

9. Funahashi A, Schlueter DP, Pintar K, Bemis EL, Siegesmund KA. Welders' pneumoconiosis: tissue elemental microanalysis by energy dispersive x ray analysis. *Br J Ind Med* (1988) 45(1):14–8. doi: 10.1136/oem.45.1.14

10. Skowronski M, Halicka A, Barinow-Wojewodzki A. Pulmonary tuberculosis in a male with silicosis. *Adv Respir Med* (2018) 86(3). doi: 10.5603/ARM.2018.0019

11. Mosquera JA, Rodrigo L, Gonzálvez F. The evolution of pulmonary tuberculosis in coal miners in Asturias, northern spain. an attempt to reduce the rate over a 15-year period, 1971-1985. *Eur J Epidemiol* (1994) 10(3):291–7. doi: 10.1007/BF01719352

12. Barboza CE, Winter DH, Seiscento M, Santos Ude P, Terra Filho M. Tuberculosis and silicosis: epidemiology, diagnosis and chemoprophylaxis. . *J Bras Pneumol* (2008) 34 (11):959–66. doi: 10.1590/s1806-37132008001100012

13. Wang CW, Colby. Histiocytic lesions TV. And proliferations in the lung. *Semin Diagn Pathol* (2007) 24(3):162–82. doi: 10.1053/j.semdp.2007.06.003

14. Zheng L, Liu X, Zhou X, Liu K. Iron-laden macrophages in the bronchoalveolar lavage in a welder: Pulmonary siderosis. *Diagn Cytopathol* (2020) 48(11):1137–40. doi: 10.1002/dc.24470

15. Colby TV, Fukuoka J, Ewaskow SP, Helmers R, Leslie KO. Pathologic approach to pulmonary hemorrhage. *Ann Diagn Pathol* (2001) 5(5):309–19. doi: 10.1053/adpa.2001.27923

16. Murali R, Zarka MA, Ocal IT, Tazelaar HD. Cytologic features of epithelioid hemangioendothelioma. *Am J Clin Pathol* (2011) 136(5):739–46. doi: 10.1309/AJCP5NK0FJCGHTFM

Atypical *ATMs*: Broadening the phenotypic spectrum of *ATM*-associated hereditary cancer

Nicholas A. Borja[1], Rachel Silva-Smith[1], Marilyn Huang[2], Dipen J. Parekh[3], Daniel Sussman[4] and Mustafa Tekin[1,5]*

[1]Dr. John T. Macdonald Foundation Department of Human Genetics, Miller School of Medicine, University of Miami, Miami, FL, United States, [2]Division of Gynecologic Oncology, Sylvester Comprehensive Cancer Center, University of Miami, Miami, FL, United States, [3]Desai Sethi Urology Institute, Miller School of Medicine, University of Miami, Miami, FL, United States, [4]Division of Digestive Health and Liver Diseases, University of Miami Miller School of Medicine, Miami, FL, United States, [5]John P. Hussmann Institute for Human Genomics, Miller School of Medicine, University of Miami, Miami, FL, United States

Heterozygous, loss-of-function germline variants in *ATM* have been associated with an increased lifetime risk of breast, pancreas, prostate, stomach, ovarian, colorectal, and melanoma cancers. We conducted a retrospective review of thirty-one unrelated patients found to be heterozygous for a germline pathogenic variant in *ATM* and identified a significant proportion of patients in this cohort with cancers not currently associated with the ATM hereditary cancer syndrome, including carcinomas of the gallbladder, uterus, duodenum, kidney, and lung as well as a vascular sarcoma. A comprehensive review of the literature found 25 relevant studies where 171 individuals with a germline deleterious *ATM* variant have been diagnosed with the same or similar cancers. The combined data from these studies were then used to estimate the prevalence of germline *ATM* pathogenic variants in these cancers, which ranged between 0.45% and 2.2%. Analysis of tumor sequencing performed in large cohorts demonstrated that the frequency of deleterious somatic *ATM* alterations in these atypical cancers equaled or exceeded the alteration frequency in breast cancer and occurred at a significantly higher rate than in other DNA-damage response tumor suppressors, namely *BRCA1* and *CHEK2*. Furthermore, multi-gene analysis of somatic alterations in these atypical cancers demonstrated significant co-occurrence of pathogenic alterations in *ATM* with *BRCA1* and *CHEK2*, while there was significant mutual exclusivity between pathogenic alterations in *ATM* and *TP53*. This indicates that germline *ATM* pathogenic variants may play a role in cancer initiation and progression in these atypical *ATM* malignancies, potentially influencing these cancers to be driven toward DNA-damage repair deficiency and away from loss of *TP53*. As such, these findings provide evidence for broadening of the *ATM*-cancer susceptibility syndrome phenotype to improve the recognition of affected patients and provide more efficacious, germline-directed therapies.

KEYWORDS

ATM, ataxia-telangiectasia mutated (ATM), germline, pathogenic variant (PV), hereditary cancer, cancer susceptibility association

Introduction

ATM (OMIM 607585) encodes the PI3K-related serine/threonine protein kinase comprising 3,056 amino acids, ataxia-telangiectasia mutated. This protein kinase primarily resides in the nucleus of dividing cells and has long been recognized as a key upstream modulator of the response to DNA double-stranded breaks, as well as oxidative and other genotoxic stresses. A critical function of ATM involves the recruitment and cooperation with DNA-damage sensing proteins such as BRCA1 in the face of double-strand breaks (1). ATM also plays a critical role in the DNA damage response through the phosphorylation of downstream substrates including CHK2 and p53, which then stimulate the cell-cycle checkpoint arrest and cellular apoptosis pathways, respectively (1, 2).

Biallelic pathogenic loss-of-function variants in *ATM* have long been associated with the genomic instability syndrome, ataxia-telangiectasia. Manifestations of the disorder include cerebellar ataxia, oculocutaneous telangiectasia, immunodeficiency, radiosensitivity, premature aging, and a predisposition to cancer development, primarily of lymphoid origin (3).

It was later recognized that women who are heterozygous for pathogenic loss-of-function variants in *ATM* have an increased risk for breast cancer, leading *ATM* to become regarded as a moderate penetrance breast cancer susceptibility gene, conferring a 2.3-fold increased risk for breast cancer compared to the general population (4, 5).

The risk of cancer among individuals heterozygous for *ATM* pathogenic variants has since been demonstrated for a broader range of malignancies. *ATM* pathogenic variant carriers appear to be at moderate-to-high increased risk for pancreatic, prostate, and gastric cancers and at low-to-moderate increased risk for ovarian and colorectal cancer as well as melanoma (6–9).

The association of *ATM* with cancer susceptibility has directly influenced clinical practice, from the creation of gene panels for molecular testing to cancer surveillance guidance and treatment recommendations. Here we present six novel cases of individuals with carcinomas of the gallbladder, uterus, duodenum, kidney, and lung as well as a sarcoma, all harboring germline *ATM* pathogenic variants, which suggests further expansion of the *ATM*-associated cancer susceptibility phenotype.

Methods

Review of patients harboring deleterious germline *ATM* variants

We retrospectively reviewed patients seen in our hereditary cancer clinic between March 2017 and December 2021 who had undergone germline testing with next-generation, multi-gene sequencing. We then identified all patients found to harbor germline likely pathogenic or pathogenic variants in *ATM* producing a loss-of-function using the criteria of the American College of Medical Genetics standards and guidelines for sequence variant interpretation (10). A comprehensive chart review through the electronic medical record was conducted to collect relevant clinical data including patient demographics, personal and family cancer history, as well as complete genetic testing results. Evidence substantiating the pathogenicity of the germline *ATM* variants among the six patients with atypical *ATM*-associated cancers was collected (Supplementary Table 1).

Multi-gene hereditary cancer syndrome testing was performed in commercial clinical laboratories accredited by the College of American Pathologists and certified by the Clinical Laboratory Improvement Amendment. Laboratories used included Ambry Genetics (Aliso Viejo, CA), GeneDx (Gaithersburg, MD), Myriad (Salt Lake City, UT), Sema4 (Stamford, CT), or Invitae (San Francisco, CA). One patient had sequencing performed at the medical institution where he had previously received care (Memorial Sloan Kettering, New York, NY). The number of analyzed genes ranged from 25-84, each of which was associated with hereditary cancers in peer-reviewed scientific literature (Supplementary Table 2).

Literature search of reported deleterious germline *ATM* variants in atypical cancers

A comprehensive review of the peer-reviewed literature through MEDLINE was conducted using PubMed for articles published between 1970 and July 2022. Search keywords included "pathogenic," "germline," "ATM," "variant," "hereditary," "cancer," "gallbladder," "uterus," "duodenum," "kidney," "lung," "epithelioid hemangioendothelioma," and then later expanded to include "biliary tract," "small bowel," "ampulla," and "sarcoma." Keywords were connected by the Boolean functions AND and OR.

All cross-sectional studies involving thirty or more patients affected with cancer of the biliary tract, uterus, small intestine/ampulla, kidney, lung, or sarcoma, who had undergone hereditary cancer predisposition testing with a multigene panel, exome, or genome sequencing were considered for inclusion. Studies using redundant patient information drawn from large datasets were excluded from the review. The study text and supplemental information were reviewed for patient characteristics, total germline pathogenic variants detected, and specific germline *ATM* variants identified.

The prevalence for each cancer type was estimated by dividing the number of individuals with a germline *ATM* pathogenic variant by the total sample size. To estimate the prevalence among those with hereditary cancer susceptibility, the number of individuals with a germline *ATM* pathogenic variant was divided by the number of those testing positive for any pathogenic variant in a hereditary cancer gene.

Obtaining frequency of somatic alterations in *ATM* for atypical cancers

De-identified genomic sequencing data from The Cancer Genome Atlas and other large-scale, cancer-specific sequencing studies were accessed and queried online through the cBioPortal for Cancer Genomics at https://www.cbioportal.org/ (11, 12). Patient cohorts were primarily selected from the TCGA pan-cancer atlas, and the

accession numbers for each tumor-specific analysis were recorded (Supplementary Methods). Somatic alterations included were loss-of-function single nucleotide variants (SNVs), indels, and copy number variants (CNVs) classified as pathogenic or likely pathogenic. Statistical analysis to compare deleterious alteration counts of *ATM*, *BRCA1*, and *CHEK2* within each tumor type was performed with Microsoft Excel version 16.64 (Microsoft, WA, USA) using the Z-test for independent proportions. A p-value equal to or less than 0.05 was considered significant.

Determining mutual exclusivity and co-occurrence among *ATM* and other DNA-damage response genes

Pathogenic alterations in the relevant cancer types accessed through cBioPortal as above were jointly analyzed to determine the relationship between variants in *ATM, BRCA1, CHEK2*, and *TP53*. A Log2 odds ratio was used to calculate how strongly the presence or absence of alterations in one gene was associated with the presence or absence of alterations in a second gene within the selected samples. A q-value derived from the Benjamini-Hochberg FDR correction procedure equal to or less than 0.05 was considered significant.

Compliance with ethical standards

All studies involving human participants were approved by the University of Miami institutional research board (IRB #20081166) and are in accordance with the 1964 Helsinki declaration and its later amendments or comparable ethical standards.

Results

We reviewed the patients seen in our hereditary cancer clinic who had undergone comprehensive multigene panel testing and were found to be heterozygous for a germline pathogenic variant in *ATM*. A total of thirty-one patients met these criteria, none of which had a pathogenic variant in any other hereditary cancer gene. Twenty-five of these patients had a personal or family history

of cancer that is consistent with the currently described spectrum of *ATM*-associated malignancies. Notably, the remaining six patients (19.4%) had a personal history of cancers not currently associated with *ATM* hereditary cancer susceptibility. Only one of these six patients was identified to harbor variants of uncertain significance in other hereditary cancer genes (Supplementary Table 3). To evaluate for genotype-phenotype correlations, we compared the pathogenic *ATM* variants in the 6 atypical cancer cases to the 25 typical cancer cases, though no clear differences were evident (Figure 1).

The personal and family history of cancer among the six patients with malignancies atypical for *ATM*-associated hereditary cancer susceptibility were then evaluated in detail (Table 1). We observed that two of the six patients had a personal history of known *ATM*-associated cancers. Patient 1 had a history of breast adenocarcinoma, and Patient 6 had a history of melanoma. All six patients had at least one 1st or 2nd-degree relative with *ATM*-associated cancer including breast, pancreatic, prostate, gastric, and colorectal adenocarcinomas. Four of the six patients meet current NCCN criteria for germline genetic testing based on either their personal history of cancer or family history of cancer (Supplementary Table 4).

Comprehensive review of atypical *ATM*-cancer associations

To better characterize the association between germline *ATM* pathogenic variants and the atypical cancers seen in our six patients, we performed a comprehensive review of all cross-sectional studies where germline sequencing was performed in patients diagnosed with carcinomas of the biliary tract, uterus, small bowel and ampulla, kidney, and lung, as well as sarcomas. We identified twenty-five broadly relevant, cross-sectional studies where next-generation sequencing of cancer susceptibility genes was performed (Supplementary Table 5, 13–37). A total of 171 unique patients harboring a germline pathogenic variant in *ATM* and diagnosed with one of the atypical *ATM* cancers were identified. Of these, we found that fewer than 20 cases of germline *ATM* pathogenic variants have been associated with biliary tract carcinoma, uterine carcinoma, small bowel carcinoma, or sarcoma, while we identified 95 cases of lung adenocarcinoma and 32 cases of renal cell carcinoma associated with germline *ATM* pathogenic variants.

FIGURE 1
Lollipop plot of germline *ATM* pathogenic variants detected in 31 consecutive patients with a personal or family history of cancer who underwent hereditary cancer susceptibility testing. The six variants associated with cancers that are atypical for *ATM* hereditary cancer susceptibility are highlighted in color (see legend).
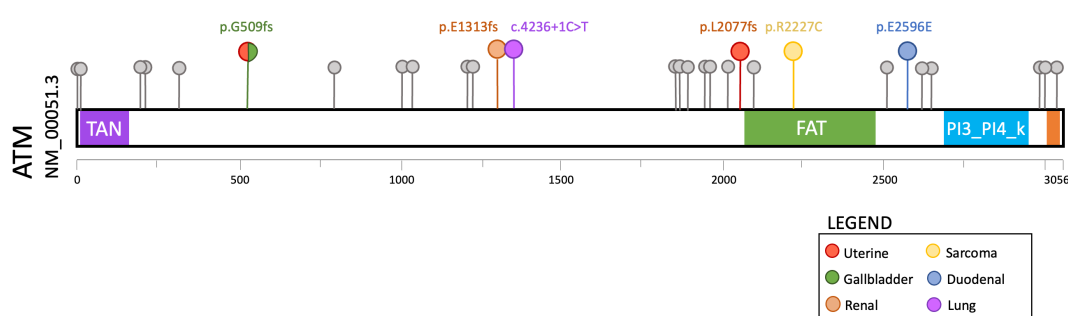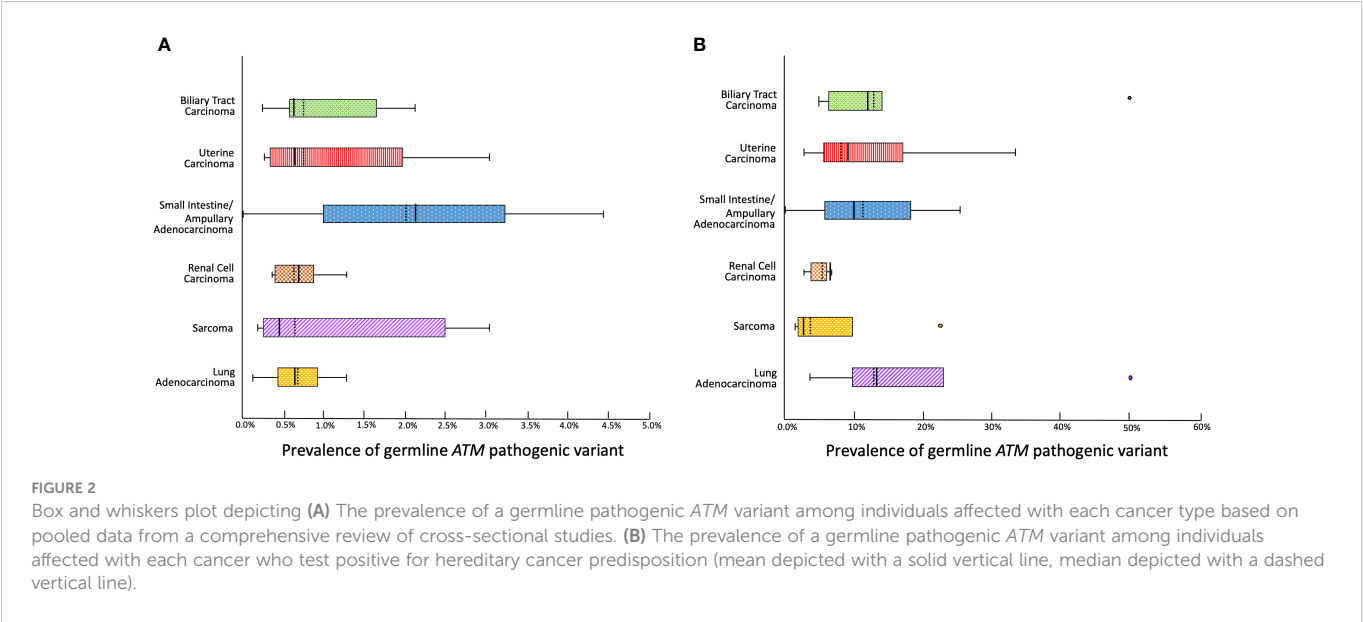
TABLE 1 Clinical summary of the six patients identified to harbor a pathogenic germline variant in *ATM* and a personal history of cancer not associated with *ATM* hereditary cancer syndrome.

Patient	Ethnicity	Cancer History (age at diagnosis)	Germline *ATM* variants	Family History of Cancer Among 1st and 2nd Degree Relatives
Patient 1	Italian & Portuguese	*Breast adenocarcinoma* (50s) Gallbladder carcinoma in situ (50s) Uterine endometroid carcinoma (60s)	c.1542delT p.Gly509Glufs*3	Mother: *breast cancer* (60s), *pancreatic cancer* (70s) Father: renal cancer (80s) Maternal aunt: *breast cancer* (60s), gallbladder cancer (70s) Paternal uncle: *colorectal cancer* (60s) Paternal grandfather: *colon cancer* (70s), *gastric cancer* (70s)
Patient 2	Ashkenazi Jewish	Uterine serous carcinoma (60s)	c.6228del p.Leu2077Phefs*5	Brother: *colon cancer* (60s) Father: *prostate cancer* (80s) Paternal uncle: *gastric cancer* (70s) Maternal aunt: bladder cancer (80s)
Patient 3	Lebanese	Duodenal adenocarcinoma (60s)	c.7788G>A p.Glu2596Glu	Brother: *prostate cancer* (50s) Mother: *breast cancer* (70s) Maternal aunt: *breast cancer* (70s) Maternal aunt: *breast cancer* (20s)
Patient 4	Ashkenazi Jewish	Clear cell renal cell carcinoma (40s)	c.3935dupG p.Glu1313Argfs*8	Mother: *rectal cancer* (70s) Maternal uncle: leukemia (70s) Maternal grandfather: leukemia (40s)
Patient 5	Caucasian	Epithelioid hemangioendothelioma of lung (40s)	c.6679C>T p.Arg2227Cys	Father: brain cancer (20s) Maternal aunt: *breast cancer* (40s), throat cancer (60s) Maternal aunt: *colon cancer* (70s) Maternal aunt: *colon cancer* (60s) Maternal aunt: *colon cancer* (70s) Paternal uncle: *melanoma* (50s)
Patient 6	Ashkenazi Jewish	*Melanoma* (10s) Lung adenocarcinoma (60s)	c.4236+1G>T	Father: *prostate cancer* (70s) Paternal grandfather: *gastric cancer* (50s) Nephew: anaplastic astrocytoma (20s) Maternal grandmother: *breast cancer* (70s)

Italicized cancers are those currently associated with *ATM* hereditary cancer predisposition syndrome.

We then estimated the prevalence of germline *ATM* pathogenic variants for each relevant cancer type by compiling data from each reviewed study (Figure 2A). The prevalence was calculated to be as low as 0.45% for sarcoma, 0.57% for uterine carcinoma, 0.6% for biliary tract carcinoma, 0.63% for lung carcinoma, and 0.87% for renal cell carcinoma. In the case of small intestine & ampullary carcinoma, the prevalence reached 2.2% albeit with a broad range due to the limited sample size. We then calculated the prevalence of germline *ATM* pathogenic variants among individuals diagnosed with an atypical *ATM* cancer who tested positive for hereditary cancer predisposition (Figure 2B). We found that among sarcoma and renal cell carcinoma patients diagnosed with a hereditary cancer susceptibility syndrome, the prevalence of a germline *ATM* pathogenic variant was 2.4% and 6.5%, respectively. Meanwhile,

FIGURE 2
Box and whiskers plot depicting **(A)** The prevalence of a germline pathogenic *ATM* variant among individuals affected with each cancer type based on pooled data from a comprehensive review of cross-sectional studies. **(B)** The prevalence of a germline pathogenic *ATM* variant among individuals affected with each cancer who test positive for hereditary cancer predisposition (mean depicted with a solid vertical line, median depicted with a dashed vertical line).

patients with biliary tract, uterine, small bowel & ampullary, as well as lung carcinomas who tested positive for a hereditary cancer susceptibility syndrome had a germline *ATM* pathogenic variant in 9% - 12.7% of cases.

These data provide evidence that germline *ATM* pathogenic variants exhibit a low penetrance for the atypical cancers investigated herein. Nevertheless, these germline *ATM* pathogenic variants were associated with a significant proportion of the known causes for hereditary cancer susceptibility in these cancers.

Somatic alterations in *ATM* detected in tumor sequencing databases across the investigated cancer types

Next, we explored available tumor sequencing data from large cohorts that closely match the tumor type and subtype described in our patient cases with the aim of further clarifying the biological relevance of *ATM* loss-of-function variants in the carcinogenesis of gallbladder, uterus, duodenum, kidney, lung, and sarcomas. We queried data available through cBioPortal and determined the frequency of somatic deleterious *ATM* variants and compared this alteration frequency to that of *BRCA1* and *CHEK2*, as these are DNA-damage response tumor suppressors also implicated in hereditary cancer, but not established to drive oncogenesis in the cancer types being investigated.

ATM variants were detected in as many as 12% of uterine carcinomas, 8% of gallbladder carcinomas, 7.8% of small bowel carcinomas, and 5% of lung adenocarcinomas, whereas *BRCA1* and *CHEK2* variants were found in less than 3% of uterine carcinomas, less than 2% of lung adenocarcinomas, less than 1% of gallbladder carcinomas, and none were found in small bowel carcinomas (Figure 3). Clear cell renal cancer had the fewest *ATM* pathogenic alterations, reported at a frequency of 2.3%, though still at a significantly higher frequency than that of *BRCA1* and *CHEK2*. In the case of sarcoma, the *ATM* alteration frequency was 2.8%, which was significantly greater than *BRCA1* but not *CHEK2*. We then compared these alteration frequencies to those seen in breast cancer, where all three genes have been implicated in carcinogenesis, and found pathogenic variants in *ATM* only occurred in 2.5% of cases and with a similar frequency to *BRCA1*, though more frequently than *CHEK2*. These data provide complementary evidence that *ATM* may contribute to cancer risk in each of these cancer types.

To better understand the influence of germline and somatic *ATM* variants on carcinogenesis in these atypical *ATM* cancers, we pooled the cancer sequencing data to examine the relationship between *ATM* alterations and the alteration of other genes in the DNA damage response and cell cycle pathways (Figure 4). We found a significant co-occurrence of pathogenic alterations in *ATM* with pathogenic alterations in *BRCA1* and *CHEK2* (Log2 OR 2.7, 2.5, p<0.01). In addition, we saw significant mutual exclusivity between *ATM* and *TP53* (Log2 OR -0.67, p<0.05). This suggests that the presence of germline *ATM* pathogenic variants may influence associated cancers to be driven toward DNA-damage repair deficiency, and away from loss of *TP53*, the most ubiquitous driver of cancer (38).
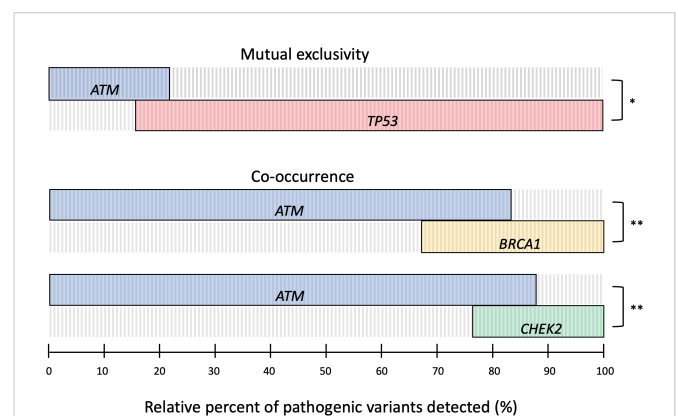
FIGURE 4

Oncoprint plot of somatic pathogenic alterations in *ATM, TP53, BRCA,* and *CHEK2* across relevant tumor sequencing data to determine the relationship between alterations. Log2 odds ratio was used to identify mutual exclusivity and co-occurrence, with significant differences defined by Benjamini–Hochberg FDR correction (* q ≤ 0.05, ** q ≤ 0.01, *** q ≤ 0.001).
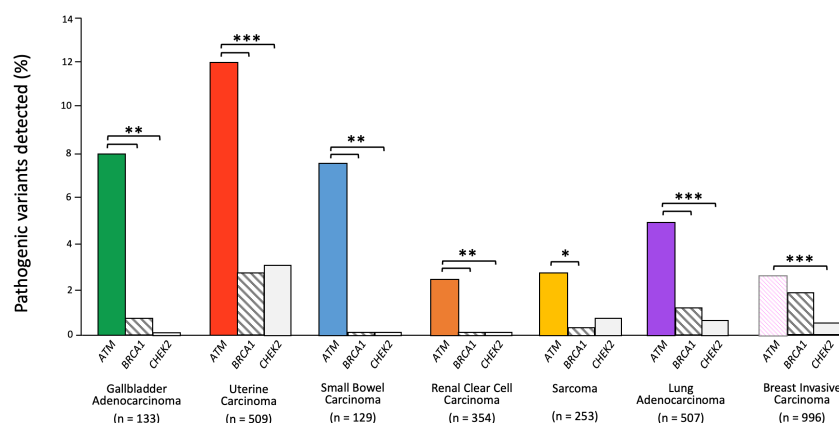
FIGURE 3

ATM somatic alteration frequency compared to *BRCA1* and *CHEK2* alterations in relevant cancers. Z-test for independent proportions was used to identify significant differences (* p ≤ 0.05, ** p ≤ 0.01, *** p ≤ 0.001, all other comparisons not significant). Tumor sequencing data was accessed through cBioPortal.

Discussion

Here we describe six unrelated patients found to be heterozygous for germline, loss-of-function variants in *ATM* and diagnosed with at least one malignancy that is not currently associated with the *ATM* cancer susceptibility syndrome, including gallbladder carcinoma, uterine carcinoma, renal cell carcinoma, duodenal adenocarcinoma, lung adenocarcinoma, and a vascular sarcoma. These atypical cancers were diagnosed in a significant proportion of patients with *ATM*-associated hereditary cancer susceptibility in our cohort. Nevertheless, our review of the literature indicates that the prevalence of germline *ATM* pathogenic variants among individuals diagnosed with these atypical cancers appears to be less than 1% in most cases.

Exploration of somatic alterations in The Cancer Genome Atlas (TCGA) datasets demonstrated there was a high frequency of pathogenic alterations in *ATM* relative to other tumor suppressors associated with hereditary cancer syndromes, suggesting that *ATM* loss may contribute to oncogenesis within these cancer types. Furthermore, our analysis reveals that alterations in *ATM* tend to co-occur with pathogenic alterations in *BRCA1* and *CHEK2* while being mutually exclusive of *TP53*. This latter finding underscores the shared functional pathway between *ATM* and *TP53* and reinforces prior work showing that DNA damage creates selection pressure for the inactivation of p53 that can be abrogated through the loss of *ATM* (39, 40). More broadly, these pathway interactions illustrate how germline *ATM* pathogenic variants may influence the acquisition of somatic alterations throughout cancer initiation and progression.

The cases reported in this series exemplify how the tumor spectra associated with cancer susceptibility syndromes are broadening through the clinical use of pan-cancer panels. The germline pathogenic variants in *ATM* detected in all six of our patients were discovered through comprehensive hereditary cancer panels. This testing approach is supported by studies demonstrating significantly higher detection rates compared to panels oriented specifically to the genes that are most relevant to the personal or family history of cancer (41–43). The heterogeneity in cancers documented among our patients with germline *ATM* variants and their families further emphasizes the value of pan-cancer panels, and certainly the importance of including *ATM* in multi-gene panels testing for hereditary cancer predisposition.

Moreover, our cases illustrate the way NCCN Guidelines may significantly limit the detection of hereditary cancer susceptibility, as many cancer types, particularly those with a low prevalence, do not currently qualify individuals for genetic testing. In our series, neither Patient 4 nor Patient 6 met guidelines for hereditary cancer testing based on their personal or family history of cancer, illustrating circumstances in which *ATM* germline variants may go undetected. This was underscored in a recent study where germline genetic testing in an unselected pan-cancer patient population found that over half of the patients who tested positive for pathogenic variants were not eligible for hereditary cancer testing based on current guidelines (44). Improving the detection of *ATM*-associated hereditary cancer is clinically meaningful as it can enable cascade genetic testing for family members who are at risk, facilitate appropriate cancer surveillance for those affected, and prompt the use of precision-based therapies.

Although no specific *ATM* genotype-phenotype correlations were discerned in this study, we did observe that the *ATM* c.1564_1565delGA variant was present in two patients with uterine cancer, and the *ATM* p.V2716A variant was present in two patients with lung adenocarcinoma. In addition, we found the germline *ATM* variant c.6679C>T identified in Patient 5 with epithelioid hemangioendothelioma was also seen in a case of endometrioid uterine cancer, and the germline *ATM* variant c.4236+1G seen in Patient 6 with lung adenocarcinoma was also present in a case of renal cell carcinoma. Meanwhile, none of the pathogenic germline *ATM* variants identified in our six patients overlapped among the somatic loss-of-function *ATM* variants present in the cancer sequencing datasets. Larger sample sizes will be needed to systematically investigate whether specific germline *ATM* variants confer a greater risk for atypical *ATM* cancers.

A limitation of this study is that we cannot exclude the possibility that our patients' malignancies were incidental to, rather than caused by the pathogenic variant in *ATM*, as the incidence of heterozygosity for pathogenic variants in *ATM* has been estimated in gnomAD for European populations to be 0.48% (45). A segregation analysis of our patients' families may have strengthened the association between atypical cancers and pathogenic variants in *ATM*, as this would have revealed whether the gallbladder carcinoma in the maternal aunt of Patient 1, the leukemias in the maternal uncle and grandfather of Patient 4, or the anaplastic astrocytoma in the paternal nephew of Patient 6 were also associated with pathogenic variants in *ATM*. Moreover, we were not able to confirm whether *ATM* loss of heterozygosity occurred in our six patients, which could have provided further evidence that *ATM* is driving carcinogenesis based on the two-hit hypothesis (46). Yet, this does not appear to be a reliable finding as the frequency of biallelic two-hit events across all cancers where a germline pathogenic variant is present has been estimated at 38.3%, with a recent study finding that *ATM* somatic second hits occurred in 11.3% in a wide spectrum of cancers including breast, pancreatic, bladder, uterine and lung cancers, among others (15, 47). A case-control analysis for each of the atypical-*ATM* cancer types could have also provided compelling evidence of an association. This has been previously performed in two cohorts of patients with lung adenocarcinoma, demonstrating a significant enrichment for germline pathogenic variants in *ATM* in cases compared to controls (48, 49). Unfortunately, the feasibility of case-control studies is limited by the rarity of many of these cancers, as well as the low penetrance of *ATM* in association with these atypical cancers.

Nevertheless, our finding of relatively frequent somatic *ATM* alterations across many of the atypical cancer types has been corroborated by an analysis showing that *ATM* was among the most frequently mutated genes in the DNA-damage response pathway across 33 distinct types of cancers (50). This evidence has also been bolstered by a recent study demonstrating a high prevalence of germline pathogenic variants in *ATM* relative to other hereditary cancer genes across a spectrum of cancers lacking testing guidelines, including bladder, brain, esophagus, and head and neck cancers (15). Furthermore, our identification that pathogenic *ATM* alterations in these atypical cancers are associated with the co-occurrence of alterations in *BRCA1* and *CHEK2*, and mutual exclusivity with *TP53*, suggests that cancers with a germline pathogenic variant in *ATM* may depend on specific molecular alterations that confer targetable vulnerabilities. This has already been

documented in patients with metastatic prostate cancer harboring a germline pathogenic variant in *ATM* sensitizing to PARP inhibition, as well as in patients with pancreatic cancer where monoallelic pathogenic variants in *ATM* produce susceptibility to combined therapies that synergistically target the DNA-damage response pathway (51, 52).

In conclusion, this study combines detailed clinical phenotyping with a comprehensive review of relevant germline *ATM* reports and large-scale tumor sequencing data to propose that germline pathogenic variants in *ATM* may be associated with the development of cancers of the gallbladder, duodenum, uterus, kidney, and lung as well as sarcoma cancers. Consideration should be given to a broadening of the *ATM*-cancer susceptibility syndrome phenotype within hereditary cancer testing guidelines, as this has the potential to improve the detection of affected patients and facilitate the use of more effective cancer treatments.

Data availability statement

The datasets presented in this study can be found in online repositories. The names of the repository/repositories and accession number(s) can be found in the article/Supplementary Material.

Ethics statement

The studies involving human participants were reviewed and approved by University of Miami institutional research board (IRB #20081166). Written informed consent for participation was not required for this study in accordance with the national legislation and the institutional requirements.

Author contributions

NB: Conceptualization, methodology, data curation, formal analysis, project administration, visualization, writing–original draft, and writing–review and editing. RS-S: Conceptualization, investigation, resources, data curation, writing–review and editing. MH: Investigation, resources, data interpretation, writing–review and editing. DP: Investigation,

Conflict of interest

The authors declare that the research was conducted in the absence of any commercial or financial relationships that could be construed as a potential conflict of interest.

Publisher's note

All claims expressed in this article are solely those of the authors and do not necessarily represent those of their affiliated organizations, or those of the publisher, the editors and the reviewers. Any product that may be evaluated in this article, or claim that may be made by its manufacturer, is not guaranteed or endorsed by the publisher.

Supplementary material

The Supplementary Material for this article can be found online at: https://www.frontiersin.org/articles/10.3389/fonc.2023.1068110/full#supplementary-material

References

1. Choi M, Kipps T, Kurzrock R. ATM Mutations in cancer: Therapeutic implications. *Mol Cancer Ther* (2016) 15:1781–91. doi: 10.1158/1535-7163.mct-15-0945

2. Shiloh Y, Ziv Y. The ATM protein kinase: Regulating the cellular response to genotoxic stress, and more. *Nat Rev Mol Cell Bio* (2013) 14:197–210. doi: 10.1038/nrm3546

3. Rothblum-Oviatt C, Wright J, Lefton-Greif MA, McGrath-Morrow SA, Crawford TO, Lederman HM. Ataxia telangiectasia: A review. *Orphanet J Rare Dis* (2016) 11:159. doi: 10.1186/s13023-016-0543-7

4. Thompson D, Duedal S, Kirner J, McGuffog L, Last J, Reiman A, et al. Cancer risks and mortality in heterozygous ATM mutation carriers. *Jnci J Natl Cancer Inst* (2005) 97:813–22. doi: 10.1093/jnci/dji141

5. Marabelli M, Cheng S, Parmigiani G. Penetrance of ATM gene mutations in breast cancer: A meta-analysis of different measures of risk. *Genet Epidemiol* (2016) 40:425–31. doi: 10.1002/gepi.21971

6. Hall MJ, Bernhisel R, Hughes E, Larson K, Rosenthal ET, Singh NA, et al. Germline pathogenic variants in the ataxia telangiectasia mutated (ATM) gene are associated with high and moderate risks for multiple cancers. *Cancer Prev Res* (2021) 14:433–40. doi: 10.1158/1940-6207.capr-20-0448

7. Chaffee KG, Oberg AL, McWilliams RR, Majithia N, Allen BA, Kidd J, et al. Prevalence of germline mutations in cancer genes among pancreatic cancer patients with positive family history. *Genet Med Off J Am Coll Med Genet* (2018) 20:119–27. doi: 10.1038/gim.2017.85

8. Pearlman R, Frankel WL, Swanson B, Zhao W, Yilmaz A, Miller K, et al. Prevalence and spectrum of germline cancer susceptibility gene mutations among patients with early-onset colorectal cancer. *JAMA Oncol* (2016) 3:464. doi: 10.1001/jamaoncol.2016.5194

9. Goldstein AM, Xiao Y, Sampson J, Zhu B, Rotunno M, Bennett H, et al. Rare germline variants in known melanoma susceptibility genes in familial melanoma. *Hum Mol Genet* (2017) 26:4886–95. doi: 10.1093/hmg/ddx368

10. Richards S, Aziz N, Bale S, Bick D, Das S, Gastier-Foster J, et al. Standards and guidelines for the interpretation of sequence variants: A joint consensus recommendation of the American college of medical genetics and genomics and the association for molecular pathology. *Genet Med* (2015) 17:405–23. doi: 10.1038/gim.2015.30

11. Gao J, Aksoy BA, Dogrusoz U, Dresdner G, Gross B, Sumer SO, et al. Integrative analysis of complex cancer genomics and clinical profiles using the cBioPortal. *Sci Signal* (2013) 6:pl1. doi: 10.1126/scisignal.2004088

12. Cerami E, Gao J, Dogrusoz U, Gross BE, Sumer SO, Aksoy BA, et al. The cBio cancer genomics portal: An open platform for exploring multidimensional cancer genomics data. *Cancer Discovery* (2012) 2:401–4. doi: 10.1158/2159-8290.cd-12-0095

13. Maynard H, Stadler ZK, Berger MF, Solit DB, Ly M, Lowery MA, et al. Germline alterations in patients with biliary tract cancers: A spectrum of significant and previously underappreciated findings. *Cancer* (2020) 126:1995–2002. doi: 10.1002/cncr.32740

14. Wardell CP, Fujita M, Yamada T, Simbolo M, Fassan M, Karlic R, et al. Genomic characterization of biliary tract cancers identifies driver genes and predisposing mutations. *J Hepatol* (2018) 68:959–69. doi: 10.1016/j.jhep.2018.01.009

15. Yap TA, Ashok A, Stoll J, Mauer E, Nepomuceno VM, Blackwell KL, et al. Prevalence of germline findings among tumors from cancer types lacking hereditary testing guidelines. *JAMA Netw Open* (2022) 5:e2213070. doi: 10.1001/jamanetworkopen.2022.13070

16. Lin J, Dong K, Bai Y, Zhao S, Dong Y, Shi J, et al. Precision oncology for gallbladder cancer: insights from genetic alterations and clinical practice. *Ann Transl Med* (2019) 7:467–7. doi: 10.21037/atm.2019.08.67

17. Bertelsen B, Tuxen IV, Yde CW, Gabrielaite M, Torp MH, Kinalis S, et al. High frequency of pathogenic germline variants within homologous recombination repair in patients with advanced cancer. *NPJ Genom Med* (2019) 4:13. doi: 10.1038/s41525-019-0087-6

18. Karpel HC, Chern J-Y, J. MS, A. JS, Pothuri B. Utility of germline multi-gene panel testing in patients with endometrial cancer. *Gynecol Oncol* (2022) 165:546–51. doi: 10.1016/j.ygyno.2022.04.003

19. Ring KL, Bruegl AS, Allen BA, Elkin EP, Singh N, Hartman A-R, et al. Germline multi-gene hereditary cancer panel testing in an unselected endometrial cancer cohort. *Modern Pathol* (2016) 29:1381–9. doi: 10.1038/modpathol.2016.135

20. Kondrashova O, Shamsani J, O'Mara TA, Newell F, Reed AEM, Lakhani SR, et al. Tumor signature analysis implicates hereditary cancer genes in endometrial cancer development. *Cancers* (2021) 13:1762. doi: 10.3390/cancers13081762

21. Long B, Lilyquist J, Weaver A, Hu C, Gnanaolivu R, Lee KY, et al. Cancer susceptibility gene mutations in type I and II endometrial cancer. *Gynecol Oncol* (2019) 152:20–5. doi: 10.1016/j.ygyno.2018.10.019

22. Latham A, Shia J, Patel Z, Reidy-Lagunes DL, Segal NH, Yaeger R, et al. Characterization and clinical outcomes of DNA mismatch repair–deficient small bowel adenocarcinoma. *Clin Cancer Res* (2021) 27:1429–37. doi: 10.1158/1078-0432.ccr-20-2892

23. Kumari N, Singh RK, Mishra SK, L R, Mohindra S, Krishnani N. Prevalence and spectrum of pathogenic germline variants in intestinal and pancreatobiliary type of ampullary cancer. *Pathol - Res Pract* (2021) 217:153309. doi: 10.1016/j.prp.2020.153309

24. Wong W, Lowery MA, Berger MF, Kemel Y, Taylor B, Zehir A, et al. Ampullary cancer: Evaluation of somatic and germline genetic alterations and association with clinical outcomes. *Cancer* (2019) 125:1441–8. doi: 10.1002/cncr.31951

25. Kong W, Yang T, Wen X, Mu Z, Zhao C, Han S, et al. Germline mutation landscape and associated clinical characteristics in Chinese patients with renal cell carcinoma. *Front Oncol* (2021) 11:737547. doi: 10.3389/fonc.2021.737547

26. Truong H, Sheikh R, Kotecha R, Kemel Y, Reisz PA, Lenis AT, et al. Germline variants identified in patients with early-onset renal cell carcinoma referred for germline genetic testing. *Eur Urol Oncol* (2021) 4:993–1000. doi: 10.1016/j.euo.2021.09.005

27. Carlo MI, Mukherjee S, Mandelker D, Vijai J, Kemel Y, Zhang L, et al. Prevalence of germline mutations in cancer susceptibility genes in patients with advanced renal cell carcinoma. *JAMA Oncol* (2018) 4:1228. doi: 10.1001/jamaoncol.2018.1986

28. Santos M, Lanillos J, Roldan-Romero JM, Caleiras E, Montero-Conde C, Cascón A, et al. Prevalence of pathogenic germline variants in patients with metastatic renal cell carcinoma. *Genet Med* (2021) 23:698–704. doi: 10.1038/s41436-020-01062-0

29. Alaiwi SA, Nassar AH, Adib E, Groha SM, Akl EW, McGregor BA, et al. Trans-ethnic variation in germline variants of patients with renal cell carcinoma. *Cell Rep* (2021) 34:108926. doi: 10.1016/j.celrep.2021.108926

30. Yngvadottir B, Andreou A, Bassaganyas L, Larionov A, Cornish AJ, Chubb D, et al. Frequency of pathogenic germline variants in cancer susceptibility genes in 1336 renal cell carcinoma cases. *Hum Mol Genet* (2022) 31:ddac089. doi: 10.1093/hmg/ddac089

31. Chan SH, Lim WK, Ishak NDB, Li S-T, Goh WL, Tan GS, et al. Germline mutations in cancer predisposition genes are frequent in sporadic sarcomas. *Sci Rep-uk* (2017) 7:10660. doi: 10.1038/s41598-017-10333-x

32. Gillani R, Camp SY, Han S, Jones JK, Chu H, O'Brien S, et al. Germline predisposition to pediatric Ewing sarcoma is characterized by inherited pathogenic variants in DNA damage repair genes. *Am J Hum Genet* (2022) 109:1026–37. doi: 10.1016/j.ajhg.2022.04.007

33. Mirabello L, Zhu B, Koster R, Karlins E, Dean M, Yeager M, et al. Frequency of pathogenic germline variants in cancer-susceptibility genes in patients with osteosarcoma. *JAMA Oncol* (2020) 6:724–34. doi: 10.1001/jamaoncol.2020.0197

34. Kim J, Light N, Subasri V, Young EL, Wegman-Ostrosky T, Barkauskas DA, et al. Pathogenic germline variants in cancer susceptibility genes in children and young adults with rhabdomyosarcoma. *Jco Precis Oncol* (2021) 5:75–87. doi: 10.1200/po.20.00218

35. Parry EM, Gable DL, Stanley SE, Khalil SE, Antonescu V, Florea L, et al. Germline mutations in DNA repair genes in lung adenocarcinoma. *J Thorac Oncol* (2017) 12:1673–8. doi: 10.1016/j.jtho.2017.08.011

36. Mukherjee S, Bandlamudi C, Hellmann MD, Kemel Y, Drill E, Rizvi H, et al. Germline pathogenic variants impact clinicopathology of advanced lung cancer. *Cancer Epidemiol Biomarkers Prev* (2022) 31:1450–9. doi: 10.1158/1055-9965.epi-21-1287

37. Tian P, Cheng X, Zhao Z, Zhang Y, Bao C, Wang Y, et al. Spectrum of pathogenic germline mutations in Chinese lung cancer patients through next-generation sequencing. *Pathol Oncol Res* (2020) 26:109–14. doi: 10.1007/s12253-019-00771-5

38. Campbell PJ, Getz G, Korbel JO, Stuart JM, Jennings JL, Stein LD, et al. Pan-cancer analysis of whole genomes. *Nature* (2020) 578:82–93. doi: 10.1038/s41586-020-1969-6

39. Negrini S, Gorgoulis VG, Halazonetis TD. Genomic instability — an evolving hallmark of cancer. *Nat Rev Mol Cell Bio* (2010) 11:220–8. doi: 10.1038/nrm2858

40. Pettitt AR, Sherrington PD, Stewart G, Cawley JC, Taylor AMR, Stankovic T. p53 dysfunction in b-cell chronic lymphocytic leukemia: Inactivation of ATM as an alternative toTP53 mutation. *Blood* (2001) 98:814–22. doi: 10.1182/blood.v98.3.814

41. Rosenthal ET, Bernhisel R, Brown K, Kidd J, Manley S. Clinical testing with a panel of 25 genes associated with increased cancer risk results in a significant increase in clinically significant findings across a broad range of cancer histories. *Cancer Genet-ny* (2017) 218:58–68. doi: 10.1016/j.cancergen.2017.09.003

42. LaDuca H, Polley EC, Yussuf A, Hoang L, Gutierrez S, Hart SN, et al. A clinical guide to hereditary cancer panel testing: Evaluation of gene-specific cancer associations and sensitivity of genetic testing criteria in a cohort of 165,000 high-risk patients. *Genet Med* (2020) 22:407–15. doi: 10.1038/s41436-019-0633-8

43. Cavaillé M, Uhrhammer N, Privat M, Ponelle-Chachuat F, Gay-Bellile M, Lepage M, et al. Feedback of extended panel sequencing in 1530 patients referred for suspicion of hereditary predisposition to adult cancers. *Clin Genet* (2021) 99:166–75. doi: 10.1111/cge.13864

44. Perkins AT, Haslem D, Goldsberry J, Shortt K, Sittig L, Raghunath S, et al. Universal germline testing of unselected cancer patients detects pathogenic variants missed by standard guidelines without increasing healthcare costs. *Cancers* (2021) 13:5612. doi: 10.3390/cancers13225612

45. Karczewski KJ, Francioli LC, Tiao G, Cummings BB, Alföldi J, Wang Q, et al. The mutational constraint spectrum quantified from variation in 141,456 humans. *Nature* (2020) 581:434–43. doi: 10.1038/s41586-020-2308-7

46. Knudson AG. Mutation and cancer: Statistical study of retinoblastoma. *Proc Natl Acad Sci* (1971) 68:820–3. doi: 10.1073/pnas.68.4.820

47. Huang K, Mashl RJ, Wu Y, Ritter DI, Wang J, Oh C, et al. Pathogenic germline variants in 10,389 adult cancers. *Cell* (2018) 173:355–370.e14. doi: 10.1016/j.cell.2018.03.039

48. Selvan ME, Zauderer MG, Rudin CM, Jones S, Mukherjee S, Offit K, et al. Inherited rare, deleterious variants in ATM increase lung adenocarcinoma risk. *J Thorac Oncol* (2020) 15:1871–9. doi: 10.1016/j.jtho.2020.08.017

49. Sang J, Zhang T, Kim J, Li M, Pesatori AC, Consonni D, et al. Rare germline deleterious variants increase susceptibility for lung cancer. *Hum Mol Genet* (2022) 31:3558–65. doi: 10.1093/hmg/ddac123

50. Knijnenburg TA, Wang L, Zimmermann MT, Chambwe N, Gao GF, Cherniack AD, et al. Genomic and molecular landscape of DNA damage repair deficiency across the cancer genome atlas. *Cell Rep* (2018) 23:239–254.e6. doi: 10.1016/j.celrep.2018.03.076

51. Gout J, Perkhofer L, Morawe M, Arnold F, Ihle M, Biber S, et al. Synergistic targeting and resistance to PARP inhibition in DNA damage repair-deficient pancreatic cancer. *Gut* (2021) 70:743–60. doi: 10.1136/gutjnl-2019-319970

52. Bono de J, Mateo J, Fizazi K, Saad F, Shore N, Sandhu S, et al. Olaparib for metastatic castration-resistant prostate cancer. *New Engl J Med* (2020) 382:2091–102. doi: 10.1056/nejmoa1911440

Case Report: Extraskeletal osteosarcoma with preceding myositis ossificans

Hiroki Imada[1], Tomoaki Torigoe[2], Yasuo Yazawa[2],
Satoshi Kanno[3], Jiro Ichikawa[4], Takehiko Yamaguchi[5]
and Tomonori Kawasaki[3]*

[1]Department of Pathology, Saitama Medical University Saitama Medical Center, Kawagoe, Japan,
[2]Department of Orthopaedic Oncology and Surgery, Saitama Medical University International Medical
Center, Hidaka, Japan, [3]Department of Pathology, Saitama Medical University International Medical
Center, Hidaka, Japan, [4]Department of Orthopedic Surgery, Graduate School of Medical Science,
University of Yamanashi, Chuo, Japan, [5]Department of Pathology, Dokkyo Medical University Nikko
Medical Center, Nikko, Japan

Extraskeletal osteosarcoma (EO) is a soft tissue sarcoma characterized by the production of bone matrix by neoplastic cells. Benign osteoid in EO, leading to a diagnostic dilemma, is rarely encountered. Herein, for the first time, we present a case with cytogenetically confirmed EO combined with or preceding myositis ossificans (MO). A 21-year-old man had a mildly painful swelling in his left knee. Imaging studies demonstrated a 39-mm mass with peripheral mineralization and cystic change on the posterolateral side of the left fibular head. He was clinically suspected of having either MO or a malignancy, such that wide resection was performed. Macroscopically, the mass was grayish to brown. In the cut section, multiple cystic lesions in addition to solid components were noted. Histopathologically, the solid components demonstrated diffuse proliferation of pleomorphic tumor cells with osteoclast-like giant cells. The malignant tumor cells formed osteoid. In the periphery, the mass was benign, showing mature bone tissue and focally non-malignant woven bone with fibroblasts, compatible with zonation. Fluorescence *in situ* hybridization (FISH) demonstrated split signals of the *USP6* gene. These findings suggested EO with preceding MO. Although the pathogenesis remains to be elucidated, the observed *USP6* rearrangement might contribute to both the diagnosis of EO with preceding MO and an understanding of the underlying histopathology.

KEYWORDS

extraskeletal osteosarcoma, myositis ossificans, USP6, high-grade sarcoma, malignant transformation

Introduction

Extraskeletal osteosarcoma (EO) is defined as soft tissue sarcoma with bone matrix production by malignant cells outside the skeletal system ([1]). The pathological diagnosis of EO is based solely on the identification of histological osteogenic differentiation. The presence of benign osteoid-simulating myositis ossificans (MO) is rarely encountered in

EO cases, possibly presenting both diagnostic and etiologic dilemmas. EO has been recognized as having complex genomic signatures (2), but most of the genetic alterations discovered to date have been non-diagnostic in clinical practice. On the other hand, MO was recently found to harbor a *USP6* rearrangement (3). However, unfortunately, the previous case reports of EO with MO lacked cytogenetic investigation. To our knowledge, this is the first report to describe a cytogenetically confirmed case in which EO was combined with or preceded MO. This is also only the second description of EO with distinct zonation of MO.

Clinical summary

A 21-year-old man consulted our hospital for a mildly painful swelling on his left knee that he had noticed 4 days earlier. A 40 × 40 × 30 mm subcutaneous mass was identified on the lateral side of the left fibular head. Laboratory test results were unremarkable. X-rays and computed tomography (CT) scans revealed a mass lesion on the posterolateral side of the left knee and the periphery of the mass showed mineralization (Figure 1). There was no continuity with the bone cortex. On magnetic resonance imaging (MRI), the mass was solid and cystic with intermediate signal intensity on T1-weighted imaging (Figure 2A), while showing heterogeneously high intensity with the fluid–fluid level on T2-weighted imaging (Figure 2B). The periphery was enhanced on FS-T1-weighted imaging with contrast (Figures 2C, D). His prior medical history, except for an injury to the same knee 10 years earlier, was unremarkable and he had never undergone radiation therapy. No evidence of metastasis was identified clinically. The core needle biopsy specimen was insufficient and did not yield a diagnosis. However, the cytology specimen suggested malignancy. Due to the tendency of the lesion to show growth and the positive cytology result, the tumor was clinically suspected of MO or hematoma with malignancy. The mass lesion was thus excised with a wide margin containing biopsy tract, without preoperative chemotherapy 6 weeks after the initial presentation. At the time of excision, the mass had not changed in size since the initial visit.

Pathological findings

Macroscopically, the gray-whitish or blackish-brown mass was located in the subcutaneous tissue, measuring 4.5 × 4 × 2.5 cm. On the cut surface, multiple cystic lesions filled with blood were noted with focal solid components (Figure 3). Histologically, the solid components were composed of diffuse proliferation of pleomorphic tumor cells, intermingled with abundant osteoclast-like giant cells (Figure 4A). Mitotic figures were numerous [22 per 10 high-power fields (HPFs)], with atypical mitoses. The tumor cells focally formed neoplastic osteoid (Figure 4B). No other morphological differentiation was confirmed. Cystic lesions included bloody materials and, internally, osteoclast-like giant cells (Figure 4C), compatible with telangiectatic or aneurysmal bone cyst-like change. The periphery of the mass consisted of benign mature bone with bland osteocytes (Figure 4D). The mature bone area was predominantly composed of lamellar bone trabeculae and focally woven bone with fibroblasts, and thus zonation was suggested (Figure 4E). EO components were adjacent to but discontinuous with mature bone lesions.

Immunohistochemically, the tumor cells showed no expression of MDM2 (Clone IF2, dilution 100×, ThermoFisher), CDK4 (Clone DCS-31, dilution 200×, Invitrogen), or H3.3 G34W (Clone RM263, dilution 800×, RevMAb Biosciences). Fluorescence *in situ* hybridization (FISH) revealed split signals of the *USP6* gene in the tumor cells (Figure 5). Based on these pathological findings, we diagnosed EO with the preceding MO.

The patient remains alive and limb function is completely preserved. Neither recurrence nor metastasis was recognized 16 months after surgery.

Discussion

MO has been regarded as an aggressively reactive process with bone formation (4). It commonly occurs in athletically active young men often with a prior history of trauma or surgery, and patients usually present with a painful mass (4). The precise etiology of MO
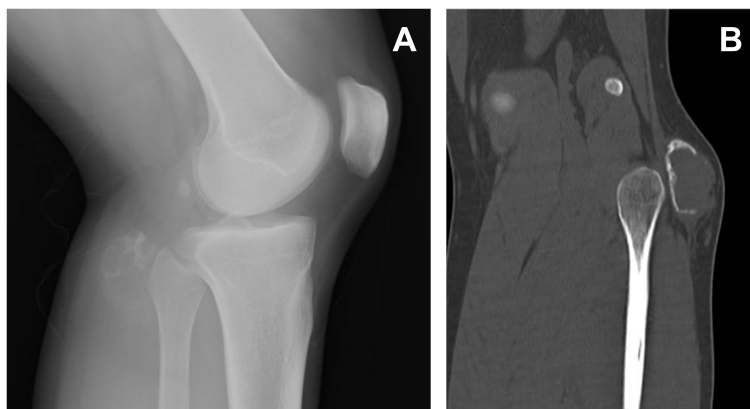

FIGURE 1
Lateral view x-ray of the left knee demonstrating a mass posterior to the fibular head **(A)**. On reconstructed CT, the mass was calcified in the periphery, but the shell was not complete and showed focal interruption **(B)**.
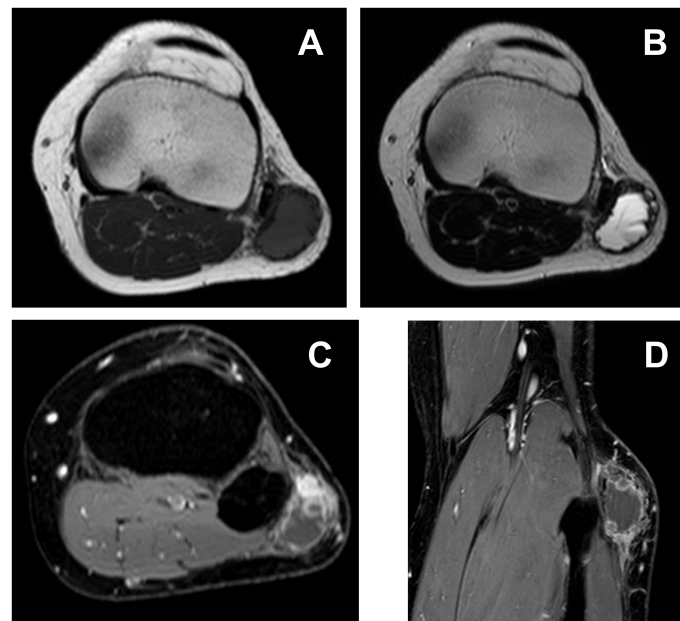
FIGURE 2
On T1-weighted imaging **(A)**, the mass shows intermediate signal intensity, while heterogeneously high intensity with fluid–fluid level can be seen on T2-weighted imaging **(B)**. Peripheral and nodular enhancement is recognizable on FS-T1-weighted imaging with contrast **(C, D)**.

has yet to be elucidated, but an inappropriate metaplastic change or osteogenic differentiation of fibroblasts has been proposed (4, 5). The presence of a zonal pattern of bone trabeculae is considered to be a distinctive feature of MO (4), but the zonation is ill-defined in some cases, especially in those with long-standing lesions. Rearrangement of the *USP6* gene was recently reported in MO (3). MO has also been recategorized as one of the *USP6*-associated neoplasms (UAN), along with other tumorous lesions showing

USP6 rearrangement, which suggests neoplastic change rather than a reactive process (6).

On the other hand, EO is a high-grade sarcoma with osteoid or bone matrix production by malignant neoplastic cells, and, by definition, the tumor has no connection to the skeletal system (1). EO is rare, comprising less than 1% of all soft tissue sarcomas and only about 4% of osteosarcomas overall (1, 7). The lower extremities, especially the thighs, are the most common site of
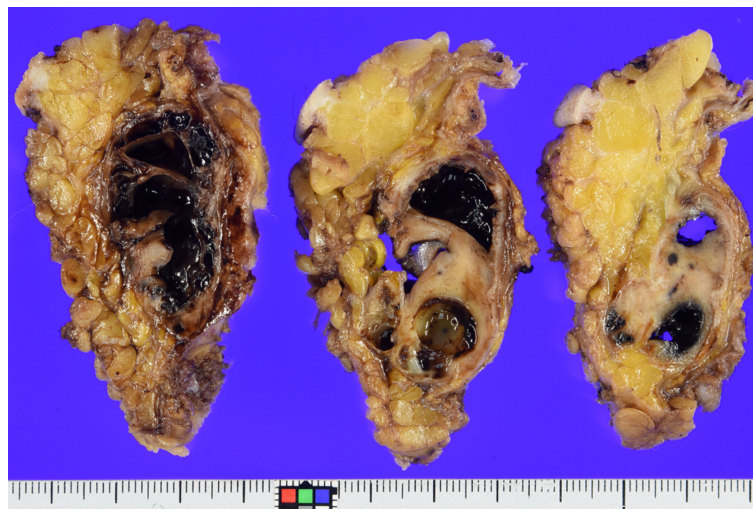

FIGURE 3
Grossly, on the cut section, the multicystic mass is seen to be subcutaneously located and mixed with hemorrhagic change and solid components. Mineralization was confirmed in the periphery, which corresponded to the imaging findings.
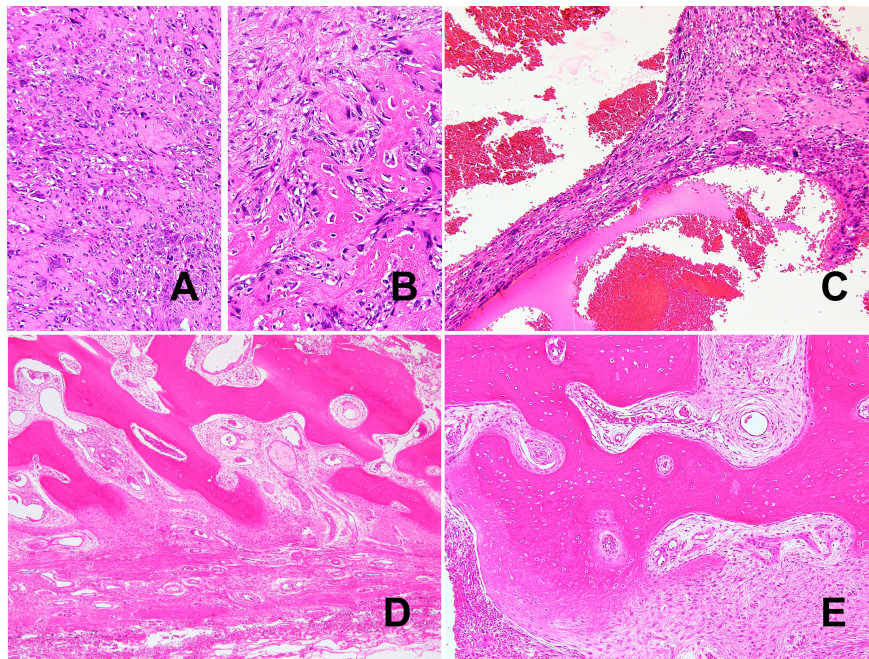
FIGURE 4
Histologically, the tumor was a high-grade pleomorphic sarcoma **(A)** with osteoid formation **(B)**. Telangiectatic or aneurysmal bone cyst-like change with abundant osteoclast-like giant cells can also be seen **(C)**. Morphologically bland-appearing, mature bone area in the periphery of the mass. **(D)**. In addition to mature lamellar bone, woven bone and fibroblasts show a continuous pattern, consistent with zonation **(E)**.

involvement (1). Middle-aged to older patients, with a slight male predominance, tend to be affected (1). EO can show various histological subtypes as with conventional osteosarcoma, and telangiectatic or aneurysmal bone cyst-like change has been reported (8). EO is usually diagnosed based on the detection of malignant osteoid formation and by ruling out other sarcomas with osteogenic differentiation such as dedifferentiated liposarcoma. Although the exact etiology of EO has not been clarified, the genomic signature has revealed features overlapping those of conventional skeletal osteosarcoma (1, 2). Because EO is usually high-grade, mature bone is not a typical feature and can, therefore, pose a diagnostic dilemma as in our present case.
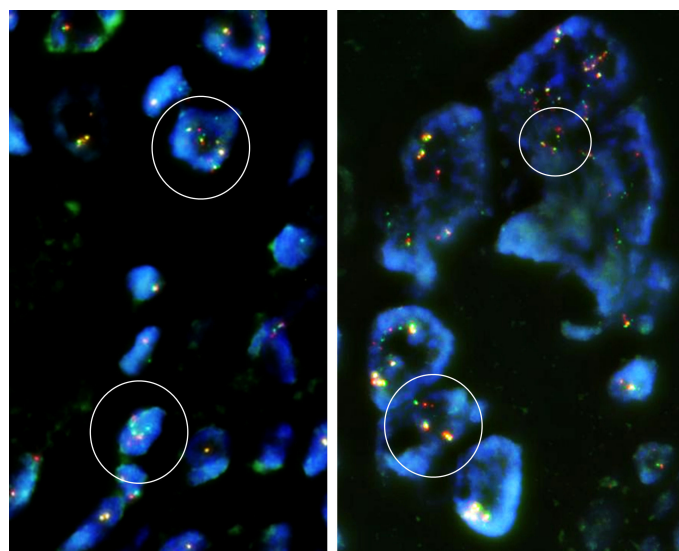

FIGURE 5
Fluorescence *in situ* hybridization (FISH) demonstrated break-apart signals of the *USP6* gene (*USP6* Split Dual Color FISH Probe, GSP Lab) in the EO component. Some of the tumor cells are polyploid, and focally split signals of the *USP6* gene are identifiable in the tumor cells (circled in white), compatible with rearrangement of the *USP6* gene.

At the center of the tumor in this patient, there was a high-grade pleomorphic sarcoma with malignant osteoid formation and telangiectatic change. This telangiectatic change corresponded to the fluid–fluid level on MRI (Figure 2). In the periphery of the tumor, mature bone trabeculae surrounded the high-grade osteosarcoma component, which was recognized on x-ray and CT scans (Figure 1). Focal zonation was confirmed in the peripheral benign bone area.

Differential diagnoses in our case included ossifying fibromyxoid tumor (OFMT) (9), osteosarcoma arising from the tiny bone or ectopic/metaplastic bone tissue (4, 9), and EO with preceding MO. OFMT is characterized by the proliferation of uniform round cells with peripheral ossification and is characterized by a rearrangement of the *PHF1* gene. The mass in our case was different from OFMT in that the tumor cells were pleomorphic. We were not able to identify either ectopic bone or continuity with the adjacent bone cortex. Therefore, OFMT and tiny bone osteosarcoma were ruled out, based on the factors discussed above. We confirmed the *USP6* rearrangement in the tumor cells, a finding not previously reported in EO. Based on the *USP6* rearrangement and peripheral mature bone tissue with focal zonation, we definitively diagnosed EO with preceding MO.

Malignant transformation of MO or osteosarcoma arising from preexisting MO is exceedingly rare, but several cases have been reported to date (4, 5, 7, 9). In these past reported cases, the ages ranged from 19 to 53 (mean, 37) years, and there was no gender predilection (4). The thigh was the location most commonly involved, though other areas including the jaw, retroperitoneum, wrist, and knee have also been reported (4). Benign bone tissue or MO component is commonly recognized in the periphery of the mass (7, 9). The prognosis is controversial but outcomes are generally dismal with most of the reported patients dying within 6 years of the initial presentation (4). The EO component is usually high-grade, but in one case report, a low-grade osteosarcoma with MO was described (10).

Most prior cases presented a diagnostic dilemma because they were diagnosed based on radiological and/or histological evidence of heterotopic benign bone tissue associated with EO (7, 9). The characteristic zonal distribution was confirmed in only one case (4). Furthermore, cytogenetic findings were not investigated in the previous cases, probably because osteosarcoma was long assumed to harbor no diagnostic cytogenetic abnormalities (1). As MO was known to harbor the *USP6* rearrangement, we speculated that *USP6* rearrangement could be detected in the sarcoma component and thus be a key factor in identifying EO arising from MO (3).

While there is no established criterion for diagnosing EO arising from MO, previously reported cases had difficulty proving the typical MO component and some of these cases are thus diagnostically questionable. In our current case, however, we identified a distinct zonation of the peripheral bone tissue that was etiologically significant in MO, as well as the *USP6* rearrangement in the high-grade osteosarcoma component that existed in the center of the tumor. Our case is the first to provide confirmation of the rearrangement of *USP6* and the second in

which the zonation of the MO component was identified. These observations support the diagnosis of EO arising from MO and suggest that MO is a neoplastic process. Unusual *USP6* rearrangement in EO may also be interpreted as MO with malignant transformation.

We have presented an exceptionally rare case of EO with preceding MO, and *USP6* rearrangement appears to reinforce the concept of malignant transformation of MO. Although the precise etiology of EO accompanied by MO remains as yet poorly understood, our current case provides the first confirmation of the rearrangement of *USP6* and is the second demonstration of zonation of the MO component.

Data availability statement

The original contributions presented in the study are included in the article/supplementary materials. Further inquiries can be directed to the corresponding author.

Ethics statement

Ethical approval was not provided for this study on human participants because Our hospital does not require ethical approval in case reports. The patients/participants provided their written informed consent to participate in this study.

Author contributions

Funding

Acknowledgments

Conflict of interest

The authors declare that the research was conducted in the absence of any commercial or financial relationships that could be construed as a potential conflict of interest.

Publisher's note

All claims expressed in this article are solely those of the authors and do not necessarily represent those of their affiliated organizations, or those of the publisher, the editors and the reviewers. Any product that may be evaluated in this article, or claim that may be made by its manufacturer, is not guaranteed or endorsed by the publisher.

References

1. WHO Classification of Tumours Editorial Board. *WHO classification of tumours: Soft tissue and bone tumours. 5th ed*. Lyon: WHO Classification of Tumours Editorial Board (2020).

2. Jour G, Wang L, Middha S, Zehir A, Chen W, Sadowska J, et al. The molecular landscape of extraskeletal osteosarcoma: A clinicopathological and molecular biomarker study. *J Pathol Clin Res* (2016) 2:9–20. doi: 10.1002/cjp2.29

3. Sukov WR, Franco MF, Erickson-Johnson M, Chou MM, Unni KK, Wenger DE, et al. Frequency of USP6 rearrangements in myositis ossificans, brown tumor, and cherubism: molecular cytogenetic evidence that a subset of "myositis ossificans-like lesions" are the early phases in the formation of soft-tissue aneurysmal bone cyst. *Skeletal Radiol* (2008) 37:321–7. doi: 10.1007/s00256-007-0442-z

4. Savant D, Kenan S, Kenan S, Kahn L. Extraskeletal osteosarcoma arising in myositis ossificans: a case report and review of the literature. *Skeletal Radiol* (2017) 46:1155–61. doi: 10.1007/s00256-017-2674-x

5. Walczak BE, Johnson CN, Howe BM. Myositis ossificans. *J Am Acad Orthop Surg* (2015) 23:612–22. doi: 10.5435/JAAOS-D-14-00269

6. Hiemcke-Jiwa LS, van Gorp JM, Fisher C, Creytens D, van Diest PJ, Flucke U. USP6-associated neoplasms: A rapidly expanding family of lesions. *Int J Surg Pathol* (2020) 28:816–25. doi: 10.1177/1066896920938878

7. Agarwal K, Agarwal S, Kumar L. Retroperitoneal extraskeletal osteosarcoma with cystic change arising from heterotopic ossification: A rare entity. *Annal Pathol Lab Med* (2015) 2:42–6.

8. Mirra JM, Fain JS, Ward WG, Eckardt JJ, Eilber F, Rosen G. Extraskeletal telangiectatic osteosarcoma. *Cancer* (1993) 71:3014–9. doi: 10.1002/1097-0142 (19930515)71:10<3014::AID-CNCR2820711021>3.0.CO;2-8

9. Konishi E, Kusuzaki K, Murata H, Tsuchihashi Y, Beabout JW, Unni KK. Extraskeletal osteosarcoma arising in myositis ossificans. *Skeletal Radiol* (2001) 30:39–43. doi: 10.1007/s002560000298

10. Okada K, Ito H, Miyakoshi N, Sageshima M, Nishida J, Itoi E. A low-grade extraskeletal osteosarcoma. *Skeletal Radiol* (2003) 32:165–9. doi: 10.1007/s00256-002-0589-6

Case Report: Surgery and genetic analysis of a complete androgen insensitivity syndrome family with testicular malignant tumors

Lu Jiang†, Peng Jia†, Baofeng Duan and Yan Zhang*

Department of Obstetrics and Gynecology, Peking University First Hospital, Beijing, China

Introduction: Complete androgen insensitivity syndrome (CAIS) is a rare sex development disorder that results from X-linked androgen receptor gene mutations. Malignant transformation of the gonads is the most feared complication in postpubertal patients.

Methods: In the current report, primary amenorrhea, infertility, and groin mass were symptoms described by a 58-year-old woman and his younger sister. Their two aunts, who shared the same clinical traits, passed away for an unknown reason.

Results: After gonadectomy, both patients were diagnosed with seminoma and an extratesticular benign tumor, and the elder sister suffered from breast cancer about a year after the operation. The diagnosis of CAIS was verified by whole-exome sequencing (WES), in which an uncommon mutation (c.2197G>A) in the AR gene was identified.

Discussion: This is the first family report of CAIS with germ cell tumors. The identified AR gene mutation based on WES can expand the understanding of CAIS.

KEYWORDS

complete androgen insensitivity syndrome, seminoma, AR gene, whole exome sequencing, case report

Introduction

Androgen insensitivity syndrome (AIS) is the most prevalent disease of sex development, with a karyotype of 46, XY and a predicted incidence of 1:20,000–1:100,000 (Tyutyusheva et al., 2021). Complete androgen insensitivity syndrome (CAIS) typically manifests as a female phenotype in a person with an XY karyotype and testes producing androgen whose levels are normal for their age, which is caused by X-linked androgen receptor (AR) gene mutations (Hughes et al., 2012; Mongan et al., 2015). In light of the effect of anti-Müllerian hormone (AMH), which is created by Sertoli cells of the testis, the uterus, cervix, and proximal vagina are absent in CAIS. Gonads are frequently discovered in the lower abdomen

Abbreviations: CAIS, complete androgen insensitivity syndrome; AR, androgen receptor; WES, whole-exome sequencing; AMH, anti-Müllerian hormone; IHC, immunohistochemistry; GCNIS, germ cell neoplasia *in situ*; PAIS, partial androgen insensitivity syndrome; MAIS, mild form androgen insensitivity syndrome; LBD, ligand-binding domain; DSD, disorders of sex development; AFP, alpha-fetoprotein; LDH, lactate dehydrogenase; hCG, human chorionic gonadotrophin.

TABLE 1 Changes in hormone levels before and after surgery of III-1.

Hormones	Before operation	After operation	References range	
		(D4)	Postmenopausal women	Men
LH (mIU/mL)	13.02	19.47	10.87–58.6	1.24–8.62
FSH (mIU/mL)	22.81	27.59	16.7–113.6	1.27–19.26
E2 (pg/mL)	31.00	16.40	0–38.9	0–38.95
PRL (ng/mL)	10.62	19.32	3.34–26.72	2.64–13.13
T (ng/mL)	4.55	0.42	0.10–0.75	1.75–7.81

LH, luteinizing hormone; FSH, follicle-stimulating hormone; E2, estradiol; PRL, prolactin; T, testosterone.

or in the inguinal canals, where they can lead to bilateral inguinal hernias or labial edema. The abundant conversion of androgens to estrogens by the P450 aromatase enzyme during puberty causes the spontaneous development of breast and female obesity along with a typical growth spurt. However, the vagina was a blind bottom, and there was hardly any pubic or axillary hair. Because of the presence of the Y chromosome, women with CAIS are typically taller than average (Hughes et al., 2012; Coutifaris et al., 2018). The most concerning consequence for women with CAIS is malignant alteration of the gonads, while the risk is positively correlated with age (Tyutyusheva et al., 2021). In this article, we present two individuals with CAIS and pathologically confirmed testicular seminoma from the same family. After whole-exome sequencing (WES), a rare AR gene mutation site (c.2197 G > A) was detected. The discovery of this study can expand the understanding of CAIS, especially the pathogenesis on a molecular scale.

Case description

In the studied family, a 58-year-old woman served as the proband (III-1), who was admitted to our hospital complaining of primary amenorrhea and increased inguinal mass for half a year. The patient stated that she has gone untreated for inguinal edema since she was a baby. She had normal sex after marriage despite having primary amenorrhea and infertility. The left inguinal mass dramatically grew to 10 cm in the past half a year, which prompted her to seek a medical assessment. Examination revealed that the person was 85 kg and 168 cm tall. The patient's pubic and axillary hair was sparse. A pelvic examination revealed normal female external genitalia, and the vagina was a blind channel with normal length (approximately 6 cm) and rugae. The cervix and uterus were absent. The left inguinal mass was approximately 10 cm × 7 cm in size, while the right side was 3 cm in diameter. Bilateral inguinal masses were inactive, without tenderness. The remainder of the physical examination was normal. Pelvic enhanced MR indicated that the uterus and ovary were absent, and there were mixed signal masses in the bilateral inguinal canal with irregular enhancement (Figure 2A). Laboratory sex hormone test results are shown in Table 1, which suggested a significantly elevated testosterone level of 4.55 ng/mL. The results of tumor markers (Alpha-fetoprotein (AFP), Lactate dehydrogenase (LDH), human chorionic gonadotrophin (hCG)) were normal, and the results of

peripheral blood karyotype analysis showed 46, XY. In the patient's lineage, two aunts (II-4 and II-6) and one younger sister (III-5) shared the proband's primary amenorrhea and infertility. Unfortunately, the first and second generations perished, and the cause was unclear. The phenotypes of her two sisters (III-3 and III-7) were normal, and III-3 died by accident (Figure 1A).

The patient had hernia sac high ligation and bilateral inguinal mass ectomy after being admitted. The general findings of the specimen showed that the left inguinal mass was well circumscribed, fleshy, bulging and hard, with a size of 10 cm × 7 cm × 6 cm, yellowish white in cross section (Figure 2B). The right mass was brown in cross section similar to testis, beside which a muscular tissue with a diameter of approximately 3 cm can be found (Figure 2C). The pathological results confirmed seminoma in the left testis, which did not invade the tunica albuginea, stage pT1, while the right mass was cryptorchidism with angioleiomyoma of the spermatic cord. The immunohistochemistry (IHC) staining results of the left inguinal mass were placental alkaline phosphatase (PLAP) ++, CD117 +++, AE1/AE3 -, AFP -, and HCG - (Figures 2D, E, F, G). The final diagnosis was left testicular seminoma (stage IA, pT1N0M0S0), and radiotherapy was offered 1 month after the operation. Notably, on the fourth day after the operation, the testosterone level decreased significantly (Table 1). The patient reported she was diagnosed with breast cancer 11 months after the surgery and underwent a breast-conserving lumpectomy during the most recent follow-up.

Her sister (III-5) was 49 years old with clinical manifestations basically consistent with those of III-1. She had primary amenorrhea and infertility, and her left inguinal mass was significantly enlarged, with a diameter of approximately 5 cm, in the past 2 years. Physical examination revealed that her weight was 74 kg with a height of 168 cm. Pelvic examination and enhanced MR indicated that the uterus and ovary were absent. The left inguinal mass was approximately 5 cm in diameter, while the right inguinal mass was 3 cm. Enhanced MR revealed a circular mixed low signal mass in both groins (Figures 3A, B). Laboratory tests suggested an elevated testosterone level of 5.12 ng/mL. The results of tumor markers (AFP, LDH, hCG) were also normal, with a peripheral blood karyotype analysis showing 46, XY. She underwent the same operation as her sister, and the final diagnosis was right testicular seminoma (stage IA, pT1N0M0S0) and left paratesticular leiomyoma. Interestingly, the leiomyoma appeared to originate from the tunica vaginalis of the left testis. Her surgical specimen photos are shown in Figure 3C.
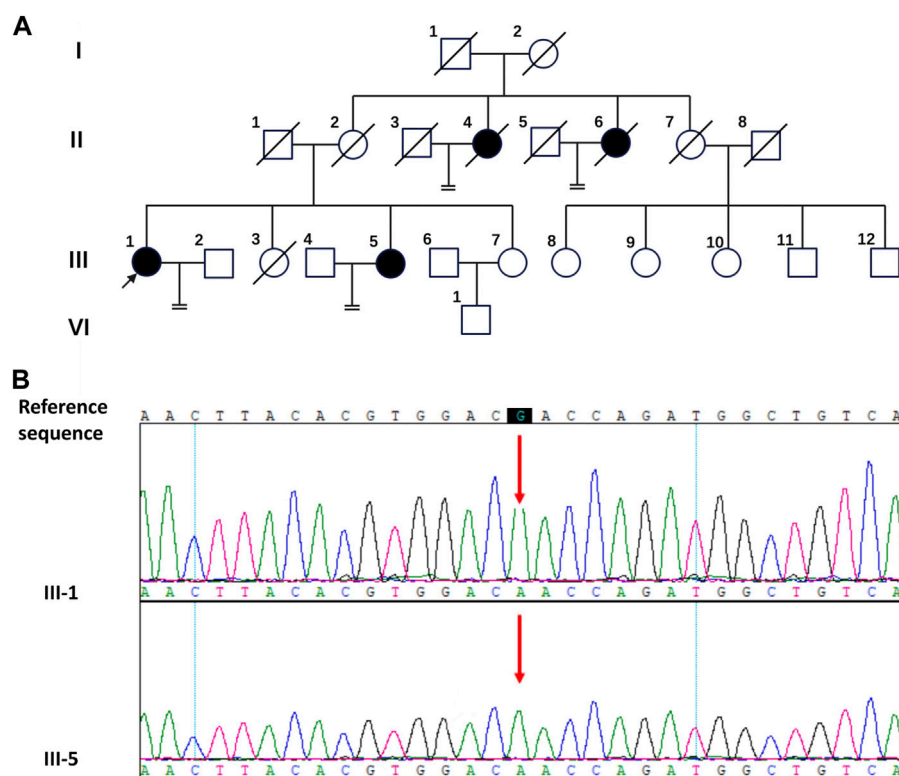
FIGURE 1
The pedigree diagram of the Chinese family with CAIS and the result of Sanger sequencing. **(A)** The pedigree diagram of the Chinese family. Black arrow indicates the proband, III-1; shapes in black indicate affected individuals, II-4, II-6, III-1and III-5. **(B)** Analysis of the DNA sequence. Sanger sequencing show the sequence encompassing the missense mutation (c.2197G>A) in the AR gene in the proband (III-1) and his sister (III-5).

For III-1 and III-5, WES investigation of mutations utilizing peripheral blood was carried out in addition to clinical evaluations, which were conducted by BGI Clinical Laboratories Co., Ltd. (Shenzhen, China). A sample of the patients' blood was used to extract the DNA, and 20,000 exons as well as the mitochondrial genome were sequenced. Sequence alignment using BWA was performed on the reference genome UCSU hg19. ExomeDepth was used to identify exon-level copy number alterations. The sequencing depth of 99.95% of the loci was over 20 × average depth. This study's most significant mutation was found in the protein-coding region of exon five of the AR gene on the X chromosome (c.2197G>A, p. Asp733Asn), which Sanger sequencing verified (Figure 1B). The c.2197G>A mutation of the AR gene has been reported in previous studies (Chaudhry et al., 2017; Cools et al., 2017). It was found in a 1-month-old female infant and a 16-year-old CAIS patient. The female infant was diagnosed with germ cell neoplasia *in situ* (GCNIS) after gonadectomy. A missense mutation (c.2197G>A) in the AR gene may be the cause of the observed pathogenicity of CAIS in this lineage when the aforementioned conditions are combined.

Discussion

The term "androgen insensitivity syndrome" refers to a group of illnesses where a person with an XY karyotype can produce normal levels of androgen but exhibits complete or partial resistance to the biological effects of androgen due to mutations in the X-linked androgen receptor gene, which codes for the ligand-activated androgen receptor, a transcription factor and member of the nuclear receptor superfamily. According to different biological phenotypes, it is usually divided into three subtypes: complete androgen insensitivity syndrome (CAIS) characterized by the feminization of the testes, partial androgen insensitivity syndrome (PAIS) with external genitalia more masculine and mild form androgen insensitivity syndrome (MAIS) with only breast development and infertility. Among CAIS patients, primary amenorrhea in adolescence or inguinal swelling in a neonate are the two most common presentations (Hughes et al., 2012). Proband III-1 and her sister III-5 in the current family were compatible with the diagnosis of CAIS when combined with clinical signs and auxiliary examinations. First, both of them presented with an inguinal mass, primary amenorrhea and infertility, scant pubic and axillary hair and typical female external genitalia. Second, imaging revealed that the uterus and ovaries were absent, and hormone tests showed that testosterone was in line with the level of men of the same age. Finally, additional genetic testing revealed that both patients had karyotypes of 46, XY. WES sequencing showed that both of them carried the same missense mutation in the AR gene (c.2197G>A).

The 920 amino acid AR protein is divided into eight exons (listed as 1–8) and seven introns, with a molecular mass of 110 kDa. The
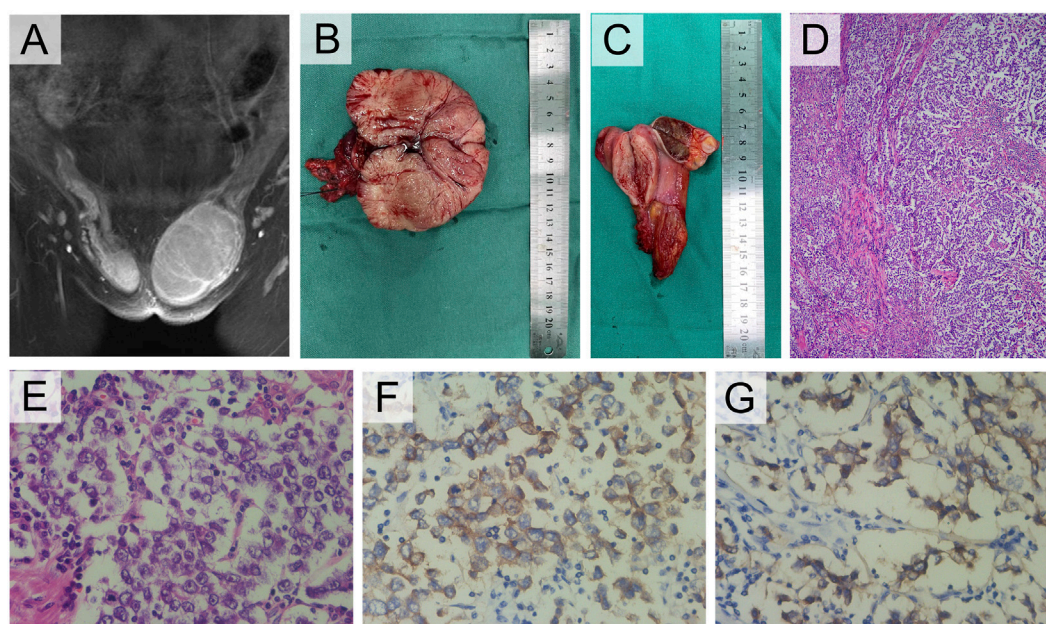
FIGURE 2
Clinical and pathological manifestations of III-1. **(A)** Enhanced MRI of groin mass. **(B)** Photograph of the left gross pathology specimen showed a lobulated fleshy mass. **(C)** The right specimen showed a brown cross section similar to testis and a muscular mass nearby. **(D)** Photomicrograph showed a sheetlike arrangement of tumor cells separated by fibrous septa. **(E)** The tumor cells exhibited cytoplasmic clearing and squared-off large nuclei (H-E stain, 400×). **(F)** The tumor cells displayed cytoplasmic expression of PLAP (IHC, 400×), and **(G)** cell membrane-localized expression of CD117 (IHC, 400×).
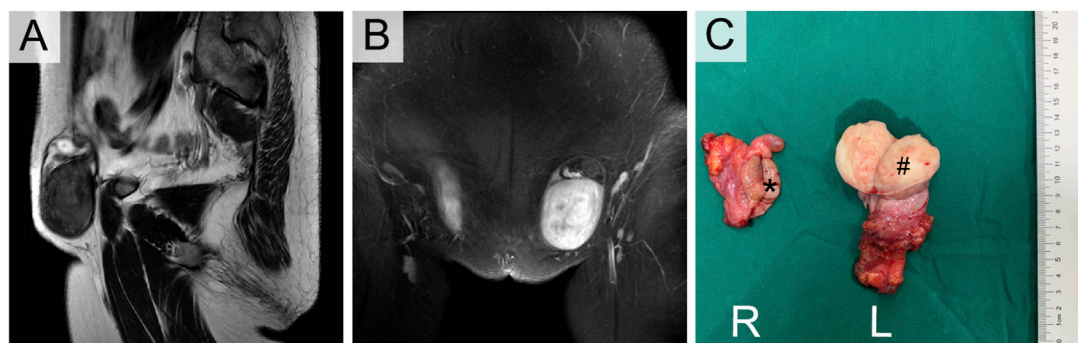
FIGURE 3
Enhanced MRI **(A,B)** and Orchiectomy specimens **(C)** of III-5. *Right testicular seminoma, # Left paratesticular leiomyoma.

single-stranded polypeptide AR receptor has four major structural domains. The ligand-binding domain (LBD, amino acids 646–920), encoded by exons 4–8, contains particular androgen binding sites, various transcription factors of coactivation and the activation function-2 (AF-2) region. It encourages the receptor's engagement with cytoplasmic heat shock proteins (HSPs), which is followed by the androgen hormone and results in the migration of the AR into the nucleus (Tyutyusheva et al., 2021). According to the HGMD database (human gene mutation database, http://www.hgmd.cf.ac.uk/ac/gene.php?gene=AR), there are 618 types of AR gene mutations, of which 443 are missense/non-sense mutations. The mutation c.2197G>A (p. Asp733Asn) found in the present

study is a single nucleotide missense mutation with few previous reports. In addition to the two CAIS patients mentioned above (Chaudhry et al., 2017; Cools et al., 2017), this mutation site is also included in the DSD-related panel designed by Eggers et al. (2016). On the current basis, according to the standard of ACMG guidelines (2015) (Richards et al., 2015), this mutation site is likely pathogenic, and there is a lack of evidence of strong pathogenicity. After adding the families reported in this study, the evidence of pathogenicity of this mutation will be further strengthened.

The likelihood of gonadal malignancies developing in DSD individuals increases when Y chromosomal material is present in the gonadal karyotype and the gonad is located in the abdominal or inguinal

region. The probability of gonadal tumors is lowest (5%) in patients with CAIS and highest (15%–60%) in those with 46, XY gonadal dysgenesis, while the rate of tumor incidence is 15% in patient with PAIS(9, 10). Age has been recognized as a significant risk factor for the development of gonadotrophic tumors. Deans et al. (2012) found that the probability of developing a neoplasm is approximately 0.02% in women under 30 and up to 22% in those over that age. Puberty testicles can provide sex hormones necessary for growth and development in children with CAIS. However, to avoid the malignant transformation of cryptorchidism, gonadectomy is usually recommended after puberty, followed by hormone replacement therapy (Hughes et al., 2012; Mongan et al., 2015). Chaudhry et al. (2017) included 133 patients with CAIS who received gonadectomy. The incidence of malignant tumors was only 1.5% (2/133). Two patients underwent gonadectomy at the ages of 30 and 68, and postoperative pathology suggested seminoma and malignant sex cord-stromal tumor, respectively. Other benign gonadal tumors included Sertoli cell adenoma, testicular hamartoma and GCNIS. GCNIS, the premalignant precursor of germ-cell tumors, is hypothesized to result from a developmental arrest of embryonic germ cells and develops from gonocytes or primordial germ cells. If gonadectomy is not performed, there will be an increasing possibility of malignant germ-cell tumors, including seminoma, non-seminoma and dysgerminoma, with increasing age (Hughes et al., 2012). Even more rarely, sex cord–stromal tumors may develop in patients with AIS, which are most commonly Sertoli-cell adenomas (Coutifaris et al., 2018). Gonadectomy after puberty should continue to be the first-line recommendation to reduce the potential increased risk of cancer. For females who want to maintain their gonads, Döhnert et al. (2017) recommended a routine yearly or biannual screening program that included endocrine assessment, gonadal imaging and the measurement of certain tumor markers (AFP, hCG, LDH, and optionally PLAP in non-smokers). In addition, preventive gonadectomy is also controversial. The prevalence rate of pre-GCNIS is 10%–15% in patients with CAIS and PAIS aged from 14 to 54 years, only a few of these diseases will progress to malignant experimental germ cell tumors, and the genetic susceptibility of different individuals may lead to diverse disease outcomes (Cools et al., 2017).

In the present study, III-1 and III-5 underwent gonadectomy at the ages of 58 and 49, respectively, and were both diagnosed with testicular seminoma. To the best of our knowledge, this is the first family to include 2 or more CAIS patients complicated with malignant germ cell tumors. Because of some social factors, both of them existed in their past lives as normal women. Although they cannot have children and menstruation, they do not want to reveal the secrets of their family until they are worried about the obvious increase in inguinal tumors. Fortunately, both of the sisters presented with stage I seminoma, with a survival rate of 99% (Döhnert et al., 2017). Considering the large size of the tumor, adjuvant radiotherapy was offered postoperatively.

In addition to testicular malignancies, it is worth mentioning that benign tumors of paratesticular tissues were found in both patients in the present study, including spermatic cord angioleiomyoma in III-1 and paratesticular leiomyoma in III-5. First, the spermatic cord is rarely the site of malignancies, between which lipomas are the most prevalent benign tumor, whereas sarcomas are the most common malignant type. Only one case of angioleiomyoma of the spermatic cord has been reported to date (Ghei et al., 2005). In addition, paratesticular leiomyoma is another rare tumor of the male reproductive system. To the best of our knowledge, there have been only four reports of

paratesticular leiomyoma (Krichen Makni et al., 2005; Goulis et al., 2006; Gorunova et al., 2011; Savaş-Erdeve et al., 2016). In the only case of a normal male phenotype, der(14)t(12;14)(q15;q24) was found, as reported in uterine leiomyomas (Gorunova et al., 2011). The other three patients all suffered from sex development disorder, including a 29-year-old girl with testicular feminization syndrome and two girls with CAIS, aged 17 and 18, respectively. Leiomyomas are typically very rare tumors of the male urogenital tract that can develop either intratesticularly or paratesticularly. The origin of these tumors is thought to be the seminiferous tubules and paratesticular structures, as well as the smooth muscle cells of the interstitial stroma (Savaş-Erdeve et al., 2016). As we mentioned above, aromatase in peripheral tissues of CAIS patients can convert androgen into estrogen. The high estrogen status of these patients may be a trigger for paratesticular leiomyoma. It is significant to note that prior to this case, there had not been any reports of breast cancer developing later in life, despite the fact that women with CAIS had sustained estrogen exposure (Mongan et al., 2015). This is the first case report of CAIS complicated by breast cancer and seminoma occurring simultaneously.

Psychosocial support is another key issue that should be considered after surgery. They can still return to their original life and work roles as women after gonadectomy. Support from their families and partners is the most important factor. Furthermore, doctors should disclose as little information about their gender development abnormalities to others as possible and give appropriate hormone replacement therapy when necessary to improve their quality of life.

In summary, this work describes an uncommon mutation in the AR gene, c.2197G>A, in a family with CAIS and an accompanying seminoma. This is the first report of multiple cases of germ cell tumors in the CAIS family. In addition, the coexistence of spermatic cord angioleiomyoma, paratesticular leiomyoma and breast cancer, as in our case, seems to be an extremely rare finding. The assessment of connections between CAIS genotypes and phenotypes, particularly tumor risk, is facilitated by the reporting of these CAIS-associated mutations, aiding future genetic consultation and diagnosis. (Abacı et al., 2015; De Toni et al., 2019).

Data availability statement

The datasets presented in this study can be found in online repositories. The names of the repository/repositories and accession number(s) can be found below: https://www.ncbi.nlm.nih.gov/, PRJNA940202.

Ethics statement

Written informed consent was obtained from the individual for the publication of any potentially identifiable images or data included in this article.

Author contributions

LJ and PJ provided and drafted the manuscript, contributed to the diagnosis, obtained informed consent, and reviewed the related literature. BD contributed to the collection of data. YZ provided critical revisions of the report for important intellectual content. All authors participated in

the care of the patient and approved the final version of the manuscript for submission.

Conflict of interest

The authors declare that the research was conducted in the absence of any commercial or financial relationships that could be construed as a potential conflict of interest.

Publisher's note

All claims expressed in this article are solely those of the authors and do not necessarily represent those of their affiliated organizations, or those of the publisher, the editors and the reviewers. Any product that may be evaluated in this article, or claim that may be made by its manufacturer, is not guaranteed or endorsed by the publisher.

References

Abacı, A., Çatlı, G., and Berberoğlu, M. (2015). Gonadal malignancy risk and prophylactic gonadectomy in disorders of sexual development. *J. Pediatr. Endocrinol. Metab.* 28 (9-10), 1019–1027. doi:10.1515/jpem-2014-0522

Chaudhry, S., Tadokoro-Cuccaro, R., Hannema, S. E., Acerini, C. L., and Hughes, I. A. (2017). Frequency of gonadal tumours in complete androgen insensitivity syndrome (CAIS): A retrospective case-series analysis. *J. Pediatr. Urol.* 13 (5), e1–e498. doi:10.1016/j.jpurol.2017.02.013

Cools, M., Wolffenbuttel, K. P., Hersmus, R., Mendonca, B. B., Kaprová, J., Drop, S. L. S., et al. (2017). Malignant testicular germ cell tumors in postpubertal individuals with androgen insensitivity: Prevalence, pathology and relevance of single nucleotide polymorphism-based susceptibility profiling. *Hum. Reprod. Oxf. Engl.* 32 (12), 2561–2573. doi:10.1093/humrep/dex300

Coutifaris, C., Kilcoyne, A., Feldman, A. S., Sabatini, M. E., and Oliva, E. (2018). Case 29-2018: A 31-year-old woman with infertility. *N. Engl. J. Med.* 379 (12), 1162–1172. doi:10.1056/NEJMcpc1807497

De Toni, L., Šabovic, I., Cosci, I., Ghezzi, M., Foresta, C., and Garolla, A. (2019). Testicular cancer: Genes, environment, hormones. *Front. Endocrinol.* 10, 408. doi:10.3389/fendo.2019.00408

Deans, R., Creighton, S. M., Liao, L. M., and Conway, G. S. (2012). Timing of gonadectomy in adult women with complete androgen insensitivity syndrome (CAIS): Patient preferences and clinical evidence. *Clin. Endocrinol. (Oxf).* 76 (6), 894–898. doi:10.1111/j.1365-2265.2012.04330.x

Döhnert, U., Wünsch, L., and Hiort, O. (2017). Gonadectomy in complete androgen insensitivity syndrome: Why and when? *Sex. Dev.* 11(4), 171–174. doi:10.1159/000478082

Eggers, S., Sadedin, S., van den Bergen, J. A., Robevska, G., Ohnesorg, T., Hewitt, J., et al. (2016). Disorders of sex development: Insights from targeted gene sequencing of a large international patient cohort. *Genome Biol.* 17 (1), 243. doi:10.1186/s13059-016-1105-y

Ghei, M., Arun, B., Maraj, B. H., Miller, R. A., and Nathan, S. (2005). Case report: Angioleiomyoma of the spermatic cord: A rare scrotal mass. *Int. Urol. Nephrol.* 37 (4), 731–732. doi:10.1007/s11255-004-4588-5

Gorunova, L., Bjerkehagen, B., and Heim, S. (2011). Paratesticular leiomyoma with a der(14)t(12;14)(q15;q24). *Cancer Genet.* 204 (8), 465–468. doi:10.1016/j.cancergen.2011.06.005

Goulis, D. G., Iliadou, P. K., Papanicolaou, A., Georgiou, I., Chatzikyriakidou, A., Gerou, S., et al. (2006). R831X mutation of the androgen receptor gene in an adolescent with complete androgen insensitivity syndrome and bilateral testicular hamartomata. *Horm. (Athens)* 5 (3), 200–204. doi:10.14310/horm.2002.11185

Hughes, I. A., Davies, J. D., Bunch, T. I., Pasterski, V., Mastroyannopoulou, K., and MacDougall, J. (2012). Androgen insensitivity syndrome. *Lancet* 380 (9851), 1419–1428. doi:10.1016/S0140-6736(12)60071-3

Krichen Makni, S., Mnif Hachicha, L., Ellouze, S., Mnif, M., Khabir, A., Ketata, H., et al. (2005). Feminizing testicular syndrome with multiple hamartomas and bilateral paratesticular leiomyomas. *Rev. Med. Interne* 26 (12), 980–983. doi:10.1016/j.revmed.2005.08.003

Mongan, N. P., Tadokoro-Cuccaro, R., Bunch, T., and Hughes, I. A. (2015). Androgen insensitivity syndrome. *Best. Pract. Res. Clin. Endocrinol. Metab.* 29 (4), 569–580. doi:10.1016/j.beem.2015.04.005

Richards, S., Aziz, N., Bale, S., Bick, D., Das, S., Gastier-Foster, J., et al. (2015). Standards and guidelines for the interpretation of sequence variants: A joint consensus recommendation of the American college of medical genetics and genomics and the association for molecular pathology. *Genet. Med.* 17 (5), 405–424. doi:10.1038/gim.2015.30

Savaş-Erdeve, Ş., Aycan, Z., Keskin, M., Çetinkaya, S., Karaman, A., Apaydın, S., et al. (2016). Complete androgen insensitivity syndrome associated with bilateral sertoli cell adenomas and unilateral paratesticular leiomyoma: A case report. *Turk J. Pediatr.* 58 (6), 654–657. doi:10.24953/turkjped.2016.06.012

Tyutyusheva, N., Mancini, I., Baroncelli, G. I., D'Elios, S., Peroni, D., Meriggiola, M. C., et al. (2021). Complete androgen insensitivity syndrome: From bench to bed. *Int. J. Mol. Sci.* 22 (3), 1264. doi:10.3390/ijms22031264

Check for updates

A novel *BRCA1* splicing variant detected in an early onset triple-negative breast cancer patient additionally carrying a pathogenic variant in *ATM*: A case report

Mara Colombo[1]*, Patrizia Mondini[1], Elisa Minenza[2],
Claudia Foglia[1], Annamaria Mosconi[2], Carmen Molica[2],
Lorenza Pistola[2], Vienna Ludovini[2] and Paolo Radice[1]

[1]Unit of Molecular Bases of Genetic Risk and Genetic Testing, Department of Experimental Oncology,
Fondazione IRCCS Istituto Nazionale dei Tumori, Milan, Italy, [2]Department of Medical Oncology,
Santa Maria della Misericordia Hospital, Perugia, Italy

The widespread adoption of gene panel testing for cancer predisposition is leading to the identification of an increasing number of individuals with clinically relevant allelic variants in two or more genes. The potential combined effect of these variants on cancer risks is mostly unknown, posing a serious problem for genetic counseling in these individuals and their relatives, in whom the variants may segregate singly or in combination. We report a female patient who developed triple-negative high grade carcinoma in the right breast at the age of 36 years. The patient underwent bilateral mastectomy followed by combined immunotherapy and chemotherapy (IMpassion030 clinical trial). Two years later she developed a skin recurrence on the right anterior chest wall. Despite intensive treatment, the patient died at 40-year-old due to disease progression. Gene panel testing of patient's DNA revealed the presence of a protein truncating variant in *ATM* [c.1672G>T; p.(Gly558Ter)] and of a not previously reported variant in the *BRCA1* exon 22 donor splice site [c.5406 +6T>C], whose clinical significance was unknown. The analysis of patient's RNA revealed the up-regulation of two alternative *BRCA1* mRNA isoforms derived from skipping of exon 22 and of exons 22-23. The corresponding predicted protein products, p.(Asp1778GlyfsTer27) and p.(Asp1778_His1822del) are both expected to affect the BRCA1 C Terminus (BRCT) domain. The two variants were observed to co-occur also in the proband's brother who, in addition, was heterozygous for a common variant (c.4837A>G) mapped to *BRCA1* exon 16. This allowed to ascertain, by transcript-specific amplification, the lack of functional mRNA isoforms expressed by the c.5406+6T>C allele and provided evidence to classify the *BRCA1* variant as pathogenic, according to the guidelines of the Evidence-based Network for the Interpretation of Germline Mutant Alleles (ENIGMA) consortium. To our knowledge, excluding two cases detected following the screening of population specific recurrent variants, only one *ATM*/*BRCA1* double heterozygote has been reported in the literature, being the

case here described the one with the youngest age at cancer onset. The systematic collection of cases with pathogenic variants in more than one cancer predisposition gene is needed to verify if they deserve *ad hoc* counseling and clinical management.

Introduction

Germline pathogenic variants in the *BRCA1* (MIM# 113705) and *BRCA2* (MIM# 600185) genes are the main risk factors for hereditary breast and ovarian cancer (HBOC). For several years, following their identification in the 1990s (1, 2), genetic tests in HBOC patients were limited to the screening of these two genes, using different mutation analysis techniques, including direct Sanger sequencing. However, it was soon apparent that only a fraction (approximately 15-25%) of HBOC families fulfilling the criteria for clinical testing carry pathogenic variants of BRCA genes (3, 4). Moreover, approximately 10-20% of tests detects the presence of variants, termed variants of uncertain significance (VUS), whose effect on cancer risk is unknown (5). More recently, other breast cancer (BC) and/or ovarian cancer (OC) predisposition genes have been identified (6). The recent advent of Next Generation Sequencing (NGS), in addition to minimizing the costs and time of genetic analyses, has enabled the simultaneous screening of multiple genes. Therefore, NGS has implemented the potential for the detection of pathogenic variants in HBOC genes other than *BRCA1* and *BRCA2* and for the identification of subjects with pathogenic variants in more than one cancer predisposition gene. In fact, although not frequently, HBOC patients have been described with double heterozygous pathogenic variants in *ATM, BRCA1, BRCA2, CHEK2, MSH6, MUTYH, NBN/NBS1* and *RAD50* following gene panel testing (7–13) with a frequency of approximately 0.3% (10, 13). Not surprisingly, double heterozygous carriers are more frequently detected in populations enriched with founder variants (14). To date, the contribute of a double heterozygosity condition for HBOC genes to the severity of the disease and its impact on the genetic counseling and clinical management of the carriers and their relatives is still debated. Further studies are therefore needed to clarify these issues.

In the present study, we report a female patient who developed triple-negative high grade carcinomas in the right breast at the ages of 36 and 38 years. Gene panel testing of patient's constitutional DNA revealed, in addition to a protein truncating variant in *ATM* [c.1672G>T; p.(Gly558Ter)], the presence of a novel VUS in the consensus sequence of the donor splice site of *BRCA1* exon 22 [c.5406+6T>C]. Gene transcript analysis revealed that the latter affected RNA splicing and allowed its classification as pathogenic. To the best of our knowledge, only three double heterozygotes for *ATM* and *BRCA1* pathogenic variants had been previously reported, being the case here described the one with the youngest age at cancer onset.

Case presentation

The case here described (therein termed proband) is a woman who at 36 years old sough genetic counseling due to the cancer history of the mother, who was diagnosed with BC and OC (Figure 1). Furthermore, she reported additional cancer cases in second- and third-degree relatives, including lung, gastrointestinal, prostate and pancreatic cancers. Based on family history, the proband was considered eligible for mutation screening of the *BRCA1, BRCA2* and *PALB2* genes. An NGS analysis, performed using a small-size panel (Myriapod® NGS BRCA1-2 panel Kit CE-IVD, Diatech Pharmacogenetics), identified the c.5406+6T>C variant in *BRCA1*. At the time of gene testing (April 2018), no data on the clinical significance of this intronic variant were reported in the BRCA Exchange (15) and ClinVar (16) repositories, nor in the literature. A few months later the proband was diagnosed by ultrasound scan with a BC. She opted for a bilateral nipple-areola complex (NAC) sparing mastectomy. A right axillary lymph node dissection was performed for a stage IIB (pT2N1aM0) cancer. The histological examination revealed a triple-negative (ER, PgR, and HER2 negative) invasive ductal G3 carcinoma (ki67 = 50%) with *in situ* component (5%). Considering the diagnosis of BC, the family history and the absence of a definitely pathogenic variant in *BRCA1, BRCA2* and *PALB2*, the genetic status of the proband was further investigated with a larger NGS-based panel (Hereditary Cancer Solution (HCS) kit, SOPHiA GENETICS) containing the following 26 genes, *ATM, APC, BARD1, BRCA1, BRCA2, BRIP1, CDH1, CHEK2, EPCAM, FAM175A, MLH1, MRE11A, MSH2, MSH6, MUTYH, NBN, PALB2, PIK3CA, PMS2, PTEN, RAD50, RAD51C, RAD51D, STK11, TP53, XRCC2*. The analysis identified the *ATM* c.1672G>T variant, located in exon 11.

The proband was enrolled in the IMpassion030 clinical trial (NCT03498716) and received adjuvant immunotherapy (atezolizumab) combined with taxan- and anthracyclin-based chemotherapy and with adjuvant radiotherapy (40Gy) for 12 months after diagnosis. Two months after the end of the treatment, the patient underwent prophylactic bilateral hystero-adnexectomy surgery. At 38 years old a skin recurrence on the right anterior chest wall with lymphangitic carcinomatosis was diagnosed consistent with triple-negative BC (ki67 = 90%). She received a combination chemotherapy of carboplatin and gemcitabine for three months as first-line treatment followed by Olaparib 600 mg/

day for two months due to disease progression. At the end of the treatment a revaluation computed tomography (CT) scan showed skin, lymph node, and pulmonary disease progression. The patient underwent a second line treatment with a combination of oral vinorelbine and capecitabine for four mouths and electrochemotherapy of skin metastases, followed by a further combination chemotherapy with cyclophosphamide-methotrexate-fluorouracil (CMF) for one month. An additional revaluation CT scan showed further disease progression. The patient died at the age of 40 years.
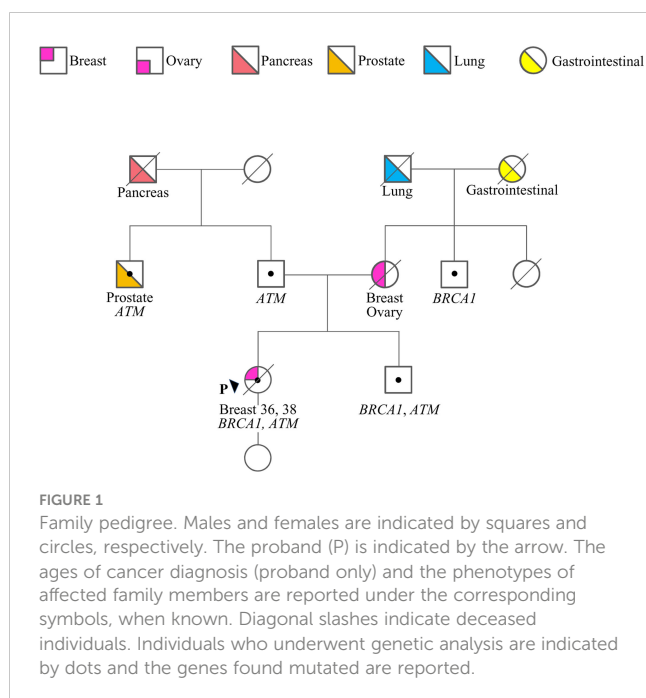
Following targeted genetic testing in the proband's parents, the c.1672G>T in *ATM* and the c.5406+6T>C in *BRCA1* variants were found to have been inherited from the father and the mother, respectively (Figure 1). While the *ATM* variant, which introduces a premature termination codon (PTC) resulting in a non-functional protein [p.(Gly558Ter)], could be considered pathogenic according to the guidelines of the American College of Medical Genetics and Genomics and the Association for Molecular Pathology (ACMG-AMP) (17), the clinical relevance of the *BRCA1* variant remained uncertain.
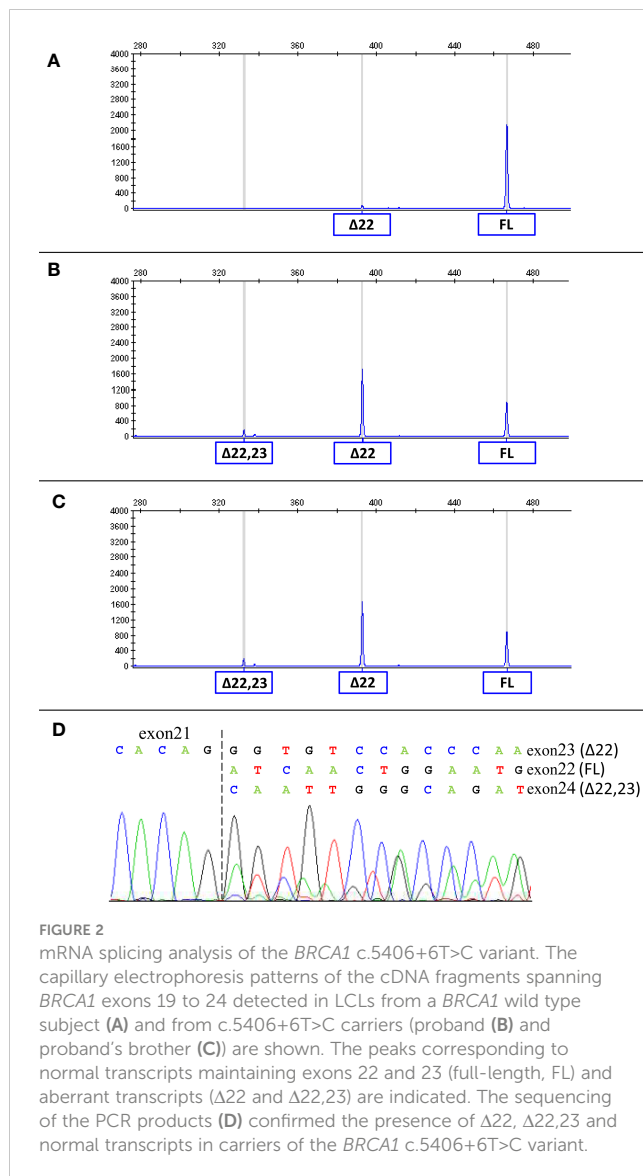
Considering that the variant in *BRCA1* is located in the consensus sequence of the donor splice site of exon 22 (according to the Breast Information Core (BIC) nomenclature) (18), a potential effect at mRNA splicing level was investigated by interrogating the Alamut Visual Plus software application (version v1.2.1 | © 2021 SOPHiA GENETICS). All tools integrated in the software predicted the variant to impact on the splicing by weakening the natural donor site of exon 22. The putative spliceogenic effect was then verified by characterizing the mRNA transcript profile as previously described (19, 20). Briefly, Epstein-Barr virus (EBV)-immortalized lymphoblastoid cell line (LCL) was established from the peripheral blood of the variant carrier. The degradation of transcripts containing premature

termination codons (PTCs) *via* nonsense mediated mRNA decay (NMD) was prevented by growing the LCL in the presence of cycloheximide. Cytoplasmic RNA was isolated from the LCL and first strand cDNA was generated for RT-PCR analysis. The primers for the amplification were designed specifically for the variant under study. Furthermore, the reverse primer was labeled with 6-carboxyfluorescein (6-FAM) in order to obtain fluorescent amplification fragments detectable by capillary electrophoresis (CE). The CE profile obtained from the LCL carrying the *BRCA1* variant was compared to that derived from *BRCA1* wild type subjects (reference) and the aberrant products not present in the reference were characterized by Sanger sequencing. Experimental conditions are reported in Supplementary Table 1. The analysis revealed the up-regulation of two isoforms derived from the out-of-frame skipping of exon 22 (Δ22, major transcript) and the in-frame skipping of exons 22 and 23 (Δ22,23, minor transcript) (Figure 2), both previously described as naturally occurring isoforms (21). The corresponding predicted protein products, p.(Asp1778GlyfsTer27) and p.(Asp1778_His1822del), are both expected to affect the BRCA1 C Terminus (BRCT) of the protein, a clinically relevant functional domain. The *BRCA1* and *ATM* variants were observed to co-occur also in the proband's brother, unaffected at the time of genetic testing (at age 33 years), who in addition was heterozygous for the common variant c.4837A>G (rs1799966) mapped to *BRCA1* exon 16. PCR fragments spanning the c.4837A>G variant were selectively amplified from the normal transcripts maintaining exon 22 using a reverse primer annealing to this exon and a forward primer annealing to the region upstream of the c.4837A>G variant. The sequence analysis of these amplification products, showing a mono-allelic expression, allowed us to ascertain the lack of functional mRNA isoforms expressed by the allele carrying the c.5406+6T>C variant (Figure 3) and to classify the variant as pathogenic (class 5) according to the *BRCA1/2* Gene Variant Classification Criteria of the Evidence-based Network for the Interpretation of Germline Mutant Alleles (ENIGMA) (22). Potential consequences on mRNA splicing were experimentally investigated following the above described approach also for the *ATM* c.1672G>T variant and excluded (data not shown).

Discussion

In this study, we describe a female patient diagnosed with triple-negative high grade BC, with two heterozygous variants in genes associated with increased risk of BC, namely the pathogenic (protein truncating) variant c.1672G>T in *ATM* and the suspected spliceogenic variant c.5406+6T>C in *BRCA1*. Neither of the two variants had been previously published or reported in publicly available databases. Due to the uncertainty on the clinical relevance of the *BRCA1* variant, we analyzed the LCL RNAs of the proband and her brother, who also carried the same variant. These investigations allowed us to classify the *BRCA1* variant as pathogenic, according to the ENIGMA guidelines. Notably, our observations are consistent with the outcomes of a saturation genome editing (SGE) assay, which were published after the identification of the variant in the case here described, that

FIGURE 1

Family pedigree. Males and females are indicated by squares and circles, respectively. The proband (P) is indicated by the arrow. The ages of cancer diagnosis (proband only) and the phenotypes of affected family members are reported under the corresponding symbols, when known. Diagonal slashes indicate deceased individuals. Individuals who underwent genetic analysis are indicated by dots and the genes found mutated are reported.

FIGURE 2
mRNA splicing analysis of the *BRCA1* c.5406+6T>C variant. The capillary electrophoresis patterns of the cDNA fragments spanning *BRCA1* exons 19 to 24 detected in LCLs from a *BRCA1* wild type subject **(A)** and from c.5406+6T>C carriers (proband **(B)** and proband's brother **(C)**) are shown. The peaks corresponding to normal transcripts maintaining exons 22 and 23 (full-length, FL) and aberrant transcripts (Δ22 and Δ22,23) are indicated. The sequencing of the PCR products **(D)** confirmed the presence of Δ22, Δ22,23 and normal transcripts in carriers of the *BRCA1* c.5406+6T>C variant.

FIGURE 3
Assessment of allele-specific expression of the normal *BRCA1* transcript. The common variant c.4837A>G, mapped to *BRCA1* exon 16, was proven to be heterozygous in the genomic DNA (gDNA) of the proband's brother (upper panel). The specific amplification of cDNA fragment maintaining exon 22 (normal transcript) and including the c.4837A>G variant was performed using a forward primer in exon 16 and a reverse primer in exon 22. The sequencing of the RT-PCR product showed a mono-allelic expression of the normal transcript (lower panel), indicating a complete spliceogenic effect of the c.5406+6T>C variant.

suggested a loss-of-function effect of the *BRCA1* c.5406+6T>C variant (23).

To the best of our knowledge, only three double heterozygotes for germline pathogenic variants in the *BRCA1* and *ATM* genes had been previously reported. Notably, two cases, both presenting the c.181T>G [p.(Cys61Gly)] variant in *BRCA1* and the c.5932G>T [p.(Glu1978Ter)] variant in *ATM*, had been detected following targeted screening of population-specific pathogenic variants (24). Conversely, the third case, carrying the c.5123C>A [p.(Ala1708Glu)] variant in *BRCA1* and c.2413C>T [p.(Arg805Ter)] variant in *ATM* was identified following a gene panel NGS analysis (7). The latter case reported multiple cancer diagnoses in addition to breast cancer, including an infiltrating carcinoma of the ampulla and a clear-cell endometrial adenocarcinoma.

Both the *ATM* and *BRCA1* genes code for key proteins involved in DNA double-strand breaks (DSBs) repair by homologous recombination (HR), a crucial mechanism for maintaining genomic integrity and preventing cancer development (25). It is debated whether, given the involvement of the two proteins in the same
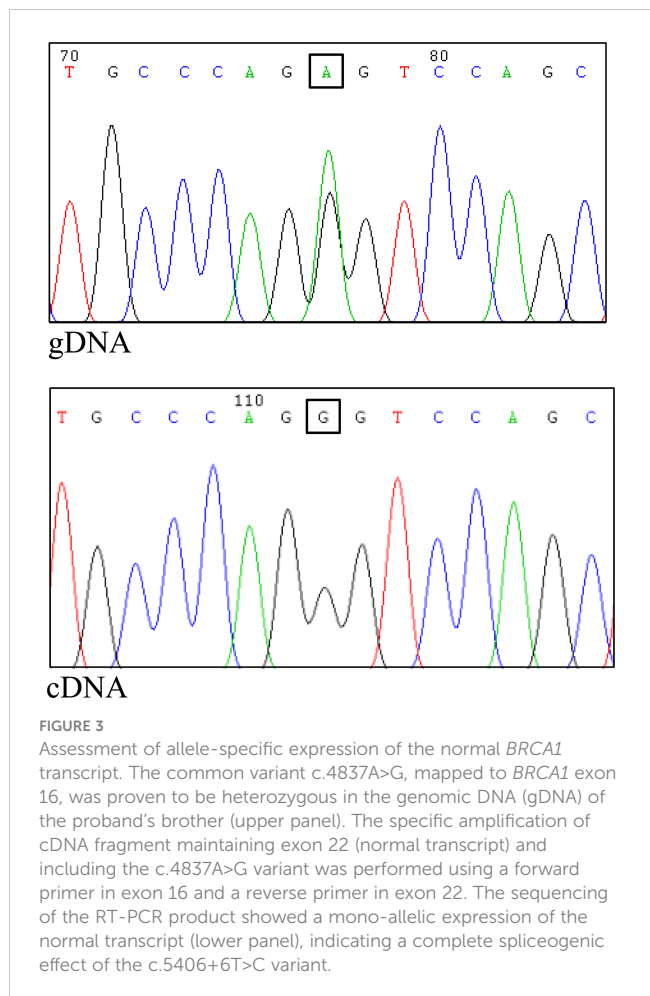
pathway, the risk of cancer and the severity of the disease can be increased in carriers of pathogenic variants in both genes, compared to single pathogenic variant carriers. Notably, it has been observed that in *Brca1*-null murine mammary tissue the heterozygous loss of *Atm* affects both mammary development, reducing ductal branching during puberty, and tumor severity, increasing invasiveness and causing undifferentiated tumor types, a phenotype not observed in the presence of *Atm* wild-type alleles (26). A later study demonstrated that in murine thymocytes the hemizygosity for both *Atm* and *Brca1* decreases radiation-induced apoptosis compared to single *Atm* or *Brca1* hemizygous cells (27). Finally, it has been observed that, compared to single *Atm* and *Brca1* heterozygous cells, mouse embryo fibroblasts double mutated in *Atm* and *Brca1* show an increased frequency of neoplastic transformation, a higher genomic instability, a delayed recognition of DNA damage induced by photon irradiation and an incomplete DNA repair (28).

Loss of function (LOF) *BRCA1* variants are associated with a high chance of cancer, with estimated cumulative risks by age 80 years of 72% and 44% for breast and ovarian cancer, respectively (29). Conversely, LOF *ATM* variants are considered moderate risk factors for breast cancer (cumulative risk by age 80 years of 27%) (30), with some limited evidence of association with ovarian cancer risk (31). To date, several common genetic variants, conferring a modest increase of breast/ovarian cancer risk in the general population, have been

ascertained to modulate the penetrance of *BRCA1* pathogenic variants (32). It is conceivable that the same modifier effect could be elicited by rare pathogenic variants in genes associated with moderate cancer risk. Consistent with this hypothesis, it has been recently reported that the occurrence of additional truncating variants in DNA repair genes might lead to an earlier onset of breast cancer in carriers of pathogenic *BRCA1* variants (33). However, in the four *BRCA1/ATM* double heterozygotes reported to date (7, 24 and present study), the age of first breast cancer diagnosis ranged from 36 to 55 years (the patient here described being the one with the earliest age of onset) with a median age of 43,2 years, similar to that (42 years) observed in carriers of single pathogenic variants in *BRCA1* (34). Analogously, when considering the tumor pathological characteristics, no specific phenotypes were observed in double heterozygous carriers compared to *BRCA1* pathogenic variant carriers. In all four cases the diagnosed breast cancers were estrogen receptor negative and in two of them (the patient described by Andres et al. (7) and our patient) they were classified as high grade triple-negative carcinomas, which are usually associated with an unfavorable prognosis. However, they are also the more represented breast cancer subtype associated with *BRCA1* pathogenic variants, being detected in approximately 65% of carriers with a breast cancer diagnosis overall (35). Conversely, the observation that both our proband and the case described by Andres et al. (7) developed multiple malignancies is in favor of a particularly aggressive clinical phenotype possible associated with the simultaneous occurrence of *BRCA1* and *ATM* pathogenic variants in the same individual. Based on genetic status and family history, the proband's healthy brother, carrying both *BRCA1* and *ATM* pathogenic variants, was recommended to undergo intensive surveillance, including endoscopic examination of the lower gastrointestinal tract every five years, yearly screening including mammography with breast magnetic resonance imaging (MRI), abdominal ultrasound scan and prostate specific antigen (PSA) test, starting from the age of 40 years.

In conclusion, the number of carriers of constitutional pathogenic variants in both *BRCA1* and *ATM* reported to date are too limited to assess if their cancer risks differ from those of individuals carrying a single *BRCA1* pathogenic variant. Therefore, the systematic collection of these cases is needed to address this issue and to define if, due to their particular genetic condition, they deserve *ad hoc* counseling and clinical management, including specific risk reduction measures.

Data availability statement

The original contributions presented in the study are included in the article/Supplementary Materials. Further inquiries can be directed to the corresponding author.

Ethics statement

The studies involving human participants were reviewed and approved by Ethics Committee of the Santa Maria della Misericordia Hospital. The patients/participants provided their written informed consent to participate in this study. Written informed consent was obtained from the individual(s) for the publication of any potentially identifiable images or data included in this article.

Author contributions

MC conceived the study, designed and performed the *in silico* and *in vitro* splicing analyses, and drafted the manuscript. VL contributed to conception of the study. EM, AM, and CM treated and followed the patient and her family. LP and VL performed the NGS analysis. PM provided technical assistance to the *in vitro* splicing experiments. CF established the LCLs. VL and EM contributed to the draft. PR made substantial contributions to conception of the study and reviewed the manuscript. All authors contributed to the article and approved the submitted version.

Funding

Acknowledgments

Conflict of interest

The authors declare that the research was conducted in the absence of any commercial or financial relationships that could be construed as a potential conflict of interest.

Publisher's note

All claims expressed in this article are solely those of the authors and do not necessarily represent those of their affiliated organizations, or those of the publisher, the editors and the reviewers. Any product that may be evaluated in this article, or claim that may be made by its manufacturer, is not guaranteed or endorsed by the publisher.

Supplementary material

The Supplementary Material for this article can be found online at: https://www.frontiersin.org/articles/10.3389/fonc.2023.1102184/full#supplementary-material

References

1. Miki Y, Swensen J, Shattuck-Eidens D, Futreal PA, Harshman K, Tavtigian S, et al. A strong candidate for the breast and ovarian cancer susceptibility gene BRCA1. *Science* (1994) 266:66–71. doi: 10.1126/science.7545954

2. Wooster R, Bignell G, Lancaster J, Swift S, Seal S, Mangion J, et al. Identification of the breast cancer susceptibility gene BRCA2. *Nature* (1995) 378:789–92. doi: 10.1038/378789a0

3. Thomas SF, Amie MD, Julia ER, Mark H, Brian EW, Beth L, et al. Clinical characteristics of individuals with germline mutations in BRCA1 and BRCA2: Analysis of 10,000 individuals. *J Clin Oncol* (2002) 20:1480–90. doi: 10.1200/JCO.2002.20.6.1480

4. Karin K, Kerstin R, Barbara W, Eric H, Jan H, Britta B, et al. Prevalence of BRCA1/2 germline mutations in 21 401 families with breast and ovarian cancer. *J Med Genet* (2016) 53:465–71. doi: 10.1136/jmedgenet-2015-103672

5. Eccles BK, Copson E, Maishman T, Abraham JE, Eccles DM. Understanding of BRCA VUS genetic results by breast cancer specialists. *BMC Cancer* (2015) 15:936. doi: 10.1186/s12885-015-1934-1

6. Bellcross CA. Hereditary breast and ovarian cancer: An updated primer for OB/GYNs. *Obstet Gynecol Clin North Am* (2022) 49:117–47. doi: 10.1016/j.ogc.2021.11.005

7. Andrés R, Menao S, Arruebo M, Quílez E, Cardiel MJ. Double heterozygous mutation in the BRCA1 and ATM genes involved in development of primary metachronous tumours: A case report. *Breast Cancer Res Treat* (2019) 177:767–70. doi: 10.1007/s10549-019-05343-4

8. Agaoglu NB, Doganay L. Concurrent pathogenic variations in patients with hereditary cancer syndromes. *Eur J Med Genet* (2021) 64:104366. doi: 10.1016/j.ejmg.2021.104366

9. Duzkale Teker N, Eyerci N. Double heterozygous mutations in the BRCA2 and ATM genes: A case report and review of the literature. *Breast Care (Basel)* (2021) 16:412–7. doi: 10.1159/000511430

10. Macquere P, Orazio S, Bonnet F, Jones N, Bubien V, Chiron J, et al. Increased incidence of pathogenic variants in ATM in the context of testing for breast and ovarian cancer predisposition. *J Hum Genet* (2022) 67:339–45. doi: 10.1038/s10038-022-01014-3

11. Mampel A, Sottile ML, Denita-Juárez SP, Vargas AL, Vargas-Roig LM. Double heterozygous pathogenic variants in the BRCA1 and BRCA2 genes in a patient with bilateral metachronous breast cancer. *Cancer Genet* (2022) 260-261:14–7. doi: 10.1016/j.cancergen.2021.11.003

12. Sánchez Castro EE, Ziegler-Rodriguez G, Castro Mujica MDC. Double heterozygous mutation in RAD50 and ATM genes in a Peruvian family with five cancer types: A case report. *Rev Fac Cien Med Univ Nac Cordoba* (2022) 79:53–6. doi: 10.31053/1853.0605.v79.n1.32795

13. Vietri MT, Caliendo G, D'Elia G, Resse M, Casamassimi A, Minucci PB, et al. Five Italian families with two mutations in BRCA genes. *Genes (Basel)* (2020) 11:1451. doi: 10.3390/genes11121451

14. Nurmi A, Muranen TA, Pelttari LM, Kiiski JI, Heikkinen T, Lehto S, et al. Recurrent moderate-risk mutations in Finnish breast and ovarian cancer patients. *Int J Cancer* (2019) 145:2692–700. doi: 10.1002/ijc.32309

15. BRCA Exchange, in: *November 18, 2022*. Available at: https://brcaexchange.org/variants.

16. ClinVar, in: *November 18, 2022*. Available at: https://www.ncbi.nlm.nih.gov/clinvar/.

17. Richards S, Aziz N, Bale S, Bick D, Das S, Gastier-Foster J, et al. Standards and guidelines for the interpretation of sequence variants: A joint consensus recommendation of the American college of medical genetics and genomics and the association for molecular pathology. *Genet Med* (2015) 17:405–24. doi: 10.1038/gim.2015.30

18. Breast Information Core (BIC), in: *November 18, 2022*. Available at: https://research.nhgri.nih.gov/bic/.

19. Caleca L, Putignano AL, Colombo M, Congregati C, Sarkar M, Magliery TJ, et al. Characterization of an Italian founder mutation in the RING-finger domain of BRCA1. *PloS One* (2014) 9:e86924. doi: 10.1371/journal.pone.0086924

20. Colombo M, Lopez-Perolio I, Meeks HD, Caleca L, Parsons MT, Li HY, et al. The BRCA2 c.68-7T > a variant is not pathogenic: A model for clinical calibration of spliceogenicity. *Hum Mutat* (2018) 39:729–41. doi: 10.1002/humu.23411

21. Colombo M, Blok MJ, Whiley P, Santamariña M, Gutiérrez-Enríquez S, Romero A, et al. Comprehensive annotation of splice junctions supports pervasive alternative splicing at the BRCA1 locus: A report from the ENIGMA consortium. *Hum Mol Genet* (2014) 23:3666–80. doi: 10.1093/hmg/ddu075

22. Evidence-based Network for the Interpretation of Germline Mutant Alleles (ENIGMA) consortium, in: *November 18, 2022*. Available at: https://enigmaconsortium.org/.

23. Findlay GM, Daza RM, Martin B, Zhang MD, Leith AP, Gasperini M, et al. Accurate classification of BRCA1 variants with saturation genome editing. *Nature* (2018) 562:217–22. doi: 10.1038/s41586-018-0461-z

24. Sokolenko AP, Bogdanova N, Kluzniak W, Preobrazhenskaya EV, Kuligina ES, Iyevleva AG, et al. Double heterozygotes among breast cancer patients analyzed for BRCA1, CHEK2, ATM, NBN/NBS1, and BLM germ-line mutations. *Breast Cancer Res Treat* (2014) 145:553–62. doi: 10.1007/s10549-014-2971-1

25. Yamamoto H, Hirasawa A. Homologous recombination deficiencies and hereditary tumors. *Int J Mol Sci* (2021) 23:348. doi: 10.3390/ijms23010348

26. Bowen TJ, Yakushiji H, Montagna C, Jain S, Ried T, Wynshaw-Boris A. Atm heterozygosity cooperates with loss of Brca1 to increase the severity of mammary gland cancer and reduce ductal branching. *Cancer Res* (2005) 65:8736–46. doi: 10.1158/0008-5472.CAN-05-1598

27. Su F, Smilenov LB, Ludwig T, Zhou L, Zhu J, Zhou G, et al. Hemizygosity for atm and Brca1 influence the balance between cell transformation and apoptosis. *Radiat Oncol* (2010) 5:15. doi: 10.1186/1748-717X-5-15

28. Wang J, Su F, Smilenov LB, Zhou L, Hu W, Ding N, et al. Mechanisms of increased risk of tumorigenesis in atm and Brca1 double heterozygosity. *Radiat Oncol* (2011) 6:96. doi: 10.1186/1748-717X-6-96

29. Kuchenbaecker KB, Hopper JL, Barnes DR, Phillips KA, Mooij TM, Roos-Blom MJ, et al. Risks of breast, ovarian, and contralateral breast cancer for BRCA1 and BRCA2 mutation carriers. *JAMA* (2017) 317:2402–16. doi: 10.1001/jama.2017.7112

30. Easton DF, Pharoah PD, Antoniou AC, Tischkowitz M, Tavtigian SV, Nathanson KL, et al. Gene-panel sequencing and the prediction of breast-cancer risk. *N Engl J Med* (2015) 372:2243–57. doi: 10.1056/NEJMsr1501341

31. Lilyquist J, LaDuca H, Polley E, Davis BT, Shimelis H, Hu C, et al. Frequency of mutations in a large series of clinically ascertained ovarian cancer cases tested on multi-gene panels compared to reference controls. *Gynecol Oncol* (2017) 147:375–80. doi: 10.1016/j.ygyno.2017.08.030

32. Barnes DR, Rookus MA, McGuffog L, Leslie G, Mooij TM, Dennis J, et al. Polygenic risk scores and breast and epithelial ovarian cancer risks for carriers of BRCA1 and BRCA2 pathogenic variants. *Genet Med* (2020) 22:1653–66. doi: 10.1038/s41436-020-0862-x

33. Sepahi I, Faust U, Sturm M, Bosse K, Kehrer M, Heinrich T, et al. Investigating the effects of additional truncating variants in DNA-repair genes on breast cancer risk in BRCA1-positive women. *BMC Cancer* (2019) 19:787. doi: 10.1186/s12885-019-5946-0

34. Brose MS, Rebbeck TR, Calzone KA, Stopfer JE, Nathanson KL, Weber BL. Cancer risk estimates for BRCA1 mutation carriers identified in a risk evaluation program. *J Natl Cancer Inst* (2002) 94:1365–72. doi: 10.1093/jnci/94.18.1365

35. Spurdle AB, Couch FJ, Parsons MT, McGuffog L, Barrowdale D, Bolla MK, et al. Refined histopathological predictors of BRCA1 and BRCA2 mutation status: A large-scale analysis of breast cancer characteristics from the BCAC, CIMBA, and ENIGMA consortia. *Breast Cancer Res* (2014) 16:3419. doi: 10.1186/s13058-014-0474-y

Molecular characteristics of multiple primary pulmonary nodules under a three-dimensional reconstruction model and relevant multi-omics analyses: a case report

Zhilin Luo[1†], Yajie Xiao[2†], Chengwen Luo[1], Liping Zhang[1], Runquan Zhou[1], Zhikun Zhao[2], Chao Sun[2], Dongfang Wu[2] and Tianhu Wang[1*]

[1]Department of Thoracic Surgery, The Third Affiliated Hospital of Chongqing Medical University, Chongqing, China, [2]Department of Medicine, YuceBio Technology Co. Ltd., Shenzhen, China

Background: In addition to CT images and pathological features, many other molecular characteristics remain unknown about multiple primary lung cancer (MPLC) from intrapulmonary metastatic lung cancer.

Case presentation: In this study, we reported a patient with an early-stage MPLC with both adenocarcinoma *in situ* (AIS) subtype and minimally invasive adenocarcinoma (MIA) subtype. The patient was diagnosed with more than 10 nodules and underwent precise surgery assisted by three-dimensional (3D) reconstruction at the left upper lung lobe. Whole-exome sequencing (WES) and multiple immunohistochemistry (mIHC) were performed to reveal the genomic profiling and tumor microenvironments of multiple nodules in this patient with MPLC. Based on 3D reconstruction location information, we found that the genomic and pathological results of adjacent lymph nodes were quite different. On the other hand, PD-L1 expression and the proportion of infiltrating lymphocytes in tumor microenvironments were all at a low status and did not vary in adjacent lymph nodes. Additionally, maximum diameter and tumor mutational burden levels were found to be significantly associated with CD8+ T cell proportion (p<0.05). Besides, CD163+ macrophages and CD4+ T cell proportion were higher in MIA nodules than in AIS nodules (p<0.05). This patient reached a recurrence-free survival of 39 months.

Conclusion: Generally, in addition to CT imaging and pathological results, genomic profiling and tumor microenvironments may facilitate identifying the potential molecular mechanisms and clinical outcomes in patients with early-stage MPLC.

KEYWORDS

multiple primary lung cancer, multi-omics analyses, genomic profiling, tumor environment, three-dimensional (3D) reconstruction

Introduction

In 2015, the World Health Organization (WHO) classified two new subtypes of lung adenocarcinoma: adenocarcinoma *in situ* (AIS) and minimally invasive adenocarcinoma (MIA) (1). Based on CT images, the AIS subtype of lung adenocarcinoma was defined as a small lesion (≤3 cm) consisting of a pure lepidic component. Whereas, the MIA type was classified as a small lesion (≤3 cm) consisting of a predominantly growing lepidic component together with some invasive small components (2).

These two subtypes of lung adenocarcinoma have been proven to have good long-term prognoses upon timely diagnosis and operation (3, 4). The 5-year recurrence-free survival (RFS) of AIS patients and MIA patients reaches nearly 100% after complete resection (5, 6). Morphologically, it is hypothesized that a gradual malignant progression can be generated from AIS to MIA. However, definite molecular mechanisms for this transformation remain unclear. Many current studies focused on early diagnosis characteristics from CT images (7–9), while only a few studies conducted comprehensive analyses for molecular profiles (10).

In this study, the patient was diagnosed with multiple primary lung cancer (MPLC) with more than 10 nodules of both AIS and MIA subtypes and subsequently underwent precise lobectomy assisted by three-dimensional (3D) reconstruction. Additionally, we compared molecular characteristics between AIS and MIA subtypes in terms of the CT images, 3D locations, genomic profiles, and tumor microenvironments in order to provide potential clinical evidence for identifying the molecular mechanisms in early lung cancer.

Case presentation

A 55-year-old man who was a mild smoker, and had no medical or family history, had his annual physical examination in January 2019 and was found with a small nodule (about 1cm) in the upper lobe of the left lung. Three months later, he was observed with multiple small ground-glass nodules (about 1cm) in the upper lobe of the left lung. After oral moxifloxacin anti-inflammatory treatment, the CT images of the patient did not improve. On the contrary, in July 2019, his CT images revealed multiple enlarged nodules in the upper lobe of the left lung and he was admitted to our hospital for further treatment (Figure 1A). Then, the patient was diagnosed with more than 10 nodules and we used a three-dimensional (3D) reconstruction model to evaluate the accurate location of these nodules and their relevant anatomical structures (Figure 1B). Subsequently, we conducted a precise operation of the left upper lung lobe, including the posterior end of the tip of the upper lobe and the anterior segment of the upper lobe. Pathological results showed that nodule 1, nodule 3, nodule 5, nodule 6, and nodule 9 were identified as MIA while nodule 4, nodule 12, and A subsegment (nodule 11) were identified as AIS. No cancer cells were found in nodule 2, nodule 7, nodule 8, and nodule 10. Based on the latest follow-up in October 2022, the patient was still in good
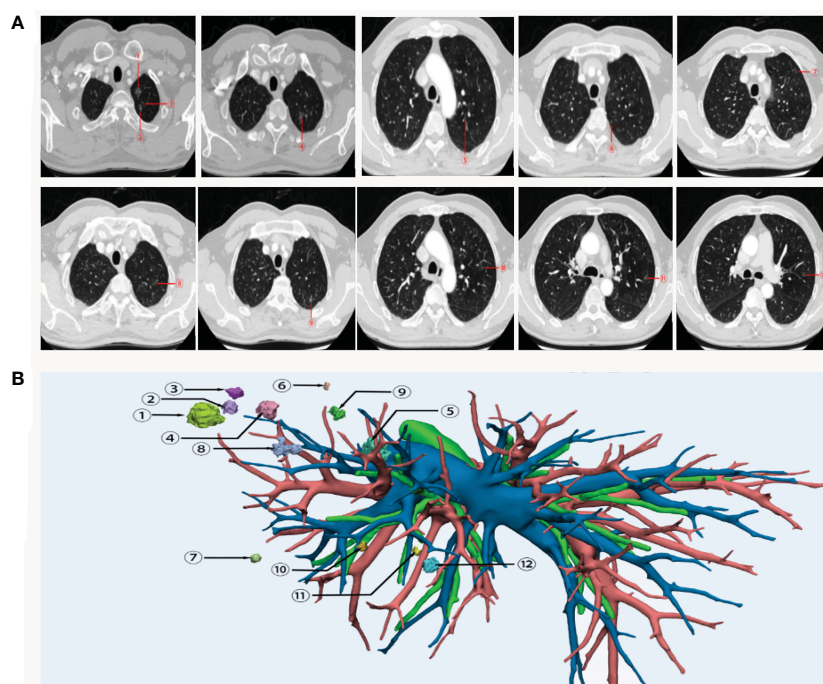

FIGURE 1
CT images **(A)** and 3D reconstruction **(B)** of this patient with early-stage MPLC. Nodule 1, nodule 3, nodule 5, nodule 6 and nodule 9 were identified as MIA. Nodule 4, nodule 12, and nodule 11 were identified as AIS. No cancer cells were found in nodule 2, nodule 7, nodule 8, and nodule 10. MPLC, multiple primary lung cancer; AIS, adenocarcinoma in situ; MIA, minimally invasive adenocarcinoma.

condition and no evidence of disease recurrence was found. Thereby this patient reached a 39-month RFS.

In this current case, whole-exome sequencing (WES) (Figure 2A) and multiple immunohistochemistry (mIHC) (Figure 2B) were performed to reveal the genomic profiling and tumor microenvironments of multiple nodules, including nodule1, nodule 4, nodule 5, nodule 6, nodule 9, and A subsegment (nodule 11). Based on WES results, all the nodules were at low tumor mutational burden (TMB) ranging from 0.46-3.68 muts/mb, low tumor neoantigen burden (TNB) ranging from 0.03-1.19 neos/mb, and low microsatellite instability (MSI) ranging from1.21-19.08%. The nodules did not present any loss at human leukocyte antigen (HLA). As shown in Figure 2A, *KRAS* mutations were observed at nodule 5,

mutations at those genes, including *MAP2K1, SEZ6L, PAX5* and *CACNB2*, were observed at nodule 6, no mutations were observed at nodule 9, and mutations at those genes, including *SIX3, KRTAP5-11, KEAP1, KRAS, GAS7, FLT4, FAT1, FAM57B, COL9A2, CD99L2*, were observed at A subsegment (nodule 11). Except for KRAS in nodule 5 and A subsegment (nodule 11), there were almost no collective mutations among all nodules. By associating with 3D locations, we found that the genomic and pathological results of adjacent lymph nodes were quite different, implying MPLC instead of intrapulmonary metastatic lung cancer (IPM). To illustrate the intratumor heterogeneity, we used opposite sections of a wax block for nodule 1 and nodule 4 to perform WES and mIHC analysis. Mutations at those genes, including *AXIN2, CDK2, TSPAN5, SUZ12, MAP2K1, LATS2,*

FIGURE 2
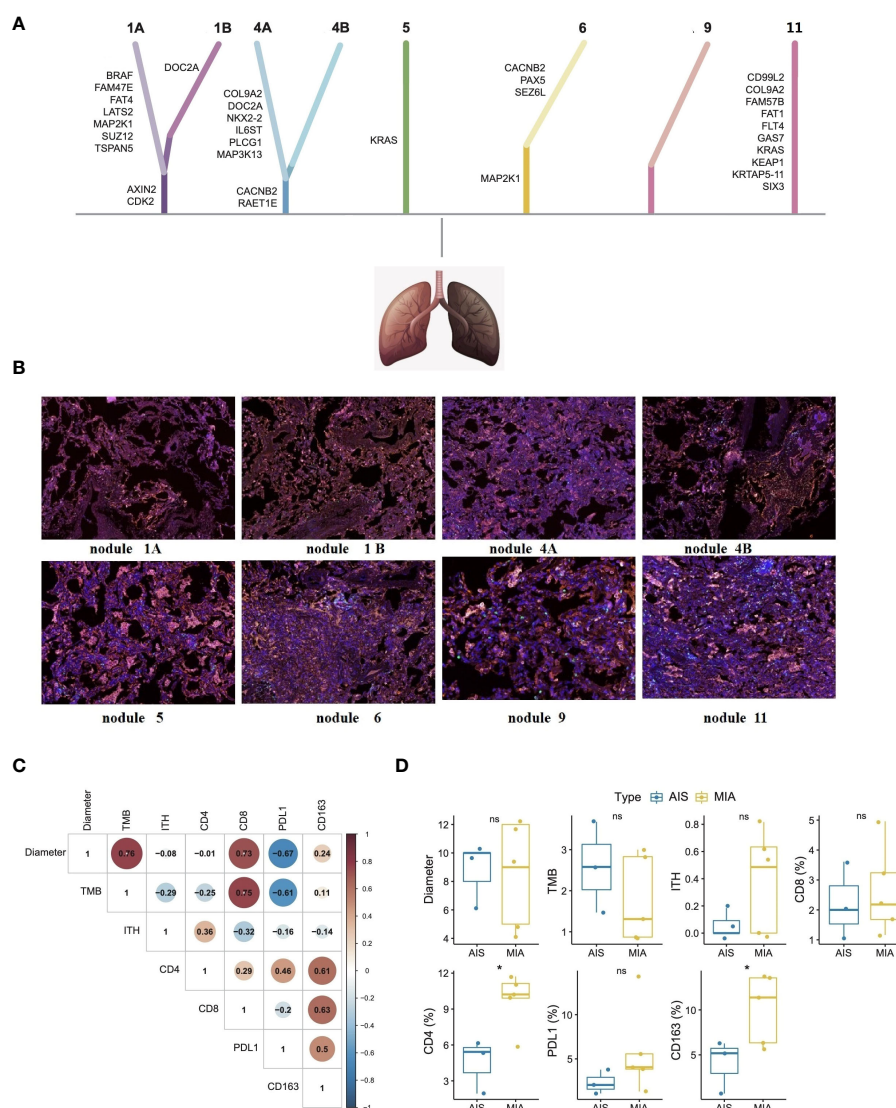Whole-exome sequencing **(A)**, mIHC analysis **(B)**, biomarker correlations **(C)**, and subtype differences **(D)** of each nodule in this patient with early-stage MPLC. Whole-exome sequencing showed that there were almost no collective mutations among all nodules. mIHC analysis showed similarly low positive levels of CD4 + T cells (yellow color), CD8 + T cells (green color), CD163+ macrophages (purple color), and PD-L1 expression (red color) in tumor microenvironments of each nodule. Fisher's exact test and Wilcox test were used to analyze the correlation or differences between different groups. *p<0.05 was considered as statistically significant. MPLC, multiple primary lung cancer; AIS, adenocarcinoma in situ; MIA, minimally invasive adenocarcinoma. ns, not statistically significant.

FAT4, FAM47E, and *BRAF*, were observed at nodule 1A, while mutation at those genes, including *CDK2, AXIN2*, and *DOC2A*, were observed at nodule 1B. Mutations at those genes, including *RAET1E, CACNB2, MAP3K13, PLCG1, IL6ST, NKX2-2, DOC2A, COL9A2*, were observed at nodule 4A while mutation at those genes, including *CACNB2* and *RAET1E*, were observed at nodule 4B. Overall, only a few mutations were simultaneously found at opposite sections of the wax block in either nodule 1 or nodule 4 (*CDK2* and *AXIN2* mutations in nodule 1A and nodule 1B; *CACNB2* and *RAET1E* mutations in nodule 4A and nodule 4B).

As seen in Figure 2B, mIHC analysis showed similarly low positive levels of CD4 + T cells (less than 17%), CD8 + T cells (less than 5%), CD163+ macrophages (less than 15%), and PD-L1 expression (less than 15%) in tumor microenvironments of each nodule. As shown in Figure 2C, maximum diameter and TMB levels were found to be significantly associated with CD8+ T cell proportion ($p < 0.05$). Unfortunately, there was no definite correlation in PD-L1 level, ITH level, CD4+ T cells proportion, and CD163+ macrophage proportion. Comparing the relevant results of MIA and AIS nodules in Figure 2D, CD163+ macrophages and CD4+ T cell proportions were higher in MIA nodules than in the AIS nodules ($p < 0.05$).

Discussion

Beyond CT imaging and pathological finding, many other molecular characteristics remain unknown about MPLC, with both AIS and MIA. Due to the patient being diagnosed with more than 10 nodules, he underwent a precise lobectomy assisted by 3D reconstruction. Combined with 3D location information, the genomic and pathological results of adjacent lymph nodes were quite different, implying MPLC instead of IPM. Besides, this patient with early-stage MPLC showed similarly low positive levels of predictive biomarkers such as TMB, TNB, MSI, and HLA loss of heterozygosity for each nodule. In addition, PD-L1 expressions as well as the proportion of infiltrating lymphocytes in tumor microenvironments were low positive in both AIS and MIA and did not vary significantly in adjacent lymph nodes. Additionally, maximum diameter and TMB level were found to be significantly associated with CD8+ T cell proportion. Besides, CD163+ macrophages and CD4+ T cell proportion were higher in MIA nodules than in AIS nodules.

Comprehensive multi-omic analysis of multidisciplinary factors leaves space for clarifying potential molecular mechanisms. As is known, genomic profiling could identify the clonality status of multiple lesions. The TRACERx project revealed the tumor evolution in patients with early-stage NSCLC and suggested that driver gene mutations in EGFR, MET, BRAF, and TP53 are the most common clonal driver mutations in lung adenocarcinoma (11). Some retrospective studies also showed that EGFR mutations were more common in MIA than in AIS (8, 12, 13). WES results of multiple nodules in this patient only revealed BRAF mutation in nodule 1, and

no other common mutations were found. Taking advantage of the 3D reconstruction technique, we found that the genomic and pathological results of adjacent lymph nodes were quite different, indicating MPLC instead of IPM. Compared with other previous studies that focused only on genomic analysis or CT findings, we combined multi-dimensional information to stereoscopically display the genomic and pathological characteristics of MPLC for distinguishing it from IPM.

Besides, the tumor microenvironment plays a crucial role in cancer evolution at all stages of NSCLC, including development, invasion, and metastasis (14, 15). The dynamic balance of anti- and pro-inflammatory immune cells can drive the immunoediting process and relative immune host response. Even after complete surgical treatment, the prognosis of NSCLC is variable and nearly half of all surgical patients develop post-surgery recurrence (16). More and more evidence suggests that adjuvant systemic therapies, such as immunotherapy, can lead to additional benefits and reduce the risk of recurrence for these early-stage surgical patients (16). Therefore, molecular biomarkers for predicting NSCLC post-surgery prognosis are urgently needed. In early-stage lung cancer, the presence of CD8+ T cells, CD4+ T cells, and CD20+ B cells were positive predictors of decreasing risks of death (17). In this study, we used multiple immunohistochemistry (mIHC) of CD4 + T cells, CD8 + T cells, CD163+ macrophages, and PD-L1 expression for analysis of immune characteristics of tumor microenvironments. The proportion of infiltrating lymphocytes of CD4 + T cells, CD8 + T cells, CD163+ macrophages, and PD-L1 expression was at a low positive level in this patient, suggesting that the immunoediting process and relative immune host response had partially initiated. In addition, higher maximum diameter and higher TMB levels were found to be significantly associated with higher CD8+ T cell proportion ($p < 0.05$), indicating that there migtht be a stronger immune host response in lesions with larger sizes. In addition, infiltrating CD163+ macrophages and CD4+ T cell proportion were higher in MIA than in AIS. Other similar studies showed that CD4+ infiltrating T cell was higher in MIA than in AIS, implying tumor invasion (18, 19). This seemed consistent with the WHO definition of the two subtypes. Contrary to genomic features, we found that the immune characteristics of adjacent lymph nodes are not very different based on the 3D reconstruction model. After undergoing precise lobectomy assisted by 3D reconstruction, the patient did not receive any adjuvant systemic therapies and reached a 39-month RFS. This study might suggest that low positive expression of multiple biomarkers in tumor microenvironments might be useful predictors of long-term prognosis of complete surgical resection without adjuvant systemic therapy.

In summary, in addition to CT imaging and pathological results, genomic profiling and tumor microenvironments may help with clarifying the potential molecular mechanism in patients with early-stage MPLC. Moreover, multiple biomarkers in tumor microenvironments may be developed as prognosis predictors for long-term outcomes of early lung cancer patients after surgery.

Data availability statement

Ethics statement

Author contributions

Acknowledgments

Conflict of interest

Publisher's note

Supplementary material

References

1. Marx A, Chan J, Coindre J, Detterbeck F, Girard N, Harris N, et al. The 2015 world health organization classification of tumors of the thymus: continuity and changes. *J Thorac Oncol* (2015) 10:1383–95. doi: 10.1097/JTO.0000000000000654

2. Jia M, Yu S, Cao L, Sun P, Gao H. Clinicopathologic features and genetic alterations in adenocarcinoma *in situ* and minimally invasive adenocarcinoma of the lung: long-term follow-up study of 121 Asian patients. *Ann Surg Oncol* (2020) 27:3052–63. doi: 10.1245/s10434-020-08241-y

3. Yotsukura M, Asamura H, Motoi N, Kashima J, Yoshida Y, Nakagawa K, et al. Long-term prognosis of patients with resected adenocarcinoma *In situ* and minimally invasive adenocarcinoma of the lung. *J Thorac Oncol* (2021) 16:1312–20. doi: 10.1016/j.jtho.2021.04.007

4. Zhang Y, Deng C, Fu F, Ma Z, Wen Z, Ma X, et al. Excellent prognosis of patients with invasive lung adenocarcinomas during surgery misdiagnosed as atypical adenomatous hyperplasia, adenocarcinoma in situ, or minimally invasive adenocarcinoma by frozen section. *Chest* (2021) 159:1265–72. doi: 10.1016/j.chest.2020.10.076

5. Zhang Y, Ma X, Shen X, Wang S, Li Y, Hu H, et al. Surgery for pre- and minimally invasive lung adenocarcinoma. *J Thorac Cardiovasc Surg* (2022) 163:456–64. doi: 10.1016/j.jtcvs.2020.11.151

6. Zhao Y, Shang J, Gao J, Han H, Gao Z, Yan Y, et al. Increased tumor intrinsic growth potential and decreased immune function orchestrate the progression of lung adenocarcinoma. *Front Immunol* (2022) 13:921761. doi: 10.3389/fimmu.2022.921761

7. Sugawara H, Watanabe H, Kunimatsu A, Abe O, Watanabe S, Yatabe Y, et al. Adenocarcinoma *in situ* and minimally invasive adenocarcinoma in lungs of smokers: image feature differences from those in lungs of non-smokers. *BMC Med Imag* (2021) 21:172. doi: 10.1186/s12880-021-00705-1

8. Chen T, Zhang X, Campisi A, Ciarrocchi A, Dell'Amore A, Song L, et al. Evaluation of dynamic image progression of minimally invasive and preinvasive lung adenocarcinomas. *Ann Transl Med* (2021) 9:804. doi: 10.21037/atm-21-1994

9. Zhang R, Tian P, Qiu Z, Liang Y, Li W. The growth feature and its diagnostic value for benign and malignant pulmonary nodules met in routine clinical practice. *J Thorac Dis* (2020) 12:2019–30. doi: 10.21037/jtd-19-3591

10. Ishida H, Shimizu Y, Sakaguchi H, Nitanda H, Kaneko K, Yamazaki N, et al. Distinctive clinicopathological features of adenocarcinoma *in situ* and minimally

invasive adenocarcinoma of the lung: a retrospective study. *Lung Cancer* (2019) 129:16–21. doi: 10.1016/j.lungcan.2018.12.020

11. Jamal-Hanjani M, Wilson G, McGranahan N, Birkbak N, Watkins T, Veeriah S, et al. Tracking the evolution of non-small-cell lung cancer. *N Engl J Med* (2017) 376:2109–21. doi: 10.1056/NEJMoa1616288

12. Kobayashi Y, Mitsudomi T, Sakao Y, Yatabe Y. Genetic features of pulmonary adenocarcinoma presenting with ground-glass nodules: the differences between nodules with and without growth. *Ann Oncol* (2015) 26:156–61. doi: 10.1093/annonc/mdu505

13. Nakamura H, Koizumi H, Kimura H, Marushima H, Saji H, Takagi M. Epidermal growth factor receptor mutations in adenocarcinoma *in situ* and minimally invasive adenocarcinoma detected using mutation-specific monoclonal antibodies. *Lung Cancer* (2016) 99:143–7. doi: 10.1016/j.lungcan.2016.07.009

14. Bagaev A, Kotlov N, Nomie K, Svekolkin V, Gafurov A, Isaeva O, et al. Conserved pan-cancer microenvironment subtypes predict response to immunotherapy. *Cancer Cell* (2021) 39:845–865.e7. doi: 10.1016/j.ccell.2021.04.014

15. Bremnes R, Busund L, Kilvær T, Andersen S, Richardsen E, Paulsen E, et al. The role of tumor-infiltrating lmphocytes in development, progression, and prognosis of non-small cell lung cancer. *J Thorac Oncol* (2016) 11:789–800. doi: 10.1016/j.jtho.2016.01.015

16. Brown L, Louie B, Jackson N, Farivar A, Aye R, Vallières E. Recurrence and survival after segmentectomy in patients with prior lung resection for early-stage non-small cell lung cancer. *Ann Thorac Surg* (2016) 102:1110–8. doi: 10.1016/j.athoracsur.2016.04.037

17. Tuminello S, Petralia F, Veluswamy R, Wang P, Flores R, Taioli E. Prognostic value of the tumor immune microenvironment for early-stage, non-small cell lung cancer. *Am J Clin Oncol* (2021) 44:350–5. doi: 10.1097/COC.0000000000000832

18. Krysan K, Tran L, Grimes B, Fishbein G, Seki A, Gardner B, et al. The immune contexture associates with the genomic landscape in lung adenomatous premalignancy. *Cancer Res* (2019) 79:5022–33. doi: 10.1158/0008-5472.CAN-19-0153

19. Zhang C, Zhang J, Xu F, Wang Y, Xie Z, Su J, et al. Genomic landscape and immune microenvironment features of preinvasive and early invasive lung adenocarcinoma. *J Thorac Oncol* (2019) 14:1912–23. doi: 10.1016/j.jtho.2019.07.031

Frontiers in
Oncology

Advances knowledge of carcinogenesis and tumor progression for better treatment and management

The third most-cited oncology journal, which highlights research in carcinogenesis and tumor progression, bridging the gap between basic research and applications to imrpove diagnosis, therapeutics and management strategies.

Discover the latest Research Topics

See more →

Frontiers in
Oncology

frontiers | Research Topics